

The Pennsylvania State University

The Graduate School

**EVOLUTION OF THE TUNGNÁRHRAUN MAFIC LAVAS: INSIGHTS INTO MAGMA
STORAGE AND ASCENT BENEATH BÁRÐARBUNGA VOLCANIC SYSTEM**

A Thesis in

Geosciences

by

Collin A. Oborn

© 2020 Collin A. Oborn

Submitted in Partial Fulfillment
of the Requirements
for the Degree of

Master of Science

December 2020

The thesis of Collin A. Oborn was reviewed and approved by the following:

Tanya Furman
Professor of Geosciences
Thesis Advisor

Peter C. La Femina
Associate Professor of Geosciences

Andrew J. Smye
Assistant Professor of Geosciences

Andrew A. Nyblade
Professor of Geosciences
Head of the Department of Geosciences

ABSTRACT

Geochemical analyses of bulk lavas and textural features of macrocryst ($>1000\text{ }\mu\text{m}$) plagioclase feldspar provide insights into the timing and structure of magma storage and ascent beneath active volcanic systems. Data from these crystals are used to infer crystallization P and T, provenance, and crustal residence times, and therefore, constrain processes of magma evolution. The Bárðarbunga volcanic system is distinct within Iceland for its consistent production of plagioclase porphyritic basalts since the last glacial maximum (~12 ka). This system is also the most productive in Iceland over the Holocene, generating voluminous, far-reaching lava flows from both its northern and southern fissures. We link the Tungnárhraun, a series of large volume ($>1\text{ km}^3$) lava flows which span nearly the entire Holocene period, to the southern Bárðarbunga fissure. Several of these flows approach plagioclase ultraphyric basalts (PUBs) with 10-20 vol% plagioclase. The macrocrysts are characterized by high anorthite cores ($>\text{An}_{80}$), which, like most PUBs, are too primitive to have grown from the host lava. The cores are surrounded by An₅₅₋₈₀ rims which have intergrowth textures with the groundmass, suggesting chemical equilibrium. The chemistry of the Tungnárhraun define three eruptive episodes: early and late periods of evolved lavas (~5.5-6 wt.% MgO) with <10 vol.% plagioclase and a middle period of more primitive lavas (~8 wt.% MgO) with 14-20 vol% plagioclase. These features suggest variation in magma storage and ascent. We explore the evolution of the Tungnárhraun through a series of plagioclase and liquid thermometers and barometers and examine their relationship to calculated host melt compositions. This project combines our extensive dataset with published data from the Tungnárhraun sequence and the Bárðardalur lavas (northern and southern extents of the volcanic system) to assess magma storage and movement through time in Iceland's most productive fissure system.

TABLE OF CONTENTS

<i>LIST OF FIGURES</i>	v
<i>LIST OF TABLES</i>	vii
INTRODUCTION	1
GEOLOGICAL BACKGROUND	5
Geologic setting of Bárðarbunga.....	5
Eruptive history of the Bárðarbunga fissure swarms.....	8
Plagioclase Ultraphyric Basalts (PUBs) of Iceland	9
METHODS	11
Samples and Analytical Techniques	11
Numerical techniques.....	12
Modeling Constraints.....	12
RESULTS	17
Petrography and Mineral Chemistry	17
Major Element Geochemistry	18
Geothermobarometry	19
Diffusion modeling	21
DISCUSSION	22
Volcanic source of the Tungnárhraun.....	22
Evolution of the Tungnárhraun – The case for three eruptive episodes.....	23
Crustal structure of the Bárðarbunga volcanic system	24
CONCLUSIONS	35
REFERENCES	43
APPENDICES	49
Appendix A – Whole Rock Chemistry	49
Appendix B – Olivine Chemistry	51
Appendix C - Plagioclase	53
Appendix D – Pyroxene Chemistry	69
Appendix E – Olivine Transects.....	75
Appendix F – Annotated Fe-Mg Interdiffusion Code (R Notebook)	95
Appendix G – Diffusion and Thermobarometry Equations.....	103

LIST OF FIGURES

Figure 1: Top – Map of the volcanic setting and systems of Iceland. WVZ = Western Volcanic Zone, EVZ = Eastern Volcanic Zone, NVZ = Northern Volcanic Zone, SISZ = South Iceland Seismic Zone, TFZ = Tjörnes Fracture Zone, RVB = Reykjanes Volcanic Belt, SVB = Snæfellsnes Volcanic Belt, MIB = Mid-Iceland Belt, ÖVB = Öræfajökull Volcanic Belt, RR = Reykjanes Ridge, KR = Kolbeinsey Ridge. Bottom – Detailed view of the volcanic systems of the EVZ. B = Bárðarbunga, V = Veiðivötn, G = Grimsvötn, L = Laki, K = Katla, E = Eldgjá, T = Torfajökull, VH = Vonarskarð, H = Hekla, S = Skjaldbreiður. The dashed circle indicates the approximate center of the Iceland Mantle Plume as depicted by Wolfe et al. (2017). Modified from Thordarson and Höskuldsson (2008)	2
Figure 2: Top – Map of the extent and Holocene lavas of the Bárðarbunga system. Notable parts of the system are labelled. After Björnsson (1988), Jóhannesson and Sæmundsson (1998a, 1998b), Gudmundsson and Högnadóttir (2007), Sigurgeirsson et al. (2015). Base data: Iceland GeoSurvey, IMO, NLSI. Basemap: IMO. Bottom – Detailed map of the northern Bárðarbunga Fissure Swarm. From Svavarssdóttir (2017)	7
Figure 3: a) Map of the Tungnárhraun lava flows, modified from Vilmundardóttir (1977). The red oval is the suggested area of origin for the Tungnárhraun. b) Map of sample locations for this study, modified from Kaldal and Vilmundardóttir (1986) and Kaldal et al. (1988).....	13
Figure 4: Top – Images of the thin sections analyzed for this study. Bottom – Select cross polarized images of plagioclase from each thin section as well as BSE images displaying representative plagioclase zoning patterns of macrocryst plagioclase.	14
Figure 5: BSE images and diffusion profiles from representative olivine. Yellow lines indicate where the profiles were taken. Profiles from THb and THd with multiple diffuse zones are included for their unique shape but were not modeled.	16
Figure 6: Plot of plagioclase macrocryst compositions in each Tungnárhraun flow. Small symbols indicate previously published data. THa and THb: Halldorsson, 2007; THh and Drekahraun: Caracciolo et al., 2020.	17
Figure 7: Whole rock compositions of the Tungnárhraun plotted on the classification scheme of Le Bas, 1986. Squares denote calculated liquid compositions and the fields represent the compositions of various volcanic systems.	19
Figure 8: Variation diagrams of major element oxides for the Tungnárhraun samples. Dataset includes WR data from THa and THb from Halldórsson, 2007. Values for Bárðarbunga's South fissure are point analyses of tephra from the Veiðivötn 1477 and Vatnaöldur 871 eruptions (Óladottir et al., 2011).....	20
Figure 9: Calculated temperature of crystallization from distinct plagioclase macrocryst parts. Dashed lines are calculated temperatures using the liquid thermometer of Yang et al., 1996; liquid composition was determined for these porphyritic samples by subtracting 20% plagioclase from whole rock averages of each flow.	21
Figure 10: Estimated diffusion times for olivine macrocrysts by flow assuming transects parallel to the C-axis at 2 kbar (upward pointing triangles), and to the A-axis at 11 kbar (downward pointing triangles).	22

Figure 11: Top – Calculated Ti contents of equilibrium melts vs. %An of the different parts of the Tungnárhraun plagioclase macrocysts. Bottom – Actual Ti [ppm] of various flows from Iceland. THa, THb, Fontur/Saxi/Brandur, and Ljósufjöll fields are groundmass Ti (Halldórssón et al., 2008; Caracciolo et al., 2020), all others are whole rock (Maclennan et al., 2003; Gurenko and Sobolev, 2005; Óladóttir et al., 2011).....	26
Figure 12: Plot of Anorthite content versus minor elements in plagioclase zones from the Tungnárhraun and Bárðardalur lava sequences. The red “A” in the inset represents the azeotrope, or reversal in the An-Ab phase diagram. Data for the Bárðardalur sequence from Svavarssdóttir (2017).....	27
Figure 13: Plot of Mg and Ti concentrations in the Tungnárhraun macrocryst plagioclase. Inset taken from Nielsen et al., (2020).	28
Figure 14: A series of cartoons detailing our proposed magma pathway evolution beneath Bárðarbunga over the Holocene, with shapes to indicate the crystal cargo at each phase of evolution. White = plagioclase, green = olivine, yellow = clinopyroxene, red = orthopyroxene. Insert show a more detailed view at each phase of evolution. We note that the actual crustal structure is likely more complicated (e.g. it’s likely that there are multiple sills between 2 and 6 kbar, evidenced by the Holuhraun III eruption). We simplify the structure for illustrative purposes.....	31

LIST OF TABLES

Table 1: Select data of the eruptive volumes of the volcanic zones of Iceland taken from Thordarson and Höskuldsson (2008).....	37
Table 2: Collected data on the volcanic parts of the Bárðarbunga volcanic system. “?” indicates an uncertain date of formation. Dates are given in CE unless otherwise noted. Information from the Icelandic Larsen (1984), Thordarson et al. (2003), Thordarson and Larsen (2007), Óladóttir et al. (2011), Larsen and Gudmundsson (2014), Svavarssdóttir (2017), Met Office (2020), University of Iceland (2020).....	37
Table 3: Holocene eruptive history of the north and south fissure swarms of Bárðarbunga. Data from: Vilmundardottir (1977), Larsen (1984), Thordarson et al. (2003), Hjartarson (2004, 2011), Thordarson and Larsen (2007), Hartley and Thordarson (2013), Larsen and Gudmundsson (2016), Svavarssdóttir (2017), Pinton et al. (2018). *Age estimate from borehole.	38
Table 4: Summary of plagioclase compositions measured for this study. Raw data can be found in Appendix B. *only one analysis, **Groundmass values are the average of 10 EPMA spot analyses.....	39
Table 5: Summary of the olivine compositions measured for this study. Raw data can be found in Appendices C and E. *only one analysis, n = number of analyses in Groundmass average....	39
Table 6: Summary of pyroxene compositions measured for this study. Raw data can be found in Appendix D. *only one analysis, n = number of analyses in Groundmass average.....	40
Table 7: Averages used in the calculation of plagioclase free liquids. ¹ Includes data from Halldórsson, 2007. ² Includes data from Caracciolo et al., 2020. *Average of measured groundmass of Caracciolo et al., 2020.....	41
Table 8: Thermometry results using a thermometer and thermobarometer presented in Druitt et al. (2012) and Putirka (2008), respectively. *one analysis (average of three EPMA spots). ¹ Includes data from Halldórsson, 2007. ² Includes data from Caracciolo et al., 2020.	42
Table 9: Olivine diffusion modeling results. Raw transect data is given in Appendix E.	42

INTRODUCTION

Fifteen million years of volcanism in Iceland record the interaction between the Mid-Atlantic Ridge and an upwelling mantle plume (Figure 1). The formation of Iceland is predominantly marked by the presence of two distinct rift zones which represent the spreading axis of the Mid-Atlantic Ridge, split into northern and southern segments and separated by a transform boundary. At the onset of Iceland's formation 15 Ma, this spreading axis was expressed as the Skagafjördur paleo-rift to the north, and the Snæfellsnes rift zone to the south. Beginning ~6-7 Ma, these rift segments have seen repeated eastward relocation as the result of the WNW drift of the plate system relative to the Iceland mantle plume (Hardarson et al., 1997). In the north, the shift to its modern-day structure began ~8-8.5 Ma, with the establishment of the present day Northern Volcanic Zone (NVZ). The Skagafjördur paleo-rift continued accretion for another 5-5.5 Myr alongside the NVZ before becoming inactive 2-3 Ma (Garcia et al., 2003). The southern segment jumped from the Snæfellsnes Rift Zone to the modern Western Volcanic Zone (WVZ) ~6-7 Ma. This segment is currently experiencing a relocation from the WVZ to the SSW-propagating Eastern Volcanic Zone (EVZ). GPS and eruptive output data suggest that spreading and volcanism of the WVZ is steadily decreasing and may eventually cease as the EVZ continues its propagation (Sæmundsson, 1978; Óskarsson et al., 1982; LaFemina et al., 2005; Sinton et al., 2005).

The modern relocation of the spreading axis from the WVZ to the EVZ is accompanied by changes in volcanism and seismicity. Volcanism in the EVZ has been volumetrically more significant than that of the WVZ since the last glacial maximum ~12 ka (Table 1). The EVZ has produced more than 163 km³ Dense Rock Equivalent (DRE) of tephra and 174 km³ of lava, or ~60% of Iceland's Holocene volcanic output from >2000 eruptions, while the WVZ has produced 94 km³ of lava (0 km³ Tephra), or ~17% of total eruptive output, from 47 eruptions (Thordarsson and Höskuldsson, 2008). Higher rates of decompression melting from the higher spreading rate of the EVZ combine with its proximity to the Iceland mantle plume contribute to this greater level of volcanic output.

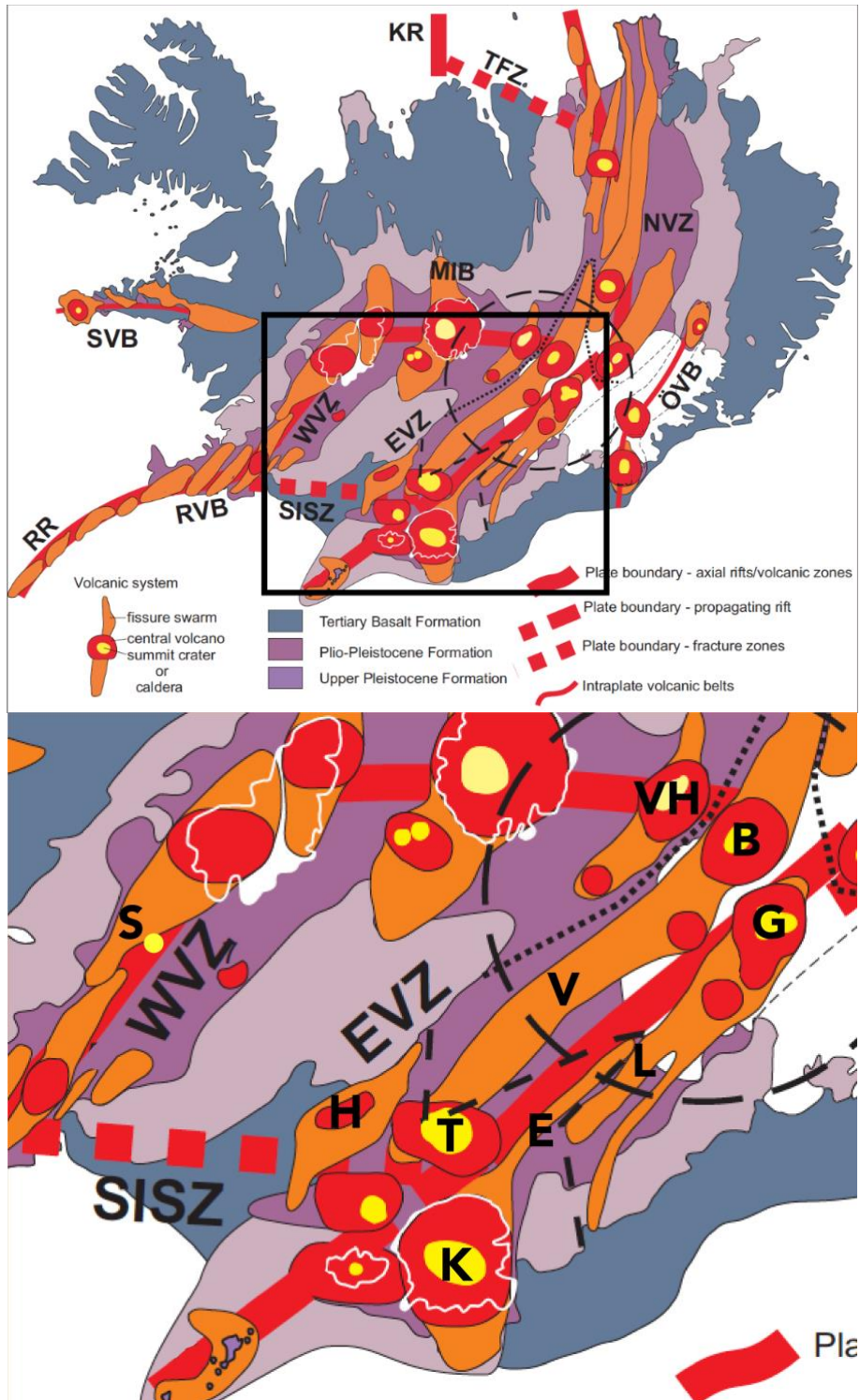


Figure 1: Top – Map of the volcanic setting and systems of Iceland. WVZ = Western Volcanic Zone, EVZ = Eastern Volcanic Zone, NVZ = Northern Volcanic Zone, SISZ = South Iceland Seismic Zone, TFZ = Tjörnes Fracture Zone, RVB = Reykjanes Volcanic Belt, SVB = Snæfellsnes Volcanic Belt, MIB = Mid-Iceland Belt, ÖVB = Öraefajökull Volcanic Belt, RR = Reykjanes Ridge, KR = Kolbeinsey Ridge. Bottom – Detailed view of the volcanic systems of the EVZ. B = Bárðarbunga, V = Veitötn, G = Grimsvötn, L = Laki, K = Katla, E = Eldgjá, T = Torfajökull, VH = Vonarskarð, H = Hekla, S = Skjaldbreiður. The dashed circle indicates the approximate center of the Iceland Mantle Plume as depicted by Wolfe et al. (2017). Modified from Thordarson and Höskuldsson (2008).

LaFemina et al. (2005) determined that accommodation of spreading along the MAR by the EVZ and WVZ is expressed by present day spreading rates of 10.2–21.0 and 1.7–7.4 mm/yr, respectively. The spreading rate increases along the EVZ from south to north, indicative of the southward propagation of the rift tip away from the plume. The South Iceland Seismic Zone, a series of bookshelf faults connecting the WVZ and EVZ, accommodates left-lateral transform motion near the southern end of the rifts (LaFemina et al., 2005). The spreading rates of both volcanic zones combine to account for the total plate rate of 18.5 mm/yr (DeMets et al., 2010). The contribution of the mantle plume to EVZ mafic lavas is also greater than that in the WVZ, as indicated by higher ${}^3\text{He}/{}^4\text{He}$ isotopic values (18-26.2 R/R_A to 12-16 R/R_A) measured in olivine and clinopyroxene phenocrysts from young mafic lavas (Kurz et al., 1985). The significant difference in volcanic output between the two zones is therefore the result of the complex process of rift relocation in Iceland.

The volcanic production of both zones is further increased by decompression melting related to isostatic rebound from the Early Holocene deglaciation, though its effect has waned in historical time. Models by Schmidt et al. (2013) indicate as much as a 135% increase in melt production beneath Iceland ($\sim 0.23 \text{ km}^3/\text{yr}$) from deglaciation-related isostatic rebound. Following extensive decompression melting of the Early Holocene, the rate of output for volcanic fissures and shield volcanoes across the WVZ increased to 30-50 times that of the late-glacial period ($24 \text{ km}^3/1000 \text{ years}$ with 1 eruption every 120 years). These rates have since fallen exponentially to 4 km^3 and an average of 1 eruption every $\sim 1 \text{ kyr}$ for the last 4 kyr (Sinton et al., 2005). Similarly, 70% of the erupted volume in the EVZ was produced in the first 5-6 kyr after deglaciation (Thorsdansson and Larsen, 2007; Thordarson and Höskuldsson, 2008).

Despite the overall reduction in eruptive volume, several of the largest Holocene basaltic fissure eruptions on Earth originated from the three systems of the EVZ: Grímsvötn, Katla, and Bárðarbunga. In historical times (after 871 CE; all historical dates which follow are CE), the 1783 eruption of Laki, a fissure of the Grimsvötn system, has been studied extensively because of its volume ($\sim 15 \text{ km}^3$), environmental impact, extremely high death toll, and availability of detailed historical accounts (Thorarinsson, 1969; Thordarson and Self, 1993, 2003; Thordarson et al., 1996; Witham and Oppenheimer, 2004). The same can be said for the $\sim 20 \text{ km}^3$ eruption of the Eldgjá

fissure from Katla in 934, though to a lesser extent (Jakobsson et al., 1979; Miller et al., 1989; Thordarson et al., 2001). Both events represent the largest Holocene eruptions from their respective volcanic systems. The volume produced by these two tremendous eruptions is smaller than that of the numerous $>1 \text{ km}^3$ eruptions of the first half of the Holocene from these fissure systems.

Each volcanic system of the EVZ has distinct chemical signatures apparent in caldera eruptives as well as fissure flows (Meyer et al., 1985). The large Laki and Eldgjá fissure eruptions are of remarkably homogeneous geochemistry. This homogeneity exists at moderate MgO contents (<7 wt. %), a common indicator of long crustal residence times, which often result in heterogeneous or compositionally zoned lavas through fractionation, magma mixing, and crustal assimilation. The geochemical compositions of Grímsvötn lavas (including Laki) do not overlap the Katla fields (including Eldgjá) in most major elements except for MgO (5.5-6.1 wt.%). Grímsvötn lavas are distinguished by lower TiO₂ and FeOT and higher SiO₂ and Al₂O₃ (Grönvold and Jóhannesson, 1984; Thordarsson et al., 1996; Passmore et al., 2012). Published samples from the Bárðarbunga system are geochemically comparable to Grímsvötn lavas, but are more primitive (6-10 wt.% MgO) and have lower TiO₂ and FeOT than Katla (Eldgjá) lavas.

Basaltic lavas in Iceland have distinct major element characteristics that differ between volcanic zones (Meyer et al., 1985; Sinton et al., 2005) as well as between volcanic systems (Figures 7 and 8; Jakobsson, 1979). The lavas of the WVZ are typically more primitive and have a wider range of MgO contents (6-14 wt.%) than their EVZ counterparts. Two large volume eruptions, Skjaldbreiður from the WVZ (9.5 ka, 13.5 km³; Figure 1) and Laki from the EVZ (1783, 14.7 km³), represent the chemical differences between their respective volcanic zones. Skjaldbreiður, with lavas ranging from 5.5-10 wt.% MgO, and Laki (5.4-6.0 wt.% MgO), are distinct in their mean MgO as well as in their relative within-flow geochemical homogeneity. The primitive contents and relative heterogeneity of the Skjaldbreiður is attributed to the injection and eruption of repeated small batches of magma with low residence times. The Skjaldbreiður shield volcano morphology results from the lack of heat available to sustain a long lived or large magma chamber compared to the EVZ, which gets abundant heat from its proximity to the plume (Meyer et al., 1985; Hansen and Grönvold, 2000; Sinton et al., 2005; Eason and Sinton, 2009).

This thesis explores the genesis and evolution of the Tungnárhraun, a series of large volume lava flows following the Tungná river from central Iceland to its southern coast. This lava sequence has been largely unstudied, apart from the detailed field characterization and mapping campaign of Vilmundardóttir (1977). This work proposed that the origin of the Tungnárhraun lies in the southern fissure of the Bárðarbunga volcanic system, the largest and most active volcanic system in Iceland over the Holocene. Another series of large volume lavas erupted to the north of the central vent, referred to as the Bárðardalur Valley lavas, were recently linked to Bárðarbunga (Svavarsdóttir et al., 2017). In this work we seek to define the volcanic system from which the Tungnárhraun were derived, to understand the nature and origin of the highly plagioclase porphyritic basalts within this sequence, and to describe the crustal structure of the Bárðarbunga magma plumbing system.

GEOLOGICAL BACKGROUND

Geologic setting of Bárðarbunga

The Bárðarbunga volcanic system defines the western edge of the EVZ (Figure 1) and has been the most active volcanic system in Iceland since the last glacial maximum (Svavarsdóttir et al., 2017). Bárðarbunga is one of several en-echelon and parallel fissure systems of the EVZ, each characterized by a topographically high volcanic center (Jakobsson, 1979). The Bárðarbunga central caldera is the topographic high of the Bárðarbunga system and forms the boundary between the EVZ and NVZ, northwest of the Grímsvötn caldera and east of the Vonarskarð system (Figure 1). The caldera and the majority of the associated fissures are located over the Iceland mantle plume (Figure 1; Wolfe et al., 1997), which has resulted in anomalously thick crust beneath the volcano (~40 km; Gudmundsson, 2003). Basaltic products of the Bárðarbunga system are found in fissure swarms and lava flows that extend both to the north and to the southwest of the caldera, into the NVZ and EVZ. This system is estimated to have erupted nearly 70 km^3 of volcanic material since the beginning of the Holocene and has averaged one eruption every 50 years for the last 1.1 kyr (Thordarson et al., 2003; Larsen and Gudmundsson, 2014).

The Bárðarbunga system consists of the Bárðarbunga central vent, an 80 km^2 caldera buried beneath the Vatnajökull glacier, and two fissure swarms which emanate from the edge of

Vatnajökull in N and SSE orientations from the caldera (Figure 2). Each fissure swarm comprises at least two separate, parallel parts: the Dynguháls region and Holuhraun volcanic field to the north, and the Veiðivötn, Vatnaöldur, and Tröllagígar fissures to the south. The extents of the northern and southern fissure swarms are bounded by the southern edge of the Dyngjufjöll mountains surrounding the Askja caldera, and the northern edge of the Torfajökull silicic complex, respectively (Figure 2). Field and geochemical data from the distal portions of each of the Bárðarbunga fissures reveal mixing of magmas with products of the Askja and Torfajökull volcanoes (Sigurdsson and Sparks, 1981; Blake, 1984). In addition, evidence exists for contemporaneous eruptions of these central volcanic systems with nearby basaltic fissures (Macdonald et al., 1990; McGarvie et al., 1990; Sigmarsdóttir and Halldórsson, 2015).

The northern extent of Bárðarbunga has been active over the entire Holocene, garnering significant attention following the 2014-15 Holuhraun eruption. The Dynguháls region is a broad name for the area directly to the north of the Bárðarbunga caldera and contains the Dynguháls fissure swarm, Urðarháls and Hrímalda volcanic fields, Kistufell table mountain, and Gígöldur crater row (Figure 2; Svavarsdóttir, 2017). The relative ages of each part of the Dynguháls region have been determined via field relations as pre-Holocene (>12 ka) for Urðarháls, ~10 ka for Kistufell, Hrímalda, and Gígöldur, and <4.5 ka for Dynguháls (Sigbjararsson, 1988; Hansen and Grönvold, 2000; Sigurgeirsson, 2015). The Holuhraun volcanic field was erupted from fissures ranging from adjacent to Dyngjújökull to ~6 km north of the glacier (Pedersen et al., 2017). The fissures represent the easternmost part of the system and have been chemically and tectonically linked to Bárðarbunga (Sigmundsson et al., 2015; Pederson et al., 2017; Halldorsson et al., 2018).

To the south, the parallel fissure swarms Veiðivötn and Vatnaöldur are 2 km apart with Veiðivötn located to the east (Figure 2; Zellmer et al., 2008). Grabens of Veiðivötn and Vatnaöldur reach up to 70 km long and 10 km wide and can contain several craters (Jóhannesson and Saemundsson, 1998). The largest of the grabens, Heljargjá, contains the nearly buried craters Fontur and Saxi, the oldest exposed Holocene craters of the Bárðarbunga system (Hjartarsson, 1988; Hansen and Grönvold, 2000; Gudmundsson and Högnadóttir, 2002; Halldórsson, 2007). A third fissure, Tröllagígar, formed in the southern fissure swarm in 1862-64. Tröllagígar is significantly shorter

than the other two crater rows of the southern fissure swarm and lies close to Vatnajökull glacier, running parallel a few kilometers to the east of Veiðivötn (Figure 2; Table 2).

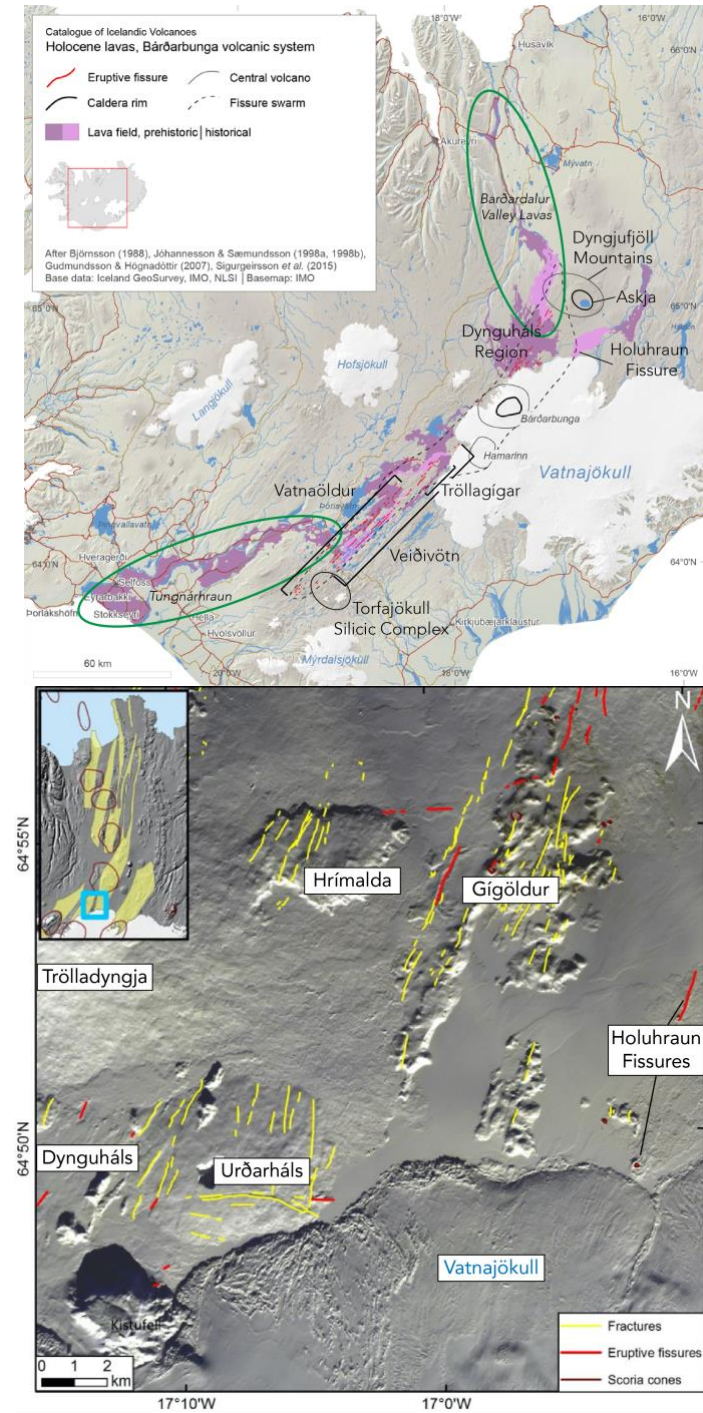


Figure 2: Top – Map of the extent and Holocene lavas of the Bárðarbunga system. Notable parts of the system are labelled. After Björnsson (1988), Jóhannesson and Sæmundsson (1998a, 1998b), Gudmundsson and Högnadóttir (2007), Sigurgeirsson et al. (2015). Base data: Iceland GeoSurvey, IMO, NLSI. Basemap: IMO. Bottom – Detailed map of the northern Bárðarbunga Fissure Swarm. From Svavarssdóttir (2017).

Eruptive history of the Bárðarbunga fissure swarms

The size and remote location of the Bárðarbunga system, combined with the thick sheet of ice over the caldera which partially obscures its relationship to other active systems, make it difficult to reconstruct its Holocene eruption history. Several large-volume, early to mid-Holocene flows were only recently attributed to the Bárðarbunga northern fissure swarm (Svavarsdóttir et al., 2017). The earliest known flows attributed to the Bárðarbunga system are Kistufell, Gígöldur, and Hrímalda at ~10 ka (Hansen and Grönvold, 2000; Breddam, 2002; Peate et al., 2010; Svavarsdóttir, 2017). The crater row of Gígöldur is a massive volcanic unit of interfingering hyaloclastites and tens of post-glacial craters which show signs of explosive volcanic activity beneath a thin sheet of ice, after the onset of deglaciation, but before the area was completely ice-free (Hansen and Grönvold, 2000; Svavarsdóttir, 2017). Hrímalda is a low, elongated table mountain striking SW-NE and situated to the west of Gígöldur. The tuya structure suggests formation towards the end of the Holocene (Sigbjarnarson, 1988; Hjartardóttir et al., 2016; Hansen and Grönvold, 2000). Associated with Hrímalda is a fissure with a rare E-W orientation, running between Hrímalda and Gígöldur, thought to be the source of the Hrímalda lavas 4.0-6.1 ka (Sigurgeirsson et al., 2015). The most prominent lava field in the northern fissure swarm is that of the Bárðardalur valley lavas. This lava field contains five distinct units: Kinnarhraun (9.5 ka), Útbruni (9.3 ka), Bárðardalshraun (>8.0 ka), Kvíahraun (4.0 ka), and Frambruni (~1362). Geography, chemistry, and mineralogy connect the Kvíahraun and Frambruni lavas to Dynguháls and the Kinnarhraun, Útbruni, and Bárðardalshraun lavas to Gígöldur (Svavarsdóttir, 2017). The only known eruptions of the Holuhraun fissure, the second part of the northern fissure swarm, are of historical age: Holuhraun I (1797), II (1867), and Holuhraun 2014-15. These three lavas have been chemically linked to the Bárðarbunga system (Hartley and Thordarson, 2013; Sigmundsson et al., 2015; Pedersen et al., 2017; Halldórsson et al., 2018), and abundant seismic activity revealed a clear pathway from beneath the caldera to the eruption site to the northeast (Sigmundsson et al., 2015; Hjartardóttir et al., 2016; Ágústdóttir et al., 2016).

The eruptive history of the southern fissure swarm is better documented than that of the northern fissure swarm. Holocene volcanism on Vatnöldur and Veiðivötn occurred both before (prehistoric) and after (historic) and the settlement of Iceland in 871. Three large volume eruptions

define the historic stage, each producing just over 1 km³ of volcanic material: Tröllahraun (1862–64), Veiðivötn 1477, and Vatnaöldur 871 (Thordarson and Larsen, 2007). Lavas produced from Veiðivötn or Vatnaöldur between the begining of the Holocene and 871 are collectively referred to as the Tungnárhraun. The number of prehistoric lavas falls between the 11 flows defined by Vilmundardóttir (1977) and as many as 17 flows identified in subsequent works on the Tungnárhraun (Thordarson et al., 2003; Pinton et al., 2018; Carraciolo et al., 2020). The source of the Tungnárhraun has not been clearly identified, though Halldórsson et al. (2008) found that the ⁸⁷Sr/⁸⁶Sr ratios of the Thjórsahraun (THa and THb) fall within the isotopic range of Bárðarbunga lavas. The ages range from 8.6 ka – 150 CE and volumes from 0.1–25 km³ as summarized in Table 3. We adopt the naming convention of Vilmundardóttir (1977) and include flow names as follows (alternative names from published literature listed in parentheses): THa/THb (Thjórsahraun), Raudhóll-Flögd, Háganga, Háahraun, Botnarhraun, THc (Thriðja Elsta Tungnárhraun), THd (Fjörda Elsta Tungnárhraun), THe (Fimmta Elsta Tungnárhraun), THf (Kvíslahraun, Sigölduhraun, Kalfahraun), Brydjahraun, THg (Hnubbahraun), THh (Thórsadálshraun), THi (Búrfellshraun), Drekahraun, THj (Tjörvahraun, THk (Hnausahraun). The total volume of the Tungnárhraun is estimated ~45 km³, or over half of the Holocene lava produced by the Bárðarbunga system. The largest and most studied are THa/THb (Thjórsahraun), which are widely considered together as the largest Holocene fissure eruption on earth at 25 km³ (Vilmundardóttir, 1977; Hjartarsson, 2011; Halldorsson et al., 2008).

Plagioclase Ultraphyric Basalts (PUBs) of Iceland

Plagioclase Ultraphyric Basalts (PUBs) are found throughout the lava pile of Iceland (Walker, 1963; Kristmannsdóttir, 1971; Gautason, 1988; Hansteen, 1993). PUBs are defined by plagioclase contents greater than that expected from cotectic relationships in MORB (>15% plag, <2% olivine). For Icelandic PUBs, plagioclase crystals are typically >500 µm and can reach up to several centimeters (Hansen and Grönvold, 2000). The large plagioclase, which are commonly referred to as macrocrysts, are An_{>85}, compositions which are too primitive to have formed from the host lava (Cullen et al., 1989; Hansen and Grönvold, 2000; Halldórsson et al., 2008). Several models have been suggested to explain the entrainment and transport of Icelandic PUBs. The most frequent interpretation, the floatation model, is that the large plagioclase are entrained from a

magma mush at mid- to deep-crustal levels beneath the volcanic systems (Hansen and Grönvold, 2000; Halldórsson et al., 2008; Neave et al., 2013). There is still some question of the extent of the crustal mush. A study of the Tertiary Grænavatn Group in eastern Iceland suggests either an isolated mush around a pipe-like conduit, or an elongated mush that runs beneath most or all of the volcanic lineament (Óskarsson et al., 2017). Experimental constraints suggest that the depth of formation and entrainment of the plagioclase macrocrysts is ≥ 6 kbar, as this is the minimum pressure where An₉₀ plagioclase is buoyant in tholeiitic magma (Kushiro and Fujii, 1977), and ≤ 11 kbar, which is roughly the crust-mantle boundary beneath the EVZ, due to the absence of orthopyroxene, which would be indicative of crystallization at deeper levels (Hansen and Grönvold, 2000). Ustunisik et al. (2020) suggest the presence of a reversal in the slope of the solidus in the Ab-An phase diagram at An_{>80} and pressures greater than 5 kbar. As a result, a basaltic liquid at ≥ 5 kbar may crystallize plagioclase feldspar with progressively higher An content as it evolves and the Mg# decreases. This supports our interpretation that the plagioclase macrocrysts in Icelandic PUBs may form in magma chambers in the lower half of the crust, though it may suggest a more complicated crustal structure for Bárðarbunga than illustrated below.

While the floatation model may be applicable to Iceland, others argue against it as a general model for PUB formation, invoking the presence of PUBs at spreading ridges without the magma chambers which accommodate a crystalline mush in the floatation model. Pressure constraints of the floatation model are higher than those experienced within the oceanic crust (Lange et al., 2013), making entrainment from crystal mushes within the crust. It is clear that magmas entraining macrocrysts of anorthitic plagioclase only need to have an upward velocity greater than or equal to the settling velocity of the plagioclase in order to counter their negative buoyancy in basalt (0.5–1 cm/s) in order to carry them to the surface (Lange et al., 2013; Neave et al., 2014; Nielsen et al., 2020). This model is bolstered by evidence from MORB plagioclase-hosted melt inclusions which indicate pressure of entrapment to be 4–6 kbar, i.e., depths greater than the normal thickness of oceanic crust (Helo et al., 2011; Drignon et al., 2019). These depths are consistent with the crystallization of high-An plagioclase in the upper mantle from a melt influenced by interaction with a depleted harzburgite (Nielsen et al., 2000; Kohut and Nielsen, 2003). While this model may be generally applicable to MOR, we consider it in combination with the floatation model given the anomalously thick crust of Iceland.

METHODS

Samples and Analytical Techniques

Samples with minimal visual weathering were collected from outcrops of seven of the Tungnárhraun lava flows in 2019 (Figure 3). Outcrops were located using Orkustofnun surface deposit maps that were georeferenced in ArcGIS using Sentinel 2 imagery and imported into the Avenza mapping app for iPhone (Vilmundardóttir, 1977; Kaldal and Vilmundardóttir, 1986; Kaldal et al., 1988). Samples were prepared for whole rock analysis by cutting >5 cm slabs with a ceramic tile saw. After polishing to remove saw marks, the slabs were reduced to ~5 mm pieces using an alumina ceramic jaw crusher and powdered in tungsten carbide disc mill for up to 2 minutes. Thin sections of nine samples were prepared by Spectrum Petrographic for microprobe work. Full thin section scans obtained with a Zeiss AxioScan.Z1 are provided in Figure 4.

Whole rock analyses for major elements were performed at the Pennsylvania State University Energy and Environmental Sustainability Labs on a Thermo iCAP 7400 Inductively Coupled Plasma Emission Spectrometer. Prior to major element analyses, powdered samples were prepared via lithium metaborate fusion (Ingamells, 1970). A total of 100 mg of powdered samples was mixed with 400 mg of lithium metaborate powder and transferred to graphite crucibles. The mixtures were heated to 900°C for 10 minutes and the melt beads were added to 100 ml of 5% HNO₃ solution in Teflon beakers for 20 minutes. Samples were further diluted by combining a 2.5 mL aliquot of sample with 10 mL each of 2% HNO₃ and Lutetium internal standard solutions. Samples were run with standards BHVO-1, BCR-1, and BIR-1 and the instrument was calibrated with 21 natural and synthetic standards.

Mineral compositions were collected using a Cameca SX Five Electron Probe Micro Analyzer (EPMA) at the Penn State Materials Characterization Laboratory. Analyses were performed with an accelerating voltage of 15 kV and a probe current of 30 nA. The instrument was standardized for Na/Al/Si/Ca on plagioclase, Mg/Cr on pyrope, K on orthoclase, Ti on SPHN, and Mn/F on almandine. Point analyses were calculated by taking the average of three points from each area of

interest. Groundmass compositions were determined by averaging 10 spot analyses of a given groundmass phase unless otherwise stated. Transect resolution was fixed at 5 μm spacing between points for the first 150 μm and then between 10-30 μm for the remainder of the desired transect. Representative transects and backscattered electron images of the corresponding crystals are given in Figure 5; all whole rock and mineral data are available in appendices A and B-E, respectively.

Numerical techniques

Plagioclase crystallization temperatures were determined using the plagioclase thermometer of Druitt et al. (2012), which assumes An₄₀ and An₈₀ crystallization at 855 and 1255°C, respectively. The liquid thermobarometric Equation 16 of Putirka (2008), derived from Yang et al. (1996), was used to calculate crystallization temperatures for groundmass compositions in equilibrium with magmas that had not accumulated the observed plagioclase feldspar macrocysts. These compositions were obtained for the Tungnárhraun samples by subtracting 20% of the average plagioclase composition for each flow from the average whole rock composition using Rock Maker (Table 7; Büttner, 2012).

Mg-Fe diffusion modeling of diffusion in olivine crystals was performed using a modified version of the finite difference method presented in Costa (2008). The original Mathematica code was rewritten in R and tested with the data of Costa and Dungan (2005) to ensure that the new code produced the same results. The code was then applied to transects of olivine macrocysts from flows THb, THd, THe, THf, THi, and THj. The model was run twice on each transect, varying the pressure and axis of diffusion from 2 kbar on the c-axis to 11 kbar on the a-axis to constrain the minimum and maximum timescales of diffusion in the absence of crystallographic information.

Modeling Constraints

Several constraints on the diffusion modeling were set according to the literature review presented above and with calculations performed on whole rock compositions. In the code rewritten from

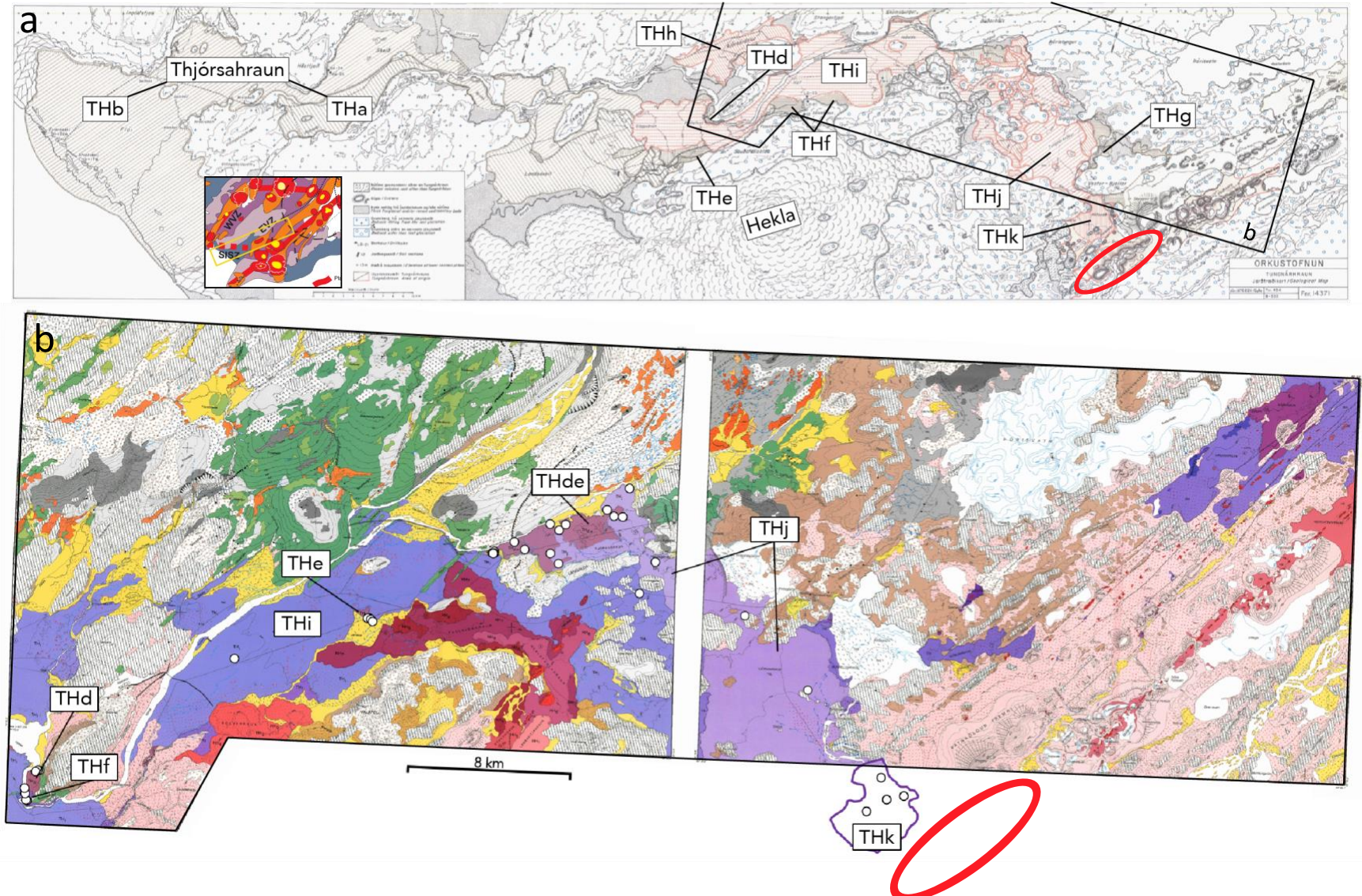


Figure 3: a) Map of the Tungnárhraun lava flows, modified from Vilmundardóttir (1977). The red oval is the suggested area of origin for the Tungnárhraun. b) Map of sample locations for this study, modified from Kaldal and Vilmundardóttir (1986) and Kaldal et al. (1988).

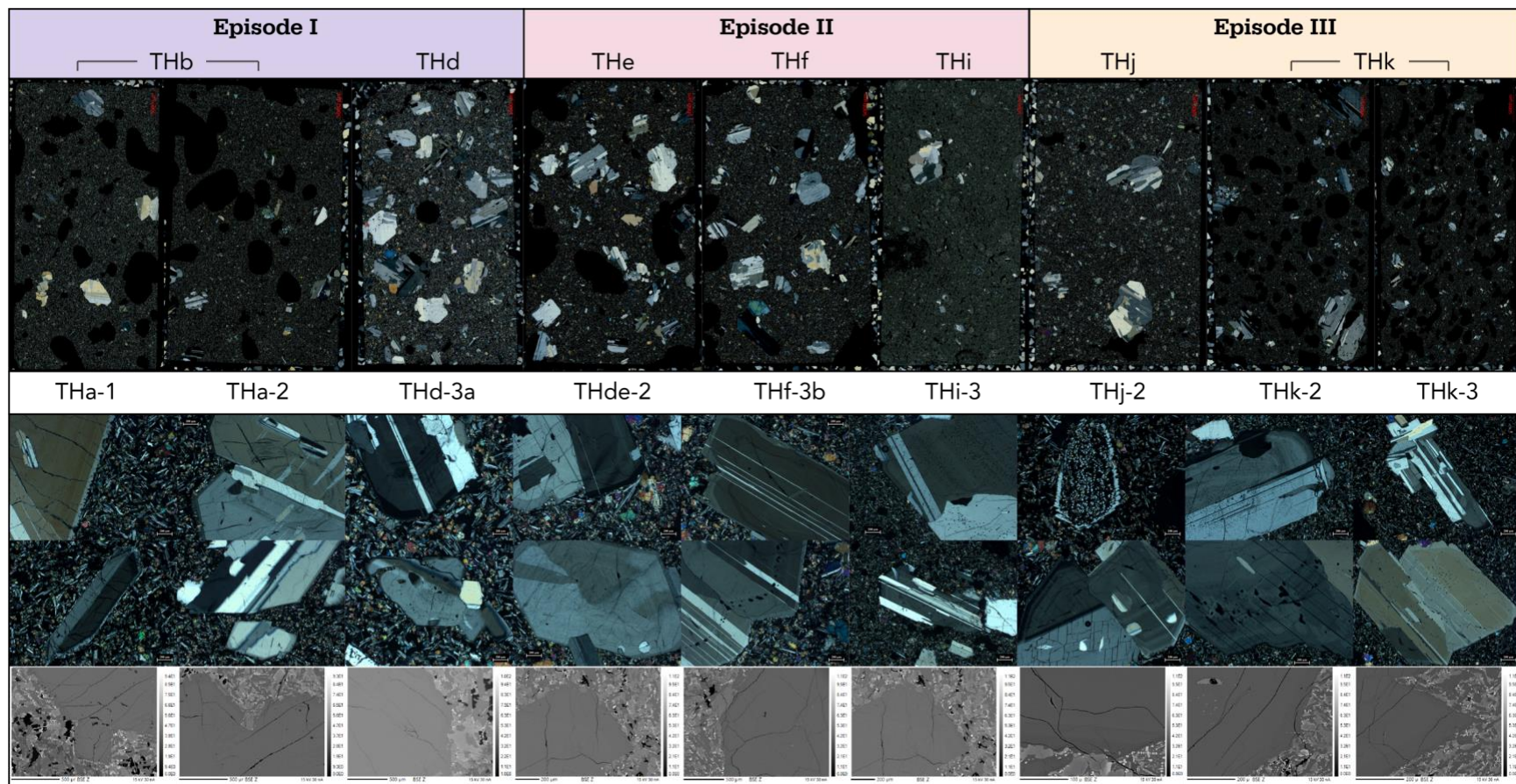


Figure 4: Top – Images of the thin sections analyzed for this study. Bottom – Select cross polarized images of plagioclase from each thin section as well as BSE images displaying representative plagioclase zoning patterns of macrocryst plagioclase.

Costa (2008; Appendix F) the constraints to be set are temperature (Temp), pressure (PRES), oxygen fugacity (fO₂), boundary conditions (rim = minFo, core = Foini), crystal orientation (ax, bx, cx), time step in seconds (dt), grid spacing (dx), and the maximum number of days for the code to run (MaxDays). In the absence of crystallographic information, we constrain the timescales of diffusion by calculating the longest and shortest possible times, corresponding to diffusion along the a-axis at the highest possible pressure and the c-axis at the lowest possible pressure, respectively. The code uses these parameters along with a calculated diffusion coefficient to step through diffusion at the selected time interval, checking the normalized root mean square error (NMRSE) at each step. The program ends when the NMRSE, after decreasing initially, increases, indicating that it has reached the optimal fit of the model to the profile.

As detailed above, pressures are constrained to 2 kbar and 11 kbar. Temperatures of diffusion were taken from estimates of the liquidus temperature derived from the whole rock data calculated using a linear equation which assumes a temperature of 1250°C for magma with 48% SiO₂ and 700°C for magmas with 78% SiO₂. The average of these temperatures from each flow were used for diffusion modeling on the corresponding olivines. Oxygen fugacity was calculated using an equation included in the original code of Costa (2008). This equation, as well as the others referred to in this section, can be found in Appendix G. The initial composition of the profile before diffusion is assumed to be the core composition which persists in most profiles for several hundred μm into the crystal. We calculate this as an average of the points prior to the inflection point, or onset of diffusion. The boundary condition is assumed to be the lowest forsterite (Fo) and outermost point along the profile, as these compositions match groundmass olivine compositions from the respective host lavas in all profiles. We chose a time step of 60 seconds and a grid spacing of 5 μm to satisfy the stability criterion for the finite difference method ($dt/dx^2*D < 0.5$), where D is the diffusion coefficient (formula given in Appendix G). Olivine diffusion modeling can reveal timescales with precision down to hours and up to tens of years (Costa and Dungan, 2005; Costa, 2008). We combine these characteristics with the relative sharpness of profiles to somewhat arbitrarily set the maximum number of days at a value high enough to contain the timescales of all profile collected, 3600 or ~10 years.

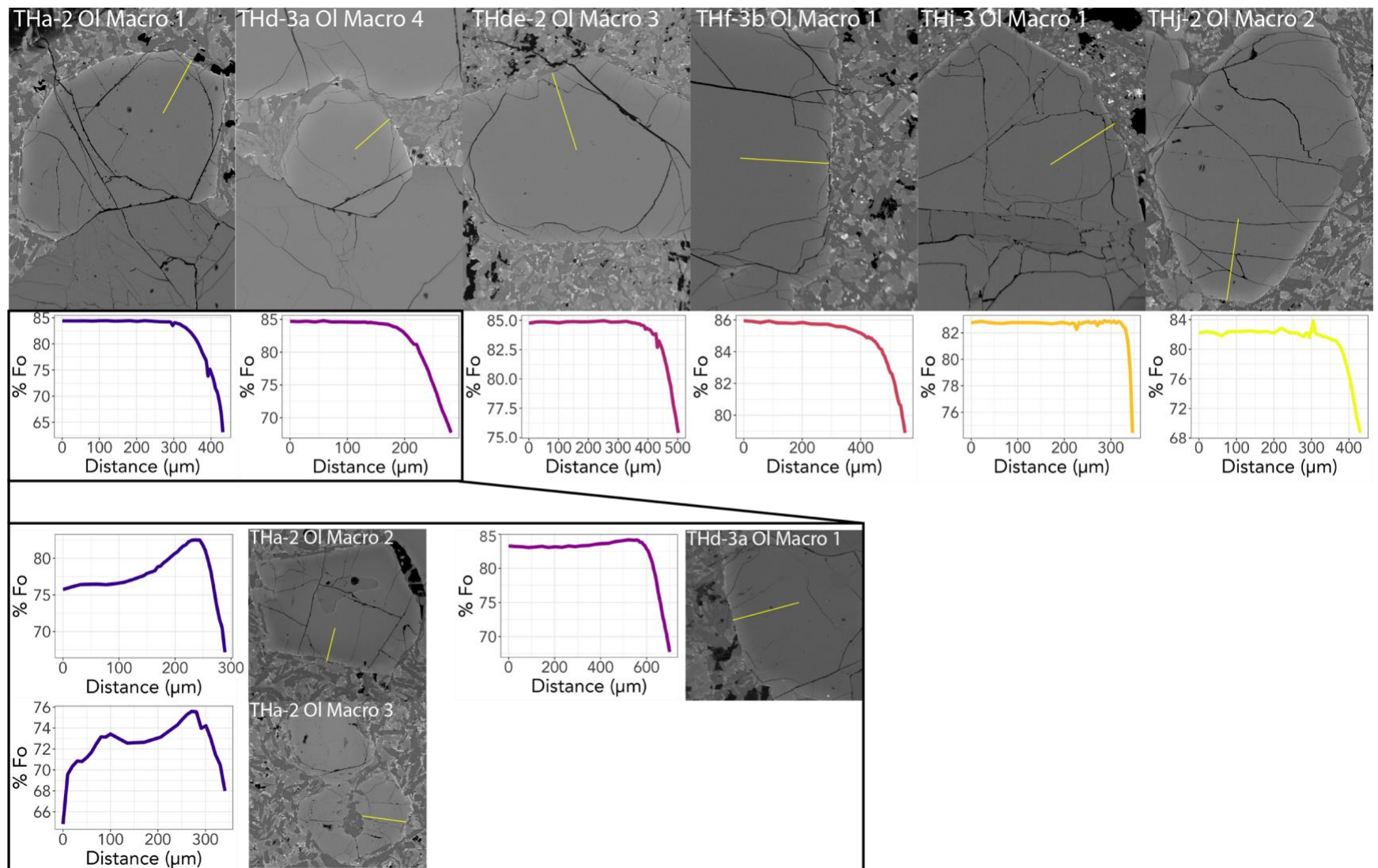


Figure 5: BSE images and diffusion profiles from representative olivine. Yellow lines indicate where the profiles were taken. Profiles from THb and THd with multiple diffuse zones are included for their unique shape but were not modeled.

RESULTS

Petrography and Mineral Chemistry

The Tungnárhraun lavas are characterized by porphyritic textures with 2-20 vol.% plagioclase feldspar macrocrysts (>1 mm; measured by ImageJ) (Table 4). Macrocrysts range from euhedral to subhedral and have normal zoning from An₈₅₋₉₁ cores to rims of lower An content (An₅₈₋₈₆) that varies widely between flows (Table 4, Figure 6). The normally zoned rims of the plagioclase macrocrysts are intergrown with the groundmass in all samples, although their compositions vary between samples. Microcrysts with composition An₅₅₋₉₀ are present in all flows and groundmass plagioclase laths are An₅₈₋₇₆ (Table 4).

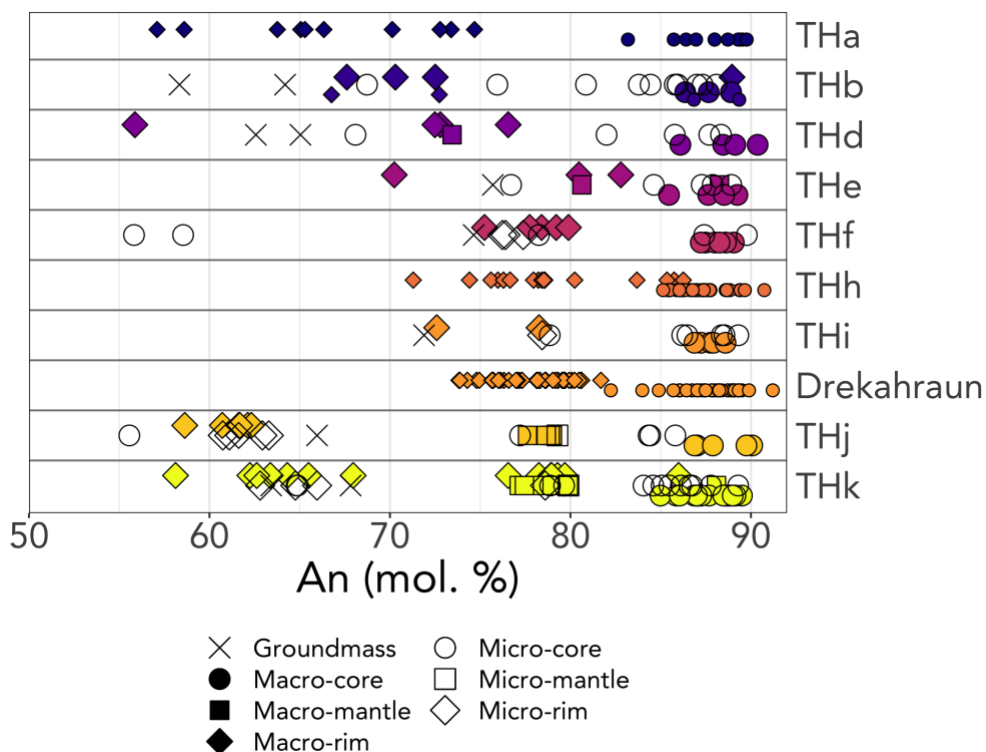


Figure 6: Plot of plagioclase macrocryst compositions in each Tungnárhraun flow. Small symbols indicate previously published data. THa and THb: Halldorsson, 2007; THh and Drekahraun: Caracciolo et al., 2020.

Flows of the Tungnárhraun contain up to ~1% olivine macrocrysts which are euhedral to subhedral and are typically found in close proximity to plagioclase macrocrysts. Olivine macrocryst cores range from Fo₈₂₋₈₇ surrounded by narrow rims of Fo₇₅₋₈₀. Olivine microcrysts are present in all samples and have compositions of Fo₆₉₋₈₄; groundmass olivine is Fo₆₅₋₇₆. CaO contents of olivine vary slightly between macrocrysts (0.35–0.41 wt.%), microcrysts (0.32–0.42 wt.%) and groundmass (0.36–0.83 wt.%) (Table 5). Groundmass olivine is mostly interstitial with occasional subhedral crystals.

Clinopyroxene macrocrysts are rare (<0.1 %) and are compositionally En₃₃₋₄₉Fs₉₋₂₇Wo₃₁₋₄₃, with 0.63–0.69 wt.% TiO₂, and 1.35–4.72 wt.% Al₂O₃. Microcrysts of pyroxene are present in all flows and most crystals have distinct rims. Microcryst cores have the compositional range En₂₈₋₅₂Fs₈₋₃₁Wo₃₈₋₄₅, 0.22–1.00 wt.% TiO₂, and 0.70–4.54 wt.% Al₂O₃ (Table 6). Groundmass pyroxene is mostly interstitial between the plagioclase laths and olivine groundmass and has a composition of En₄₄₋₄₉Fs₁₀₋₂₅Wo₃₁₋₄₁, 0.60–1.22 wt.% TiO₂, and 1.97–3.21 wt.% Al₂O₃.

Large (>1 mm) glomerocrysts are also found in all flows, consisting primarily of euhedral plagioclase microcrysts (0.1–1 mm) with occasional euhedral to anhedral olivine and clinopyroxene microcrysts. The glomerocrysts share similar internal textures and compositions with the macrocrysts.

Major Element Geochemistry

The Tungnárhraun lavas are classified on the basis of total alkali and silica contents as tholeiitic basalts (Table 7, Figure 7). The lavas define two distinct ranges of MgO content: flows THa, THb, THd, THj, and THk have lower MgO (5.6 – 6.9 wt.%) than THe, THf, and THi (7.5–7.9 wt.% MgO; Figure 8). The calculated megacryst-absent liquid compositions are classified as tholeiitic basalt and basaltic andesite with 49.7–52.4 wt. % SiO₂ and 1.8–4.0 wt. % Na₂O + K₂O (Table 7, Figure 7). MgO contents of these calculated liquids are between 6.9 and 9.1 wt. %.

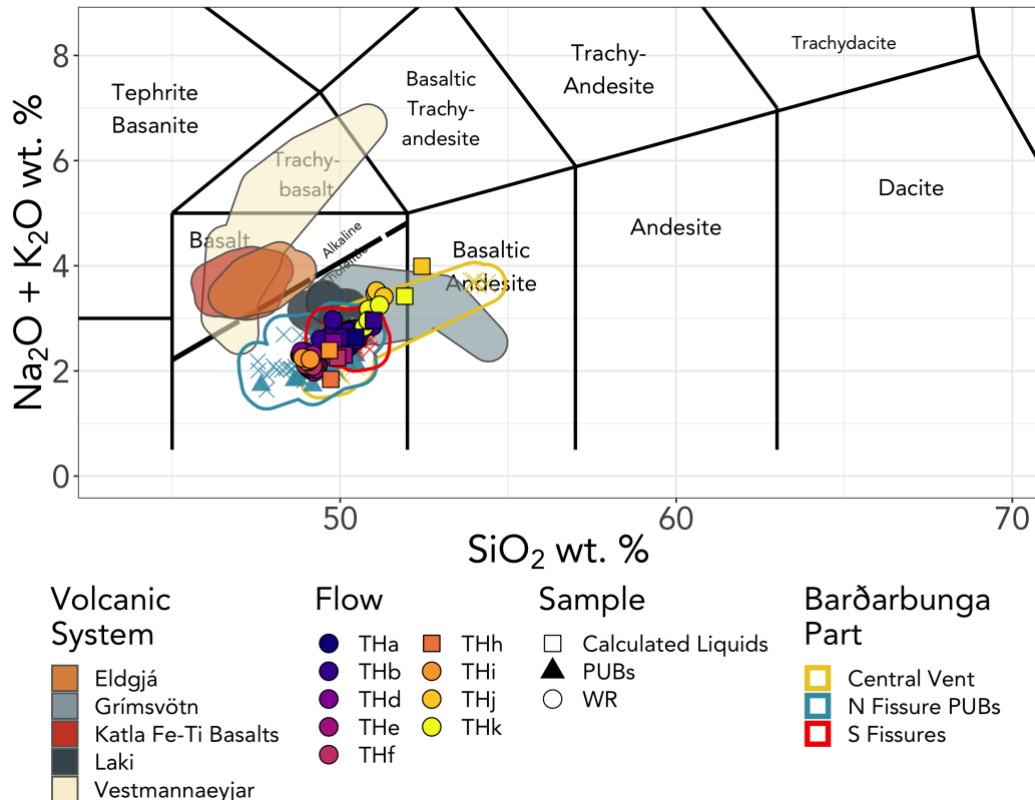
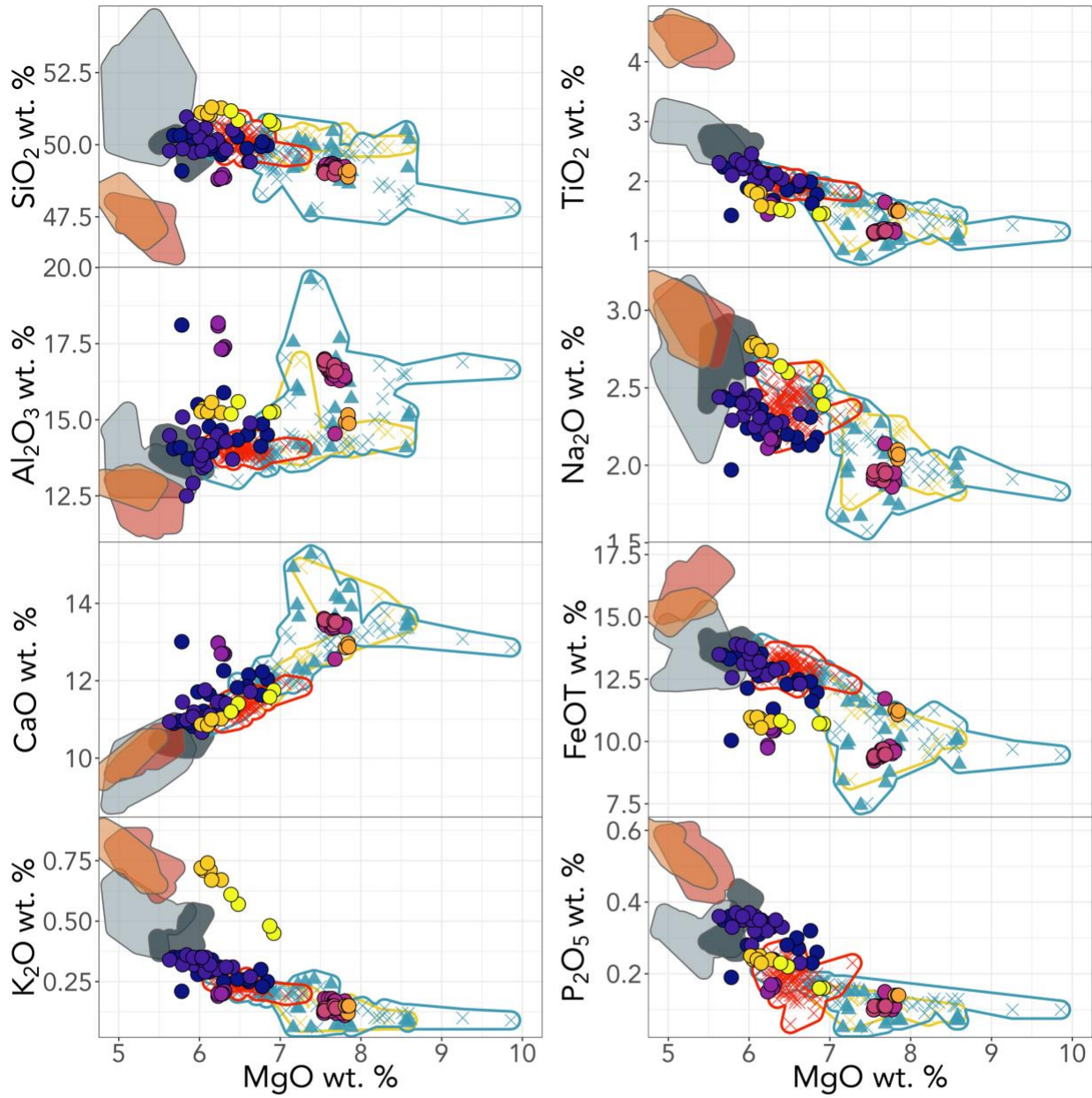


Figure 7: Whole rock compositions of the Tungnárhraun plotted on the classification scheme of Le Bas, 1986. Squares denote calculated liquid compositions and the fields represent the compositions of various volcanic systems.

Geothermobarometry

Crystallization temperatures for the plagioclase macrocrysts were calculated following Druitt et al. (2012). The results (Figure 9; Table 8) indicate growth at higher temperatures for the crystal cores than the surrounding mantles and rims. Plagioclase macrocryst cores yield remarkably consistent temperatures between 1277–1367°C throughout the Tungnárhraun. Plagioclase feldspar macrocrysts of the low-MgO samples yield temperatures from 1014 – 1220°C (THa, THb, and THd) and 1036 – 1315°C (THj and THk). In contrast, plagioclase feldspars in the high-MgO group (THe, THf, and THi) and THh yield generally hotter temperatures between 1157 – 1318°C.



Volcanic System	Flow	Sample	Barðarbunga Part
Eldgjá	THa	○ New WR	Yellow square
Grímsvötn	THb	×	Blue square
Katla Fe-Ti Basalts	THd	○	Cyan square
Laki	THe	○	Red square
	THf	○	Black square
	THi	○	Orange square
	THj	○	Yellow circle
	THk	○	Yellow triangle
		×	Black cross
		▲	Black triangle
			Black square with diagonal line

Figure 8: Variation diagrams of major element oxides for the Tungnárhraun samples. Dataset includes WR data from THa and THb from Halldórsson, 2007. Values for Bárðarbunga's South fissure are point analyses of tephra from the Veiðivötn 1477 and Vatnaöldur 871 eruptions (Óladottir et al., 2011).

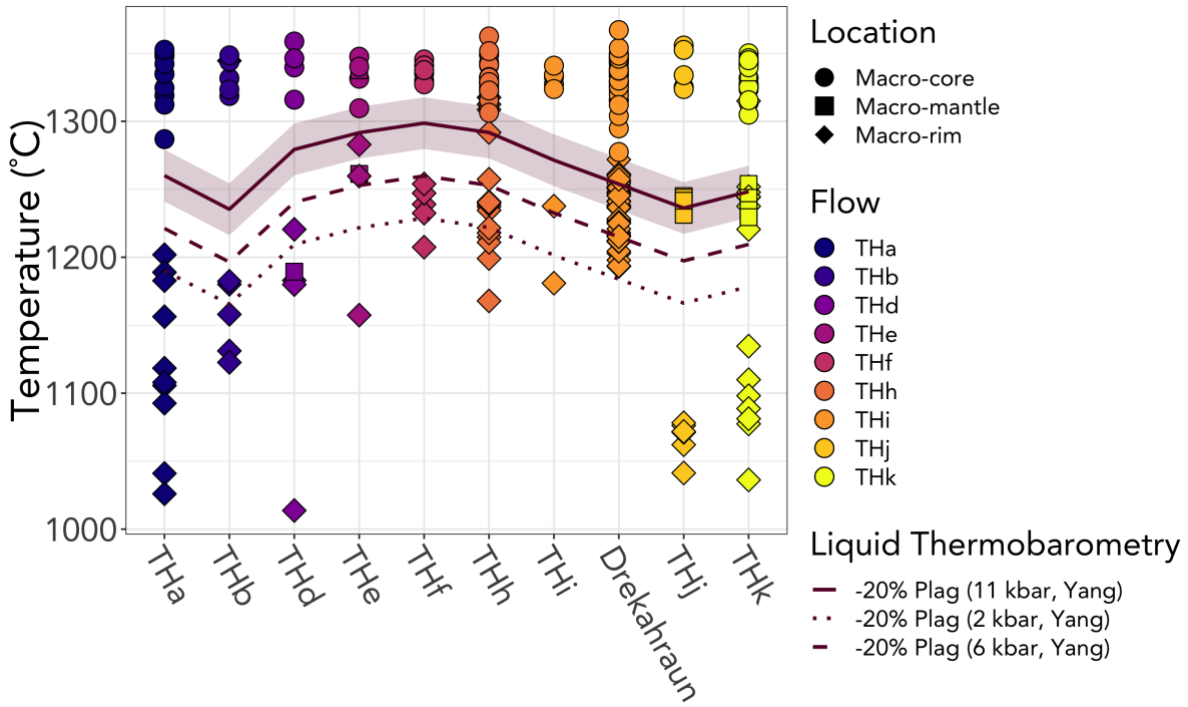


Figure 9: Calculated temperature of crystallization from distinct plagioclase macrocryst parts. Dashed lines are calculated temperatures using the liquid thermometer of Yang et al., 1996; liquid composition was determined for these porphyritic samples by subtracting 20% plagioclase from whole rock averages of each flow.

Calculations using the liquid thermobarometer of Yang et al. (1996) on the megacryst-absent calculated liquid compositions (Table 7) at 2, 6, and 11 kbar produce temperatures of 1165 – 1225°C, 1196 – 1260°C, and 1235 – 1299°C, respectively. Plagioclase and liquid thermometry calculations are summarized in Table 6 and are compared to the results of the plagioclase thermometry in Figure 9.

Diffusion modeling

Mg-Fe interdiffusion modeling (following Costa, 2008) on olivine macrocrysts from each flow indicates timescales of diffusion between 2 and 2512 days (6.9 years). Models run at 2 kbar on the c-axis produce timescales of less than a year between entrainment and eruption (2–277 days). Models calculated at 11 kbar along the a-axis have a much wider range of timescales from 16 to 2512 days (Figure 10 and Table 9).

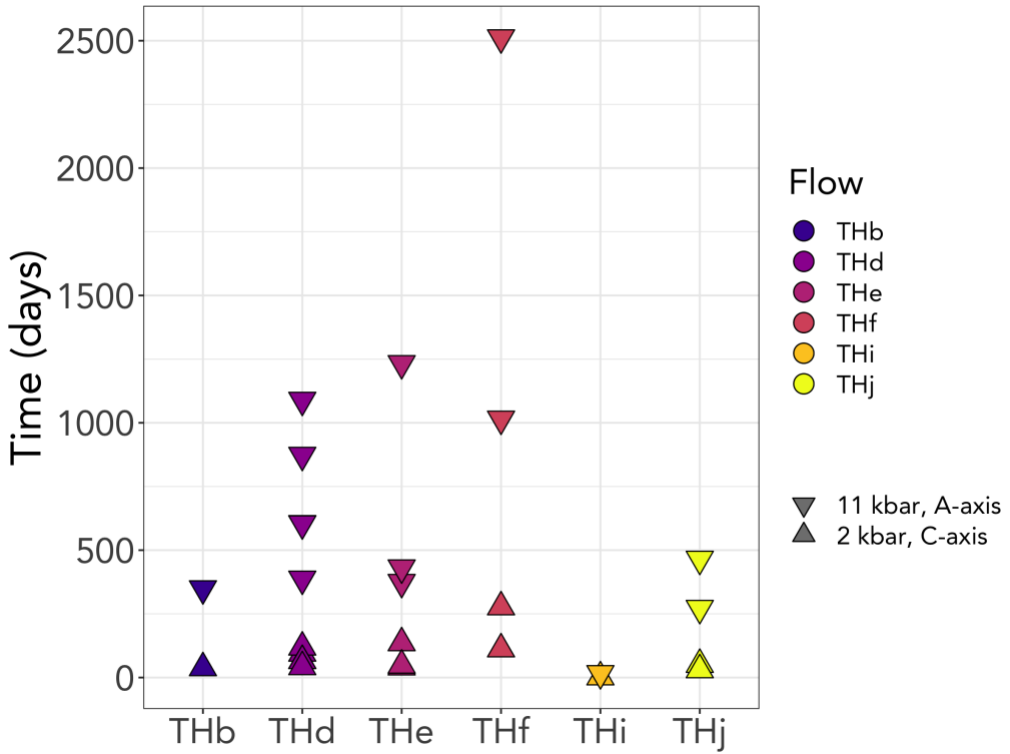


Figure 10: Estimated diffusion times for olivine macrocrysts by flow assuming transects parallel to the C-axis at 2 kbar (upward pointing triangles), and to the A-axis at 11 kbar (downward pointing triangles).

DISCUSSION

Volcanic source of the Tungnárhraun

The source vent for the Tungnárhraun lavas has not been clearly identified. These flows represent a significant portion of the total Holocene magmatic production of Iceland, providing valuable insight into the magma budget of the Eastern Volcanic Zone. At a practical level, linking them to a source is paramount to hazard evaluation for the most volcanically active region of Iceland. Geographic and geochemical considerations eliminate the nearby systems of Hekla, Torfajökull, and Katla (Figure 1). All flows of the Tungnárhraun have been found in bore holes significantly inland of Hekla (Vilmundardóttir, 1977), Torfajökull is primarily a silicic center (Macdonald et al., 1990; McGarvie et al., 1990; Gunnarsson et al., 1998), and the distinct high TiO₂ (>4 wt.%) of low MgO (<6 wt.%) basalts from Katla and Eldgjá eliminate this system as the source (Figure 8; Jakobsson et al., 1979; Miller et al., 1989). These factors leave the two largest and most active systems of the EVZ and Iceland as potential sources of the Tungnárhraun; Bárðarbunga and Grímsvötn.

The Grímsvötn and Bárðarbunga systems are notoriously similar in size and volcanic activity. Geochemical and seismic data from the eruption of Gjálp 1996 revealed a complicated subsurface relationship which prevents Grímsvötn from being excluded from consideration as the source of the Tungnárhraun on geography alone (Sigmarsson et al., 2000; Steinhörsson et al., 2000). Vilmundardóttir (1977) proposed that the origin for the Tungnárhraun lies somewhere in the southern end of the Veiðivötn fissure (Figure 3), which would link them to the Bárðarbunga volcanic system. However, the two most recent lava flows in this area (Vatnaöldur 871, Veiðivötn 1477) have covered the northernmost parts of the latest Tungnárhraun, making it impossible to resolve this question solely on field relations (Pinton et al., 2018; Caracciolo et al., 2020).

Constraints on the source of the Tungnárhraun are found in the chemistry of the lavas produced by the Grímsvötn and Bárðarbunga systems. The Tungnárhraun lie mostly within the compositional field of Bárðarbunga and outside the distinct composition ranges of other EVZ volcanic systems at 5.5-8 wt.% MgO, TiO₂ of 1-2.5 wt.%, and FeOT of 9-14 wt.%, allowing us to attribute the Tungnárhraun to the Bárðarbunga volcanic system (Figure 8). Despite major element similarities between Laki and THa and THb, isotopic data preclude a Grímsvötn system source in favor of Bárðarbunga (Halldórsson et al., 2008).

Evolution of the Tungnárhraun – The case for three eruptive episodes

From the whole rock chemistry of the Tungnárhraun, we identify three temporal eruptive episodes which generated these lavas and adopt Roman numeral nomenclature (Episode I/II/III). Episode I lavas (THa, THb, and THd) are typified by moderate MgO (<7 wt.%) and major element contents which mostly lie on the trend of EVZ lavas between historical Bárðarbunga southern fissure lavas and the Laki eruption (Figure 8), significantly overlapping the compositional fields of both (e.g. 0.21-0.36 wt.% K₂O, 10.3-13.9 wt.% FeOT). Episode II lavas (THe, THf, and THi) are distinguished from those of Episode I by higher MgO (7.5-8.0 wt.%) and major element contents which plot squarely within the composition field of Bárðarbunga northern fissure PUBs (Figure 8; e.g. 0.11-0.18 K₂O, 9.2-11.7 wt.% FeOT). In Episode III (THj and THk) lavas return to moderate MgO contents but are distinguished from Episode I by their unusually high K₂O (0.45-0.74 wt.%) and lower FeOT(10.6-11.0 wt.%; Figure 8). We note that the chemistry of each eruptive episode

would be more homogenous if not for the inclusion of THd and THi in Episodes I and II. Both flows show major element differences in CaO, Al₂O₃, Na₂O, and K₂O consistent with the high contents of anorthitic plagioclase; this mineralogy identifies them as transition lavas (discussed below).

The chemistry, internal structure, and abundance of plagioclase feldspars provide further support for division of the Tungnáhraun into three eruptive episodes. The estimated amount of plagioclase increases from <5% in THb to 20-30% in THd, THe, and THf and then decreases to 5-10% in THi, THj, and THk (Table 4). The compositions of plagioclase macrocryst rims separate the high and moderate MgO groups of the Tungnáhraun (Figure 6). Rims from Episode I are An₅₆₋₈₈, lower and more heterogeneous than the An₇₂₋₈₀ rims of Episode. Samples of Drekahraun and Þjórsárdalshraun (THh) fall within the time period of Episode II and plagioclase macrocrysts from these flows have rim compositions identical to those in THe, THf, and THi (Caracciolo et al., 2020). Episode III has low An rims similar to those in Episode I (An₅₇₋₈₂), but plagioclase crystals in these flows have a zone of intermediate composition (An₇₇₋₈₀) referred to as a mantle (e.g. Cullen et al., 1989; Neave et al., 2013). The rims of Episode III plagioclase have a similar range of compositions to the rims of Episode I crystals, but all compositions fall exclusively within three tightly grouped An composition ranges as defined by the rims (An₅₇₋₆₈), mantles (An₇₇₋₈₀), and cores (An₈₅₋₉₀). The mantles of Episode III have identical compositions to plagioclase rims of Episode II, suggesting that the plagioclase xenocrysts in Episode III are reworked from the Episode II eruptions. Changes in the equilibrium An composition indicated by the macrocryst rims, phenocrystic microcrysts, and groundmass plagioclase (Figure 6) suggest that closed-system fractionation within each eruptive episode occurs at different stages relative to plagioclase entrainment.

Crustal structure of the Bárðarbunga volcanic system

Several lines of evidence lead us to conclude that the plagioclase feldspar megacrysts in the Tungnáhraun are xenocrystic in origin. First, each megacryst is surrounded by a distinct zone of lower-An plagioclase. The rims have an intergrowth texture with groundmass phases and compositions that are in equilibrium with the groundmass plagioclase. The boundaries between

these zones are notably sharp indicating rapid transfer or uptake into magmas with distinct compositions from those which formed the prior zone. Second, the plagioclase thermometer of Druitt et al. (2012) returns the highest temperature of crystallization for the macrocryst cores (1275-1365°C). These temperatures exceed those produced via application of the thermobarometer of Yang et al. (1996) to average calculated host liquid compositions (1126-1299 ± 15°C) at the range of crustal pressures beneath the EVZ (2-11 kbar), as constrained by previous works (Hansen and Grönvold, 2000). Finally, following Bindeman et al. (1996), the Ti contents of the plagioclase cores suggest formation from an equilibrium liquid with significantly lower Ti (<5000 ppm) than Bárðarbunga southern fissure swarm lavas (>10,000 ppm), including calculated and measured groundmass compositions from THa-THk (Halldorsson et al., 2008; this study, Figure 11). In Iceland, lavas with this range of Ti contents are restricted to very primitive basalt (Borgahraun; 10-13% MgO; MacLennan et al., 2003) or gabbro (Midfell xenoliths; Gurenko and Sobolev, 2006). The plagioclase macrocryst cores in the Tungnárhraun must have crystallized from a more mafic liquid than the host lavas (Figure 11). In addition, the plagioclase rims have Ti contents (5000-15,000 ppm) characteristic of lavas erupted from Bárðarbunga's southern fissures, including the Tungnárhraun lavas ($\text{TiO}_2 = 1.1\text{-}2.5 \text{ wt.\%} = 6,715\text{-}14,750 \text{ ppm}$). We conclude that the plagioclase macrocrysts formed from a more mafic liquid than that in which they were erupted, and that they did not spend enough time in the host liquid to experience significant diffusive homogenization across the compositional boundaries, features typical of global PUBs (Cullen et al., 1989; Hansen and Grönvold, 2000; Halldórsson et al., 2008; Ustunisik et al., 2020).

Compositional transects across the Tungnárhraun plagioclase megacrysts reveal a counterintuitive difference in MgO between their rims and cores. Noting that the observed Ti contents of high-An plagioclase (Figure 11) are associated with more primitive basaltic liquids, we would expect the plagioclase cores of the Tungnárhraun to have higher MgO contents than the lower-An rims. However, our recently obtained data, along with the data presented below, show lower or equivalent MgO contents in the crystal cores compared to the rims. This difference can be reconciled with the presence of an azeotrope, or reversal, in the An-Ab phase diagram, present at depths greater than ~5 kbar (Lindsley et al., 1969; Nekvasil et al., 2015; Ustunisik et al., 2020). Ustunisik et al. (2020) place this reversal between An₈₀₋₈₅, suggesting that a magma with a sufficiently high Ca#, evolving or fractionating at 5 kbar or greater, will produce progressively

higher anorthite plagioclase as the Mg# of the liquid decreases. This effect is opposite to the “normal” trend of plagioclase formation and can be seen in our data, which shows opposing trends of the macrocryst cores and rims on a plot of MgO versus %An (Figure 12). We note that these divergent trends are consistent with our conclusion that the different zones of the plagioclase formed from different processes. Following the work of Nielsen et al. (2020), trends on a plot of Ti versus Mg (Figure 13) indicate that the cores form in a magma mixing environment, occurring as magmas recharge the crustal mush, and macrocryst rims crystallize from progressively melted mantle, potentially as the melting of the mantle from deglaciation takes hold and progressive melts mobilize the mush.

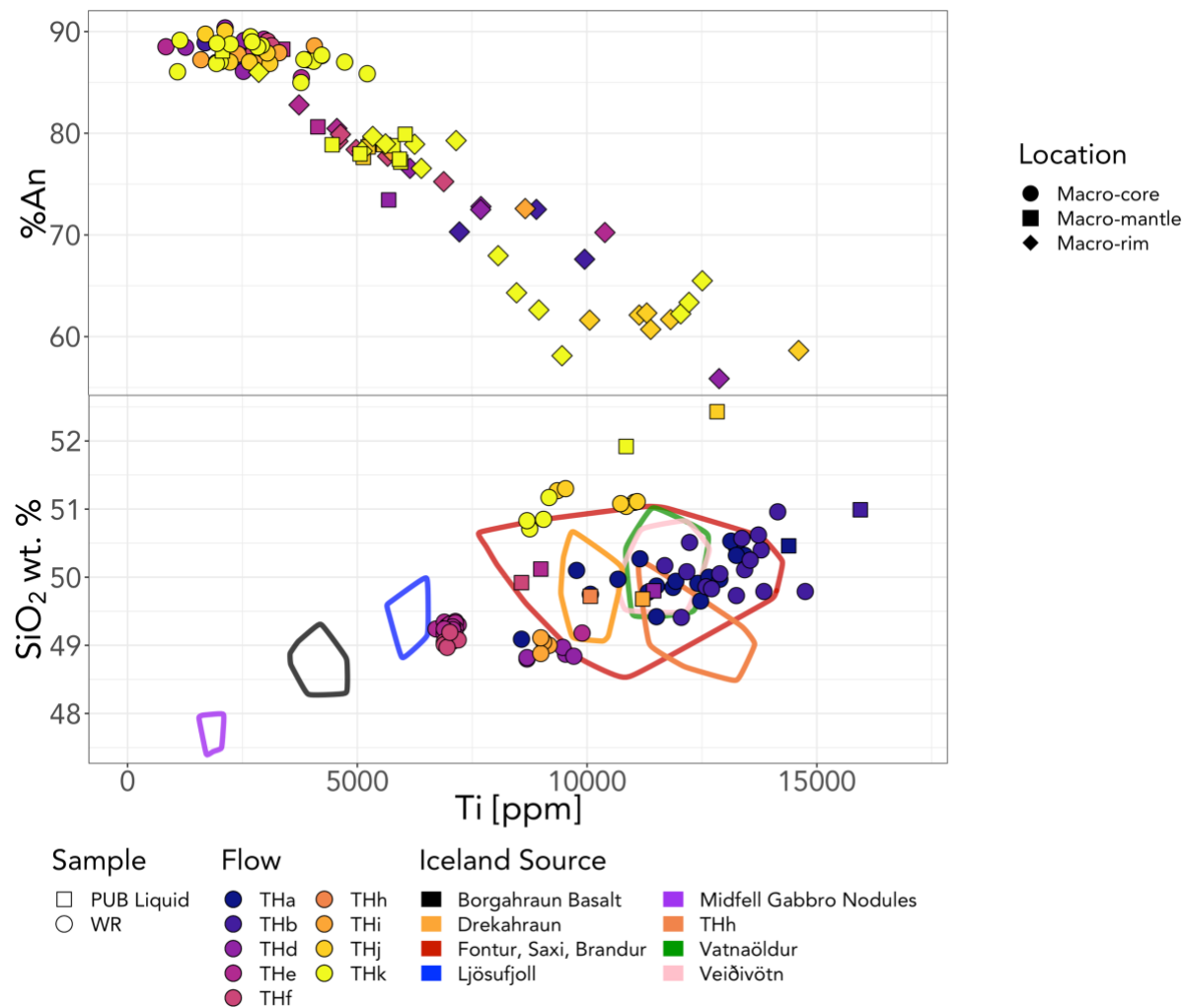


Figure 11: Top – Calculated Ti contents of equilibrium melts vs. %An of the different parts of the Tungnárhauvn plagioclase macrocrysts. Bottom – Actual Ti [ppm] of various flows from Iceland. THa, THb, Fontur/Saxi/Brandur, and Ljósufjöll fields are groundmass Ti (Halldórsson et al., 2008; Caracciolo et al., 2020), all others are whole rock (MacLennan et al., 2003; Gurenko and Sobolev, 2005; Óladóttir et al., 2011).

We argue for a hybrid model of plagioclase entrainment that integrates the two extant hypotheses for PUB formation discussed above, and which reveals the subsurface structure beneath the Tungnáhraun. We note that Iceland has anomalously thick crust for a slow spreading center and the large volume basalt flows strongly imply the existence of crustal magma chambers. We therefore suggest that the negative buoyancy (plagioclase floatation) model applies at depths >6 kbar and the magma ascent model dominates the system at depths <6 kbar.

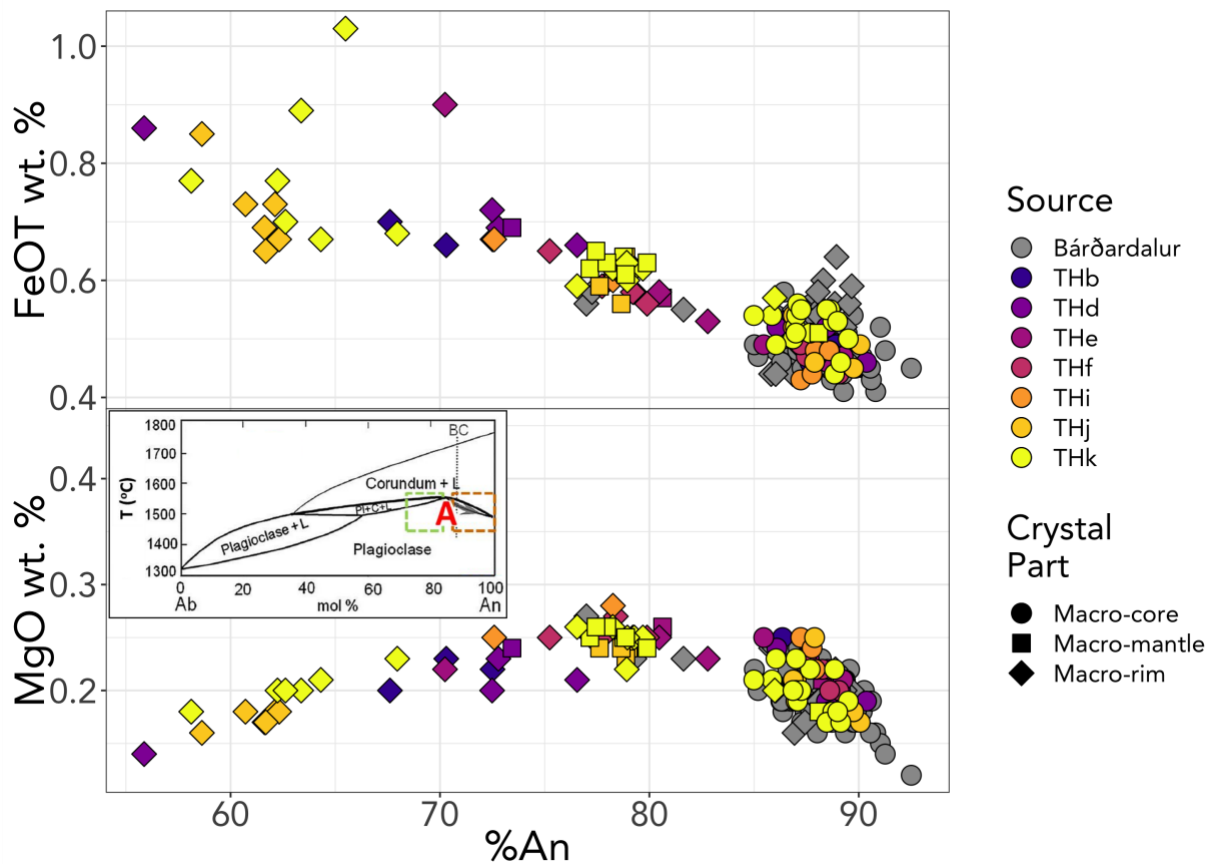


Figure 12: Plot of Anorthite content versus minor elements in plagioclase zones from the Tungnáhraun and Bárðardalur lava sequences. The red “A” in the inset represents the azeotrope, or reversal in the An-Ab phase diagram. Data for the Bárðardalur sequence from Svavarssdóttir (2017).

Incorporation of plagioclase could occur in response to injection of hot mafic magma that either entrains a significant crystal cargo from a mush near the base of the crust or mobilizes plagioclase that settled from previous magmas along the same pathway. From its plagioclase entrainment or fractionation depth, the magma must make its way to the surface at a rate greater than ~0.5 cm/s in order to retain the plagioclase. Ascent would take ~76 days if the magma is assumed to retain

all of the assimilated plagioclase, from the maximum depth constraint of 33 km (11 kbar). In the rapid end-member ascent scenario, travel from 18 km (6 kbar) at 1.0 cm/s would take ~20 days. These values are consistent with the lower range of eruptive time scales calculated by Mg-Fe diffusion modeling of olivine macrocrysts from the Tungnárhraun. The olivine crystals are considered xenocrysts entrained at the same time as the plagioclase, as they commonly form glomerocrysts and are zoned from highly forsteritic (Fo_{82-86}) cores to equilibrium compositions at the rim ($\text{Fo}_{<75}$) that match those of the groundmass crystals. This general model is considered for each eruptive episode of the Tungnárhraun is detailed below.

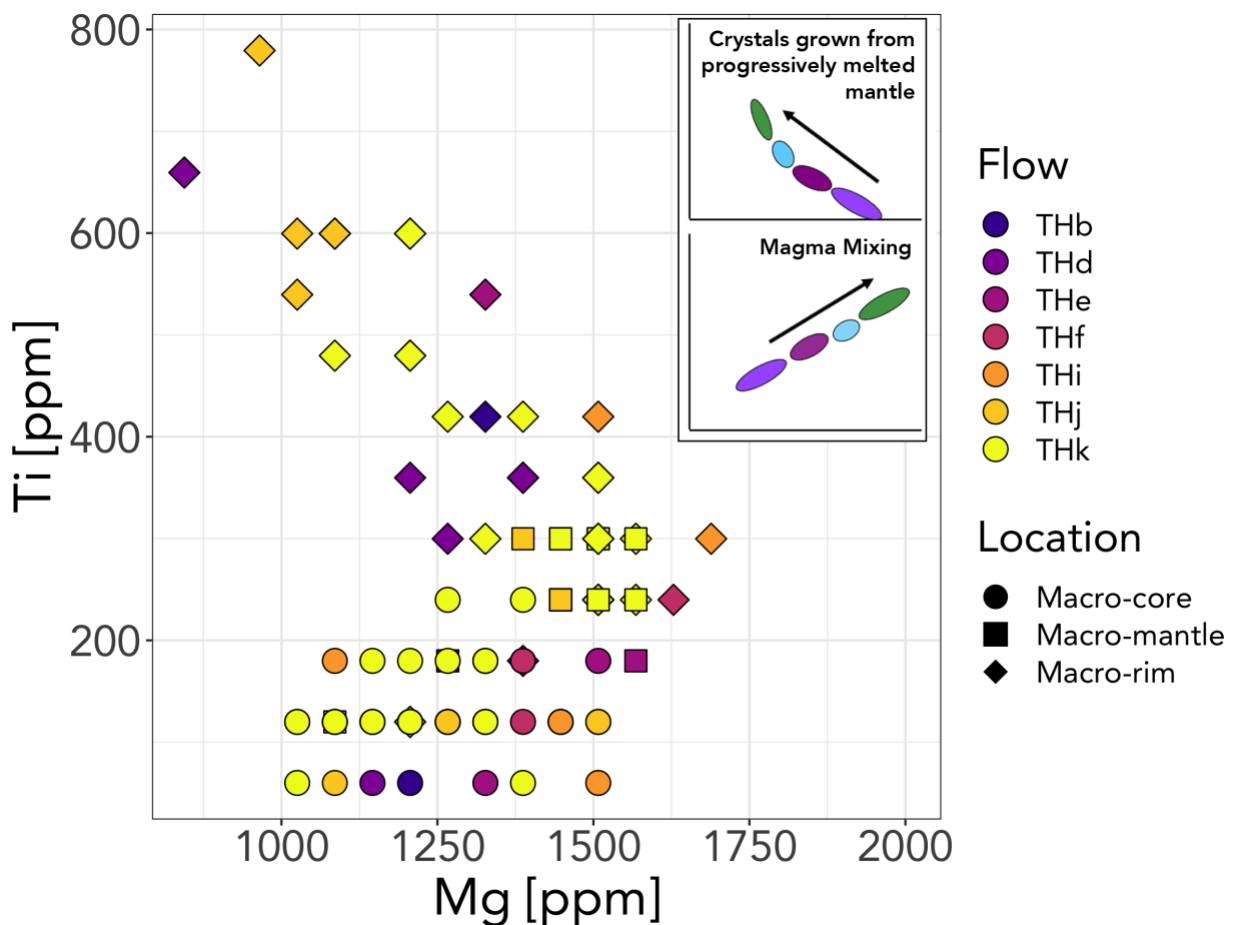
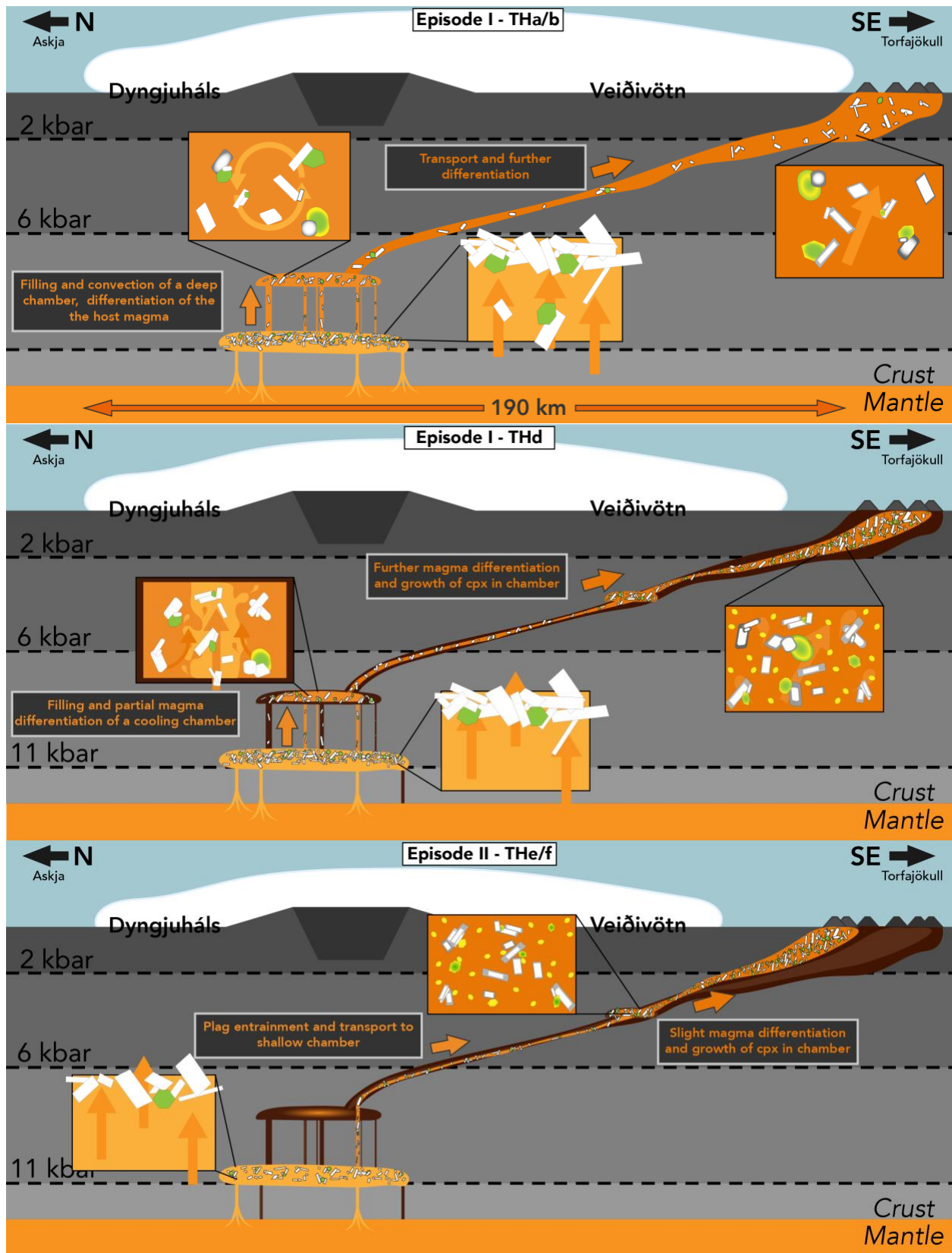


Figure 13: Plot of Mg and Ti concentrations in the Tungnárhraun macrocryst plagioclase. Inset taken from Nielsen et al., (2020).

During Episode I, large volumes of mafic magma accumulated in a chamber in the lower half of the crust, where subsequent replenishing batches of mafic magma injected liquid and fresh crystal cargo into the convecting chamber. The low MgO contents of Episode I lavas indicate a higher degree of fractionation than is observed in subsequent events, and a wide range of plagioclase rim

compositions and oscillatory zoning suggest that differentiation occurred alongside entrainment as the chamber underwent convective overturn. This scenario is likely given the time needed to accumulate the large volumes of THa and THb lava flows; mixing with replenishing batches of magma injected periodically prevents further differentiation. The new batches of magma injected into the chamber during this time likely introduced new macrocrysts of plagioclase and olivine. The final injection triggered the evacuation of the magma chamber and provided the majority of the euhedral plagioclase found in the lavas. Olivine composition profiles record at least one magma recharge that partially equilibrated with the crystal cores prior to rim growth: these crystals have a higher forsterite zone ($\text{Fo}_{\geq 76}$) around an intermediate core (Fo_{76}), which diffused to the final equilibrium boundary condition during mixing and transport (Figures 5). Two profiles showing this feature are from subhedral olivine found alongside highly resorbed plagioclase, both evidence of reworking by fresh magma. The lone profile with a classic error function shape is from a euhedral olivine attached to a large, mostly intact plagioclase and was likely introduced in the final magma infusion that triggered the eruption after 38 and 349 days.

Lava flow THd represents a transition from the deep magma body generated after the end of the last glacial maximum resulting from stress field changes related to deglaciation and isostatic rebound. An analogous shift likely occurred in the area of the northern fissure swarm around the same time given its similar glaciation history (Svavarsdóttir, 2017). This deglaciation-related shift would allow the deep magma chamber to evacuate prior to accumulating the large volume of magma as was erupted in THa and THb. Flow THd contains a relatively higher amount of euhedral plagioclase and olivine mixed with rare disintegrated and sub- to anhedral plagioclase. This assemblage suggests that the magma which triggered the evacuation of the deep chamber retained abundant plagioclase entrained from the basal mush, while mixing with the remaining liquid and crystals from the large magma chamber that fed the THa and THb eruptions. On its way to the surface, THd was likely stored for a short time in a shallow magma chamber, where it crystallized clinopyroxene, olivine, and plagioclase microcrysts that are compositionally distinct from the groundmass (Figure 14).



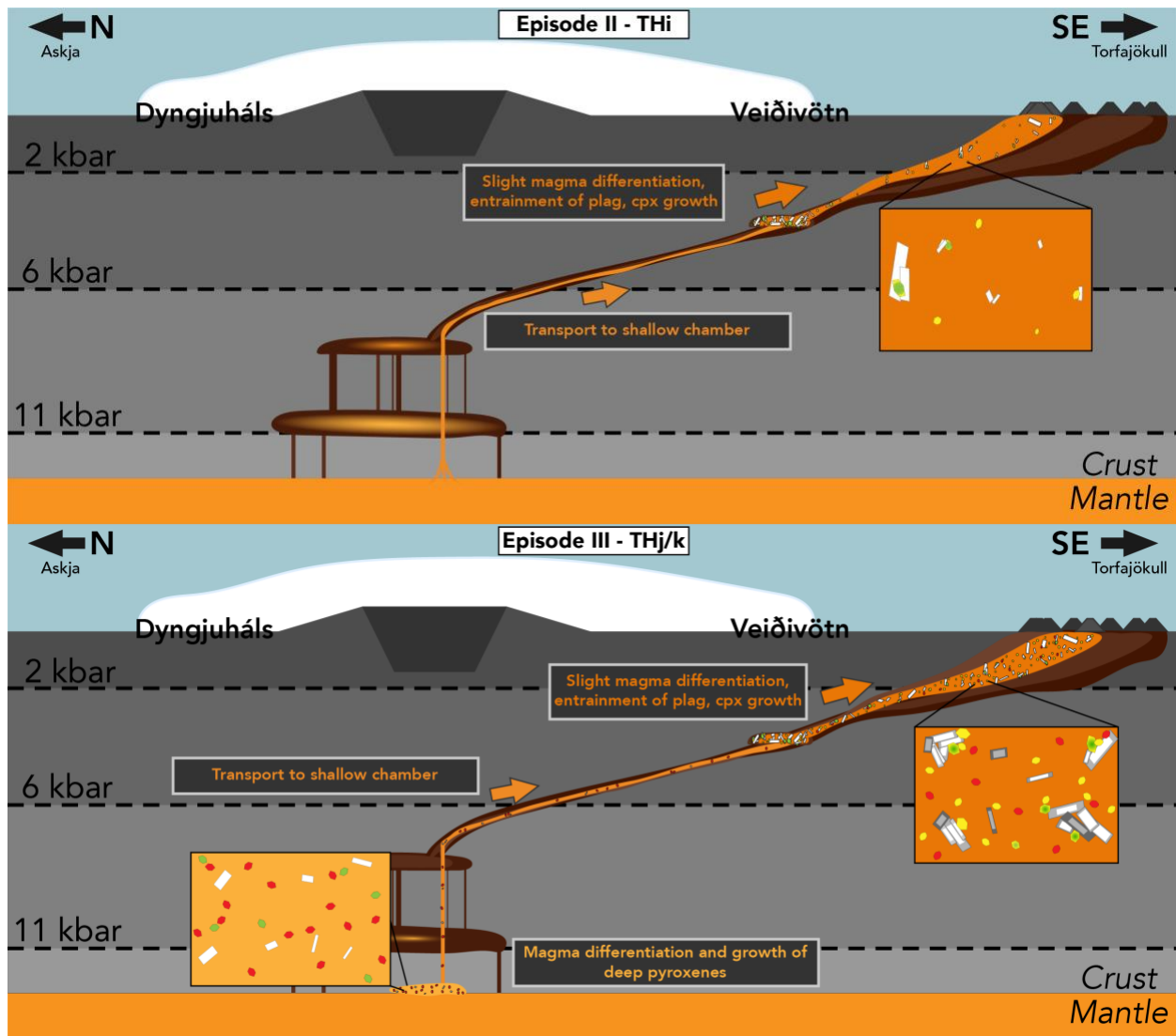


Figure 14: A series of cartoons detailing our proposed magma pathway evolution beneath Bárðarbunga over the Holocene, with shapes to indicate the crystal cargo at each phase of evolution. White = plagioclase, green = olivine, yellow = clinopyroxene, red = orthopyroxene. Insert show a more detailed view at each phase of evolution. We note that the actual crustal structure is likely more complicated (e.g. it's likely that there are multiple sills between 2 and 6 kbar, evidenced by the Holuhraun III eruption). We simplify the structure for illustrative purposes.

Episode II lavas continue to draw from the cumulate mush formed from the melts produced in the mantle after deglaciation, where temperatures are hot enough to trigger significant diffusive equilibration of olivine, but not of plagioclase. The residence time of the macrocrysts in crustal chambers overprints the subsequent diffusion during transport as maximum diffusion timescales increase through Episode II, while mineralogy remains relatively constant. Magmas follow the pathway of THd, making their way to the surface quickly enough to avoid differentiation and the loss of plagioclase and olivine through gravitational settling (Figure 14). Minimal fractionation

results in relatively more mafic host liquids more closely resembling those which formed the macrocryst phases. Plagioclase macrocrysts remain with the Episode II liquids from entrainment to eruption, as evidenced by generally thicker rims than Episode I (up to 200 μm). Episode II lavas and THd contain abundant microcrysts, primarily clinopyroxene, that are compositionally distinct from the groundmass. Much like THd, the THi flow is a transition lava representing a change in the magma pathway between eruptive episodes, in this case as the melting effects of deglaciation wane. The drop in the amount of plagioclase in THi signals the depletion, solidification, or avoidance of the mush at the base of the crust. The lack of plagioclase megacrysts, their remarkably thin rims (<50 μm ; Figure 6), and the abrupt compositional profile of the lone olivine macrocryst, leads us to conclude that THi bypassed the mush of the rift, injecting instead through the shallow magma chamber of a previous Episode II magma, mobilizing a minimal amount of crystals for a short time before erupting (2-16 days; Figures 12 and 14).

The magmas of Episode III follow the path of THi, undergoing minor differentiation at the base of the crust, bypassing the mush of the rift, and fractionating further in the shallow chamber of Episode II, where they mobilize clumps of plagioclase and olivine macrocrysts as glomerocrysts. The plagioclase macrocrysts of this episode have an intermediate mantle that is compositionally identical to the rims of Episode II. Episode III plagioclase are characterized by 1) high An core macrocrysts with an intermediate (“Episode II”) mantle and a low An rim, 2) intermediate An microcrysts with low-An rims and 3) low-An microcrysts in equilibrium with the host lava. We note that the large plagioclase crystals are found almost exclusively as glomerocrysts consisting of macrocrysts with grain boundaries indicative of comagmatic growth. Storage in the shallow magma chamber allowed THj and THk to crystallize abundant clinopyroxene microcrysts, a significant proportion of which have compositions trending toward orthopyroxene, suggesting a period of differentiation near the base of the crust (>11 kbar) at the edge of the orthopyroxene stability field (Figure 14). The combination of differentiation periods near the surface and base of the crust increases K₂O and decreases FeOT of the Episode III lavas which diverge from the rest of Bárðarbunga and the Tungnárhraun.

The 2014-15 eruption on the Holuhraun fissure (Holuhraun III), one of the most well monitored fissure eruptions on Earth, provides a real-world analog against which we examine our model of

magma movement. The magma from this eruption traveled ~48 km laterally at ~6-7 km depth for over two weeks before erupting on the part of the Holuhraun fissure away from the edge of Vatnajökull (Ágústsdóttir et al., 2019). This movement supports the occurrence of significant lateral magma migration away from the Bárðarbunga central conduit. Microseismic data indicates a secondary vertical pathway at 7-22 km depth located ~10 km SE of the central caldera and a zone of melt accumulation at ~2 kbar, the top of the range predicted in our model for a secondary magma chamber (Hudson et al., 2013). Geodetic and geobarometric data indicate magma equilibration and storage between 8-12 km, again consistent with a shallow storage chamber in the mid to upper crust (Sigmundsson et al., 2015; Ágústdóttir et al., 2016; Gudmundsson et al., 2016).

The secondary conduit of the Holuhraun III eruption lies between the Bárðarbunga caldera and the Gjálp 1996 eruption. This eruption occurred on a fissure oriented between Bárðarbunga and Grímsvötn and has been chemically linked to Grímsvötn despite syn-eruptive seismic activity around the Bárðarbunga caldera (Sigmarsson et al., 2000). As with Gjálp, the 2014-15 Holuhraun eruption was associated with widespread seismic activity. In addition to seismicity associated with dike propagation, local networks recorded seismicity on the Kistufell and Úrðarháls segments of the Northern Fissure Swarm, as well as on Askja and its associated fissure, indicating a complex interaction between volcanic systems in central Iceland (Green et al., 2015).

The vast majority of Holocene Icelandic PUBs erupted from parts of Bárðarbunga including the largest flows of the Bárðardalur Valley (Kinnarhraun, Bárðardalshraun) and Gígöldur in the northern fissure. The chemistry and $^{87}\text{Sr}/^{86}\text{Sr}$ ratios of the plagioclase macrocrysts from these flows are consistent with values measured in THa and THb lavas by Halldórsson et al. (2008) and suggest crystallization from a crystal mush. While the Bárðardalur lavas are more primitive than the Tungnáhraun (7-9 wt.% MgO), these flows also separate into distinct groups: a non-PUB group with 7-8 wt.% MgO and a more primitive (8-9 wt.% MgO) PUB group (Svavarssdóttir, 2017). This bimodal distribution suggests that entrainment of PUB plagioclase at Bárðarbunga occurs preferentially in magmas with lower crustal residence times. As in the Tungnárhraun, the amount of plagioclase in the Bárðardalur lavas declines as decompression melting and volcanic output began to slow ~4.0 ka. Around this time, both large lava sequences have a ~1 km³ transition lava, THi in the Tungnárhraun and Kvíahraun in the Bárðardalur, which maintain the high MgO contents

of the PUBs but have notably lower volumes of plagioclase (<10%). For the Tungnárhraun, we conclude that this transition lava marks the depletion of the mush which provided the macrocryst cargo. During the genesis of this transition lava, either the pathway from the source of the melt to the source of the plagioclase closed or the pathway of magma migration changed away from the mush. Either scenario could be the result of the changing stress field after deglaciation. The An content and minor element composition of Bárðardalur plagioclase macrocryst cores also have the same range as plagioclase from the Tungnárhraun (Figure 12). Given the timing of the transition lava in each sequence and the identical compositions of plagioclase macrocrysts, we suggest that the northern and southern fissure swarms shared the source of their plagioclase from the beginning of the Holocene until ~4.0 ka. When distinguishing between the elongate and plagioclase mush models of Óskarsson et al. (2017), we conclude that the homogeneity of the plagioclase core compositions could not be maintained within a mush that spans the length of Bárðarbunga fissures. Therefore, the large volume Holocene lava sequences of Bárðarbunga likely travelled to the surface through centralized pipe-like conduit before being forced to the periphery by the weight of the central volcano and overlying ice sheet. This model is supported by the relative differentiation between the two systems as a conduit below Bárðarbunga would give the Tugnárhraun a longer distance to travel to the end of its respective fissure, and therefore more time to fractionate prior to eruption.

We link the Tungnárhraun flows to the Bárðarbunga system on the basis of whole rock chemistry and the occurrence of PUBs. This interpretation, coupled with the recent linkage of the Bárðardalur valley lavas to the Bárðarbunga system, make Bárðarbunga by far the most productive system in Iceland over the Holocene. PUBs are found throughout the accessible lava pile in Iceland, though the majority are associated with Bárðarbunga, presumably originating from the same mush pile. Like all PUBs, the macrocryst plagioclase and olivine phases are xenocrysts and could not have formed from the host liquid. Whole rock chemistry and mineral chemistry and morphology reveal a complicated and evolving magma pathway, which, between the two fissure swarms, does not diverge until a relatively shallow level, before magams are forced into one of the two fissures by the weight of the overlying volcano and Vatnajökull ice-sheet. This structure prevails until ~4.0 ka when the shifting crustal stress field caused a change in the magma pathway feeding the system. While our model of Bárðarbunga's crustal structure may be relatively simplistic in the face of the

complex nature of Askja-Bárðarbunga and Bárðarbunga-Grímsvötn interactions, geochemical, geophysical, and geodetic data from the large-volume Holuhraun III eruption largely supports the idea of magma storage in the mid to upper crust.

CONCLUSIONS

Measured bulk rock geochemistry allows us to connect the Tungnárhraun lava sequence to the Bárðarbunga volcanic system. While compositions vary between eruptive episodes, the whole rock chemistry remains within the large fingerprint of Bárðarbunga volcanics, and largely outside of the homogeneous composition fields of the nearby Grímsvötn and Katla volcanic systems.

We interpret the Tungnárhraun as reflecting three phases of eruptive activity, each of which is linked to the interplay between magma production by the Iceland plume and magma extrusion in response to changing weight of glacier cover at the end of the Ice Age. In Episode I, a large convecting magma chamber, sustained by the heat of the mantle plume, experienced numerous injections of mafic magma and microcrystal cargo. The depth of this chamber is constrained to the lower half of the crust by published studies on PUB formation in Iceland and elsewhere. The eruption of this large volume was triggered by the deglaciation of Iceland and a final injection of mafic magma. This period of activity ended with the eruption of a transition lava, THd, the final eruption from the deep-seated magma chamber. THd begins the PUB sequence within the Tungnárhraun, mixing with the remaining magma in the chamber before being stored at shallow levels beneath Bárðarbunga prior to eruption. Episode II represents a PUB sequence within the Tungnárhraun. Compositional zoning of macrocryst phases indicate that they sat in a hot mush for a significant amount of time prior to entrainment by the host liquid. In this period, magmas travelled quickly and did not differentiate as much as Episode I magmas. Abundant clinopyroxene microcrysts in the host lava suggests storage in an upper crustal magma chamber post-plagioclase entrainment. Episode II is capped by another transition lava, THi, which signifies the waning effects of deglaciation-related melting and the cooling of the shallow magma chamber. During Episode III, a wide range of pyroxene composition indicate magmas fractionate at both deep and shallow levels. The absence of plagioclase with only two zones suggests that they bypass the mush of the rift. In the absence of their own plagioclase, these magmas rework the macrocryst cargo left

behind in the shallow magma chamber of Episode II resulting in a distinct three zone internal morphology. We support our interpretations with data from the recent large volume eruption Holuhraun III in 2014-15 which erupted from a discrete chamber within the same range of depths we suggest for the shallow magma chamber which fed the Episode II and III eruptions. Given the co-seismic events which have occurred on nearby systems during the Holuhraun III and Gjálp eruptions, it is likely that the crustal structure of Bárðarbunga is complex, though we provide a necessary first step in understanding its evolution.

Upon comparison of the Tungnárhraun to data from the Bárðardalur Valley lavas, we conclude that both sequences of large volume eruptions entrained plagioclase macrocrysts from the same crustal mush. Given the significant overlap in minor element composition and homogeneity, we suggest that this mush is likely concentrated around a pipe-like conduit and not an elongate form which runs a significant distance beneath Bárðarbunga. The relative evolution of each sequence is consistent with a shorter magma pathway for the northern fissure than the southern, in line with a central conduit beneath Bárðarbunga, closer to Askja than Torfajökull.

Finally, the addition of the Tungnárhraun in this work and the recent connection of the Bárðardalur lavas and their associated fissures definitively make the Bárðarbunga volcanic system the largest and most productive volcanic system in Iceland over the Holocene.

Table 1 – Eruptive volumes of Icelandic neovolcanic zones

<i>Volcanic Zone</i>	<i>Number of Eruptions</i>	<i>Volume of lava (km³)</i>	<i>Volume of tephra (km³ DRE)</i>	<i>Total Volume (km³ DRE)</i>	<i>Percent of Iceland's eruptive output</i>
NVZ	146	90	12	94	16.5
WVZ	47	94	0	94	16.6
EVZ	2023	174	412	337	59.5

Table 1: Select data of the eruptive volumes of the volcanic zones of Iceland taken from Thordarson and Höskuldsson (2008).

Table 2 – Components of the Bárðarbunga volcanic system

Name	Date of Formation	Date of last known eruption (name)	Location Description
<i>Northern Fissure Swarm</i>			
Kistufell	~10 ka	~10 ka	Tuya and fissure at the edge of Vatnajökull, NNE of Bárðarbunga
Dynguháls Fissure Swarm	<4.5 ka	~1362 (Frambruni)	From the edge of Vatnajökull, N of Bárðarbunga, W of Kistufell
Urðarháls	>12 ka	>12 ka	Fissure and lava field N of Kistufell
Hrímalda	~10 ka	~10 ka	Low ridge NNE of Urðarháls
Hrímalda-Gígöldur Fissure	4.0-6.1 ka	4.0-6.1 ka	E-W trending between Hrímalda and Gígöldur
Gígöldur Crater Row	~10 ka	8.0-9.3 (Bárðardalshraun)	Trending roughly N-S, NNW of Urðarháls
Holuhraun Fissure	1797	2014-15	Discontinuous fissure from the edge of Vatnajökull, E of Gígöldur
Askja(?)	~10 ka	1961 (Vikraborgir)	Caldera surrounded by the Dyngufjöll mountains, N of Gígöldur
<i>Subglacial</i>			
Bárðarbunga Caldera	?	2008	Beneath W edge of Vatnajökull
Hamarinn Shield Volcano	?	?	Beneath Vatnajökull, SSE of Bárðarbunga
Gjálp(?)	1996(?)	1996	Fissure trending ESE beneath Vatnajökull towards Grimsvötn
<i>Southern Fissure Swarm</i>			
Veiðivötn	?	1477	SW trending fissure from Bárðarbunga
Vatnöldur	?	871	SW trending fissure W and parallel to Veiðivötn
Tröllagigar	?	1862-64 (Tröllahraun)	Short SW trending fissure extending from Vatnajökull, E of Veiðivötn
Torfajökull(?)	2.6 Ma-12 ka	1477	Oblong silicic complex at the SW extent of the Veiðivötn and Vatnöldur fissures

Table 2: Collected data on the volcanic parts of the Bárðarbunga volcanic system. “?” indicates an uncertain date of formation. Dates are given in CE unless otherwise noted. Information from the Icelandic Larsen (1984), Thordarson et al. (2003), Thordarson and Larsen (2007), Óladóttir et al. (2011), Larsen and Gudmundsson (2014), Svavarssdóttir (2017), Met Office (2020), University of Iceland (2020).

Table 3 – Holocene eruptive history of Bárðarbunga fissure swarms

Name	Date	Volume (km ³)	Vol% Plagioclase	Alternate Names
<i>Northern Fissure Swarm</i>				
Kinnarhraun	9.5 ka	4.8	15-30	
Útbruni	9.3 ka	1.0	2-5	
Bárðardalshraun	>8.0 ka	8.0	10-30	
Krepputungahraun	7.0 ka	7.0	?	
Kvíahraun	4.0 ka	~1	2-5	
Frambruni	1362	4	Less than PUB	Fjallsendahraun
Holuhraun I	1797	~1	Less than PUB	
Holuhraun II	1867	~1	Less than PUB	
Holuhraun (III?)	2014-15	1.44	Less than PUB	
<i>Southern Fissure Swarm</i>				
THa	8.6 ka	5	2-30	
THb	>8.0 ka	13.5	2-30	Thjórsahraun
Raudhóll-Flögd	>8.0 ka	1	?	
Háganga	>8.0 ka	1	?	
Háahraun-Botnarhraun	7.35-8.15 ka	1.1	?	
THc	6.8 ka*	1.4	?	Thriðja Elsta Tungnárhraun
THd	6.9-7.1 ka	3.8	25-30	Fjörða Elsta Tungnárhraun
THe	6.4-6.8 ka	1.0	20-35	Fimmta Elsta Tungnárhraun
THf	5.3-6.2 ka	3.4	20-25	Sigalda, Kvíslahraun, Sigölduhraun, Kalfahraun
THg	6.0 ka*	0.4	?	Hnubbahraun
Byrdjahraun	4.0 ka	1	?	
THh	4.0 ka*	2.4	?	Thórsadálshraun
THi	3.38-3.46 ka	3.9	5-10	Búrfellshraun, Dreki, Drekahraun
Drekahraun	3.0-3.05 ka	2.6	5-10	THi
THj	2.32-2.5 ka	0.7	2-10	Tjörvahraun
THk	~800*	0.1	5-10	Hnausahraun
Vatnaöldur 871	871	1.1	Less than PUB	
Veiðivötn 1477	1477	1.1	Less than PUB	
Tröllahraun	1862-64	0.3	Less than PUB	
Total		74.04		

Table 3: Holocene eruptive history of the north and south fissure swarms of Bárðarbunga. Data from: Vilmundardottir (1977), Larsen (1984), Thordarson et al. (2003), Hjartarson (2004, 2011), Thordarson and Larsen (2007), Hartley and Thordarson (2013), Larsen and Gudmundsson (2016), Svavarsdóttir (2017), Pinton et al. (2018). *Age estimate from borehole.

Table 4 – Plagioclase Compositions

Flow	Sample	% Volume Plagioclase (ImageJ)		Plagioclase (%An)						Groundmass**	
				Macrocrysts (>1000 µm)			Microcrysts (100-1000 µm)				
		Estimated	ImageJ	Core	Mantle	Rim	Core	Rim			
THb	THa-1	< 5	4.4	87.7 – 88.9	-	67.6 – 89	68.7 – 87.3	-	58.3		
THb	THa-2	< 5	2.6	86.4 – 88.9	-	70.3 – 72.5	80.8 – 88.1	-	64.2		
THd	THd-3a	25-30	18.8	86.1 – 90.4	73.4*	55.9 – 76.6	68.1 – 88.3	-	65.0		
THe	THde-2	20	14.3	85.5 – 89.3	80.6 – 88.3	70.2 – 82.8	76.7 – 88.9	-	75.7		
THf	THf-3b	20	14.9	87.2 – 89.1	-	75.2 – 79.9	55.9 – 89.8	76.2 – 77.4	74.6		
THi	THi-3	< 5	2.6	86.9 – 88.6	-	72.6 – 78.3	78.9 – 89.3	78.4*	71.9		
THj	THj-2	5	7.2	86.9 – 90.1	77.6 – 79.0	58.6 – 62.3	55.6 – 85.8	60.7 – 63.3	66.0		
THk	THk-2	10	10.9	85.7 – 89.5	78.8*	62.2 – 86.0	64.8 – 86.6	-	67.8		
THk	THk-3	5	2.2	85.0 – 89.1	77.2 – 88.1	58.1 – 79.0	64.9 – 89.3	62.8 – 78.6	63.4		

Table 4: Summary of plagioclase compositions measured for this study. Raw data can be found in Appendix B. *only one analysis, **Groundmass values are the average of 10 EPMA spot analyses.

Table 5 – Olivine Compositions

Flow	Sample	% Volume Olivine Macrocrysts		Macrocrysts (>1000 µm)		Microcrysts (100-1000 µm)		Groundmass		n	
				Core		Core					
		Estimated	ImageJ	Fo %	CaO	Fo %	CaO	Fo %	CaO		
THb	THa-1	0	-	-	-	70.7 – 79.1	0.32 – 0.36	65.4	0.41	1	
THb	THa-2	< 1	0.47	84.3*	0.37*	-	-	68.9	0.83	3	
THd	THd-3a	< 5	0.60	83.5 – 84.5	0.37	69.3 – 84.8	0.33 – 0.37	67.0	0.39	3	
THe	THde-2	< 5	0.73	84.9 – 86.2	0.38 – 0.41	79.2 – 84.2	0.36 – 0.42	74.5	0.45	2	
THf	THf-3b	< 1	0.46	85.6 – 85.8	0.37	82.3 – 83.3	0.35 – 0.37	75.8	0.39	4	
THi	THi-3	< 1	0.28	82.7*	0.36*	81.2 – 83.7	0.35 – 0.38	71.8	0.36	4	
THj	THj-2	< 1	0.11	81.9 – 82.3	0.35 – 0.36	-	-	66.3	0.42	5	
THk	THk-2	0	-	-	-	82.3*	0.38*	75.4	0.40	1	
THk	THk-3	< 1	-	-	-	82.0 – 82.1	0.36 – 0.37	73.1	0.48	4	

Table 5: Summary of the olivine compositions measured for this study. Raw data can be found in Appendices C and E. *only one analysis, n = number of analyses in Groundmass average

Table 6 – Pyroxene Compositions

Flow	Sample	Pyroxene (En-Fs-Wo %)												
		Macrocrysts (>1000 µm)						Microcrysts (100-1000 µm)						
		Core			Rim			Core			Rim			
		En	Fs	Wo	En	Fs	Wo	En	Fs	Wo	En	Fs	Wo	
THb	THa-1	47.8*	9.3*	42.9*	-	-	-	46.1 – 50.2	9.0 – 14.9	37.8 – 42.6	-	-	-	
THb	THa-2	-	-	-	-	-	-	42.1 – 48.4	8.4 – 13.8	41.6 – 44.1	-	-	-	
THd	THd-3a	-	-	-	-	-	-	47.3 – 48.1	8.3 – 11.2	41.5 – 43.6	-	-	-	
THe	THde-2	-	-	-	-	-	-	47.1 – 50.0	8.3 – 8.6	41.4 – 44.6	-	-	-	
THf	THf-3b	-	-	-	-	-	-	47.8 – 51.1	8.1 – 8.9	40.1 – 43.7	-	-	-	
THi	THi-3	-	-	-	-	-	-	47.8 – 48.6	10.1 – 10.4	41.3 – 41.8	-	-	-	
THj	THj-2	-	-	-	-	-	-	47.5 – 50.6	9.2 – 10.6	38.8 – 43.0	46.2*	12.5*	41.3*	
THk	THk-2	-	-	-	-	-	-	28.3 – 50.7	9.7 – 30.8	39.6 – 42.5	47.9 – 49.6	11.0 – 11.7	38.8 – 41.1	
THk	THk-3	33.2 – 34.0	25.4 – 26.7	39.3 – 31.4	47.0 – 47.9	10.5 41.6 – 42.5	41.6 – 31.3 – 49.5	8.9 – 27.5	40.1 – 43.4	46.8 – 49.4	10.8 – 13.4	39.4 – 42.0		

Flow	Sample	Groundmass			n
		En	Fs	Wo	
THb	THa-1	43.8	24.9	31.4	9
THb	THa-2	46.7	14.9	38.4	7
THd	THd-3a	46.0	14.7	39.3	7
THe	THde-2	47.8	12.0	40.2	8
THf	THf-3b	48.6	10.5	40.9	5
THi	THi-3	47.0	12.4	40.6	6
THj	THj-2	44.9	18.6	36.4	5
THk	THk-2	48.7	12.4	38.9	9
THk	THk-3	45.7	14.1	40.2	6

Table 6: Summary of pyroxene compositions measured for this study. Raw data can be found in Appendix D. *only one analysis, n = number of analyses in Groundmass average.

Table 7 – Rock Maker Calculated Compositions

Flow	SiO ₂	TiO ₂	Al ₂ O ₃	Fe ₂ O ₃	FeO	MnO	MgO	CaO	Na ₂ O	K ₂ O	P ₂ O ₅	BaO	Total
<i>Whole Rock Averages</i>													
THa ¹	49.92	1.98	14.65	2.05	10.46	0.21	6.29	11.61	2.24	0.29	0.30	-	100.00
THb ¹	50.12	2.19	14.03	2.15	10.96	0.22	6.10	11.23	2.35	0.33	0.33	-	100.00
THd	48.98	1.55	17.44	1.69	8.63	0.17	6.23	12.86	2.10	0.20	0.16	-	99.98
THe	49.29	1.22	16.48	1.59	8.10	0.17	7.57	13.35	1.95	0.16	0.11	-	100.01
THf	49.12	1.17	16.72	1.56	7.95	0.17	7.66	13.48	1.92	0.14	0.11	-	100.00
THi	48.96	1.52	15.13	1.82	9.29	0.20	7.85	12.91	2.04	0.15	0.14	-	99.98
THj	51.15	1.74	15.33	1.78	9.06	0.19	6.12	10.93	2.76	0.70	0.24	-	100.00
THk	50.89	1.49	15.32	1.76	8.95	0.19	6.67	11.49	2.53	0.53	0.19	-	100.00
<i>Plagioclase Composition Averages</i>													
THa ¹	47.51	0.00	33.09	0.38	0.22	0.00	0.00	17.02	1.96	0.07	-	0.00	100.25
THb ¹	46.45	0.02	34.21	0.53	0.00	0.00	0.23	17.99	1.35	0.01	-	0.00	100.79
THd	46.24	0.02	34.38	0.52	0.00	0.01	0.21	18.14	1.29	0.01	-	0.00	100.81
THe	46.49	0.02	34.17	0.51	0.00	0.01	0.23	17.97	1.38	0.02	-	0.00	100.79
THf	46.42	0.02	34.41	0.42	0.04	0.00	0.22	17.97	1.31	0.01	-	0.00	100.83
THh ²	45.85	0.03	34.45	0.61	0.00	0.01	0.17	17.58	1.42	0.02	-	0.01	100.12
THi ²	46.58	0.02	34.33	0.34	0.13	0.00	0.22	17.69	1.37	0.01	-	0.00	100.69
THj	46.42	0.02	34.41	0.43	0.07	0.00	0.20	17.88	1.33	0.01	-	0.00	100.77
THk	46.42	0.02	34.25	0.50	0.02	0.01	0.20	17.83	1.39	0.01	-	0.00	100.64
<i>Rock Maker Output (-20% Plagioclase)</i>													
THa	50.46	2.4	10.68	2.47	12.61	0.26	7.65	10.45	2.3	0.34	0.37	-	99.99
THb	50.99	2.66	9.69	2.6	13.25	0.27	7.38	9.79	2.57	0.39	0.4	-	99.99
THd	49.8	1.91	14.01	2.04	10.38	0.21	7	11.9	2.3	0.25	0.19	-	99.99
THe	50.12	1.5	12.87	1.91	9.76	0.21	8.64	12.55	2.11	0.19	0.14	-	100
THf	49.92	1.43	13.11	1.88	9.58	0.21	8.77	12.7	2.08	0.17	0.13	-	99.98
THh ^{2*}	48.97	1.37	15.96	1.70	8.67	0.16	7.85	13.46	1.65	0.10	0.09	-	100.00
THi	49.68	1.87	11.16	2.2	11.2	0.24	9.03	12.06	2.21	0.18	0.17	-	100
THj	52.43	2.14	11.39	2.14	10.91	0.23	6.9	9.57	3.12	0.87	0.3	-	100
THk	51.92	1.81	11.26	2.12	10.81	0.23	8.07	10.13	2.78	0.64	0.23	-	100

Table 7: Averages used in the calculation of plagioclase free liquids. ¹Includes data from Halldórsson, 2007. ²Includes data from Caracciolo et al., 2020. *Average of measured groundmass of Caracciolo et al., 2020.

Table 8 – Thermometry Results

Flow	Plagioclase Thermometry; Druitt et al., 2012 (°C)			Liquid Thermometry; Putirka, 2008 (°C)		
	Macrocrysts (>1000 µm)			Eq. 16	SEE = ±19 °C	
	Core	Mantle	Rim		2 kbar	6 kbar
THa ¹	1287 – 1353	-	1026 – 1202	1178	1209	1248
THb ¹	1323 – 1349	-	1122 – 1182	1166	1197	1236
THd	1316 – 1359	1189*	1014 – 1220	1201	1233	1271
THe	1310 – 1348	1261 – 1338	1157 – 1283	1222	1253	1292
THf	1327 – 1346	-	1207 – 1254	1229	1260	1299
THh ²	1306 – 1362	-	1168 – 1318	1222	1253	1292
THi ²	1277 – 1367	-	1193 – 1272	1209	1240	1279
THj	1324 – 1356	1231 – 1245	1041 – 1078	1165	1196	1235
THk	1305 – 1350	1227 – 1336	1036 – 1315	1190	1221	1260

Table 8: Thermometry results using a thermometer and thermobarometer presented in Druitt et al. (2012) and Putirka (2008), respectively. *one analysis (average of three EPMA spots). ¹Includes data from Halldórsson, 2007. ²Includes data from Caracciolo et al., 2020.

Table 9 – Olivine Fe - Mg Diffusion Modeling Results

Sample	Crystal	Flow	Temperature (°C)	2 kbar, C-axis	11 kbar, A-axis
THa-2	Macro 1	THb	1149	38	349
THd-3a	Macro 1	THd	1137	95	873
THd-3a	Macro 2	THd	1137	119	1089
THd-3a	Macro 4	THd	1137	66	605
THd-3a	Micro 2	THd	1137	66	604
THd-3a	Micro 5	THd	1137	42	387
THde-2	Macro 1	THe	1175	136	1233
THde-2	Macro 2	THe	1175	41	374
THde-2	Macro 3	THe	1175	48	431
THf-3b	Macro 1	THf	1177	112	1015
THf-3b	Macro 2	THf	1177	277	2512
THi-3	Macro 1	THi	1190	2	16
THj-2	Macro 1	THj	1153	51	465
THj-2	Macro 2	THj	1153	30	272

Table 9: Olivine diffusion modeling results. Raw transect data is given in Appendix E.

REFERENCES

- Ágústdóttir, T., Woods, J., Greenfield, T., Green, R. G., White, R. S., Winder, T., ... & Soosalu, H. (2016). Strike-slip Faulting During the 2014 Bárðarbunga-Holuhraun Dike Intrusion, Central Iceland. *GRL*.
- Blake, S. (1984). Magma mixing and hybridization processes at the alkalic, silicic, Torfajökull central volcano triggered by tholeiitic Veiðivötn fissuring, south Iceland. *Journal of Volcanology and Geothermal Research*, 22(1-2), 1-31.
- Bindeman, I. N., Davis, A. M., & Drake, M. J. (1998). Ion microprobe study of plagioclase-basalt partition experiments at natural concentration levels of trace elements. *Geochimica et Cosmochimica Acta*, 62(7), 1175-1193.
- Breddam, K. (2002). Kistufell: primitive melt from the Iceland mantle plume. *Journal of Petrology*, 43(2), 345-373.
- Büttner, S. H. (2012). Rock Maker: an MS Excel™ spreadsheet for the calculation of rock compositions from proportional whole rock analyses, mineral compositions, and modal abundance. *Mineralogy and Petrology*, 104(1-2), 129-135.
- Caracciolo, A., Bali, E., Guðfinnsson, G. H., Kahl, M., Halldórsson, S. A., Hartley, M. E., & Gunnarsson, H. (2020). Temporal evolution of magma and crystal mush storage conditions in the Bárðarbunga-Veiðivötn volcanic system, Iceland. *Lithos*, 352, 105234.
- Costa, F., & Dungan, M. (2005). Short time scales of magmatic assimilation from diffusion modeling of multiple elements in olivine. *Geology*, 33(10), 837-840.
- Costa, F., Dohmen, R., & Chakraborty, S. (2008). Time scales of magmatic processes from modeling the zoning patterns of crystals. *Reviews in Mineralogy and Geochemistry*, 69(1), 545-594.
- Cullen, A., Vicenzi, E., & McBirney, A. R. (1989). Plagioclase-ultraphyric basalts of the Galapagos Archipelago. *Journal of Volcanology and Geothermal Research*, 37(3-4), 325-337.
- DeMets, C., Gordon, R. G., & Argus, D. F. (2010). Geologically current plate motions. *Geophysical Journal International*, 181(1), 1-80.
- Drignon, M. J., Nielsen, R. L., Tepley III, F. J., & Bodnar, R. J. (2019). Upper mantle origin of plagioclase megacrysts from plagioclase-ultraphyric mid-oceanic ridge basalt. *Geology*, 47(1), 43-46.
- Druitt, T. H., Costa, F., Deloule, E., Dungan, M., & Scaillet, B. (2012). Decadal to monthly timescales of magma transfer and reservoir growth at a caldera volcano. *Nature*, 482(7383), 77-80.
- Eason, D. E., & Sinton, J. M. (2009). Lava shields and fissure eruptions of the Western Volcanic Zone, Iceland: Evidence for magma chambers and crustal interaction. *Journal of Volcanology and Geothermal Research*, 186(3-4), 331-348.
- Garcia, S., Arnaud, N. O., Angelier, J., Bergerat, F., & Homberg, C. (2003). Rift jump process in Northern Iceland since 10 Ma from $^{40}\text{Ar}/^{39}\text{Ar}$ geochronology. *Earth and Planetary Science Letters*, 214(3-4), 529-544.

- Gautason, B., 1988. Uppruni Plagíóklasbasalts. 4. árs verkefni, Háskóli Íslands. In Icelandic.
- Gronvold, K., & Jóhannesson, H. (1984). Eruption in Grímsvötn 1983; course of events and chemical studies of the tephra. *Jökull*, (34), 1-8.
- Gudmundsson, Ó. (2003). The dense root of the Iceland crust. *Earth and Planetary Science Letters*, 206(3-4), 427-440.
- Gudmundsson, M. T. and T. Högnadóttir (2002). Lava Thicknesses North and West of Þórisvatn: Results from Gravitymeasurements (in Icelandic). RH-01-2003. Reykjavík, Science Institute, University of Iceland: 30.
- Gunnarsson, B., Marsh, B. D., & Taylor Jr, H. P. (1998). Generation of Icelandic rhyolites: silicic lavas from the Torfajökull central volcano. *Journal of Volcanology and Geothermal Research*, 83(1-2), 1-45.
- Gurenko, A. A., & Sobolev, A. V. (2006). Crust-primitive magma interaction beneath neovolcanic rift zone of Iceland recorded in gabbro xenoliths from Midfell, SW Iceland. *Contributions to Mineralogy and Petrology*, 151(5), 495.
- Halldórsson, S. A. (2007). Petrology and Geochemistry of the Þjórsá Lava, Iceland. *Skemman: University of Iceland's Thesis Database*, 1-137. Retrieved 2020, from <https://skemman.is/>
- Halldórsson, S. A., Bali, E., Hartley, M. E., Neave, D. A., Peate, D. W., Guðfinnsson, G. H., ... & Jakobsson, S. (2018). Petrology and geochemistry of the 2014–2015 Holuhraun eruption, central Iceland: compositional and mineralogical characteristics, temporal variability and magma storage. *Contributions to Mineralogy and Petrology*, 173(8), 64.
- Halldórsson, S. A., Oskarsson, N., Gronvold, K., Sigurdsson, G., Sverrisdottir, G., & Steinþorsson, S. (2008). Isotopic-heterogeneity of the Thjorsa lava—implications for mantle sources and crustal processes within the Eastern Rift Zone, Iceland. *Chemical Geology*, 255(3-4), 305-316.
- Hansen, H., & Grönvold, K. (2000). Plagioclase ultraphyric basalts in Iceland: the mush of the rift. *Journal of Volcanology and Geothermal Research*, 98(1-4), 1-32.
- Hansteen, T.H., 1993. Lithospheric evolution of a tholeiitic picrite and a spatially associated plagioclase – phryic olivine tholeiite from the Hengill Area, SW Iceland. In: Investigations on fluid and silicate melt inclusions in minerals and their application to problems related to genesis and evolution of upper mantle and crustal rocks. PhD dissertation, University of Copenhagen
- Hardarson, B. S., & Godfrey Fitton, J. (1997). Mechanisms of crustal accretion in Iceland. *Geology*, 25(11), 1043-1046.
- Hartley, M. E., & Thordarson, T. (2013). The 1874–1876 volcano-tectonic episode at Askja, North Iceland: Lateral flow revisited. *Geochemistry, Geophysics, Geosystems*, 14(7), 2286-2309.
- Helo, C., Longpré, M. A., Shimizu, N., Clague, D. A., & Stix, J. (2011). Explosive eruptions at mid-ocean ridges driven by CO₂-rich magmas. *Nature Geoscience*, 4(4), 260-263.
- Hjartardóttir, Á. R., Einarsson, P., Magnúsdóttir, S., Björnsdóttir, P., & Brandsdóttir, B. (2016). Fracture systems of the Northern Volcanic Rift Zone, Iceland: an onshore part of the Mid-

Atlantic plate boundary. *Geological Society, London, Special Publications*, 420(1), 297-314.

- Hjartarson, A. Á. (1988). The Thjorsa lava, the largest Holocene lava flow on Earth. *Naturufraeðingurinn*, 58, 1-16.
- Hjartarson, A. Á. (2004). Hraunin Í Bárðardal. *Naturufraeðingurinn*, 72(3-4), 155-163.
- Hjartarson, A. Á. (2011). Víðáttumestu hraun Íslands. *Náttúrufræðingurinn*, 81, 37-49.
- Ingamells, C. O. (1970). Lithium metaborate flux in silicate analysis. *Analytica Chimica Acta*, 52(2), 323-334.
- Jakobsson, S. P. (1979). Petrology of recent basalts of the Eastern Volcanic Zone, Iceland.
- Jóhannesson, H., & Sæmundsson, K. (1998). Geological map of Iceland, 1: 500,000. *Bedrock Geology. Naturufrædistofnun Íslands, Reykjavík*.
- Kaldal, I., & Vilmundardóttir, E. G. (1986). Map of superficial deposits, Búrfell-Langalda, 3540 J. National Energy Authority, Hydro Power Division and the National Power Company. Reykjavík, Iceland.
- Kaldal, I., Vilmundardóttir, E. G., & Larsen, G. (1988). Map of superficial deposits, Sigalda-Veiðivötn, 3340 J. National Energy Authority, Hydro Power Division and the National Power Company. Reykjavík, Iceland
- Kohut, E. J., & Nielsen, R. L. (2003). Low-pressure phase equilibria of anhydrous anorthite-bearing mafic magmas. *Geochemistry, Geophysics, Geosystems*, 4(7).
- Kristmannsdóttir, H. (1971). Anorthosite inclusions in Tertiary dolerite from the island groups Hrappsey and Purkey, West Iceland. *The Journal of Geology*, 79(6), 741-748.
- Kurz, M. D., Meyer, P. S., & Sigurdsson, H. (1985). Helium isotopic systematics within the neovolcanic zones of Iceland. *Earth and Planetary Science Letters*, 74(4), 291-305.
- Kushiro, I., & Fujii, T. (1977). Floatation of plagioclase in magma at high pressures and its bearing on the origin of anorthosite. *Proceedings of the Japan Academy, Series B*, 53(7), 262-266.
- LaFemina, P. C., Dixon, T. H., Malervisi, R., Árnadóttir, T., Sturkell, E., Sigmundsson, F., & Einarsson, P. (2005). Geodetic GPS measurements in south Iceland: Strain accumulation and partitioning in a propagating ridge system. *Journal of Geophysical Research: Solid Earth*, 110(B11).
- Lange, A. E., Nielsen, R. L., Tepley III, F. J., & Kent, A. J. (2013). The petrogenesis of plagioclasephyric basalts at mid-ocean ridges. *Geochemistry, Geophysics, Geosystems*, 14(8), 3282-3296.
- Larsen, G., & Gudmundsson, M. T. (2014). Volcanic system: Bárðarbunga system. Catalogue of Icelandic Volcanoes, 1-11. Retrieved 2020, from <http://icelandicvolcanos.is/>
- Le Bas, M., Maitre, R. L., Streckeisen, A., Zanettin, B., & IUGS Subcommission on the Systematics of Igneous Rocks. (1986). A chemical classification of volcanic rocks based on the total alkali-silica diagram. *Journal of petrology*, 27(3), 745-750.

- Macdonald, R., McGarvie, D. W., Pinkerton, H., Smith, R. L., & Palacz, A. (1990). Petrogenetic evolution of the Torfajökull Volcanic Complex, Iceland I. Relationship between the magma types. *Journal of Petrology*, 31(2), 429-459.
- Maclennan, J., McKenzie, D., Hilton, F., Gronvöld, K., & Shimizu, N. (2003). Geochemical variability in a single flow from northern Iceland. *Journal of Geophysical Research: Solid Earth*, 108(B1), ECV-4.
- McGarvie, D. W., Macdonald, R., Pinkerton, H., & Smith, R. L. (1990). Petrogenetic evolution of the Torfajökull Volcanic Complex, Iceland II. The role of magma mixing. *Journal of Petrology*, 31(2), 461-481.
- Meyer, P. S., Sigurdsson, H., & Schilling, J. G. (1985). Petrological and geochemical variations along Iceland's neovolcanic zones. *Journal of Geophysical Research: Solid Earth*, 90(B12), 10043-10072.
- Miller, J. (1989). *The 10th century eruption of Eldgjá, southern Iceland* (Vol. 8903). Nordic Volcanological Institute, University of Iceland.
- Neave, D. A., MacLennan, J., Hartley, M. E., Edmonds, M., & Thordarson, T. (2014). Crystal storage and transfer in basaltic systems: the Skuggafjöll eruption, Iceland. *Journal of Petrology*, 55(12), 2311-2346.
- Nielsen, R. L., Sours-Page, R. E., & Harpp, K. S. (2000). Role of a Cl-bearing flux in the origin of depleted ocean floor magmas. *Geochemistry, Geophysics, Geosystems*, 1(5).
- Nielsen, R. L., Ustunisik, G., Lange, A. E., Tepley III, F. J., & Kent, A. J. (2020). Trace Element and Isotopic Characteristics of Plagioclase Megacrysts in Plagioclase Ultraphyric Basalts (PUB). *Geochemistry, Geophysics, Geosystems*, 21(2), e2019GC008638.
- Óladóttir, B. A., Larsen, G., & Sigmarsdóttir, O. (2011). Holocene volcanic activity at Grímsvötn, Bárðarbunga and Kverkfjöll subglacial centres beneath Vatnajökull, Iceland. *Bulletin of Volcanology*, 73(9), 1187-1208.
- Óskarsson, B. V., Andersen, C. B., Riishuus, M. S., Sørensen, E. V., & Tegner, C. (2017). The mode of emplacement of Neogene flood basalts in Eastern Iceland: The plagioclase ultraphyric basalts in the Grænavatn group. *Journal of Volcanology and Geothermal Research*, 332, 26-50.
- Oskarsson, N., Sigvaldason, G. E., & Steinhorsson, S. (1982). A dynamic model of rift zone petrogenesis and the regional petrology of Iceland. *Journal of Petrology*, 23(1), 28-74.
- Passmore, E., MacLennan, J., Fitton, G., & Thordarson, T. (2012). Mush disaggregation in basaltic magma chambers: evidence from the AD 1783 Laki eruption. *Journal of Petrology*, 53(12), 2593-2623.
- Peate, D. W., Breddam, K., Baker, J. A., Kurz, M. D., Barker, A. K., Prestvik, T., ... & Skovgaard, A. C. (2010). Compositional characteristics and spatial distribution of enriched Icelandic mantle components. *Journal of Petrology*, 51(7), 1447-1475.
- Pedersen, G. B. M., Höskuldsson, A., Dürig, T., Thordarson, T., Jónsdóttir, I., Riishuus, M. S., ... & Sigmundsson, F. (2017). Lava field evolution and emplacement dynamics of the 2014–2015 basaltic fissure eruption at Holuhraun, Iceland. *Journal of Volcanology and Geothermal Research*, 340, 155-169.

- Pinton, A., Giordano, G., Speranza, F., & Þórðarson, Þ. (2018). Paleomagnetism of Holocene lava flows from the Reykjanes Peninsula and the Tungnaá lava sequence (Iceland): implications for flow correlation and ages. *Bulletin of Volcanology*, 80(1), 10.
- Putirka, K. D. (2008). Thermometers and barometers for volcanic systems. *Reviews in mineralogy and geochemistry*, 69(1), 61-120.
- Saemundsson, K. (1978). Fissure swarms and central volcanoes of the neovolcanic zones of Iceland in Crustal evolution in northern Britain and adjacent regions. *Geological journal Liverpool*, (10), 415-432.
- Schmidt, P., Lund, B., Hieronymus, C., MacLennan, J., Árnadóttir, T., & Pagli, C. (2013). Effects of present-day deglaciation in Iceland on mantle melt production rates. *Journal of Geophysical Research: Solid Earth*, 118(7), 3366-3379.
- Sigbjarnarson, G. (1988). Krepputunga og Brúardalir: lýsingar á korteiningum jarðfræðikorts. *Orkustofnun*.
- Sigmarsson, O., & Halldórsson, S. A. (2015). Delimiting Bárðarbunga and Askja volcanic systems with Sr-and Nd-isotope ratios. *Jökull*, 65, 17-27.
- Sigmundsson, F., Hooper, A., Hreinsdóttir, S., Vogfjörd, K. S., Ófeigsson, B. G., Heimisson, E. R., ... & Drouin, V. (2015). Segmented lateral dyke growth in a rifting event at Bárðarbunga volcanic system, Iceland. *Nature*, 517(7533), 191-195.
- Sigurdsson, H., & Sparks, R. S. J. (1981). Petrology of rhyolitic and mixed magma ejecta from the 1875 eruption of Askja, Iceland. *Journal of Petrology*, 22(1), 41-84.
- Sigurgeirsson, M., Á. Hjartarson, I. Kaldal, K. Sæmundsson, S. G. Kristinsson and S. Víkingsson (2015). Jarðfræðikort af Norðurgosbelti. Syðri hluti – Ódáðhraun. *Reykjavík, Iceland Geosurvey*, 1.
- Sinton, J., Grönvold, K., & Sæmundsson, K. (2005). Postglacial eruptive history of the western volcanic zone, Iceland. *Geochemistry, Geophysics, Geosystems*, 6(12).
- Svavarsdóttir, S. I. (2017). Geochemistry and petrology of Holocene lavas in the Bárðardalur region and their association with the Bárðarbunga volcanic system. *Skemman: University of Iceland's Thesis Database*, 1-130. Retrieved 2020, from <https://skemman.is/>
- Svavarsdóttir, S. I., Halldórsson, S. A., & Guðfinnsson, G. H. (2017). Geochemistry and petrology of Holocene lavas in the Bárðardalur region, N-Iceland. Part I: Geochemical constraints on source provenance. *Jökull*, 67, 17-42.
- Thorarinsson, S. (1969). The Lakagigar eruption of 1783. *Bulletin Volcanologique*, 33(3), 910-929.
- Thordarson, T., & Höskuldsson, Á. (2008). Postglacial volcanism in Iceland. *Jökull*, 58(198), e228.
- Thordarson, T., & Larsen, G. (2007). Volcanism in Iceland in historical time: Volcano types, eruption styles and eruptive history. *Journal of Geodynamics*, 43(1), 118-152.
- Thordarson, T., & Self, S. (1993). The Laki (Skaftár Fires) and Grímsvötn eruptions in 1783–1785. *Bulletin of Volcanology*, 55(4), 233-263.

- Thordarson, T., & Self, S. (2003). Atmospheric and environmental effects of the 1783–1784 Laki eruption: A review and reassessment. *Journal of Geophysical Research: Atmospheres*, 108(D1), AAC-7.
- Thordarson, T., Miller, D. J., Larsen, G., Self, S., & Sigurdsson, H. (2001). New estimates of sulfur degassing and atmospheric mass-loading by the 934 AD Eldgjá eruption, Iceland. *Journal of Volcanology and Geothermal Research*, 108(1-4), 33-54.
- Thordarson, T., Self, S., Miller, D. J., Larsen, G., & Vilmundardóttir, E. G. (2003). Sulphur release from flood lava eruptions in the Veidivötn, Grímsvötn and Katla volcanic systems, Iceland. *Geological Society, London, Special Publications*, 213(1), 103-121.
- Thordarson, T., Self, S., Oskarsson, N., & Hulsebosch, T. (1996). Sulfur, chlorine, and fluorine degassing and atmospheric loading by the 1783–1784 AD Laki (Skaftár Fires) eruption in Iceland. *Bulletin of Volcanology*, 58(2-3), 205-225.
- Ustunisik, G. K., Nielsen, R. L., & Walker, D. (2020). The Missing Magmas of MOR. *Presented at Goldschmidt 2020 (Online)*. <https://doi.org/10.46427/gold2020.2654>
- Vilmundardottir, E. G. (1977). Tungnarhraun, Orustofnun geologic report. *Rep. OS ROD*, 7702, 156.
- Walker, G. P. L. (1963). The Breiddalur central volcano, eastern Iceland. *Quarterly Journal of the Geological Society*, 119(1-4), 29-63.
- Witham, C. S., & Oppenheimer, C. (2004). Mortality in England during the 1783–4 Laki Craters eruption. *Bulletin of Volcanology*, 67(1), 15-26.
- Wolfe, C. J., Bjarnason, I. T., VanDecar, J. C., & Solomon, S. C. (1997). Seismic structure of the Iceland mantle plume. *Nature*, 385(6613), 245-247.
- Yang, H. J., Frey, F. A., Rhodes, J. M., & Garcia, M. O. (1996). Evolution of Mauna Kea volcano: Inferences from lava compositions recovered in the Hawaii Scientific Drilling Project. *Journal of Geophysical Research: Solid Earth*, 101(B5), 11747-11767.
- Zellmer, G. F., Rubin, K. H., Grönvold, K., & Jurado-Chichay, Z. (2008). On the recent bimodal magmatic processes and their rates in the Torfajökull–Veidivötn area, Iceland. *Earth and Planetary Science Letters*, 269(3-4), 388-398.

APPENDICES

Appendix A – Whole Rock Chemistry

Sample #	THa-1	THa-2	THd-1	THd-2a	THd-2b	THd-3a	THd-3b	THde-1	THde-2	THde-3	THde-4
Flow	THb	THb	THd	THd	THd	THd	THd	THe	THe	THe	THe
Latitude	63.8286193	63.9895586	64.0728	64.07289	64.07289	64.0723	64.0723	64.1819	64.1826	64.18729	64.18433
Longitude	-21.027841	-20.63805	-19.85442	-19.85594	-19.85594	-19.858	-19.858	-19.41861	-19.4165	-19.39717	-19.38642
<i>SiO₂</i>	48.95	49.04	48.58	47.59	47.94	48.44	48.57	49.18	48.91	49.33	48.95
<i>TiO₂</i>	2.42	1.99	1.58	1.53	1.43	1.44	1.61	1.12	1.14	1.15	1.19
<i>Al₂O₃</i>	13.61	14.77	17.29	16.82	17.76	18.03	17.22	16.98	16.46	16.90	16.28
<i>Fe₂O₃</i>	14.76	13.35	11.34	11.08	10.56	10.56	11.47	10.07	10.17	10.31	10.53
<i>MnO</i>	0.23	0.21	0.18	0.17	0.16	0.16	0.18	0.16	0.16	0.16	0.17
<i>MgO</i>	5.93	6.58	6.27	6.11	6.12	6.18	6.23	7.54	7.56	7.57	7.63
<i>CaO</i>	10.49	11.63	12.62	12.37	12.75	12.87	12.63	13.53	13.41	13.51	13.28
<i>Na₂O</i>	2.57	2.32	2.14	2.10	2.08	2.09	2.16	1.91	1.92	1.93	1.93
<i>K₂O</i>	0.34	0.27	0.21	0.19	0.18	0.20	0.19	0.12	0.16	0.18	0.12
<i>P₂O₅</i>	0.27	0.23	0.17	0.16	0.15	0.15	0.16	0.11	0.10	0.11	0.11
<i>BaO</i>	0.01	0.00	0.00	0.00	0.00	0.00	0.00	0.00	0.00	0.00	0.00
<i>SrO</i>	0.02	0.02	0.02	0.02	0.02	0.02	0.02	0.02	0.02	0.02	0.02
<i>Total</i>	99.61	100.41	100.40	98.15	99.15	100.14	100.45	100.75	100.01	101.16	100.22
THde-5	THde-6	THde-7	THde-8	THe-1a	THe-2	THe-3a	THe-3b	THe-4	THj-1a	THj-1b	THj-3
THe	THe	THe	THe	THe	THe	THe	THe	THe	THe	THe	THe
64.19641	64.19625	64.17915	64.20143	64.14978	64.14963	64.14923	64.14923	64.14834	64.19373	64.19373	64.20138
-19.34724	-19.36275	-19.35162	-19.29079	-19.53728	-19.53844	-19.53524	-19.53524	-19.53347	-19.35326	-19.35326	-19.29952
49.00	48.92	48.85	48.95	48.66	48.83	48.20	48.55	48.17	48.98	48.51	49.17
1.15	1.14	1.18	1.16	1.18	1.18	1.14	1.16	1.17	1.17	1.14	1.65
16.52	16.88	16.18	16.61	16.29	16.22	16.30	16.36	15.97	16.37	16.18	14.53
10.28	10.15	10.47	10.24	10.36	10.47	10.18	10.27	10.51	10.52	10.33	12.81
0.16	0.16	0.17	0.16	0.17	0.17	0.16	0.16	0.17	0.17	0.16	0.20
7.55	7.51	7.56	7.51	7.54	7.73	7.61	7.52	7.59	7.63	7.68	7.68
13.41	13.50	13.24	13.33	13.17	13.35	13.15	13.29	13.17	13.31	13.19	12.56
1.94	1.90	1.93	1.93	1.91	1.87	1.82	1.87	1.90	1.95	1.92	2.14
0.18	0.12	0.18	0.13	0.15	0.11	0.12	0.13	0.14	0.17	0.17	0.17
0.11	0.10	0.11	0.11	0.10	0.11	0.10	0.11	0.11	0.11	0.11	0.15
0.00	0.00	0.00	0.00	0.00	0.00	0.00	0.00	0.00	0.00	0.00	0.00
0.02	0.02	0.02	0.02	0.02	0.02	0.02	0.02	0.02	0.02	0.02	0.02
100.32	100.40	99.89	100.16	99.54	100.07	98.81	99.44	98.91	100.39	99.41	101.08

<i>Sample #</i>	THf-1a	THf-1b	THf-2a	THf-2b	THf-3a	THf-3b	THf-4a	THf-4b	THi-1a	THi-1b	THi-2
<i>Flow</i>	THf	THi	THi	THi							
<i>Latitude</i>	64.05939	64.05939	64.05966	64.05966	64.06242	64.06242	64.06475	64.06475	64.12794	64.12794	64.18184
<i>Longitude</i>	-19.86431	-19.86431	-19.86538	-19.86538	-19.86678	-19.86678	-19.86789	-19.86789	-19.66824	-19.66824	-19.4166
<i>SiO₂</i>	48.63	48.94	48.49	48.37	48.64	49.10	48.58	48.89	48.73	48.61	48.82
<i>TiO₂</i>	1.17	1.16	1.19	1.14	1.14	1.15	1.15	1.16	1.50	1.52	1.51
<i>Al₂O₃</i>	16.49	16.76	16.40	16.58	16.81	16.98	16.66	16.49	14.86	14.89	14.86
<i>Fe₂O₃</i>	10.33	10.30	10.46	10.19	10.14	10.29	10.28	10.30	12.18	12.13	12.25
<i>MnO</i>	0.17	0.16	0.17	0.16	0.16	0.16	0.16	0.16	0.19	0.19	0.19
<i>MgO</i>	7.58	7.53	7.56	7.56	7.48	7.57	7.61	7.64	7.79	7.78	7.78
<i>CaO</i>	13.42	13.55	13.29	13.38	13.50	13.61	13.43	13.44	12.81	12.81	12.80
<i>Na₂O</i>	1.96	1.95	1.88	1.92	1.93	1.96	1.95	1.93	2.02	2.05	2.07
<i>K₂O</i>	0.15	0.14	0.14	0.14	0.13	0.13	0.15	0.14	0.14	0.12	0.15
<i>P₂O₅</i>	0.11	0.10	0.11	0.10	0.10	0.11	0.11	0.11	0.14	0.14	0.14
<i>BaO</i>	0.00	0.00	0.00	0.00	0.00	0.00	0.00	0.00	0.00	0.00	0.00
<i>SrO</i>	0.02	0.02	0.02	0.02	0.02	0.02	0.02	0.02	0.02	0.02	0.02
<i>Total</i>	100.01	100.61	99.70	99.55	100.06	101.07	100.11	100.28	100.37	100.26	100.59
THi-3	THi-4	THj-2	THj-4	THj-5	THj-6	THj-7	THj-8	THk-1	THk-2	THk-3	THk-4
THi	THi	THj	THj	THj	THj	THj	THj	THk	THk	THk	THk
64.18162	64.16862	64.18336	64.20405	64.21406	64.1298	64.18278	64.16086	64.08576	64.08365	64.09319	64.07784
-19.41764	-19.26878	-19.36061	-19.3069	-19.28562	-19.12123	-19.25495	-19.18993	-19.01645	-19.03384	-19.04055	-19.05323
48.82	48.58	50.45	50.28	50.76	50.27	50.35	50.86	50.06	50.17	50.70	50.43
1.50	1.48	1.82	1.78	1.83	1.53	1.76	1.57	1.48	1.44	1.51	1.44
15.14	14.72	15.17	15.03	15.17	14.93	15.04	15.44	15.35	15.10	15.05	15.12
12.09	12.15	11.66	11.77	11.90	11.59	11.82	11.44	11.39	11.58	11.73	11.63
0.19	0.19	0.19	0.19	0.19	0.19	0.19	0.19	0.19	0.19	0.19	0.19
7.83	7.77	5.97	6.04	5.98	6.15	6.02	6.10	6.38	6.85	6.34	6.81
12.94	12.74	10.75	10.77	10.79	10.81	10.69	10.91	11.24	11.63	11.10	11.49
2.10	2.05	2.76	2.72	2.75	2.68	2.74	2.72	2.56	2.37	2.62	2.46
0.15	0.15	0.70	0.70	0.72	0.66	0.73	0.66	0.56	0.44	0.61	0.48
0.14	0.14	0.24	0.24	0.25	0.23	0.23	0.23	0.22	0.16	0.23	0.16
0.00	0.00	0.01	0.01	0.01	0.01	0.01	0.01	0.01	0.01	0.01	0.01
0.02	0.02	0.03	0.03	0.03	0.02	0.03	0.02	0.02	0.02	0.02	0.02
100.93	99.99	99.76	99.56	100.37	99.06	99.61	100.15	99.45	99.95	100.11	100.24

Values given in weight percent oxide.

Appendix B – Olivine Chemistry

<i>Spot Name</i>	<i>SiO₂</i>	<i>TiO₂</i>	<i>Al₂O₃</i>	<i>Cr₂O₃</i>	<i>FeO</i>	<i>MnO</i>	<i>MgO</i>	<i>CaO</i>	<i>Na₂O</i>	<i>K₂O</i>	<i>Total</i>
THa1.ol_micro2_1	38.39	0.02	0.02	0.00	23.81	0.32	37.43	0.30	0.01	-0.01	100.29
THa1.ol_micro2_2	37.72	0.02	0.03	0.00	27.54	0.36	34.59	0.33	-0.01	-0.01	100.60
THa1.ol_micro2_3	37.95	0.01	0.03	0.00	26.04	0.36	35.82	0.32	0.00	-0.01	100.54
THa1.ol_micro3_1	39.03	0.01	0.04	0.01	21.12	0.29	39.91	0.38	0.01	0.00	100.81
THa1.ol_micro3_2	39.69	0.01	0.03	0.02	16.89	0.24	43.30	0.34	0.00	0.01	100.52
THa1.ol_micro3_3	39.22	0.00	0.03	0.02	18.74	0.24	41.71	0.37	0.00	0.00	100.33
THa1.ol_groundmass_9	37.28	0.05	0.03	0.00	29.88	0.40	32.62	0.41	0.02	0.00	100.69
THa2.ol_groundmass_1	37.03	0.05	0.30	0.00	26.74	0.37	34.38	0.41	0.00	0.01	99.30
THa2.ol_groundmass_4	37.81	0.04	0.19	0.01	26.52	0.36	34.88	0.40	0.01	0.01	100.23
THa2.ol_groundmass_10	39.08	0.17	0.50	0.01	25.32	0.36	33.57	1.67	0.07	0.01	100.77
THd3a.ol_micro1_1	38.70	0.00	0.03	0.01	22.56	0.31	38.63	0.34	0.07	0.05	100.71
THd3a.ol_micro1_2	39.04	0.01	0.03	0.01	20.49	0.29	40.53	0.33	0.01	0.00	100.73
THd3a.ol_micro1_3	38.36	0.02	0.04	0.00	24.20	0.34	37.33	0.31	0.00	0.02	100.61
THd3a.ol_micro2_1	40.33	0.00	0.04	0.02	14.22	0.22	45.29	0.36	0.01	0.00	100.49
THd3a.ol_micro2_2	40.19	0.00	0.03	0.03	14.82	0.22	44.94	0.37	0.00	0.01	100.62
THd3a.ol_micro2_3	40.00	0.00	0.03	0.02	15.69	0.23	44.12	0.36	0.01	-0.01	100.48
THd3a.ol_micro5_lighter_1	37.72	0.03	0.01	0.00	26.44	0.36	35.48	0.31	0.02	0.00	100.39
THd3a.ol_micro5_lighter_2	37.54	0.03	0.03	0.00	28.27	0.39	33.85	0.35	0.02	0.00	100.48
THd3a.ol_micro5_lighter_3	37.96	0.00	0.03	0.01	25.89	0.34	35.93	0.33	0.00	0.01	100.50
THd3a.groundmass.ol_4	37.17	0.06	0.02	0.00	28.73	0.39	33.37	0.41	0.00	0.02	100.18
THd3a.groundmass.ol_7	37.27	0.06	0.03	0.00	28.61	0.40	33.52	0.38	0.00	-0.01	100.27
THd3a.groundmass.ol_9	37.53	0.05	0.03	0.01	28.24	0.40	33.73	0.37	0.01	0.00	100.35
THde2.ol_micro1_1	39.77	0.00	0.03	0.01	16.47	0.23	43.50	0.37	0.01	0.01	100.38
THde2.ol_micro1_2	39.77	-0.01	0.04	0.01	16.59	0.24	43.61	0.35	0.00	0.00	100.61
THde2.ol_micro1_3	39.73	0.01	0.03	0.00	16.74	0.23	43.28	0.37	0.00	-0.01	100.39
THde2.ol_micro3_1	39.06	0.01	0.06	0.00	19.32	0.25	40.65	0.37	0.01	0.02	99.75
THde2.ol_micro3_2	39.29	-0.01	0.03	0.01	17.23	0.24	42.59	0.39	0.01	0.00	99.80
THde2.ol_micro3_3	39.25	0.00	0.01	0.01	19.51	0.27	41.13	0.33	0.01	0.01	100.54
THde2.ol_micro4_1	39.47	0.01	0.03	0.02	14.26	0.21	44.38	0.48	0.03	0.01	98.91
THde2.ol_micro4_2	40.31	0.00	0.05	0.02	14.23	0.21	45.24	0.38	0.01	0.01	100.46
THde2.ol_micro4_3	40.37	0.02	0.05	0.02	14.45	0.21	45.22	0.39	0.02	0.02	100.75
THde2.ol_micro7_1	39.71	0.01	0.05	0.01	17.36	0.24	42.93	0.39	0.00	0.01	100.71
THde2.ol_micro7_2	39.92	0.02	0.05	0.01	16.89	0.25	43.45	0.36	0.01	0.00	100.97
THde2.ol_micro7_3	39.69	0.01	0.03	0.01	17.12	0.25	43.21	0.35	0.01	-0.01	100.69
THde2.groundmass.ol_7	38.60	0.04	0.03	0.00	22.65	0.33	38.49	0.45	0.01	0.00	100.58
THde2.groundmass.ol_9	38.43	0.05	0.04	0.00	22.51	0.32	38.30	0.45	0.01	0.01	100.10
THde2.cpx_micro1_1	39.84	0.00	0.04	0.02	16.20	0.25	43.43	0.35	0.02	0.02	100.17

<i>Spot Name</i>	<i>SiO₂</i>	<i>TiO₂</i>	<i>Al₂O₃</i>	<i>Cr₂O₃</i>	<i>FeO</i>	<i>MnO</i>	<i>MgO</i>	<i>CaO</i>	<i>Na₂O</i>	<i>K₂O</i>	<i>Total</i>
THde2_cpx_micro1_2	39.42	0.00	0.04	0.01	18.40	0.25	41.61	0.38	0.01	0.01	100.13
THde2_cpx_micro1_3	39.36	0.00	0.05	0.01	18.32	0.25	41.86	0.35	0.01	0.01	100.23
THd3a_cpx_micro2_1	38.20	0.03	0.04	0.00	25.61	0.36	36.38	0.32	0.01	-0.01	100.95
THd3a_cpx_micro2_2	38.07	0.02	0.03	0.01	26.53	0.36	35.52	0.35	0.00	0.00	100.89
THd3a_cpx_micro2_3	38.73	0.01	0.03	0.00	23.57	0.32	38.14	0.33	0.00	0.00	101.13
THf3b_oliv_micro3_1	39.91	0.02	0.04	0.01	17.32	0.24	43.08	0.32	0.01	0.01	100.97
THf3b_oliv_micro3_2	40.21	0.01	0.03	0.03	15.66	0.23	44.45	0.37	0.01	0.01	101.00
THf3b_oliv_micro3_3	40.09	0.01	0.03	0.02	15.57	0.23	44.40	0.35	0.01	0.01	100.73
THf3b_oliv_micro4_1	40.20	-0.01	0.03	0.01	15.74	0.22	44.50	0.34	0.00	0.02	101.06
THf3b_oliv_micro4_2	40.24	0.01	0.05	0.02	15.25	0.21	44.87	0.39	0.00	0.00	101.03
THf3b_oliv_micro4_3	40.17	0.00	0.04	0.02	14.94	0.22	44.95	0.38	0.01	0.01	100.74
THf3b_groundmass_oliv_3	38.83	0.01	0.04	0.01	22.06	0.32	39.17	0.40	0.01	-0.01	100.83
THf3b_groundmass_oliv_4	38.72	0.04	0.05	0.00	22.10	0.32	39.14	0.44	0.01	-0.01	100.81
THf3b_groundmass_oliv_5	39.37	0.02	0.03	0.00	20.73	0.28	40.43	0.37	0.01	-0.01	101.26
THf3b_groundmass_oliv_6	38.86	-0.01	0.02	0.01	21.96	0.29	39.52	0.36	0.01	0.01	101.04
THi3_oliv_micro2_1	40.25	0.01	0.03	0.01	15.94	0.23	44.30	0.35	0.00	-0.01	101.13
THi3_oliv_micro2_2	40.01	0.02	0.04	0.01	15.84	0.23	44.39	0.36	0.00	-0.01	100.90
THi3_oliv_micro2_3	40.06	0.01	0.04	0.01	15.98	0.24	44.31	0.33	0.00	0.00	100.99
THi3_oliv_micro3_1	40.32	0.01	0.03	0.01	14.98	0.21	45.07	0.34	0.01	0.00	100.98
THi3_oliv_micro3_2	40.42	0.01	0.04	0.01	15.03	0.23	45.16	0.35	0.01	-0.01	101.25
THi3_oliv_micro3_3	40.12	0.01	0.05	0.01	14.96	0.21	44.95	0.35	0.00	0.00	100.67
THi3_oliv_micro4_1	39.95	0.01	0.04	0.00	16.66	0.24	43.67	0.38	0.00	0.01	100.95
THi3_oliv_micro4_2	39.70	0.01	0.04	0.00	17.51	0.26	43.18	0.39	-0.01	0.00	101.08
THi3_oliv_micro4_3	39.77	0.02	0.03	0.01	17.21	0.25	43.32	0.36	0.01	-0.02	100.98
THi3_oliv_micro5_1	39.99	0.00	0.03	0.01	16.22	0.24	44.25	0.35	-0.02	-0.01	101.09
THi3_oliv_micro5_2	40.04	0.02	0.03	0.01	16.18	0.24	44.12	0.36	0.01	0.00	101.00
THi3_oliv_micro5_3	39.67	0.02	0.03	0.01	17.79	0.27	42.96	0.37	0.01	0.01	101.12
THi3_groundmass_oliv_1	39.37	0.01	0.04	0.01	20.34	0.28	40.62	0.39	0.00	0.00	101.05
THi3_groundmass_oliv_8	39.69	0.04	0.03	0.01	17.27	0.24	43.31	0.37	0.00	0.01	100.95
THi3_groundmass_oliv_9	36.67	0.02	0.04	0.00	32.38	0.43	30.31	0.36	0.01	0.00	100.22
THi3_groundmass_oliv_10	37.56	0.02	0.03	0.01	28.81	0.39	33.63	0.34	0.00	0.01	100.80
THj2_groundmass_oliv_3	37.66	0.04	0.02	0.00	28.05	0.41	34.14	0.40	0.00	-0.02	100.72
THj2_groundmass_oliv_4	37.63	0.03	0.04	0.00	27.76	0.40	34.33	0.40	0.01	-0.02	100.60
THj2_groundmass_oliv_6	36.50	0.09	0.04	0.00	32.79	0.48	30.08	0.43	0.01	0.00	100.43
THj2_groundmass_oliv_8	37.72	0.06	0.02	0.00	27.75	0.41	34.27	0.44	0.01	0.00	100.68
THj2_groundmass_oliv_9	37.16	0.08	0.04	0.00	29.08	0.41	33.00	0.44	0.02	0.02	100.26
THk2_oliv_micro2_1	39.97	0.01	0.03	0.01	16.11	0.23	44.07	0.37	0.01	-0.02	100.81

<i>Spot Name</i>	<i>SiO₂</i>	<i>TiO₂</i>	<i>Al₂O₃</i>	<i>Cr₂O₃</i>	<i>FeO</i>	<i>MnO</i>	<i>MgO</i>	<i>CaO</i>	<i>Na₂O</i>	<i>K₂O</i>	<i>Total</i>
THk2_oliv_micro2_2	39.91	0.00	0.03	0.01	16.05	0.23	44.00	0.39	0.01	0.00	100.63
THk2_oliv_micro2_3	39.93	-0.01	0.03	0.00	16.22	0.24	43.98	0.37	0.01	0.01	100.79
THk2_groundmass_oliv_10	38.51	0.02	0.03	0.00	21.85	0.33	38.94	0.40	-0.02	-0.01	100.09
THk3_oliv_micro1_1	39.87	0.02	0.03	0.01	16.53	0.25	43.92	0.36	0.00	0.00	100.99
THk3_oliv_micro1_2	40.01	0.01	0.03	0.01	16.49	0.24	43.88	0.37	0.00	-0.01	101.04
THk3_oliv_micro1_3	40.06	-0.01	0.03	0.01	16.48	0.24	43.94	0.35	0.01	-0.01	101.11
THk3_oliv_micro2_1	39.88	0.01	0.04	0.01	16.38	0.23	44.02	0.36	-0.01	0.00	100.93
THk3_oliv_micro2_2	40.10	0.01	0.02	0.01	16.45	0.24	43.88	0.37	0.01	0.00	101.09
THk3_oliv_micro2_3	39.82	0.00	0.03	0.00	16.40	0.24	43.92	0.38	0.00	0.00	100.79
THk3_groundmass_oliv_1	38.21	0.05	0.03	0.01	22.79	0.34	37.81	0.43	0.01	0.01	99.67
THk3_groundmass_oliv_3	38.08	0.06	0.03	0.00	23.78	0.37	37.15	0.48	0.01	0.01	99.98
THk3_groundmass_oliv_8	38.17	0.03	0.04	0.00	23.59	0.34	37.36	0.51	0.01	0.01	100.05
THk3_groundmass_oliv_10	38.13	0.02	0.02	0.00	23.98	0.34	37.18	0.48	0.01	0.03	100.19

Appendix C - Plagioclase

<i>Spot Name</i>	<i>SiO₂</i>	<i>TiO₂</i>	<i>Al₂O₃</i>	<i>Cr₂O₃</i>	<i>FeO</i>	<i>MnO</i>	<i>MgO</i>	<i>CaO</i>	<i>Na₂O</i>	<i>K₂O</i>	<i>Total</i>
THa1_plag1_rim_1	52.39	0.10	29.94	0.01	0.66	0.01	0.17	13.20	3.96	0.09	100.53
THa1_plag1_rim_2	51.37	0.07	30.71	0.01	0.73	0.00	0.21	14.29	3.36	0.09	100.84
THa1_plag1_rim_3	51.56	0.08	30.37	0.00	0.72	0.00	0.23	13.95	3.50	0.05	100.47
THa1_plag1_core_1	46.06	0.04	34.35	0.00	0.43	0.00	0.21	18.12	1.18	0.00	100.39
THa1_plag1_core_2	46.94	0.02	33.97	0.00	0.43	0.00	0.25	17.89	1.50	0.01	101.02
THa1_plag1_core_3	46.81	0.00	34.08	0.00	0.43	0.00	0.25	17.68	1.48	0.02	100.76
THa1.ol_plag_cluster1_plag_1	52.47	0.07	30.01	0.01	0.77	0.00	0.23	13.43	3.78	0.08	100.84
THa1.ol_plag_cluster1_plag_2	51.50	0.06	30.72	0.00	0.77	0.00	0.19	14.19	3.47	0.08	100.98
THa1.ol_plag_cluster1_plag_3	50.59	0.06	30.92	0.00	0.76	0.00	0.21	14.46	3.19	0.05	100.25
THa1_plag_micro1_1	47.68	0.02	33.29	0.00	0.54	0.01	0.26	17.08	1.82	0.03	100.73
THa1_plag_micro1_2	47.62	0.03	33.28	0.00	0.52	0.01	0.26	17.25	1.83	0.01	100.82
THa1_plag_micro1_3	47.57	0.02	33.40	0.00	0.54	0.00	0.26	17.06	1.81	0.01	100.67
THa1_plag_micro2_1	49.80	0.06	31.42	0.00	0.57	0.01	0.30	15.23	2.81	0.04	100.23
THa1_plag_micro2_2	49.71	0.04	31.64	0.00	0.63	0.00	0.28	15.52	2.72	0.03	100.58
THa1_plag_micro2_3	49.33	0.04	32.14	0.00	0.58	0.00	0.26	15.78	2.56	0.01	100.71
THa1_plag_micro3_1	47.12	0.03	33.72	0.00	0.61	0.01	0.18	17.27	1.67	0.03	100.62
THa1_plag_micro3_2	46.72	0.03	34.06	0.00	0.54	0.01	0.18	17.63	1.51	0.01	100.68
THa1_plag_micro3_3	47.07	0.03	33.84	0.00	0.57	0.01	0.18	17.54	1.59	0.01	100.84
THa1_plag_micro4_1	46.52	0.04	34.08	-0.01	0.52	0.00	0.19	17.71	1.41	0.03	100.50
THa1_plag_micro4_2	46.44	0.03	34.18	0.00	0.50	0.01	0.18	17.77	1.44	0.02	100.57
THa1_plag_micro4_3	46.57	0.01	34.33	0.00	0.51	0.01	0.20	17.85	1.39	0.01	100.87

<i>Spot Name</i>	<i>SiO₂</i>	<i>TiO₂</i>	<i>Al₂O₃</i>	<i>Cr₂O₃</i>	<i>FeO</i>	<i>MnO</i>	<i>MgO</i>	<i>CaO</i>	<i>Na₂O</i>	<i>K₂O</i>	<i>Total</i>
THa1_plag_macro2_rim_1	46.31	0.02	34.35	0.00	0.46	0.00	0.21	17.94	1.23	0.01	100.53
THa1_plag_macro2_rim_2	45.59	0.02	34.72	0.00	0.47	0.01	0.17	18.55	1.03	0.03	100.59
THa1_plag_macro2_rim_3	46.66	0.03	34.13	0.00	0.46	0.01	0.21	17.79	1.42	0.03	100.74
THa1_plag_macro2_core_1	45.94	0.02	34.49	0.00	0.47	0.01	0.19	18.45	1.18	0.02	100.77
THa1_plag_macro2_core_2	46.30	0.02	34.29	0.00	0.47	0.00	0.20	18.02	1.34	0.02	100.66
THa1_plag_macro2_core_3	46.07	0.00	34.27	0.00	0.44	0.01	0.21	18.16	1.22	0.01	100.41
THa1_plag_groundmass_1	54.24	0.13	28.96	0.00	1.11	0.02	0.18	12.16	4.52	0.16	101.48
THa1_plag_groundmass_2	53.12	0.13	29.40	0.00	0.82	0.01	0.17	12.62	4.24	0.11	100.63
THa1_plag_groundmass_3	53.06	0.08	29.64	0.00	0.87	0.02	0.17	12.85	4.17	0.11	100.96
THa1_plag_groundmass_4	54.18	0.13	28.70	0.00	0.86	0.00	0.15	11.77	4.67	0.14	100.60
THa1_plag_groundmass_5	53.48	0.09	29.31	0.00	0.86	0.00	0.20	12.71	4.26	0.12	101.03
THa1_plag_groundmass_6	52.95	0.09	29.64	0.00	0.84	0.01	0.13	12.74	4.15	0.13	100.69
THa1_plag_groundmass_7	56.07	0.19	27.36	0.00	1.00	0.01	0.13	10.29	5.53	0.24	100.81
THa1_plag_groundmass_8	54.83	0.15	28.43	0.00	0.91	0.01	0.15	11.35	4.99	0.19	101.00
THa1_plag_groundmass_9	53.57	0.11	29.32	0.00	0.85	0.02	0.19	12.45	4.30	0.12	100.93
THa1_plag_groundmass_10	55.90	0.17	27.09	0.00	1.02	0.00	0.24	10.50	5.31	0.19	100.42
THa2_plag_macro1_rim_1	50.51	0.08	31.02	0.00	0.69	0.00	0.22	14.68	3.15	0.06	100.42
THa2_plag_macro1_rim_2	49.57	0.06	31.87	0.00	0.66	0.02	0.24	15.47	2.65	0.03	100.58
THa2_plag_macro1_rim_3	51.45	0.08	30.86	0.00	0.64	0.00	0.21	14.17	3.39	0.06	100.86
THa2_plag_macro1_core_1	46.83	0.01	33.81	0.00	0.48	0.01	0.25	17.58	1.57	0.00	100.54
THa2_plag_macro1_core_2	46.85	0.02	33.88	0.00	0.50	0.00	0.24	17.71	1.49	0.03	100.72
THa2_plag_macro1_core_3	46.98	0.03	33.87	0.00	0.50	-0.01	0.25	17.58	1.52	0.02	100.74
THa2_plag_micro1_1	47.05	0.03	33.96	0.00	0.46	0.00	0.24	17.63	1.55	0.02	100.94
THa2_plag_micro1_2	46.72	0.01	34.36	0.00	0.48	0.02	0.22	17.86	1.38	0.02	101.07
THa2_plag_micro1_3	46.70	0.01	33.95	0.00	0.47	0.01	0.23	17.70	1.43	0.01	100.52
THa2_plag_micro2_1	47.82	0.04	33.34	0.00	0.47	0.00	0.28	17.09	1.78	0.02	100.84
THa2_plag_micro2_2	47.34	0.03	33.73	0.00	0.47	0.01	0.25	17.45	1.64	0.00	100.92
THa2_plag_micro2_3	47.81	0.02	33.28	0.00	0.48	0.00	0.27	17.07	1.81	0.02	100.76
THa2_plag_micro3_1	49.42	0.08	31.97	-0.01	0.76	0.00	0.26	15.56	2.62	0.05	100.71
THa2_plag_micro3_2	48.29	0.03	33.11	0.00	0.57	0.01	0.22	16.81	2.03	0.03	101.10
THa2_plag_micro3_3	47.30	0.03	33.38	0.00	0.58	0.02	0.22	17.21	1.76	0.03	100.53
THa2_plag_micro4_1	45.88	0.03	34.78	0.00	0.51	-0.01	0.14	18.33	1.13	0.01	100.81
THa2_plag_micro4_2	46.46	0.03	34.28	0.00	0.57	0.00	0.18	17.89	1.34	0.02	100.77
THa2_plag_micro4_3	46.88	0.02	33.94	0.00	0.55	0.00	0.19	17.49	1.50	0.03	100.60
THa2_plag_micro5_1	46.86	0.03	34.02	0.00	0.51	0.00	0.19	17.57	1.56	0.01	100.75
THa2_plag_micro5_2	47.00	0.01	33.89	0.00	0.52	0.01	0.19	17.63	1.58	0.00	100.84
THa2_plag_micro5_3	47.00	0.03	33.93	0.00	0.57	0.00	0.20	17.48	1.62	0.00	100.83

<i>Spot Name</i>	<i>SiO₂</i>	<i>TiO₂</i>	<i>Al₂O₃</i>	<i>Cr₂O₃</i>	<i>FeO</i>	<i>MnO</i>	<i>MgO</i>	<i>CaO</i>	<i>Na₂O</i>	<i>K₂O</i>	<i>Total</i>
THa2_plag_macro2_rim_1	51.70	0.09	30.50	0.00	0.68	0.01	0.21	13.87	3.50	0.06	100.63
THa2_plag_macro2_rim_2	51.05	0.05	30.86	0.00	0.59	0.00	0.22	14.33	3.21	0.08	100.40
THa2_plag_macro2_rim_3	51.03	0.04	30.99	0.00	0.70	0.00	0.25	14.61	3.15	0.06	100.83
THa2_plag_macro2_core_1	46.42	0.02	34.28	-0.01	0.48	0.01	0.21	17.98	1.32	0.01	100.73
THa2_plag_macro2_core_2	45.54	0.02	35.05	0.01	0.41	0.01	0.18	18.63	1.02	0.02	100.86
THa2_plag_macro2_core_3	46.61	0.02	34.13	0.00	0.48	0.00	0.22	18.10	1.41	0.01	100.98
THa2_plag_micro6_1	47.00	0.03	34.12	0.00	0.43	0.00	0.25	17.81	1.53	0.01	101.18
THa2_plag_micro6_2	47.02	0.03	33.73	0.00	0.46	0.00	0.25	17.58	1.59	0.02	100.70
THa2_plag_micro6_3	47.15	0.04	33.94	0.00	0.43	0.01	0.25	17.55	1.64	0.01	101.02
THa2_plag_groundmass_1	52.00	0.09	30.05	0.00	0.86	0.01	0.17	13.45	3.74	0.09	100.47
THa2_plag_groundmass_2	53.55	0.11	28.79	0.00	0.81	0.01	0.17	12.24	4.51	0.14	100.34
THa2_plag_groundmass_3	52.31	0.16	29.56	0.00	1.20	0.02	0.28	13.33	3.76	0.11	100.73
THa2_plag_groundmass_4	52.69	0.11	29.76	-0.01	0.95	0.02	0.19	13.15	4.02	0.12	100.99
THa2_plag_groundmass_5	52.04	0.08	30.31	0.00	0.79	0.00	0.19	13.67	3.67	0.10	100.87
THa2_plag_groundmass_6	51.73	0.10	30.28	0.00	0.80	0.01	0.22	13.78	3.64	0.09	100.64
THa2_plag_groundmass_7	52.37	0.10	30.10	0.00	0.89	0.01	0.23	13.41	3.88	0.09	101.08
THa2_plag_groundmass_8	52.66	0.21	28.85	0.00	1.49	0.02	0.27	12.96	3.93	0.12	100.51
THa2_plag_groundmass_9	53.88	0.13	28.94	0.00	0.96	0.00	0.17	11.95	4.57	0.13	100.72
THa2_plag_groundmass_10	52.85	0.11	29.86	-0.01	0.83	0.01	0.20	13.00	3.93	0.10	100.88
THd3a_plag_macro1_rim_1	49.61	0.05	31.93	-0.01	0.64	0.01	0.21	15.60	2.72	0.06	100.83
THd3a_plag_macro1_rim_2	49.71	0.05	31.70	0.00	0.66	0.00	0.21	15.31	2.82	0.06	100.52
THd3a_plag_macro1_rim_3	48.41	0.05	32.69	0.00	0.54	0.01	0.22	16.52	2.39	0.02	100.84
THd3a_plag_macro1_core_1	45.81	0.01	34.56	0.00	0.43	0.00	0.19	18.59	1.11	0.00	100.70
THd3a_plag_macro1_core_2	45.87	0.02	34.88	0.00	0.44	0.00	0.18	18.53	1.10	0.00	101.03
THd3a_plag_macro1_core_3	45.68	0.02	34.85	0.00	0.43	0.01	0.19	18.69	1.07	0.01	100.93
THd3a_plag_micro1_1	47.55	0.03	33.37	0.00	0.60	0.01	0.21	17.12	1.82	0.02	100.73
THd3a_plag_micro1_2	47.45	0.05	33.43	0.00	0.60	0.01	0.23	17.18	1.76	0.01	100.71
THd3a_plag_micro1_3	48.47	0.04	31.74	0.00	0.55	0.00	0.28	15.91	2.47	0.03	99.50
THd3a_plag_macro2_rim_1	50.51	0.04	31.66	0.00	0.66	0.01	0.23	15.07	2.97	0.04	101.19
THd3a_plag_macro2_rim_2	51.35	0.08	30.85	0.01	0.70	0.01	0.23	14.24	3.36	0.07	100.90
THd3a_plag_macro2_rim_3	49.73	0.07	31.77	0.00	0.64	0.00	0.23	15.51	2.81	0.06	100.82
THd3a_plag_macro2_core_1	46.75	0.02	33.84	0.01	0.48	0.00	0.23	17.68	1.51	0.01	100.53
THd3a_plag_macro2_core_2	47.71	0.02	33.29	0.00	0.48	0.01	0.26	17.23	1.82	0.02	100.86
THd3a_plag_macro2_core_3	46.33	0.02	34.12	0.00	0.49	0.01	0.22	17.88	1.36	0.01	100.44
THd3a_plag_macro3_rim_1	50.16	0.06	31.73	0.00	0.73	0.00	0.20	15.34	2.85	0.03	101.11
THd3a_plag_macro3_rim_2	51.61	0.07	30.79	0.00	0.67	0.01	0.18	14.04	3.51	0.08	100.96
THd3a_plag_macro3_rim_3	49.59	0.06	31.35	0.00	0.73	0.01	0.21	14.93	2.83	0.05	99.76

<i>Spot Name</i>	<i>SiO₂</i>	<i>TiO₂</i>	<i>Al₂O₃</i>	<i>Cr₂O₃</i>	<i>FeO</i>	<i>MnO</i>	<i>MgO</i>	<i>CaO</i>	<i>Na₂O</i>	<i>K₂O</i>	<i>Total</i>
THd3a_plag_macro3_core_1	46.19	0.01	34.52	0.00	0.49	0.00	0.19	18.22	1.28	0.00	100.90
THd3a_plag_macro3_core_2	46.05	0.02	34.34	0.00	0.49	0.01	0.18	18.06	1.25	0.01	100.40
THd3a_plag_macro3_core_3	46.46	0.00	34.35	0.00	0.49	0.01	0.19	17.89	1.36	0.01	100.77
THd3a_plag_macro4_rim_1	53.02	0.10	29.39	0.00	0.78	0.00	0.18	12.80	4.27	0.10	100.65
THd3a_plag_macro4_rim_2	54.05	0.09	28.84	0.00	0.84	0.01	0.14	12.08	4.60	0.14	100.78
THd3a_plag_macro4_rim_3	57.50	0.15	26.79	0.00	0.92	0.00	0.10	9.63	5.85	0.27	101.22
THd3a_plag_macro4_mantle_1	50.54	0.05	31.15	0.00	0.65	0.01	0.25	14.67	3.21	0.04	100.58
THd3a_plag_macro4_mantle_2	49.47	0.05	32.15	0.00	0.67	0.01	0.22	15.65	2.63	0.05	100.88
THd3a_plag_macro4_mantle_3	50.48	0.04	31.22	0.00	0.65	0.01	0.25	14.83	3.09	0.05	100.62
THd3a_plag_macro4_core_1	46.49	0.03	34.29	0.00	0.45	0.01	0.22	17.86	1.48	0.02	100.84
THd3a_plag_macro4_core_2	45.73	0.03	34.72	0.00	0.44	0.00	0.19	18.48	1.09	0.01	100.68
THd3a_plag_macro4_core_3	45.78	0.00	34.74	0.00	0.42	0.00	0.18	18.61	1.10	0.02	100.84
THd3a_plag_micro2_1	51.43	0.07	30.42	0.00	0.66	0.01	0.20	13.86	3.53	0.08	100.27
THd3a_plag_micro2_2	51.54	0.08	30.40	0.00	0.66	0.01	0.20	13.79	3.58	0.08	100.34
THd3a_plag_micro2_3	51.49	0.08	30.39	-0.01	0.65	0.01	0.20	13.97	3.51	0.08	100.38
THd3a_plag_micro3_1	45.65	0.01	34.06	0.00	0.45	0.00	0.20	18.08	1.26	0.03	99.73
THd3a_plag_micro3_2	45.86	0.01	34.51	0.00	0.47	0.00	0.19	18.42	1.21	0.01	100.68
THd3a_plag_micro3_3	46.47	0.01	33.93	0.00	0.48	0.01	0.23	17.87	1.47	0.00	100.47
THd3a_plag_micro4_1	46.37	0.00	34.32	0.00	0.40	0.01	0.24	18.03	1.39	0.01	100.77
THd3a_plag_micro4_2	46.54	0.03	34.12	0.00	0.41	0.01	0.26	17.86	1.43	0.00	100.67
THd3a_plag_micro4_3	46.42	0.01	34.47	-0.01	0.41	0.01	0.24	18.16	1.36	0.01	101.10
THd3a_plag_micro5_1	46.74	0.03	33.94	-0.01	0.48	0.01	0.23	17.68	1.55	0.01	100.66
THd3a_plag_micro5_2	47.34	0.04	33.72	0.00	0.58	0.00	0.21	17.35	1.75	0.02	101.01
THd3a_plag_micro5_3	46.65	0.01	34.05	0.00	0.53	0.01	0.20	17.74	1.50	0.02	100.71
THd3a_groundmass_arc_plag_1	52.26	0.09	29.92	0.00	0.81	0.01	0.18	13.38	3.89	0.10	100.66
THd3a_groundmass_arc_plag_2	51.82	0.08	30.17	0.00	0.79	-0.01	0.16	13.64	3.70	0.10	100.47
THd3a_groundmass_arc_plag_3	52.59	0.10	29.93	0.00	0.83	0.01	0.19	13.33	3.99	0.09	101.05
THd3a_groundmass_arc_plag_4	54.01	0.14	28.34	0.00	0.97	0.02	0.19	11.82	4.60	0.16	100.25
THd3a_groundmass_arc_plag_5	54.25	0.13	28.50	0.00	0.92	0.00	0.19	11.89	4.60	0.13	100.59
THd3a_groundmass_plag_1	51.99	0.11	29.78	0.00	1.01	0.01	0.30	13.57	3.75	0.09	100.61
THd3a_groundmass_plag_2	54.92	0.15	28.13	0.00	1.18	0.01	0.15	11.26	4.92	0.18	100.90
THd3a_groundmass_plag_3	51.45	0.11	28.89	0.00	0.78	0.00	0.20	12.76	3.92	0.09	98.21
THd3a_groundmass_plag_4	52.48	0.10	29.98	0.00	0.72	0.00	0.19	13.38	3.94	0.11	100.90
THd3a_groundmass_plag_5	50.98	0.05	30.87	0.00	0.87	0.01	0.20	14.49	3.30	0.07	100.84
THd3a_groundmass_plag_6	52.48	0.08	30.19	0.00	0.79	0.01	0.18	13.45	3.86	0.09	101.13
THd3a_groundmass_plag_7	52.56	0.07	29.71	0.00	0.75	0.00	0.21	13.19	4.02	0.09	100.61
THd3a_groundmass_plag_8	51.05	0.05	31.01	-0.01	0.76	0.01	0.19	14.38	3.38	0.07	100.90

<i>Spot Name</i>	<i>SiO₂</i>	<i>TiO₂</i>	<i>Al₂O₃</i>	<i>Cr₂O₃</i>	<i>FeO</i>	<i>MnO</i>	<i>MgO</i>	<i>CaO</i>	<i>Na₂O</i>	<i>K₂O</i>	<i>Total</i>
THd3a_groundmass_plag_9	52.30	0.09	30.11	0.00	0.70	0.01	0.20	13.44	3.84	0.11	100.80
THd3a_groundmass_plag_10	52.55	0.08	29.81	0.00	0.82	0.01	0.16	13.19	3.94	0.08	100.66
THde2_plag_micro1_1	46.91	0.02	33.72	0.00	0.50	0.01	0.23	17.57	1.57	0.01	100.56
THde2_plag_micro1_2	48.25	0.03	32.68	0.00	0.58	0.01	0.33	16.64	2.16	0.03	100.71
THde2_plag_micro1_3	46.43	0.03	34.04	0.00	0.53	0.01	0.21	17.93	1.46	0.03	100.66
THde2_plag_macro1_rim_1	49.97	0.04	31.91	0.00	0.62	0.01	0.23	15.30	2.79	0.03	100.90
THde2_plag_macro1_rim_2	51.46	0.07	30.94	0.00	0.77	0.00	0.19	14.23	3.43	0.07	101.15
THde2_plag_macro1_rim_3	52.00	0.15	29.60	0.00	1.27	0.02	0.25	13.48	3.73	0.08	100.57
THde2_plag_macro1_mantle_1	47.75	0.03	33.04	0.00	0.55	0.01	0.24	16.79	2.05	0.02	100.47
THde2_plag_macro1_mantle_2	48.02	0.03	32.65	0.00	0.54	0.01	0.25	16.71	2.05	0.03	100.29
THde2_plag_macro1_mantle_3	49.09	0.04	32.11	0.01	0.52	0.01	0.28	16.08	2.43	0.03	100.60
THde2_plag_macro1_core_1	46.39	0.03	34.16	0.00	0.46	0.00	0.23	17.98	1.35	0.01	100.60
THde2_plag_macro1_core_2	46.90	0.04	34.07	0.00	0.47	0.01	0.24	17.74	1.50	0.03	101.00
THde2_plag_macro1_core_3	46.44	0.03	34.31	0.00	0.48	0.01	0.22	18.04	1.31	0.01	100.85
THde2_plag_micro2_1	46.43	0.02	34.28	0.00	0.48	0.00	0.22	17.99	1.39	0.02	100.84
THde2_plag_micro2_2	46.71	0.03	33.91	0.00	0.49	0.00	0.24	17.76	1.51	0.02	100.67
THde2_plag_micro2_3	46.37	0.05	33.98	0.00	0.46	0.00	0.22	17.90	1.38	0.03	100.40
THde2_plag_micro3_1	49.91	0.04	31.87	0.00	0.49	0.00	0.26	15.47	2.72	0.04	100.80
THde2_plag_micro3_2	49.39	0.04	31.98	0.00	0.52	0.00	0.27	15.63	2.57	0.05	100.46
THde2_plag_micro3_3	49.42	0.03	32.17	0.00	0.52	0.01	0.26	15.83	2.49	0.05	100.76
THde2_plag_macro2_1	46.37	0.03	34.25	0.00	0.48	0.01	0.23	18.02	1.36	0.03	100.77
THde2_plag_macro2_2	47.13	0.05	33.56	0.00	0.47	0.00	0.27	17.52	1.70	0.01	100.71
THde2_plag_macro2_3	47.61	0.01	33.25	0.00	0.42	0.01	0.26	17.05	1.85	0.01	100.47
THde2_plag_micro4_1	46.26	0.02	34.55	0.00	0.43	0.00	0.22	17.93	1.34	0.00	100.76
THde2_plag_micro4_2	46.49	0.01	34.38	0.00	0.45	0.00	0.23	17.84	1.37	0.00	100.79
THde2_plag_micro4_3	46.40	0.03	34.27	0.00	0.45	0.00	0.23	18.03	1.37	0.03	100.80
THde2_plag_macro3_rim_1	47.95	0.02	32.88	0.00	0.56	0.01	0.24	16.84	2.02	0.03	100.54
THde2_plag_macro3_rim_2	48.09	0.05	33.06	0.00	0.54	0.01	0.25	16.97	2.01	0.04	101.01
THde2_plag_macro3_rim_3	49.48	0.04	32.15	0.00	0.55	0.00	0.26	15.87	2.56	0.04	100.96
THde2_plag_macro3_core_1	46.04	0.04	34.51	0.00	0.45	0.01	0.21	18.11	1.22	0.02	100.61
THde2_plag_macro3_core_2	46.23	0.02	34.12	0.00	0.44	0.01	0.22	18.11	1.29	0.02	100.47
THde2_plag_macro3_core_3	45.80	0.01	34.76	0.00	0.42	0.00	0.20	18.51	1.10	0.01	100.82
THde2_plag_micro7_1	46.31	0.02	34.55	0.00	0.44	0.00	0.21	18.15	1.36	0.01	101.05
THde2_plag_micro7_2	46.29	-0.01	34.38	0.00	0.42	0.00	0.22	18.15	1.30	0.02	100.78
THde2_plag_micro7_3	45.05	0.03	34.16	0.00	0.42	0.01	0.20	18.28	1.08	0.01	99.24
THde2_plag_macro4_rim_1	46.00	0.01	34.39	0.00	0.47	0.01	0.19	18.11	1.29	0.01	100.49
THde2_plag_macro4_rim_2	48.74	0.03	32.48	0.00	0.50	0.00	0.27	16.30	2.28	0.02	100.63

<i>Spot Name</i>	<i>SiO₂</i>	<i>TiO₂</i>	<i>Al₂O₃</i>	<i>Cr₂O₃</i>	<i>FeO</i>	<i>MnO</i>	<i>MgO</i>	<i>CaO</i>	<i>Na₂O</i>	<i>K₂O</i>	<i>Total</i>
THde2_plag_macro4_rim_3	48.36	0.05	32.59	0.00	0.54	0.01	0.24	16.39	2.22	0.04	100.45
THde2_plag_macro4_mantle_1	45.93	0.01	34.60	0.00	0.43	0.01	0.19	18.38	1.18	0.01	100.74
THde2_plag_macro4_mantle_2	46.83	0.04	33.78	0.00	0.44	0.01	0.24	17.81	1.55	0.01	100.70
THde2_plag_macro4_mantle_3	46.02	0.03	34.45	0.00	0.44	0.00	0.21	18.17	1.24	0.02	100.59
THde2_plag_macro4_core_1	45.64	0.00	34.97	0.00	0.42	0.00	0.19	18.83	1.01	0.00	101.06
THde2_plag_macro4_core_2	46.86	0.01	33.77	0.00	0.46	0.00	0.25	17.67	1.52	0.01	100.56
THde2_plag_macro4_core_3	46.43	0.01	34.24	-0.01	0.40	0.00	0.23	18.07	1.36	0.02	100.75
THde2_groundmass_plag_1	48.85	0.05	32.41	0.00	0.74	0.01	0.21	16.04	2.40	0.03	100.74
THde2_groundmass_plag_2	50.25	0.08	31.04	0.00	0.77	0.01	0.28	14.96	3.03	0.07	100.47
THde2_groundmass_plag_3	48.24	0.02	32.73	-0.01	0.74	0.00	0.20	16.72	2.16	0.05	100.88
THde2_groundmass_plag_4	49.37	0.05	31.89	0.00	0.78	0.01	0.24	15.81	2.70	0.06	100.90
THde2_groundmass_plag_5	50.31	0.04	31.34	0.00	0.64	0.01	0.27	15.01	2.96	0.06	100.64
THde2_groundmass_plag_6	49.90	0.06	31.97	0.00	0.68	0.01	0.20	15.32	2.76	0.04	100.95
THde2_groundmass_plag_7	50.30	0.08	31.18	0.00	0.80	0.01	0.24	14.95	3.15	0.05	100.77
THde2_groundmass_plag_8	48.96	0.07	31.66	0.00	0.77	0.01	0.22	15.45	2.49	0.05	99.69
THde2_groundmass_plag_9	50.44	0.05	31.24	0.00	0.63	0.00	0.23	14.90	3.07	0.05	100.62
THde2_groundmass_plag_10	48.91	0.06	32.18	0.00	0.72	0.01	0.25	15.96	2.46	0.06	100.60
THf3b_plag_macro1_rim_1	49.12	0.03	32.22	0.00	0.55	0.00	0.30	15.90	2.38	0.03	100.53
THf3b_plag_macro1_rim_2	50.26	0.08	31.60	0.00	0.70	0.01	0.23	14.97	2.99	0.05	100.89
THf3b_plag_macro1_rim_3	50.43	0.07	31.80	0.00	0.66	0.01	0.22	15.02	2.89	0.06	101.16
THf3b_plag_macro1_core_1	46.73	0.03	34.18	0.01	0.46	0.02	0.24	17.78	1.48	0.01	100.93
THf3b_plag_macro1_core_2	46.67	0.01	34.25	0.00	0.43	0.01	0.22	17.87	1.35	0.03	100.83
THf3b_plag_macro1_core_3	46.51	0.03	34.35	0.00	0.44	0.01	0.24	17.85	1.36	0.01	100.81
THf3b_plag_micro1_1	47.04	0.02	33.92	0.00	0.47	0.00	0.24	17.65	1.50	0.00	100.85
THf3b_plag_micro1_2	46.63	0.01	34.32	0.00	0.47	0.01	0.24	17.79	1.38	0.02	100.86
THf3b_plag_micro1_3	46.44	0.03	34.29	0.01	0.46	-0.01	0.21	17.96	1.35	0.00	100.75
THf3b_plag_macro2_rim_1	48.79	0.02	32.36	0.00	0.56	0.01	0.28	16.09	2.34	0.03	100.50
THf3b_plag_macro2_rim_2	48.92	0.03	32.74	0.00	0.58	0.00	0.27	16.37	2.25	0.03	101.18
THf3b_plag_macro2_rim_3	49.68	0.07	32.01	0.00	0.64	0.01	0.27	15.43	2.63	0.04	100.77
THf3b_plag_macro2_mantle_1	46.48	0.01	34.27	0.00	0.48	0.00	0.23	17.83	1.37	0.03	100.69
THf3b_plag_macro2_mantle_2	46.51	0.05	34.40	0.00	0.45	0.01	0.22	17.92	1.37	0.02	100.95
THf3b_plag_macro2_mantle_3	46.11	0.03	34.73	0.00	0.42	0.00	0.19	18.19	1.21	0.02	100.90
THf3b_plag_macro2_dark_1	46.26	0.02	34.68	0.00	0.39	-0.01	0.20	18.26	1.21	0.00	101.02
THf3b_plag_macro2_dark_2	46.03	0.02	34.89	0.00	0.39	0.00	0.20	18.36	1.12	0.02	101.04
THf3b_plag_macro2_dark_3	45.64	0.02	34.92	0.00	0.35	0.00	0.17	18.44	1.05	0.03	100.61
THf3b_plag_micro2_rim_1	49.10	0.02	32.40	0.00	0.55	0.00	0.26	16.06	2.36	0.02	100.77
THf3b_plag_micro2_rim_2	50.06	0.06	31.87	0.00	0.58	0.00	0.23	15.20	2.81	0.04	100.85

<i>Spot Name</i>	<i>SiO₂</i>	<i>TiO₂</i>	<i>Al₂O₃</i>	<i>Cr₂O₃</i>	<i>FeO</i>	<i>MnO</i>	<i>MgO</i>	<i>CaO</i>	<i>Na₂O</i>	<i>K₂O</i>	<i>Total</i>
THf3b_plag_micro2_rim_3	49.65	0.05	31.64	0.00	0.56	0.02	0.25	15.27	2.77	0.05	100.26
THf3b_plag_micro2_core_1	46.27	0.02	34.43	0.00	0.40	0.00	0.23	18.01	1.32	0.01	100.70
THf3b_plag_micro2_core_2	46.01	0.02	34.55	0.00	0.43	0.00	0.21	18.15	1.16	0.02	100.54
THf3b_plag_micro2_core_3	45.46	0.03	35.02	0.00	0.43	0.01	0.18	18.49	0.95	0.00	100.55
THf3b_plag_macro3_rim_1	48.01	0.03	32.84	0.00	0.58	0.01	0.23	16.43	2.00	0.03	100.17
THf3b_plag_macro3_rim_2	50.65	0.06	31.53	0.00	0.59	0.01	0.26	14.78	3.05	0.04	100.96
THf3b_plag_macro3_rim_3	48.69	0.05	32.58	0.00	0.54	0.00	0.26	16.06	2.38	0.02	100.59
THf3b_plag_macro3_core_1	46.38	0.04	34.50	0.00	0.43	0.00	0.21	17.90	1.29	0.01	100.76
THf3b_plag_macro3_core_2	46.25	0.02	34.49	0.00	0.45	0.00	0.20	18.06	1.28	0.02	100.76
THf3b_plag_macro3_core_3	46.27	0.02	34.48	0.00	0.46	0.00	0.20	18.05	1.25	0.00	100.72
THf3b_plag_micro3_rim_1	50.77	0.05	32.36	0.00	0.65	0.00	0.28	15.86	2.69	0.05	102.70
THf3b_plag_micro3_rim_2	49.69	0.05	31.88	-0.01	0.64	0.01	0.29	15.41	2.68	0.02	100.68
THf3b_plag_micro3_rim_3	48.71	0.05	32.58	0.00	0.56	0.01	0.26	16.17	2.23	0.04	100.60
THf3b_plag_micro3_core_1	55.44	0.03	28.24	0.00	0.38	0.01	0.22	11.09	4.94	0.12	100.47
THf3b_plag_micro3_core_2	55.20	0.03	28.51	0.00	0.40	0.01	0.18	11.37	4.82	0.12	100.63
THf3b_plag_micro3_core_3	55.20	0.03	28.52	0.00	0.38	0.00	0.17	11.43	4.83	0.12	100.68
THf3b_plag_macro4_rim_1	48.32	0.03	32.96	0.00	0.52	0.00	0.24	16.50	2.08	0.03	100.69
THf3b_plag_macro4_rim_2	49.40	0.04	32.11	0.00	0.57	0.00	0.28	15.79	2.50	0.04	100.71
THf3b_plag_macro4_rim_3	48.91	0.05	32.31	0.00	0.62	0.02	0.24	15.89	2.35	0.03	100.41
THf3b_plag_macro4_core_1	46.51	0.03	34.42	0.00	0.45	0.00	0.23	18.02	1.35	0.01	101.01
THf3b_plag_macro4_core_2	46.67	0.02	34.16	0.00	0.44	0.01	0.23	17.79	1.37	0.02	100.71
THf3b_plag_macro4_core_3	46.47	0.02	34.44	0.01	0.43	0.02	0.21	18.04	1.32	0.01	100.97
THf3b_plag_micro4_1	49.43	0.05	32.14	0.00	0.53	0.00	0.29	15.84	2.46	0.02	100.77
THf3b_plag_micro4_2	49.08	0.04	32.47	0.00	0.53	0.01	0.28	15.94	2.36	0.02	100.72
THf3b_plag_micro4_3	49.13	0.02	32.25	0.00	0.56	0.03	0.28	15.87	2.45	0.03	100.62
THf3b_plag_macro5_1	46.64	0.04	34.32	0.00	0.47	0.00	0.23	17.78	1.41	0.01	100.90
THf3b_plag_macro5_2	46.63	0.02	34.16	-0.01	0.46	0.00	0.24	17.77	1.43	0.00	100.71
THf3b_plag_macro5_3	46.71	0.03	34.18	0.00	0.45	0.00	0.22	17.73	1.45	0.02	100.78
THf3b_plag_micro5_rim_1	49.53	0.04	31.92	0.00	0.58	0.01	0.26	15.62	2.62	0.05	100.62
THf3b_plag_micro5_rim_2	49.61	0.05	31.92	0.00	0.55	0.01	0.25	15.42	2.63	0.04	100.47
THf3b_plag_micro5_rim_3	49.49	0.04	31.94	0.01	0.56	0.00	0.24	15.56	2.61	0.05	100.48
THf3b_plag_micro5_core_1	54.46	0.02	29.17	0.00	0.37	0.01	0.18	11.93	4.48	0.11	100.72
THf3b_plag_micro5_core_2	54.64	0.04	28.73	0.00	0.48	0.01	0.12	11.62	4.66	0.11	100.42
THf3b_plag_micro5_core_3	54.23	0.03	29.02	0.00	0.51	0.00	0.14	11.88	4.51	0.11	100.44
THf3b_plag_macro6_rim_1	48.78	0.03	31.99	0.00	0.49	0.02	0.27	16.12	2.38	0.04	100.12
THf3b_plag_macro6_rim_2	48.46	0.04	32.87	0.00	0.52	0.01	0.25	16.45	2.12	0.03	100.75
THf3b_plag_macro6_rim_3	48.77	0.04	32.75	0.01	0.60	0.00	0.25	16.33	2.24	0.02	101.00

<i>Spot Name</i>	<i>SiO₂</i>	<i>TiO₂</i>	<i>Al₂O₃</i>	<i>Cr₂O₃</i>	<i>FeO</i>	<i>MnO</i>	<i>MgO</i>	<i>CaO</i>	<i>Na₂O</i>	<i>K₂O</i>	<i>Total</i>
THf3b_plag_macro6_core_1	46.46	0.01	34.47	0.00	0.46	0.00	0.22	17.99	1.32	0.00	100.94
THf3b_plag_macro6_core_2	45.91	0.02	34.49	0.00	0.44	0.00	0.20	18.17	1.16	0.02	100.40
THf3b_plag_macro6_core_3	46.75	0.03	34.06	0.00	0.47	0.00	0.23	17.56	1.47	0.00	100.57
THf3b_groundmass_plag_1	49.80	0.07	31.69	0.00	0.58	0.01	0.28	15.23	2.75	0.05	100.45
THf3b_groundmass_plag_2	50.03	0.05	31.53	0.00	0.69	0.01	0.27	15.05	2.87	0.04	100.53
THf3b_groundmass_plag_3	49.91	0.04	32.42	0.00	0.65	0.02	0.21	15.50	2.60	0.04	101.39
THf3b_groundmass_plag_4	49.38	0.03	31.92	0.00	0.68	0.01	0.26	15.71	2.57	0.05	100.60
THf3b_groundmass_plag_5	49.42	0.06	31.66	0.00	0.71	0.01	0.27	15.47	2.63	0.03	100.25
THf3b_groundmass_plag_6	50.38	0.08	31.48	0.00	0.95	0.01	0.12	14.84	3.02	0.05	100.93
THf3b_groundmass_plag_7	49.59	0.03	32.15	0.00	0.58	0.01	0.23	15.60	2.65	0.02	100.86
THf3b_groundmass_plag_8	50.70	0.07	31.64	0.00	0.68	0.02	0.24	14.88	2.96	0.05	101.24
THf3b_groundmass_plag_9	50.90	0.04	31.10	0.00	0.84	0.01	0.15	14.28	3.20	0.08	100.60
THf3b_groundmass_plag_10	49.71	0.04	31.79	0.01	0.69	0.00	0.16	15.04	2.90	0.06	100.39
THi3_plag_micro1_1	48.48	0.03	32.97	-0.01	0.68	0.01	0.15	16.23	2.04	0.03	100.61
THi3_plag_micro1_2	49.88	0.16	30.67	0.00	1.37	0.02	0.36	15.15	2.62	0.09	100.30
THi3_plag_micro1_3	48.89	0.04	32.65	0.00	0.70	0.00	0.18	16.19	2.30	0.02	100.97
THi3_plag_micro2_1	46.15	0.02	34.62	0.00	0.51	-0.01	0.17	18.24	1.16	0.02	100.88
THi3_plag_micro2_2	46.12	0.02	34.58	0.01	0.51	0.01	0.18	18.05	1.20	0.02	100.69
THi3_plag_micro2_3	46.03	0.02	34.65	0.00	0.51	0.01	0.17	18.11	1.21	0.02	100.72
THi3_plag_macro1_1	47.17	0.01	34.41	-0.01	0.39	0.01	0.25	17.84	1.42	0.00	101.49
THi3_plag_macro1_2	46.68	0.02	34.15	0.00	0.42	0.00	0.25	17.64	1.47	0.02	100.65
THi3_plag_macro1_3	46.76	0.01	34.27	0.00	0.41	0.01	0.25	17.81	1.40	0.01	100.93
THi3_plag_macro2_1	46.38	0.02	34.38	0.00	0.41	0.00	0.23	17.84	1.34	-0.01	100.59
THi3_plag_macro2_2	46.68	0.02	34.33	0.00	0.41	0.00	0.24	17.92	1.37	0.01	100.98
THi3_plag_macro2_3	46.81	0.02	34.29	0.00	0.46	0.01	0.24	17.64	1.39	0.01	100.84
THi3_plag_macro3_1	46.54	0.02	34.37	0.00	0.45	0.00	0.23	17.72	1.39	0.02	100.72
THi3_plag_macro3_2	46.25	0.04	34.39	0.01	0.44	0.01	0.22	18.03	1.28	0.01	100.67
THi3_plag_macro3_3	46.50	0.02	34.20	-0.01	0.47	0.01	0.21	17.86	1.38	0.01	100.66
THi3_plag_macro4_rim_1	48.99	0.05	32.32	0.00	0.60	0.00	0.26	15.91	2.39	0.03	100.56
THi3_plag_macro4_rim_2	49.00	0.04	32.51	0.00	0.58	0.01	0.28	15.99	2.39	0.02	100.83
THi3_plag_macro4_rim_3	49.37	0.05	32.13	0.00	0.57	0.01	0.29	15.82	2.49	0.03	100.74
THi3_plag_macro4_core_1	12.59	-0.01	8.86	0.00	0.10	0.00	0.11	4.62	0.47	0.14	26.88
THi3_plag_macro4_core_2	46.12	0.06	34.62	0.00	0.46	0.01	0.18	16.82	1.18	0.02	99.46
THi3_plag_macro4_core_3	46.14	0.01	34.54	0.00	0.46	0.00	0.19	17.91	1.27	0.01	100.52
THi3_plag_micro3_1	46.65	0.01	34.03	0.00	0.60	0.00	0.19	17.52	1.49	0.01	100.50
THi3_plag_micro3_2	46.84	0.04	33.83	0.00	0.58	0.00	0.19	17.50	1.50	0.02	100.49
THi3_plag_micro3_3	46.95	0.03	33.81	0.00	0.57	0.01	0.19	17.37	1.62	0.02	100.57

<i>Spot Name</i>	<i>SiO₂</i>	<i>TiO₂</i>	<i>Al₂O₃</i>	<i>Cr₂O₃</i>	<i>FeO</i>	<i>MnO</i>	<i>MgO</i>	<i>CaO</i>	<i>Na₂O</i>	<i>K₂O</i>	<i>Total</i>
THi3_plag_micro4_rim_1	48.62	0.03	32.68	0.00	0.59	0.01	0.24	16.14	2.29	0.02	100.60
THi3_plag_micro4_rim_2	49.21	0.04	32.21	0.00	0.55	0.00	0.26	15.79	2.46	0.02	100.53
THi3_plag_micro4_rim_3	49.10	0.05	32.32	0.00	0.54	0.00	0.26	15.79	2.45	0.05	100.56
THi3_plag_micro4_core_1	46.19	0.01	34.50	0.00	0.49	0.00	0.18	18.00	1.26	0.03	100.65
THi3_plag_micro4_core_2	45.83	0.02	34.79	0.00	0.46	0.01	0.17	18.25	1.12	0.00	100.66
THi3_plag_micro4_core_3	46.64	0.01	34.09	-0.01	0.48	0.00	0.18	17.65	1.45	0.01	100.51
THi3_plag_macro5_rim_1	49.54	0.06	32.02	0.00	0.65	0.00	0.25	15.36	2.71	0.02	100.61
THi3_plag_macro5_rim_2	50.43	0.07	31.49	0.00	0.65	0.02	0.25	14.77	3.05	0.04	100.76
THi3_plag_macro5_rim_3	51.52	0.09	30.90	0.00	0.68	0.02	0.24	14.19	3.39	0.10	101.12
THi3_plag_macro5_core_1	46.86	0.02	34.26	0.00	0.49	0.00	0.21	17.79	1.41	0.00	101.05
THi3_plag_macro5_core_2	46.75	0.02	34.23	0.00	0.49	0.00	0.21	17.65	1.47	0.02	100.85
THi3_plag_macro5_core_3	47.00	0.02	33.88	-0.01	0.51	0.00	0.22	17.48	1.51	0.03	100.65
THi3_plag_micro5_1	46.95	0.02	33.90	0.01	0.56	0.01	0.20	17.44	1.54	0.02	100.66
THi3_plag_micro5_2	46.91	0.02	34.11	0.00	0.55	0.01	0.18	17.67	1.50	0.00	100.94
THi3_plag_micro5_3	46.66	0.03	34.05	0.00	0.55	0.01	0.18	17.54	1.48	0.03	100.53
THi3_plag_micro6_1	45.68	0.02	34.78	0.00	0.46	0.01	0.15	18.35	1.11	0.02	100.57
THi3_plag_micro6_2	46.12	0.03	34.38	0.00	0.47	0.01	0.18	17.78	1.29	0.01	100.25
THi3_plag_micro6_3	46.85	0.01	34.07	0.00	0.48	-0.01	0.21	17.51	1.48	0.01	100.61
THi3_groundmass_plag_1	51.27	0.07	30.49	0.00	0.87	0.01	0.32	14.11	3.43	0.04	100.60
THi3_groundmass_plag_2	50.78	0.06	30.71	0.00	0.91	0.00	0.13	14.15	3.37	0.08	100.18
THi3_groundmass_plag_3	49.72	0.04	31.91	0.00	0.73	0.01	0.28	15.43	2.65	0.02	100.79
THi3_groundmass_plag_4	49.62	0.05	31.90	-0.01	0.91	0.02	0.10	15.22	2.71	0.06	100.58
THi3_groundmass_plag_5	48.67	0.03	32.74	0.00	0.88	0.01	0.19	15.98	2.30	0.04	100.84
THi3_groundmass_plag_6	50.43	0.07	31.67	0.00	1.05	0.02	0.16	14.85	3.07	0.07	101.38
THi3_groundmass_plag_7	52.20	0.09	30.10	0.01	1.15	0.01	0.20	13.56	3.70	0.09	101.10
THi3_groundmass_plag_8	51.65	0.08	30.41	0.00	1.15	0.02	0.17	13.86	3.52	0.07	100.92
THi3_groundmass_plag_9	49.27	0.09	32.09	0.00	1.03	0.01	0.09	15.25	2.71	0.04	100.59
THi3_groundmass_plag_10	52.07	0.07	30.15	0.00	1.07	0.01	0.17	13.57	3.72	0.09	100.92
THj2_plag_micro1_rim_1	53.89	0.12	29.02	-0.01	0.92	0.00	0.17	12.01	4.52	0.27	100.92
THj2_plag_micro1_rim_2	52.91	0.06	29.71	0.00	0.79	0.01	0.18	12.52	4.15	0.22	100.55
THj2_plag_micro1_rim_3	52.74	0.08	29.69	0.00	0.81	0.01	0.18	12.87	4.04	0.19	100.61
THj2_plag_micro1_core_1	47.37	0.04	33.67	0.00	0.59	0.00	0.19	17.09	1.74	0.03	100.73
THj2_plag_micro1_core_2	47.56	0.02	33.58	0.00	0.58	-0.01	0.20	16.85	1.87	0.01	100.67
THj2_plag_micro1_core_3	47.19	0.03	34.03	-0.01	0.61	0.00	0.18	17.31	1.59	0.01	100.94
THj2_plag_macro1_rim_1	53.09	0.11	29.65	0.00	0.72	0.00	0.17	12.55	4.17	0.20	100.65
THj2_plag_macro1_rim_2	52.99	0.10	29.83	0.00	0.69	0.01	0.18	12.83	4.09	0.21	100.92
THj2_plag_macro1_rim_3	53.18	0.08	29.74	-0.01	0.77	0.01	0.18	12.73	4.17	0.23	101.09

<i>Spot Name</i>	<i>SiO₂</i>	<i>TiO₂</i>	<i>Al₂O₃</i>	<i>Cr₂O₃</i>	<i>FeO</i>	<i>MnO</i>	<i>MgO</i>	<i>CaO</i>	<i>Na₂O</i>	<i>K₂O</i>	<i>Total</i>
THj2_plag_macro1_mantle_1	49.17	0.04	32.27	0.00	0.61	0.01	0.25	16.00	2.44	0.05	100.84
THj2_plag_macro1_mantle_2	48.90	0.05	32.47	0.00	0.57	0.00	0.25	16.06	2.36	0.04	100.69
THj2_plag_macro1_mantle_3	48.58	0.04	32.80	0.00	0.59	0.00	0.23	16.37	2.23	0.04	100.88
THj2_plag_macro1_core_1	46.94	0.03	34.29	0.00	0.52	0.00	0.19	17.71	1.46	0.02	101.17
THj2_plag_macro1_core_2	46.62	0.02	34.10	0.00	0.51	0.01	0.20	17.49	1.48	0.01	100.42
THj2_plag_macro1_core_3	46.59	0.01	34.32	0.00	0.49	0.01	0.18	17.84	1.41	0.02	100.87
THj2_plag_micro2_1	47.30	0.02	33.82	0.01	0.53	0.00	0.21	17.37	1.58	0.02	100.87
THj2_plag_micro2_2	47.19	0.04	33.89	0.00	0.54	0.00	0.21	17.32	1.57	0.03	100.79
THj2_plag_micro2_3	47.13	0.03	34.06	0.00	0.54	0.01	0.21	17.48	1.57	0.03	101.05
THj2_plag_micro3_rim_1	52.45	0.10	29.80	0.00	0.69	0.00	0.20	12.96	4.00	0.18	100.38
THj2_plag_micro3_rim_2	52.85	0.08	29.86	0.00	0.67	0.01	0.18	13.02	4.08	0.22	100.96
THj2_plag_micro3_rim_3	52.81	0.09	29.93	-0.01	0.65	0.01	0.18	12.91	4.00	0.18	100.75
THj2_plag_micro3_core_1	48.25	0.03	32.84	0.00	0.70	0.00	0.16	16.11	2.25	0.07	100.40
THj2_plag_micro3_core_2	49.74	0.04	31.97	-0.01	0.75	0.00	0.17	15.19	2.76	0.10	100.70
THj2_plag_micro3_core_3	49.02	0.07	32.07	0.00	0.81	0.00	0.14	15.46	2.38	0.21	100.16
THj2_plag_macro2_rim_1	53.45	0.11	29.48	0.01	0.73	0.00	0.17	12.47	4.18	0.21	100.81
THj2_plag_macro2_rim_2	54.22	0.10	28.96	0.00	0.75	0.01	0.20	11.85	4.48	0.26	100.81
THj2_plag_macro2_rim_3	52.83	0.09	29.70	0.00	0.69	0.01	0.17	12.67	4.12	0.22	100.50
THj2_plag_macro2_core_1	46.96	0.03	34.05	0.00	0.50	0.01	0.22	17.60	1.50	0.03	100.88
THj2_plag_macro2_core_2	46.45	0.02	34.38	0.00	0.50	0.00	0.20	17.72	1.38	-0.01	100.64
THj2_plag_macro2_core_3	46.68	0.02	34.09	0.00	0.51	0.01	0.20	17.59	1.47	0.01	100.60
THj2_plag_macro3_rim_1	54.25	0.14	28.57	0.00	0.88	0.00	0.15	11.64	4.71	0.28	100.62
THj2_plag_macro3_rim_2	53.43	0.14	28.68	0.01	0.89	0.00	0.17	11.91	4.39	0.26	99.88
THj2_plag_macro3_rim_3	53.45	0.10	29.21	0.00	0.76	0.00	0.16	12.28	4.35	0.25	100.56
THj2_plag_macro3_core_1	45.81	0.02	34.73	0.00	0.46	0.00	0.16	18.41	1.05	0.02	100.66
THj2_plag_macro3_core_2	46.18	0.01	34.46	0.00	0.47	0.01	0.18	18.08	1.20	0.00	100.59
THj2_plag_macro3_core_3	45.77	0.02	34.92	0.00	0.47	0.01	0.17	18.26	1.07	0.01	100.70
THj2_plag_micro4_rim_1	53.09	0.10	29.47	0.00	0.74	-0.01	0.17	12.52	4.16	0.22	100.46
THj2_plag_micro4_rim_2	53.22	0.09	29.48	0.00	0.77	0.01	0.18	12.53	4.23	0.22	100.71
THj2_plag_micro4_rim_3	53.86	0.10	29.19	0.01	0.76	0.01	0.18	12.06	4.42	0.24	100.82
THj2_plag_micro4_inner_1	53.66	0.10	29.49	0.00	0.73	0.01	0.17	12.31	4.21	0.24	100.91
THj2_plag_micro4_inner_2	53.17	0.10	29.51	-0.01	0.75	0.00	0.17	12.54	4.22	0.22	100.68
THj2_plag_micro4_inner_3	58.00	0.03	26.47	0.00	0.50	0.01	0.08	8.66	5.98	0.50	100.24
THj2_plag_micro4_inner_4	54.23	0.09	28.62	0.00	0.74	0.01	0.15	11.67	4.62	0.28	100.40
THj2_plag_micro4_inner_5	54.88	0.07	28.42	0.00	0.66	0.00	0.14	11.21	4.83	0.32	100.52
THj2_plag_macro4_rim_1	53.09	0.10	29.69	-0.01	0.63	0.01	0.18	12.72	4.05	0.21	100.66
THj2_plag_macro4_rim_2	53.20	0.09	29.68	0.00	0.70	0.01	0.18	12.61	4.14	0.21	100.82

<i>Spot Name</i>	<i>SiO₂</i>	<i>TiO₂</i>	<i>Al₂O₃</i>	<i>Cr₂O₃</i>	<i>FeO</i>	<i>MnO</i>	<i>MgO</i>	<i>CaO</i>	<i>Na₂O</i>	<i>K₂O</i>	<i>Total</i>
THj2_plag_macro4_rim_3	53.17	0.10	29.68	0.00	0.69	0.00	0.18	12.59	4.09	0.19	100.69
THj2_plag_macro4_outer_mantle_1	49.91	0.05	31.94	0.00	0.59	0.01	0.24	15.32	2.81	0.04	100.91
THj2_plag_macro4_outer_mantle_2	48.97	0.03	32.51	0.01	0.59	0.01	0.24	16.03	2.34	0.04	100.76
THj2_plag_macro4_outer_mantle_3	48.83	0.04	32.57	0.00	0.56	0.00	0.24	16.09	2.32	0.04	100.69
THj2_plag_macro4_inner_mantle_1	47.02	0.02	34.00	0.00	0.53	0.00	0.20	17.44	1.62	0.01	100.83
THj2_plag_macro4_inner_mantle_2	46.71	0.02	34.20	0.00	0.54	0.00	0.20	17.61	1.44	0.01	100.72
THj2_plag_macro4_inner_mantle_3	47.14	0.03	33.97	0.00	0.49	0.00	0.20	17.48	1.54	0.01	100.87
THj2_plag_macro4_core_1	46.40	0.04	34.38	0.00	0.50	0.01	0.19	17.90	1.32	0.01	100.76
THj2_plag_macro4_core_2	46.55	0.02	34.20	0.00	0.50	0.00	0.20	17.61	1.41	0.01	100.50
THj2_plag_macro4_core_3	46.60	0.02	34.16	0.01	0.53	0.01	0.23	17.62	1.45	0.01	100.64
THj2_plag_micro5_1	52.81	0.07	29.91	0.00	0.65	0.01	0.24	13.04	4.02	0.08	100.84
THj2_plag_micro5_2	48.56	0.03	32.66	0.00	0.63	0.01	0.20	16.27	2.28	0.03	100.68
THj2_plag_micro5_3	52.90	0.07	29.68	0.00	0.63	0.00	0.27	13.08	4.02	0.07	100.73
THj2_plag_macro5_rim_1	52.89	0.06	29.62	0.00	0.68	0.01	0.18	12.62	4.13	0.21	100.39
THj2_plag_macro5_rim_2	53.31	0.10	29.40	0.00	0.71	0.01	0.16	12.32	4.25	0.25	100.52
THj2_plag_macro5_rim_3	52.78	0.10	29.69	0.00	0.66	0.01	0.17	12.66	4.12	0.22	100.40
THj2_plag_macro5_mantle_1	48.74	0.04	32.50	0.00	0.60	0.00	0.23	16.04	2.34	0.05	100.54
THj2_plag_macro5_mantle_2	48.53	0.04	32.60	0.00	0.63	0.00	0.22	16.03	2.32	0.05	100.42
THj2_plag_macro5_mantle_3	48.72	0.06	32.44	0.00	0.64	0.00	0.23	16.02	2.35	0.06	100.51
THj2_plag_macro5_core_1	46.40	0.02	34.44	0.00	0.44	0.00	0.24	17.77	1.34	0.03	100.67
THj2_plag_macro5_core_2	46.63	0.04	34.35	0.00	0.42	-0.01	0.26	17.84	1.35	0.01	100.90
THj2_plag_macro5_core_3	46.31	0.02	34.35	-0.01	0.42	0.00	0.26	17.86	1.35	0.01	100.57
THj2_plag_micro6_rim_1	52.76	0.11	29.84	0.00	0.64	0.00	0.16	12.67	4.00	0.21	100.39
THj2_plag_micro6_rim_2	53.08	0.10	29.90	0.01	0.61	0.00	0.18	12.81	3.99	0.20	100.88
THj2_plag_micro6_rim_3	52.91	0.09	29.77	0.00	0.61	0.02	0.18	12.81	4.08	0.19	100.66
THj2_plag_micro6_mantle_1	48.70	0.05	32.79	0.00	0.65	0.01	0.22	16.10	2.26	0.06	100.82
THj2_plag_micro6_mantle_2	48.74	0.02	32.53	0.00	0.63	-0.01	0.21	16.14	2.23	0.06	100.55
THj2_plag_micro6_mantle_3	48.92	0.01	32.50	0.01	0.65	0.01	0.21	16.04	2.38	0.05	100.77
THj2_plag_micro6_core_1	47.22	0.03	33.51	0.01	0.54	0.01	0.22	17.19	1.72	0.03	100.48
THj2_plag_micro6_core_2	47.57	0.04	33.57	0.00	0.53	0.01	0.22	17.08	1.83	0.01	100.86
THj2_plag_micro6_core_3	47.11	0.03	33.64	0.00	0.54	0.01	0.22	17.15	1.69	0.01	100.40
THj2_plag_macro6_rim_1	53.34	0.10	29.96	0.00	0.62	0.02	0.17	12.94	4.14	0.19	101.48
THj2_plag_macro6_rim_2	53.77	0.11	29.76	0.00	0.62	0.01	0.18	12.77	4.30	0.22	101.73
THj2_plag_macro6_rim_3	53.75	0.09	29.59	0.00	0.66	0.00	0.17	12.49	4.27	0.21	101.24
THj2_plag_macro6_mantle_1	49.23	0.05	32.50	0.00	0.57	0.01	0.25	15.93	2.42	0.05	101.00
THj2_plag_macro6_mantle_2	49.18	0.05	32.74	0.00	0.53	0.01	0.24	16.18	2.33	0.04	101.30
THj2_plag_macro6_mantle_3	49.11	0.03	32.61	0.00	0.55	0.01	0.23	16.00	2.37	0.05	100.96

<i>Spot Name</i>	<i>SiO₂</i>	<i>TiO₂</i>	<i>Al₂O₃</i>	<i>Cr₂O₃</i>	<i>FeO</i>	<i>MnO</i>	<i>MgO</i>	<i>CaO</i>	<i>Na₂O</i>	<i>K₂O</i>	<i>Total</i>
THj2_plag_macro6_core_1	46.10	0.00	34.69	0.00	0.42	0.00	0.21	18.16	1.19	0.01	100.78
THj2_plag_macro6_core_2	45.90	0.02	34.86	0.00	0.45	0.01	0.17	18.38	1.14	0.01	100.94
THj2_plag_macro6_core_3	46.00	0.03	34.93	0.00	0.41	0.01	0.16	18.25	1.11	0.01	100.90
THj2_groundmass_plag_1	53.77	0.10	29.13	0.00	0.83	0.01	0.19	12.16	4.39	0.26	100.84
THj2_groundmass_plag_2	53.63	0.14	28.72	0.00	0.80	0.01	0.19	12.21	4.44	0.25	100.40
THj2_groundmass_plag_3	53.74	0.11	29.12	0.00	0.86	0.00	0.17	11.99	4.40	0.25	100.65
THj2_groundmass_plag_4	53.72	0.13	29.17	0.01	0.85	0.01	0.17	12.08	4.48	0.25	100.87
THj2_groundmass_plag_5	48.36	0.04	32.56	0.00	0.82	0.01	0.16	16.01	2.27	0.09	100.32
THj2_groundmass_plag_6	52.77	0.08	29.79	0.01	0.78	0.01	0.18	12.98	4.01	0.19	100.79
THj2_groundmass_plag_7	49.23	0.04	32.06	0.00	0.83	0.00	0.17	15.40	2.62	0.11	100.45
THj2_groundmass_plag_8	48.65	0.04	32.69	0.00	0.67	0.00	0.24	16.10	2.36	0.05	100.79
THj2_groundmass_plag_9	54.18	0.11	28.72	0.00	0.79	0.01	0.19	11.79	4.56	0.28	100.63
THj2_groundmass_plag_10	51.92	0.08	30.54	0.00	0.89	0.01	0.18	13.68	3.58	0.17	101.05
THk2_plag_macro1_rim_1	52.69	0.12	29.77	0.00	0.76	0.00	0.21	13.07	3.93	0.16	100.71
THk2_plag_macro1_rim_2	51.94	0.07	30.41	0.00	0.69	0.02	0.24	13.84	3.59	0.14	100.95
THk2_plag_macro1_rim_3	55.06	0.12	27.92	0.00	0.84	0.00	0.16	11.09	4.77	0.34	100.29
THk2_plag_macro1_mantle_1	48.91	0.04	32.32	-0.01	0.66	0.01	0.26	16.02	2.46	0.01	100.68
THk2_plag_macro1_mantle_2	48.70	0.06	32.39	0.00	0.60	0.01	0.24	16.11	2.34	0.01	100.46
THk2_plag_macro1_mantle_3	48.65	0.05	32.36	0.00	0.56	0.00	0.26	16.03	2.35	0.03	100.28
THk2_plag_macro1_core_1	46.44	0.01	34.02	0.00	0.47	0.02	0.19	17.57	1.40	0.01	100.13
THk2_plag_macro1_core_2	46.49	0.00	34.04	0.00	0.51	0.01	0.20	17.55	1.53	0.00	100.34
THk2_plag_macro1_core_3	46.53	0.03	34.07	0.00	0.49	0.01	0.21	17.70	1.43	0.00	100.46
THk2_plag_macro2_rim_1	51.97	0.05	30.25	0.00	0.71	0.02	0.25	13.45	3.69	0.12	100.50
THk2_plag_macro2_rim_2	52.29	0.06	30.23	0.00	0.68	0.01	0.22	13.53	3.76	0.13	100.91
THk2_plag_macro2_rim_3	51.90	0.21	27.48	0.00	1.56	0.03	0.88	13.05	3.94	0.17	99.21
THk2_plag_macro2_core_1	46.49	0.04	34.11	0.00	0.49	0.00	0.20	17.59	1.49	0.02	100.43
THk2_plag_macro2_core_2	47.38	0.04	33.50	0.01	0.52	0.00	0.22	17.04	1.78	0.02	100.51
THk2_plag_macro2_core_3	46.58	0.04	34.07	0.00	0.51	0.00	0.20	17.52	1.44	0.02	100.38
THk2_plag_micro1_1	51.80	0.07	30.25	-0.01	0.78	0.01	0.19	13.63	3.46	0.18	100.37
THk2_plag_micro1_2	54.96	0.36	26.38	0.00	2.81	0.05	0.21	11.52	3.57	0.57	100.41
THk2_plag_micro1_3	52.62	0.10	29.33	0.00	1.16	0.01	0.26	13.02	3.72	0.24	100.48
THk2_plag_micro2_happy_1	48.95	0.06	32.45	0.00	0.63	0.00	0.26	15.94	2.51	0.04	100.84
THk2_plag_micro2_happy_2	49.08	0.03	32.20	0.00	0.62	0.02	0.25	15.89	2.50	0.03	100.63
THk2_plag_micro2_happy_3	48.17	0.04	33.06	0.00	0.61	0.00	0.23	16.62	2.10	0.02	100.85
THk2_plag_micro2_unhappy_1	48.29	0.04	32.71	0.01	0.67	0.00	0.22	16.31	2.18	0.06	100.47
THk2_plag_micro2_unhappy_2	47.88	0.04	32.95	0.00	0.64	0.01	0.23	16.58	2.00	0.03	100.35
THk2_plag_micro2_unhappy_3	50.24	0.05	31.43	0.00	0.64	0.00	0.26	15.07	2.86	0.04	100.59

<i>Spot Name</i>	<i>SiO₂</i>	<i>TiO₂</i>	<i>Al₂O₃</i>	<i>Cr₂O₃</i>	<i>FeO</i>	<i>MnO</i>	<i>MgO</i>	<i>CaO</i>	<i>Na₂O</i>	<i>K₂O</i>	<i>Total</i>
THk2_plag_macro3_rim_1	48.74	0.06	32.72	-0.01	0.60	0.00	0.25	16.25	2.32	0.02	100.96
THk2_plag_macro3_rim_2	48.75	0.06	32.53	0.00	0.60	0.00	0.26	16.14	2.34	0.02	100.69
THk2_plag_macro3_rim_3	48.55	0.05	32.48	-0.01	0.61	0.01	0.25	16.10	2.30	0.02	100.37
THk2_plag_macro3_core_1	46.32	0.03	33.86	0.01	0.50	0.01	0.21	17.43	1.51	0.02	99.88
THk2_plag_macro3_core_2	46.40	0.01	34.19	0.00	0.51	0.01	0.19	17.83	1.36	0.01	100.51
THk2_plag_macro3_core_3	46.72	0.01	33.98	-0.01	0.51	0.00	0.21	17.62	1.46	0.02	100.52
THk2_plag_macro4_1	46.48	0.03	34.23	0.00	0.56	0.00	0.19	17.74	1.42	0.01	100.66
THk2_plag_macro4_2	46.63	0.03	34.02	0.00	0.51	0.00	0.19	17.59	1.46	0.02	100.44
THk2_plag_macro4_3	46.52	0.04	34.19	0.01	0.52	0.01	0.19	17.77	1.46	-0.01	100.71
THk2_plag_macro5_rim_1	46.67	0.02	34.09	0.00	0.52	0.00	0.20	17.59	1.51	0.01	100.61
THk2_plag_macro5_rim_2	46.36	0.02	34.00	0.00	0.53	0.01	0.20	17.56	1.49	0.01	100.17
THk2_plag_macro5_rim_3	47.07	0.03	33.51	0.00	0.55	0.00	0.22	17.18	1.67	0.03	100.27
THk2_plag_macro5_incl_zone_1	46.41	0.04	34.37	0.01	0.50	0.01	0.19	17.94	1.33	0.02	100.81
THk2_plag_macro5_incl_zone_2	46.44	0.01	34.38	0.00	0.54	0.00	0.18	17.99	1.32	0.02	100.90
THk2_plag_macro5_incl_zone_3	45.51	0.02	34.37	0.00	0.50	0.01	0.18	18.17	1.15	0.02	99.92
THk2_plag_macro5_core_1	46.64	0.03	34.09	0.00	0.49	0.01	0.22	17.76	1.46	0.01	100.70
THk2_plag_macro5_core_2	46.41	0.04	34.22	0.00	0.47	0.00	0.23	17.80	1.39	0.01	100.59
THk2_plag_macro5_core_3	46.27	0.02	34.37	0.00	0.47	-0.01	0.20	18.02	1.29	0.01	100.65
THk2_plag_macro6_rim_1	48.64	0.03	32.45	0.00	0.58	0.01	0.26	16.04	2.35	0.05	100.41
THk2_plag_macro6_rim_2	48.59	0.05	32.64	0.00	0.58	0.00	0.25	16.36	2.25	0.02	100.73
THk2_plag_macro6_rim_3	48.49	0.05	32.72	0.00	0.60	0.01	0.24	16.29	2.21	0.01	100.62
THk2_plag_macro6_muddle_1	46.95	0.03	33.92	0.00	0.52	0.01	0.21	17.69	1.54	0.03	100.89
THk2_plag_macro6_muddle_2	46.56	0.03	34.00	0.00	0.54	0.00	0.21	17.57	1.52	0.03	100.46
THk2_plag_macro6_muddle_3	46.09	0.03	34.55	0.00	0.47	0.00	0.18	18.44	1.24	0.01	101.01
THk2_plag_macro6_core_1	46.50	0.01	34.08	0.00	0.49	0.01	0.21	17.84	1.38	0.01	100.52
THk2_plag_macro6_core_2	45.98	0.03	34.68	0.00	0.45	0.01	0.18	18.40	1.12	0.01	100.85
THk2_plag_macro6_core_3	45.65	0.03	34.85	0.00	0.46	0.01	0.17	18.36	1.03	0.01	100.57
THk2_plag_micro3_1	46.89	0.03	33.89	0.00	0.51	0.01	0.20	17.53	1.67	0.02	100.74
THk2_plag_micro3_2	46.71	0.03	34.08	0.00	0.52	0.00	0.18	17.63	1.48	0.03	100.64
THk2_plag_micro3_3	46.65	0.03	34.08	0.00	0.51	0.00	0.19	17.56	1.51	0.03	100.55
THk2_plag_micro4_1	47.80	0.04	33.05	0.00	0.52	0.00	0.23	16.78	1.99	0.01	100.42
THk2_plag_micro4_2	46.93	0.02	33.62	0.00	0.55	0.01	0.23	17.27	1.70	0.01	100.33
THk2_plag_micro4_3	46.89	0.02	33.48	0.00	0.53	0.00	0.22	17.28	1.68	0.01	100.11
THk2_plag_micro5_1	47.05	0.04	33.62	0.00	0.55	0.01	0.21	17.26	1.61	0.02	100.36
THk2_plag_micro5_2	47.23	0.03	33.63	0.00	0.54	0.01	0.22	17.45	1.66	0.02	100.79
THk2_plag_micro5_3	46.79	0.04	33.91	0.00	0.52	0.01	0.21	17.55	1.60	0.01	100.64
THk2_plag_macro7_rim_1	48.94	0.04	32.26	0.00	0.57	0.01	0.26	15.92	2.41	0.04	100.43

<i>Spot Name</i>	<i>SiO₂</i>	<i>TiO₂</i>	<i>Al₂O₃</i>	<i>Cr₂O₃</i>	<i>FeO</i>	<i>MnO</i>	<i>MgO</i>	<i>CaO</i>	<i>Na₂O</i>	<i>K₂O</i>	<i>Total</i>
THk2_plag_macro7_rim_2	49.13	0.04	32.29	0.00	0.61	0.00	0.25	15.81	2.44	0.05	100.65
THk2_plag_macro7_rim_3	48.76	0.04	32.46	-0.01	0.59	0.01	0.27	15.99	2.39	0.04	100.55
THk2_plag_macro7_core_1	46.72	0.01	34.00	0.00	0.48	0.02	0.20	17.51	1.57	0.00	100.49
THk2_plag_macro7_core_2	46.36	0.02	34.22	0.00	0.46	0.01	0.21	17.80	1.41	0.01	100.50
THk2_plag_macro7_core_3	46.38	0.02	34.25	0.00	0.45	0.00	0.20	17.72	1.45	0.01	100.47
THk2_plag_micro6_1	46.11	0.01	34.66	0.00	0.48	0.00	0.17	18.12	1.23	0.00	100.79
THk2_plag_micro6_2	47.65	0.00	33.47	0.00	0.51	0.00	0.22	17.04	1.83	0.03	100.77
THk2_plag_micro6_3	46.49	0.02	34.29	0.00	0.53	0.01	0.19	17.85	1.42	0.04	100.86
THk2_plag_macro8_rim_1	46.64	0.03	33.95	0.00	0.58	0.01	0.20	17.59	1.58	0.02	100.60
THk2_plag_macro8_rim_2	49.04	0.06	32.20	0.00	0.60	0.01	0.24	15.64	2.63	0.07	100.49
THk2_plag_macro8_rim_3	50.14	0.06	31.86	0.00	0.61	-0.01	0.24	15.26	2.83	0.08	101.08
THk2_plag_macro8_core_1	46.71	0.04	34.24	0.00	0.47	0.01	0.23	17.72	1.42	0.02	100.85
THk2_plag_macro8_core_2	46.88	0.05	34.07	0.00	0.46	0.01	0.23	17.81	1.48	0.02	100.99
THk2_plag_macro8_core_3	46.90	0.02	34.24	0.00	0.49	0.01	0.22	17.77	1.47	0.02	101.13
THk2_groundmass_plag_1	53.02	0.09	29.70	-0.01	0.75	0.01	0.20	12.75	4.23	0.16	100.91
THk2_groundmass_plag_2	52.18	0.08	29.82	0.00	0.81	0.00	0.27	13.38	3.78	0.14	100.46
THk2_groundmass_plag_3	51.80	0.09	30.07	0.00	0.82	0.01	0.26	13.55	3.77	0.14	100.51
THk2_groundmass_plag_4	49.84	0.07	31.61	0.00	0.74	0.00	0.25	15.16	2.83	0.08	100.57
THk2_groundmass_plag_5	55.10	0.12	27.66	0.00	1.25	0.02	0.22	11.08	4.96	0.29	100.69
THk2_groundmass_plag_6	53.72	0.13	29.19	0.00	0.99	0.01	0.16	12.18	4.38	0.23	100.99
THk2_groundmass_plag_7	49.53	0.08	31.98	0.01	0.83	0.01	0.26	15.56	2.60	0.06	100.91
THk2_groundmass_plag_8	49.16	0.04	32.09	0.00	0.70	0.00	0.26	15.73	2.51	0.03	100.52
THk2_groundmass_plag_9	49.55	0.03	31.80	0.00	0.68	0.00	0.27	15.38	2.74	0.05	100.51
THk2_groundmass_plag_10	51.97	0.07	30.16	0.00	0.76	0.00	0.25	13.70	3.66	0.13	100.70
THk3_plag_micro1_rim_1	53.17	0.10	29.78	0.00	0.80	0.01	0.20	13.08	3.96	0.24	101.35
THk3_plag_micro1_rim_2	52.32	0.06	30.19	0.00	0.67	0.00	0.21	13.45	3.68	0.15	100.74
THk3_plag_micro1_rim_3	51.85	0.05	30.59	0.00	0.69	0.02	0.23	13.89	3.55	0.12	100.99
THk3_plag_micro1_core_1	52.59	0.04	29.93	0.01	0.67	0.01	0.20	13.06	3.99	0.15	100.65
THk3_plag_micro1_core_2	51.95	0.06	30.76	-0.01	0.66	0.01	0.21	13.88	3.57	0.14	101.25
THk3_plag_micro1_core_3	52.65	0.10	29.68	0.00	0.92	0.01	0.17	12.83	3.97	0.25	100.59
THk3_plag_micro2_rim_1	48.79	0.04	32.60	0.00	0.63	0.00	0.25	16.18	2.31	0.04	100.84
THk3_plag_micro2_rim_2	48.90	0.05	32.47	0.00	0.61	0.00	0.25	16.02	2.38	0.05	100.74
THk3_plag_micro2_rim_3	49.15	0.03	32.39	0.00	0.60	0.01	0.26	15.99	2.47	0.04	100.92
THk3_plag_micro2_core_1	47.16	0.03	33.57	0.00	0.55	0.00	0.22	17.09	1.76	0.01	100.38
THk3_plag_micro2_core_2	46.61	0.05	33.99	0.01	0.52	0.01	0.20	17.67	1.51	0.03	100.59
THk3_plag_micro2_core_3	47.38	0.04	33.65	-0.01	0.54	0.00	0.22	17.20	1.74	0.02	100.79
THk3_plag_macro1_rim_1	53.10	0.06	29.70	-0.01	0.67	0.01	0.22	12.79	4.02	0.20	100.77

<i>Spot Name</i>	<i>SiO₂</i>	<i>TiO₂</i>	<i>Al₂O₃</i>	<i>Cr₂O₃</i>	<i>FeO</i>	<i>MnO</i>	<i>MgO</i>	<i>CaO</i>	<i>Na₂O</i>	<i>K₂O</i>	<i>Total</i>
THk3_plag_macro1_rim_2	52.40	0.06	30.13	0.00	0.63	0.00	0.21	13.30	3.76	0.19	100.68
THk3_plag_macro1_rim_3	52.33	0.09	29.97	0.01	0.70	0.00	0.21	13.05	3.84	0.19	100.38
THk3_plag_macro1_mantle_1	49.66	0.04	31.74	0.01	0.61	-0.01	0.25	15.30	2.66	0.04	100.30
THk3_plag_macro1_mantle_2	48.68	0.03	32.54	0.00	0.55	0.01	0.24	16.16	2.29	0.04	100.54
THk3_plag_macro1_mantle_3	49.25	0.07	31.98	-0.01	0.62	0.00	0.26	15.63	2.67	0.04	100.53
THk3_plag_macro1_core_1	46.57	0.03	34.12	0.00	0.50	0.01	0.20	17.62	1.47	0.01	100.52
THk3_plag_macro1_core_2	47.27	0.02	33.71	0.01	0.52	0.00	0.21	17.23	1.77	0.01	100.75
THk3_plag_macro1_core_3	47.51	0.04	33.62	0.00	0.50	0.00	0.22	17.11	1.82	0.01	100.84
THk3_plag_macro2_rim_1	48.78	0.06	32.38	0.00	0.58	0.01	0.26	15.46	2.60	0.02	100.16
THk3_plag_macro2_rim_2	49.06	0.05	31.86	0.00	0.56	0.01	0.26	15.60	2.57	0.03	100.00
THk3_plag_macro2_rim_3	49.52	0.04	31.82	0.00	0.58	0.00	0.27	15.49	2.65	0.03	100.40
THk3_plag_macro2_mantle_1	45.97	0.02	34.26	0.00	0.48	0.00	0.18	17.90	1.34	0.00	100.14
THk3_plag_macro2_mantle_2	46.01	0.01	34.55	-0.01	0.47	-0.01	0.17	18.26	1.22	0.02	100.71
THk3_plag_macro2_mantle_3	46.36	0.03	34.04	0.00	0.47	0.00	0.20	17.69	1.44	0.02	100.25
THk3_plag_macro2_core_1	46.81	0.03	34.01	0.01	0.47	0.01	0.22	17.61	1.52	0.02	100.69
THk3_plag_macro2_core_2	47.04	0.00	33.80	0.00	0.45	0.00	0.24	17.37	1.64	0.01	100.54
THk3_plag_macro2_core_3	46.57	0.00	34.08	0.00	0.46	0.00	0.23	17.67	1.53	0.02	100.58
THk3_plag_micro3_rim_1	52.72	0.09	29.82	0.01	0.88	0.01	0.22	12.98	4.06	0.17	100.94
THk3_plag_micro3_rim_2	52.36	0.10	30.11	0.00	0.70	0.01	0.20	13.37	3.81	0.15	100.80
THk3_plag_micro3_rim_3	52.05	0.08	30.16	0.00	0.69	0.00	0.20	13.30	3.74	0.16	100.39
THk3_plag_micro3_mantle_1	48.40	0.05	32.66	0.00	0.59	0.01	0.24	16.36	2.19	0.04	100.53
THk3_plag_micro3_mantle_2	48.41	0.06	32.49	0.00	0.57	0.00	0.24	16.13	2.29	0.02	100.20
THk3_plag_micro3_mantle_3	48.53	0.06	32.65	0.00	0.59	0.01	0.25	16.16	2.25	0.02	100.50
THk3_plag_micro3_core_1	46.70	0.01	34.20	0.00	0.55	0.01	0.19	17.77	1.45	0.02	100.90
THk3_plag_micro3_core_2	46.68	0.03	34.08	0.00	0.52	0.01	0.20	17.63	1.50	0.02	100.65
THk3_plag_micro3_core_3	45.57	0.01	34.72	0.00	0.50	0.01	0.17	18.24	1.15	0.00	100.38
THk3_plag_macro3_rim_1	52.47	0.09	29.84	0.00	0.80	0.00	0.21	13.08	3.96	0.20	100.65
THk3_plag_macro3_rim_2	53.62	0.14	29.09	0.01	1.00	0.01	0.20	12.18	4.32	0.23	100.80
THk3_plag_macro3_rim_3	52.02	0.08	30.11	0.00	0.83	0.02	0.20	13.43	3.69	0.16	100.54
THk3_plag_macro3_mantle_1	48.74	0.05	32.54	0.00	0.63	0.01	0.25	16.19	2.29	0.04	100.74
THk3_plag_macro3_mantle_2	48.49	0.07	32.74	0.00	0.62	0.01	0.24	16.17	2.20	0.03	100.58
THk3_plag_macro3_mantle_3	48.38	0.03	32.72	0.00	0.58	0.00	0.23	16.35	2.22	0.03	100.54
THk3_plag_macro3_core_1	46.57	0.02	33.98	0.00	0.52	0.00	0.20	17.64	1.48	0.00	100.41
THk3_plag_macro3_core_2	45.67	0.01	34.64	0.00	0.49	0.01	0.17	18.31	1.10	0.00	100.41
THk3_plag_macro3_core_3	45.96	0.02	34.65	0.00	0.49	-0.01	0.16	18.12	1.19	0.02	100.61
THk3_plag_micro4_1	46.44	0.01	34.14	0.01	0.51	0.01	0.18	17.73	1.48	0.02	100.53
THk3_plag_micro4_2	46.61	0.03	34.12	0.00	0.49	0.00	0.18	17.86	1.48	0.02	100.79

<i>Spot Name</i>	<i>SiO₂</i>	<i>TiO₂</i>	<i>Al₂O₃</i>	<i>Cr₂O₃</i>	<i>FeO</i>	<i>MnO</i>	<i>MgO</i>	<i>CaO</i>	<i>Na₂O</i>	<i>K₂O</i>	<i>Total</i>
THk3_plag_micro4_3	46.68	0.03	33.95	0.00	0.53	0.00	0.19	17.66	1.51	0.00	100.54
THk3_plag_micro5_1	47.57	0.05	33.43	0.00	0.57	0.01	0.21	16.95	1.89	0.01	100.67
THk3_plag_micro5_2	47.07	0.03	33.93	0.00	0.54	0.01	0.18	17.61	1.60	0.02	100.99
THk3_plag_micro5_3	46.82	0.02	33.63	0.00	0.57	0.00	0.19	17.21	1.69	0.03	100.16
THk3_plag_micro6_1	45.88	0.03	34.70	0.00	0.44	0.01	0.17	18.21	1.18	0.01	100.61
THk3_plag_micro6_2	45.72	0.01	34.63	0.00	0.44	0.00	0.16	18.24	1.17	0.02	100.40
THk3_plag_micro6_3	46.05	0.02	34.57	0.00	0.47	0.00	0.17	18.08	1.24	0.02	100.60
THk3_plag_micro7_rim_1	53.15	0.11	29.62	-0.01	0.71	0.01	0.21	12.86	4.04	0.17	100.87
THk3_plag_micro7_rim_2	52.91	0.08	29.47	0.01	0.72	0.00	0.22	12.66	4.12	0.18	100.35
THk3_plag_micro7_rim_3	52.94	0.08	29.40	-0.01	0.75	0.02	0.24	12.91	4.06	0.18	100.58
THk3_plag_micro7_core_1	50.48	0.04	31.42	0.00	0.58	0.00	0.23	14.85	3.04	0.05	100.68
THk3_plag_micro7_core_2	47.59	0.08	32.75	0.00	1.06	0.02	0.33	16.83	1.81	0.15	100.63
THk3_plag_micro7_core_3	47.16	0.09	33.18	0.00	0.93	0.01	0.18	16.96	1.83	0.08	100.43
THk3_plag_macro4_rim_1	48.73	0.05	32.50	0.00	0.60	0.00	0.25	16.13	2.37	0.04	100.66
THk3_plag_macro4_rim_2	48.79	0.04	32.69	0.00	0.52	0.00	0.25	16.28	2.43	0.03	101.02
THk3_plag_macro4_rim_3	48.82	0.06	32.73	0.00	0.57	0.00	0.24	16.30	2.31	0.03	101.04
THk3_plag_macro4_core_1	46.27	0.01	34.67	0.00	0.41	-0.01	0.22	18.15	1.27	0.02	101.01
THk3_plag_macro4_core_2	46.11	0.02	34.52	0.00	0.40	-0.01	0.21	18.23	1.22	0.01	100.72
THk3_plag_macro4_core_3	46.33	0.02	34.61	0.00	0.42	0.01	0.23	18.19	1.28	0.01	101.09
THk3_plag_macro5_rim_1	51.79	0.08	29.84	0.00	0.65	0.00	0.21	13.22	3.68	0.17	99.64
THk3_plag_macro5_rim_2	50.30	0.04	31.52	0.00	0.69	-0.01	0.24	14.91	2.92	0.06	100.66
THk3_plag_macro5_rim_3	52.18	0.08	29.19	0.00	0.69	0.01	0.23	13.16	3.91	0.16	99.62
THk3_plag_macro5_mantle_1	49.00	0.02	32.35	0.00	0.60	0.01	0.25	16.15	2.40	0.04	100.81
THk3_plag_macro5_mantle_2	48.77	0.04	32.54	0.01	0.53	0.00	0.25	16.13	2.33	0.02	100.62
THk3_plag_macro5_mantle_3	48.76	0.05	32.35	0.00	0.60	0.00	0.26	16.06	2.37	0.04	100.48
THk3_plag_macro5_core_1	46.60	0.02	33.95	0.00	0.53	0.01	0.20	17.50	1.53	0.02	100.37
THk3_plag_macro5_core_2	45.92	0.03	34.64	0.00	0.50	0.01	0.16	18.36	1.16	0.01	100.78
THk3_plag_macro5_core_3	45.86	0.02	34.67	0.00	0.50	0.00	0.16	18.18	1.19	0.00	100.58
THk3_plag_macro6_rim_1	52.84	0.06	29.89	0.00	0.65	0.00	0.21	13.05	3.95	0.18	100.83
THk3_plag_macro6_rim_2	53.29	0.08	29.94	0.00	0.73	0.01	0.21	13.06	4.01	0.17	101.49
THk3_plag_macro6_rim_3	53.56	0.10	29.34	0.00	0.71	0.02	0.18	12.23	4.32	0.20	100.66
THk3_plag_macro6_mantle_1	49.08	0.05	32.46	0.00	0.60	0.01	0.26	15.81	2.46	0.03	100.75
THk3_plag_macro6_mantle_2	48.91	0.05	32.45	0.00	0.62	0.01	0.25	15.90	2.44	0.05	100.67
THk3_plag_macro6_mantle_3	49.36	0.03	32.39	0.00	0.60	0.00	0.26	15.83	2.45	0.02	100.93
THk3_plag_macro6_core_1	46.26	-0.01	34.55	0.00	0.43	0.01	0.18	17.97	1.32	0.02	100.74
THk3_plag_macro6_core_2	45.64	0.02	34.73	0.00	0.44	0.01	0.17	18.34	1.13	0.01	100.50
THk3_plag_macro6_core_3	45.92	0.02	34.74	0.01	0.43	0.02	0.18	18.19	1.19	0.02	100.70

<i>Spot Name</i>	<i>SiO₂</i>	<i>TiO₂</i>	<i>Al₂O₃</i>	<i>Cr₂O₃</i>	<i>FeO</i>	<i>MnO</i>	<i>MgO</i>	<i>CaO</i>	<i>Na₂O</i>	<i>K₂O</i>	<i>Total</i>
THk3_plag_macro7_rim_1	53.47	0.07	29.30	0.00	0.78	0.01	0.20	12.33	4.28	0.21	100.65
THk3_plag_macro7_rim_2	54.14	0.09	28.66	0.00	0.71	0.01	0.18	11.60	4.61	0.25	100.26
THk3_plag_macro7_rim_3	53.85	0.09	28.47	0.00	0.80	0.01	0.17	11.48	4.73	0.27	99.87
THk3_plag_macro7_mantle_1	49.14	0.03	32.16	0.00	0.60	-0.01	0.25	15.82	2.56	0.05	100.61
THk3_plag_macro7_mantle_2	49.27	0.06	32.20	0.00	0.64	0.00	0.27	15.75	2.50	0.02	100.70
THk3_plag_macro7_mantle_3	49.04	0.06	32.23	0.00	0.61	0.01	0.26	15.91	2.52	0.02	100.66
THk3_plag_macro7_core_1	46.14	0.03	34.53	0.00	0.49	0.01	0.18	18.23	1.27	0.02	100.89
THk3_plag_macro7_core_2	45.46	0.02	34.84	0.00	0.49	0.00	0.16	18.48	1.08	0.01	100.54
THk3_plag_macro7_core_3	46.39	0.02	34.40	0.00	0.50	0.01	0.19	17.96	1.35	0.02	100.83
THk3_groundmass_plag_1	54.61	0.40	26.95	0.01	1.53	0.02	0.22	11.08	4.15	0.60	99.56
THk3_groundmass_plag_2	53.17	0.09	29.41	0.01	0.84	0.01	0.25	12.68	4.16	0.21	100.82
THk3_groundmass_plag_3	52.63	0.34	27.68	0.00	2.38	0.04	0.24	12.46	3.65	0.41	99.84
THk3_groundmass_plag_4	53.16	0.11	29.02	0.00	0.91	0.01	0.25	12.46	4.24	0.22	100.38
THk3_groundmass_plag_5	49.33	0.06	32.10	-0.01	0.71	0.01	0.27	15.72	2.56	0.03	100.78
THk3_groundmass_plag_6	49.88	0.05	31.58	0.00	0.75	0.00	0.28	15.26	2.78	0.05	100.63
THk3_groundmass_plag_7	54.36	0.13	28.53	0.00	1.00	0.01	0.19	11.67	4.64	0.26	100.78
THk3_groundmass_plag_8	54.35	0.10	28.58	0.00	0.95	0.01	0.19	11.83	4.64	0.27	100.91
THk3_groundmass_plag_9	52.68	0.10	29.68	0.00	0.82	0.01	0.21	12.90	4.00	0.20	100.60
THk3_groundmass_plag_10	53.78	0.11	29.08	0.00	0.90	0.01	0.18	12.30	4.43	0.23	101.03

Appendix D – Pyroxene Chemistry

<i>Spot Name</i>	<i>SiO₂</i>	<i>TiO₂</i>	<i>Al₂O₃</i>	<i>Cr₂O₃</i>	<i>FeO</i>	<i>MnO</i>	<i>MgO</i>	<i>CaO</i>	<i>Na₂O</i>	<i>K₂O</i>	<i>Total</i>
THa1_cpx_macro1_1	51.14	0.58	4.70	0.26	6.05	0.14	16.76	20.14	0.21	0.01	100.00
THa1_cpx_macro1_2	50.79	0.75	4.88	0.45	5.62	0.14	16.05	21.06	0.22	0.00	99.96
THa1_cpx_macro1_3	51.16	0.66	4.57	0.43	5.56	0.13	16.60	20.57	0.21	0.01	99.92
THa2_cpx_micro1_1	49.84	1.04	5.12	0.08	11.79	0.24	12.06	18.70	0.41	0.02	99.28
THa2_cpx_micro1_2	51.16	0.75	3.10	0.12	7.18	0.14	14.83	22.31	0.20	0.01	99.77
THa2_cpx_micro1_3	51.25	0.53	3.42	0.39	5.73	0.14	16.10	21.49	0.19	-0.02	99.23
THa1.ol_plag_cluster1.ol.1	50.82	0.56	4.68	0.49	5.85	0.14	17.06	19.84	0.21	0.00	99.67
THa1.ol_plag_cluster1.ol.2	51.21	0.50	4.37	0.46	5.43	0.14	16.62	20.83	0.19	0.01	99.76
THa1.ol_plag_cluster1.ol.3	51.20	0.58	4.24	0.53	5.36	0.11	16.64	20.99	0.21	0.01	99.86
THa1.ol.micro1.1	50.84	0.83	4.40	0.25	7.53	0.19	16.93	18.69	0.23	0.00	99.88
THa1.ol.micro1.2	50.62	0.77	4.47	0.27	6.88	0.16	15.98	20.64	0.26	-0.01	100.05
THa1.ol.micro1.3	50.65	0.88	4.26	0.24	7.07	0.17	16.34	19.81	0.22	0.01	99.65
THa1.ol.micro4.core.1	50.79	0.65	4.79	0.49	5.74	0.15	16.35	20.41	0.22	0.00	99.58
THa1.ol.micro4.core.2	51.13	0.59	4.52	0.49	5.79	0.15	16.95	19.93	0.22	0.00	99.76
THa1.ol.micro4.core.3	53.51	0.30	2.07	0.24	5.90	0.17	19.18	18.36	0.17	0.00	99.90

<i>Spot Name</i>	<i>SiO₂</i>	<i>TiO₂</i>	<i>Al₂O₃</i>	<i>Cr₂O₃</i>	<i>FeO</i>	<i>MnO</i>	<i>MgO</i>	<i>CaO</i>	<i>Na₂O</i>	<i>K₂O</i>	<i>Total</i>
THa1.ol_micro5_1	50.98	1.09	3.06	0.14	9.43	0.24	15.87	18.61	0.25	-0.01	99.65
THa1.ol_micro5_2	51.36	0.89	2.99	0.19	8.27	0.21	16.18	19.61	0.24	0.00	99.93
THa1.ol_micro5_3	52.68	0.68	1.37	0.07	10.16	0.27	17.53	16.92	0.15	0.00	99.83
THa1.ol_micro_transect1	51.29	0.66	4.39	0.32	5.72	0.14	16.59	20.62	0.20	0.01	99.94
THa1.ol_micro_transect1	51.17	0.59	4.52	0.29	5.92	0.14	16.56	20.66	0.21	0.01	100.07
THa1.ol_micro_transect1	51.12	0.57	4.53	0.33	5.71	0.14	16.54	20.85	0.21	0.00	99.99
THa1.ol_micro_transect1	51.55	0.48	4.10	0.49	5.36	0.13	16.66	21.06	0.20	-0.01	100.04
THa1.ol_micro_transect1	50.04	1.13	3.77	0.07	10.12	0.25	15.05	18.74	0.34	0.00	99.49
THa1.ol_micro_transect1	49.71	1.17	3.84	0.07	10.21	0.24	14.93	18.60	0.30	-0.01	99.08
THa1.ol_micro_transect1	49.72	1.21	4.05	0.13	10.25	0.24	15.09	18.34	0.31	-0.01	99.35
THa1.ol_micro_transect1	49.95	1.22	4.14	0.11	10.11	0.25	15.14	18.80	0.34	0.00	100.06
THa1.ol_micro_transect1	52.12	0.65	2.03	0.13	7.78	0.19	16.56	19.83	0.24	0.01	99.55
THa1.ol_micro_transect1	51.57	0.95	2.77	0.12	9.75	0.24	16.25	18.21	0.20	-0.01	100.05
THa1.ol_groundmass_1	50.95	1.08	3.15	0.14	9.64	0.23	15.49	18.86	0.25	0.01	99.79
THa1.ol_groundmass_2	49.14	1.81	2.50	0.01	16.24	0.34	12.37	16.88	0.25	0.01	99.54
THa1.ol_groundmass_3	48.63	1.34	1.78	0.01	23.47	0.48	9.68	13.83	0.20	0.01	99.44
THa1.ol_groundmass_4	52.42	0.64	0.90	0.01	15.64	0.40	17.90	11.48	0.11	0.00	99.49
THa1.ol_groundmass_5	51.73	0.92	2.04	0.07	10.31	0.26	15.95	18.58	0.20	0.01	100.06
THa1.ol_groundmass_6	51.69	0.82	1.88	0.06	11.03	0.27	16.12	17.09	0.18	0.01	99.15
THa1.ol_groundmass_7	50.61	1.33	2.67	0.02	12.34	0.29	15.36	16.89	0.22	0.00	99.73
THa1.ol_groundmass_8	50.71	1.20	1.79	0.01	17.34	0.39	15.59	12.39	0.18	0.01	99.63
THa1.ol_groundmass_10	51.67	0.75	1.02	0.00	20.20	0.47	16.96	8.73	0.11	-0.01	99.92
THa2.ol_micro1_1	51.29	0.60	3.88	0.46	5.80	0.16	16.50	21.00	0.23	0.00	99.92
THa2.ol_micro1_2	51.27	0.61	3.91	0.43	6.07	0.16	16.98	20.12	0.25	-0.01	99.81
THa2.ol_micro1_3	51.32	0.60	3.84	0.43	5.77	0.14	16.71	20.74	0.22	-0.01	99.76
THa2.ol_micro2_1	52.99	0.43	2.25	0.35	5.79	0.14	17.67	20.19	0.21	0.00	100.01
THa2.ol_micro2_2	51.53	0.57	3.52	0.47	5.69	0.14	16.75	20.95	0.23	-0.02	99.86
THa2.ol_micro2_3	51.31	0.60	3.86	0.50	5.62	0.15	16.52	20.94	0.22	-0.01	99.73
THa2.ol_micro3_1	51.03	0.96	3.66	0.22	7.85	0.19	16.52	19.21	0.23	0.00	99.87
THa2.ol_micro3_2	51.25	0.54	4.09	0.44	5.60	0.13	16.61	20.83	0.21	0.02	99.73
THa2.ol_micro3_3	51.24	0.55	4.05	0.55	5.86	0.14	16.58	20.60	0.21	0.01	99.78
THa2.ol_micro4_1	52.15	0.51	3.10	0.45	5.32	0.13	16.83	21.51	0.24	0.00	100.23
THa2.ol_micro4_2	52.01	0.53	3.19	0.49	5.20	0.12	16.74	21.47	0.20	0.01	99.97
THa2.ol_micro4_3	52.51	0.48	2.95	0.44	5.26	0.14	17.09	21.26	0.21	-0.01	100.34
THa2.ol_micro5_1	51.02	0.92	3.67	0.34	7.27	0.18	16.17	20.04	0.23	0.01	99.84
THa2.ol_micro5_2	50.50	0.77	5.02	0.56	5.71	0.14	16.17	20.78	0.23	0.00	99.88
THa2.ol_micro5_3	50.04	1.30	4.36	0.19	8.57	0.20	15.96	18.90	0.25	0.01	99.78
THa2.ol_groundmass_2	52.09	0.75	2.44	0.11	8.14	0.20	16.54	19.66	0.20	0.00	100.12

<i>Spot Name</i>	<i>SiO₂</i>	<i>TiO₂</i>	<i>Al₂O₃</i>	<i>Cr₂O₃</i>	<i>FeO</i>	<i>MnO</i>	<i>MgO</i>	<i>CaO</i>	<i>Na₂O</i>	<i>K₂O</i>	<i>Total</i>
THa2_ol_groundmass_3	52.03	0.80	2.62	0.11	8.44	0.19	16.25	19.75	0.20	0.00	100.39
THa2_ol_groundmass_5	51.38	0.89	2.43	0.08	9.50	0.21	15.44	19.09	0.22	0.00	99.22
THa2_ol_groundmass_6	51.79	0.92	2.33	0.04	11.16	0.28	16.26	17.30	0.21	0.00	100.28
THa2_ol_groundmass_7	52.52	0.68	1.78	0.07	8.99	0.22	16.78	18.95	0.18	0.01	100.18
THa2_ol_groundmass_8	52.18	0.64	2.17	0.09	7.65	0.18	16.37	20.41	0.20	0.00	99.89
THa2_ol_groundmass_9	52.54	0.70	1.55	0.04	11.17	0.29	17.10	16.27	0.17	0.00	99.83
THd3a_cpx_micro1_1	51.70	0.63	2.84	0.27	6.60	0.15	16.52	20.99	0.24	0.00	99.94
THd3a_cpx_micro1_2	51.66	0.61	3.23	0.27	6.83	0.18	16.79	19.91	0.25	0.00	99.73
THd3a_cpx_micro1_3	50.77	0.77	4.24	0.22	7.46	0.17	16.24	19.54	0.27	-0.01	99.69
THd3a_groundmass_arc_cpx_1	50.49	0.99	4.06	0.13	7.97	0.18	15.85	19.87	0.24	0.00	99.77
THd3a_groundmass_arc_cpx_2	52.10	0.79	2.10	0.03	9.79	0.24	16.11	19.11	0.21	0.01	100.50
THd3a_groundmass_arc_cpx_3	51.65	0.90	1.74	0.04	10.92	0.25	15.23	18.98	0.20	0.00	99.92
THd3a_groundmass_arc_cpx_4	52.11	0.72	1.95	0.04	9.47	0.23	16.02	19.37	0.22	0.00	100.12
THd3a_groundmass_arc_cpx_5	51.38	0.88	2.61	0.05	8.90	0.21	15.69	19.83	0.21	0.00	99.76
THd3a_ol_micro3_1	52.75	0.54	2.10	0.18	6.36	0.17	17.33	20.57	0.20	-0.01	100.21
THd3a_ol_micro3_2	50.93	0.81	3.95	0.49	6.55	0.17	16.24	20.41	0.25	0.00	99.80
THd3a_ol_micro3_3	52.12	0.51	2.54	0.25	6.54	0.15	17.08	20.37	0.23	0.01	99.80
THd3a_ol_micro4_1	51.32	0.48	3.99	0.68	4.98	0.12	16.53	21.27	0.22	0.01	99.61
THd3a_ol_micro4_2	52.12	0.40	3.13	0.49	4.79	0.11	17.06	21.59	0.21	0.01	99.91
THd3a_ol_micro4_3	50.95	0.64	4.19	0.51	5.76	0.13	16.68	20.55	0.24	0.00	99.66
THd3a_ol_micro5_darker_1	52.95	0.37	2.30	0.06	5.97	0.15	17.15	21.09	0.20	-0.01	100.25
THd3a_ol_micro5_darker_2	52.82	0.41	2.35	0.06	6.09	0.15	17.16	20.95	0.18	0.00	100.17
THd3a_ol_micro5_darker_3	52.80	0.40	2.42	0.06	6.05	0.15	17.06	21.12	0.20	0.00	100.27
THd3a_groundmass_ol_1	52.15	0.75	2.03	0.07	9.04	0.21	16.63	18.87	0.19	0.00	99.95
THd3a_groundmass_ol_2	51.19	1.02	2.78	0.11	9.96	0.24	15.69	18.59	0.25	0.00	99.83
THd3a_groundmass_ol_3	52.24	0.69	1.90	0.05	8.67	0.22	16.16	20.09	0.20	0.00	100.23
THd3a_groundmass_ol_5	51.94	0.84	2.05	0.06	9.68	0.23	15.82	19.30	0.22	0.00	100.14
THd3a_groundmass_ol_6	52.10	0.70	1.89	0.05	9.24	0.21	16.06	19.52	0.20	0.00	99.98
THd3a_groundmass_ol_8	51.25	0.83	2.93	0.17	9.04	0.23	16.41	18.80	0.22	0.01	99.89
THd3a_groundmass_ol_10	51.47	0.91	2.77	0.12	8.67	0.21	16.20	19.40	0.20	0.01	99.96
THde2_ol_micro2_1	51.06	0.50	4.56	0.65	5.12	0.13	16.37	21.11	0.23	0.00	99.72
THde2_ol_micro2_2	50.71	0.62	4.46	0.56	5.12	0.12	16.11	21.67	0.21	0.00	99.58
THde2_ol_micro2_3	50.99	0.65	4.59	0.67	5.08	0.12	16.24	21.45	0.21	0.00	100.00
THde2_ol_micro6_1	50.66	0.64	4.47	0.66	5.12	0.13	16.44	21.02	0.22	0.00	99.35
THde2_ol_micro6_2	51.35	0.44	3.53	0.54	5.01	0.12	16.81	20.87	0.21	0.01	98.90
THde2_ol_micro6_3	53.28	0.36	2.06	0.26	6.01	0.18	19.26	18.52	0.16	-0.01	100.09
THde2_groundmass_ol_1	52.49	0.55	1.26	0.01	12.55	0.32	17.75	13.92	0.14	-0.01	98.99
THde2_groundmass_ol_2	51.40	0.77	3.66	0.25	6.55	0.16	16.55	20.32	0.21	-0.01	99.87

<i>Spot Name</i>	<i>SiO₂</i>	<i>TiO₂</i>	<i>Al₂O₃</i>	<i>Cr₂O₃</i>	<i>FeO</i>	<i>MnO</i>	<i>MgO</i>	<i>CaO</i>	<i>Na₂O</i>	<i>K₂O</i>	<i>Total</i>
THde2_groundmass_ol_3	52.17	0.64	2.95	0.06	7.06	0.17	16.63	20.41	0.21	0.00	100.30
THde2_groundmass_ol_4	52.49	0.59	2.18	0.06	7.34	0.18	16.58	20.58	0.18	0.00	100.17
THde2_groundmass_ol_5	52.79	0.59	2.08	0.07	7.35	0.17	16.71	20.61	0.19	-0.01	100.56
THde2_groundmass_ol_6	52.70	0.56	2.11	0.10	6.77	0.17	16.70	20.96	0.18	0.01	100.25
THde2_groundmass_ol_8	53.01	0.49	1.74	0.08	6.73	0.18	17.42	20.03	0.17	0.01	99.86
THde2_groundmass_ol_10	51.84	0.64	3.24	0.17	6.14	0.14	16.75	21.11	0.21	0.00	100.25
THf3b_oliv_micro1_1	52.50	0.41	2.79	0.37	4.86	0.12	17.01	21.72	0.20	-0.01	99.98
THf3b_oliv_micro1_2	51.78	0.62	3.59	0.38	5.32	0.14	16.77	21.31	0.20	0.00	100.10
THf3b_oliv_micro1_3	52.13	0.48	3.27	0.37	5.08	0.13	17.06	21.05	0.18	0.00	99.75
THf3b_oliv_micro2_1	51.14	0.58	4.36	0.51	5.21	0.13	16.47	21.05	0.23	0.00	99.68
THf3b_oliv_micro2_2	51.30	0.54	4.52	0.50	5.35	0.12	16.78	20.93	0.23	0.00	100.26
THf3b_oliv_micro2_3	50.65	0.83	4.73	0.37	5.77	0.15	16.35	20.64	0.20	0.00	99.68
THf3b_oliv_micro5_1	52.03	0.48	3.40	0.49	5.05	0.12	16.95	21.07	0.21	0.00	99.81
THf3b_oliv_micro5_2	53.42	0.39	2.36	0.07	5.90	0.16	18.65	19.57	0.18	0.01	100.72
THf3b_oliv_micro5_3	53.28	0.33	2.16	0.06	5.67	0.17	18.84	18.88	0.18	-0.02	99.57
THf3b_oliv_micro6_1	52.60	0.49	2.79	0.21	6.02	0.16	17.60	20.18	0.19	0.00	100.24
THf3b_oliv_micro6_2	52.54	0.40	2.81	0.35	5.59	0.15	17.89	19.81	0.19	0.00	99.75
THf3b_oliv_micro6_3	53.26	0.33	2.46	0.40	5.33	0.16	18.72	19.49	0.18	0.00	100.32
THf3b_groundmass_oliv_1	53.59	0.39	1.84	0.15	5.79	0.16	17.83	20.38	0.16	0.01	100.30
THf3b_groundmass_oliv_2	53.17	0.34	2.34	0.29	5.62	0.16	18.53	19.47	0.19	-0.01	100.10
THf3b_groundmass_oliv_8	49.73	1.32	4.88	0.06	8.18	0.19	15.90	19.25	0.27	0.00	99.78
THf3b_groundmass_oliv_9	52.18	0.68	2.92	0.16	6.25	0.15	16.72	20.93	0.20	0.01	100.19
THf3b_groundmass_oliv_10	52.51	0.54	2.11	0.08	7.14	0.19	16.95	20.48	0.19	-0.01	100.19
THi3_cpx_micro1_1	52.15	0.60	3.08	0.03	6.49	0.14	16.78	20.84	0.20	0.00	100.30
THi3_cpx_micro1_2	52.10	0.59	2.88	0.01	7.19	0.16	16.72	20.48	0.25	0.00	100.37
THi3_cpx_micro1_3	53.42	0.44	2.03	0.03	6.07	0.16	17.50	20.82	0.19	0.01	100.65
THi3_oliv_micro1_1	53.21	0.43	1.95	0.13	6.30	0.17	18.54	19.32	0.16	0.00	100.20
THi3_oliv_micro1_2	51.02	0.93	4.31	0.22	6.46	0.14	16.40	20.63	0.21	0.00	100.32
THi3_oliv_micro1_3	50.94	0.82	4.10	0.25	6.30	0.15	16.47	20.73	0.22	0.02	99.98
THi3_groundmass_oliv_2	52.00	0.88	2.74	0.10	8.32	0.18	16.57	19.44	0.20	-0.01	100.42
THi3_groundmass_oliv_3	51.98	0.54	3.42	0.27	5.71	0.13	17.09	20.73	0.21	-0.01	100.08
THi3_groundmass_oliv_4	52.30	0.70	3.10	0.16	7.04	0.17	16.93	19.74	0.19	0.01	100.33
THi3_groundmass_oliv_5	52.00	0.67	2.96	0.21	7.05	0.18	16.92	19.70	0.18	0.01	99.88
THi3_groundmass_oliv_6	51.36	1.05	4.14	0.07	8.44	0.20	15.07	19.45	0.30	0.04	100.11
THi3_groundmass_oliv_7	52.50	0.80	2.91	0.06	9.46	0.22	15.73	19.15	0.28	0.00	101.10
THj2_oliv_micro1_rim1	51.90	0.87	3.10	0.09	7.18	0.16	16.47	20.37	0.27	0.02	100.42
THj2_oliv_micro1_rim2	51.79	0.85	3.09	0.08	7.33	0.18	16.36	20.38	0.25	-0.01	100.31
THj2_oliv_micro1_rim3	52.19	0.81	1.80	0.02	9.03	0.22	15.96	19.81	0.21	0.01	100.06

<i>Spot Name</i>	<i>SiO₂</i>	<i>TiO₂</i>	<i>Al₂O₃</i>	<i>Cr₂O₃</i>	<i>FeO</i>	<i>MnO</i>	<i>MgO</i>	<i>CaO</i>	<i>Na₂O</i>	<i>K₂O</i>	<i>Total</i>
THj2_oliv_micro1_core_1	53.67	0.40	1.91	0.11	7.01	0.19	19.00	18.27	0.15	-0.01	100.70
THj2_oliv_micro1_core_2	53.26	0.37	2.31	0.15	5.80	0.16	18.11	20.12	0.19	-0.01	100.46
THj2_oliv_micro1_core_3	50.79	0.94	4.69	0.16	7.34	0.18	16.99	19.23	0.21	0.00	100.54
THj2_oliv_micro2_1	51.64	0.72	3.49	0.10	6.68	0.16	16.44	20.56	0.19	0.01	99.99
THj2_oliv_micro2_2	51.99	0.62	3.46	0.26	5.73	0.13	16.75	21.03	0.22	0.01	100.19
THj2_oliv_micro2_3	52.01	0.54	3.26	0.26	5.45	0.15	16.83	21.34	0.20	-0.01	100.03
THj2_oliv_micro3_1	52.00	0.55	3.38	0.24	5.65	0.13	16.89	20.93	0.22	0.00	99.99
THj2_oliv_micro3_2	51.76	0.61	3.58	0.26	5.88	0.15	17.02	20.98	0.20	-0.01	100.43
THj2_oliv_micro3_3	52.36	0.53	2.92	0.22	5.81	0.14	17.22	20.73	0.18	0.01	100.13
THj2_oliv_micro4_1	53.22	0.41	1.87	0.09	6.97	0.17	18.59	18.84	0.17	0.00	100.33
THj2_oliv_micro4_2	51.41	0.55	3.05	0.23	5.62	0.14	16.62	20.92	0.19	0.03	98.75
THj2_oliv_micro4_3	52.05	0.60	3.17	0.21	5.86	0.15	16.69	21.00	0.21	0.01	99.95
THj2_oliv_micro5_1	50.82	0.99	4.11	0.26	6.36	0.15	16.12	20.65	0.22	-0.01	99.68
THj2_oliv_micro5_2	52.48	0.53	2.88	0.20	5.87	0.16	17.03	20.96	0.19	0.02	100.30
THj2_oliv_micro5_3	50.98	0.85	4.30	0.21	6.75	0.16	16.71	19.73	0.22	0.01	99.89
THj2_groundmass_oliv_1	51.17	1.25	2.36	0.01	13.14	0.34	16.31	15.23	0.20	-0.01	100.01
THj2_groundmass_oliv_2	50.26	1.47	2.87	0.01	13.94	0.35	15.08	15.71	0.26	-0.01	99.95
THj2_groundmass_oliv_5	51.57	0.99	2.16	0.02	10.17	0.26	15.84	18.75	0.21	0.00	99.97
THj2_groundmass_oliv_7	50.72	1.19	3.30	0.03	9.46	0.24	15.46	19.61	0.27	0.01	100.28
THj2_groundmass_oliv_10	50.75	1.22	2.96	0.01	10.76	0.25	15.11	18.55	0.25	-0.01	99.85
THk2_oliv_micro1_1	52.51	0.43	2.41	0.18	5.74	0.15	17.44	20.62	0.19	0.01	99.68
THk2_oliv_micro1_2	52.88	0.40	2.02	0.15	5.84	0.16	17.99	20.25	0.19	0.01	99.88
THk2_oliv_micro1_3	52.86	0.42	1.84	0.12	6.98	0.18	18.88	18.05	0.14	-0.01	99.46
THk2_oliv_micro3_1	53.13	0.46	1.77	0.07	7.38	0.21	18.85	17.91	0.16	0.00	99.95
THk2_oliv_micro3_2	51.44	0.65	3.57	0.17	5.98	0.14	16.60	21.01	0.22	0.00	99.79
THk2_oliv_micro3_3	52.86	0.42	1.95	0.12	5.98	0.17	17.74	20.37	0.16	0.00	99.76
THk2_oliv_micro4_1	51.12	0.81	3.98	0.21	6.50	0.16	16.58	20.25	0.22	0.01	99.83
THk2_oliv_micro4_2	51.34	0.66	3.76	0.30	5.84	0.14	16.63	20.97	0.22	-0.01	99.85
THk2_oliv_micro4_3	50.68	0.96	4.51	0.22	6.70	0.16	16.11	20.57	0.22	0.01	100.14
THk2_oliv_micro5_1	52.16	0.49	2.74	0.20	5.52	0.14	16.98	21.23	0.20	0.01	99.66
THk2_oliv_micro5_2	50.62	0.86	4.34	0.14	6.95	0.16	16.67	19.45	0.23	0.01	99.43
THk2_oliv_micro5_3	53.01	0.48	2.40	0.12	6.90	0.19	18.78	17.95	0.16	0.01	100.00
THk2_oliv_micro6_rim_1	52.74	0.51	2.13	0.10	7.10	0.20	18.30	18.59	0.19	-0.01	99.87
THk2_oliv_micro6_rim_2	51.66	0.74	3.37	0.12	7.33	0.20	17.11	19.40	0.22	-0.01	100.15
THk2_oliv_micro6_rim_3	51.76	0.68	3.12	0.06	7.58	0.21	17.16	19.18	0.19	0.00	99.94
THk2_oliv_micro6_core_1	50.56	0.33	1.02	0.00	18.54	0.67	9.52	18.77	0.28	0.01	99.68
THk2_oliv_micro6_core_2	50.57	0.41	1.15	0.00	17.84	0.68	9.52	19.22	0.28	0.00	99.67
THk2_oliv_micro6_core_3	50.23	0.47	1.35	0.00	18.44	0.68	9.26	18.98	0.29	0.00	99.71

<i>Spot Name</i>	<i>SiO₂</i>	<i>TiO₂</i>	<i>Al₂O₃</i>	<i>Cr₂O₃</i>	<i>FeO</i>	<i>MnO</i>	<i>MgO</i>	<i>CaO</i>	<i>Na₂O</i>	<i>K₂O</i>	<i>Total</i>
THk2.oliv.micro7.rim_1	51.35	0.89	3.02	0.09	7.42	0.18	16.50	19.99	0.21	-0.01	99.65
THk2.oliv.micro7.rim_2	52.21	0.56	2.87	0.09	6.51	0.15	17.09	20.50	0.21	0.01	100.18
THk2.oliv.micro7.rim_3	51.76	0.67	3.24	0.14	6.85	0.17	17.07	19.88	0.24	0.00	100.00
THk2.oliv.micro7.core_1	51.28	0.23	0.77	0.00	16.36	0.85	10.66	18.92	0.38	0.02	99.48
THk2.oliv.micro7.core_2	51.89	0.25	0.83	0.00	14.64	0.80	11.81	19.52	0.42	0.01	100.17
THk2.oliv.micro7.core_3	51.84	0.22	0.82	0.00	13.82	0.73	11.93	20.08	0.42	-0.01	99.88
THk2.groundmass.oliv_1	51.45	0.88	3.72	0.12	7.85	0.20	17.31	18.14	0.21	0.00	99.88
THk2.groundmass.oliv_2	52.02	0.69	2.88	0.09	7.76	0.19	17.02	19.38	0.20	0.02	100.25
THk2.groundmass.oliv_3	52.27	0.55	2.51	0.10	6.89	0.20	17.38	19.85	0.21	0.03	99.98
THk2.groundmass.oliv_4	52.15	0.67	2.79	0.09	7.29	0.20	16.86	20.01	0.23	0.00	100.28
THk2.groundmass.oliv_5	52.86	0.56	2.17	0.10	7.49	0.19	17.59	19.23	0.18	-0.01	100.36
THk2.groundmass.oliv_6	51.89	0.64	3.11	0.12	6.94	0.17	16.87	20.04	0.24	0.00	100.01
THk2.groundmass.oliv_7	52.64	0.68	2.04	0.03	8.67	0.23	17.10	18.79	0.18	0.01	100.37
THk2.groundmass.oliv_8	52.78	0.53	1.71	0.04	8.80	0.23	17.84	17.76	0.19	0.00	99.87
THk2.groundmass.oliv_9	51.53	0.89	3.11	0.09	8.59	0.20	16.85	18.64	0.22	0.00	100.12
THk3.oliv.micro3.rim_1	52.98	0.49	1.73	0.05	7.13	0.21	17.56	19.49	0.18	0.01	99.82
THk3.oliv.micro3.rim_2	52.91	0.55	1.86	0.05	7.26	0.21	17.57	19.69	0.18	0.01	100.28
THk3.oliv.micro3.rim_3	53.25	0.50	1.77	0.05	7.18	0.21	17.78	19.54	0.17	0.00	100.44
THk3.oliv.micro3.core_1	52.95	0.45	2.36	0.21	5.61	0.15	17.60	20.94	0.18	0.02	100.47
THk3.oliv.micro3.core_2	52.30	0.53	3.20	0.26	5.62	0.14	16.96	21.13	0.20	0.01	100.36
THk3.oliv.micro3.core_3	52.01	0.63	3.34	0.27	5.58	0.13	16.48	21.65	0.21	0.00	100.30
THk3.oliv.micro4_1	51.75	0.56	3.39	0.27	5.68	0.13	16.64	21.32	0.19	0.00	99.93
THk3.oliv.micro4_2	51.56	0.60	3.54	0.29	5.61	0.13	16.52	21.17	0.22	0.01	99.66
THk3.oliv.micro4_3	50.96	0.82	3.96	0.20	6.23	0.15	16.30	20.70	0.22	0.04	99.58
THk3.oliv.micro5.rim_1	52.28	0.56	2.46	0.10	6.76	0.19	16.75	20.58	0.23	0.01	99.92
THk3.oliv.micro5.rim_2	51.93	0.60	2.54	0.10	6.48	0.16	16.45	20.98	0.20	0.01	99.44
THk3.oliv.micro5.rim_3	52.01	0.65	2.70	0.09	7.07	0.19	16.82	20.32	0.21	0.01	100.07
THk3.oliv.micro5.mantle_1	51.84	0.24	0.75	0.00	14.56	0.82	11.76	19.47	0.42	0.01	99.87
THk3.oliv.micro5.mantle_2	51.68	0.24	0.75	0.00	14.61	0.84	11.76	19.37	0.43	-0.02	99.68
THk3.oliv.micro5.mantle_3	51.85	0.26	0.77	0.00	14.61	0.83	11.77	19.39	0.44	0.02	99.93
THk3.oliv.micro5.core_1	51.80	0.23	0.64	0.00	15.21	0.84	11.84	18.88	0.37	0.02	99.82
THk3.oliv.micro5.core_2	51.98	0.25	0.80	0.00	15.15	0.83	12.00	19.15	0.37	0.01	100.54
THk3.oliv.micro5.core_3	51.71	0.20	0.66	-0.01	15.36	0.84	11.75	19.03	0.34	0.01	99.89
THk3.oliv.micro6_1	53.07	0.43	2.27	0.19	5.66	0.16	17.81	20.38	0.21	0.00	100.17
THk3.oliv.micro6_2	53.15	0.48	1.75	0.07	7.09	0.19	18.17	19.03	0.17	0.00	100.11
THk3.oliv.micro6_3	51.66	0.58	3.53	0.21	5.90	0.15	16.74	20.93	0.23	0.00	99.92
THk3.oliv.macro1.rim_1	51.81	0.66	2.96	0.10	6.72	0.18	16.66	20.66	0.21	-0.01	99.94
THk3.oliv.macro1.rim_2	52.49	0.60	2.50	0.08	6.63	0.17	16.73	21.07	0.22	0.00	100.47

<i>Spot Name</i>	<i>SiO₂</i>	<i>TiO₂</i>	<i>Al₂O₃</i>	<i>Cr₂O₃</i>	<i>FeO</i>	<i>MnO</i>	<i>MgO</i>	<i>CaO</i>	<i>Na₂O</i>	<i>K₂O</i>	<i>Total</i>
THk3_oliv_macro1_rim_3	52.29	0.62	2.59	0.09	6.56	0.16	16.67	21.16	0.24	0.00	100.37
THk3_oliv_macro1_core_1	50.55	0.73	1.74	0.00	15.55	0.55	11.25	19.15	0.32	0.00	99.82
THk3_oliv_macro1_core_2	50.84	0.63	1.50	0.00	15.53	0.55	11.31	19.12	0.28	0.01	99.77
THk3_oliv_macro1_core_3	50.61	0.71	1.71	0.00	14.79	0.48	11.04	20.15	0.31	0.02	99.82
THk3_oliv_macro2_rim_1	52.88	0.58	1.82	0.07	6.97	0.19	17.13	20.61	0.19	0.00	100.44
THk3_oliv_macro2_rim_2	52.90	0.52	1.86	0.07	6.47	0.16	17.18	20.65	0.19	0.00	100.00
THk3_oliv_macro2_rim_3	53.10	0.50	1.81	0.07	6.63	0.18	17.13	20.81	0.18	0.02	100.40
THk3_oliv_macro2_core_1	50.99	0.57	1.17	0.00	15.69	0.57	11.44	19.08	0.24	0.01	99.76
THk3_oliv_macro2_core_2	50.58	0.74	1.61	0.00	16.73	0.59	11.57	17.92	0.29	0.00	100.04
THk3_oliv_macro2_core_3	51.07	0.58	1.27	0.00	16.05	0.58	11.56	18.62	0.25	0.01	99.99
THk3_oliv_micro7_rim_1	51.62	0.81	3.17	0.09	7.60	0.20	16.60	19.46	0.21	0.00	99.76
THk3_oliv_micro7_rim_2	51.21	0.80	3.34	0.10	7.71	0.21	15.73	20.62	0.27	0.01	100.00
THk3_oliv_micro7_rim_3	51.32	1.02	3.40	0.04	9.63	0.24	16.48	17.68	0.22	0.01	100.02
THk3_oliv_micro7_core_1	50.54	0.59	1.42	0.00	16.58	0.60	10.81	18.84	0.29	0.01	99.69
THk3_oliv_micro7_core_2	50.61	0.53	1.33	0.00	16.64	0.61	10.60	19.27	0.30	0.00	99.89
THk3_oliv_micro7_core_3	50.34	0.57	1.52	0.00	16.16	0.58	10.14	19.75	0.32	-0.01	99.39
THk3_oliv_micro8_1	51.19	0.84	3.98	0.07	7.25	0.16	16.24	20.41	0.20	0.00	100.34
THk3_oliv_micro8_2	52.19	0.56	3.18	0.25	5.66	0.14	16.79	21.33	0.22	0.01	100.34
THk3_oliv_micro8_3	52.03	0.64	3.29	0.19	6.21	0.15	17.12	20.53	0.22	-0.01	100.37
THk3_groundmass_oliv_2	51.05	0.80	3.88	0.21	6.11	0.14	16.44	20.83	0.19	0.00	99.66
THk3_groundmass_oliv_4	51.44	1.08	4.15	0.06	8.36	0.20	14.47	18.77	0.42	0.36	99.29
THk3_groundmass_oliv_5	51.96	0.77	2.73	0.05	8.26	0.22	16.76	19.10	0.19	0.01	100.03
THk3_groundmass_oliv_6	51.92	0.66	2.26	0.05	7.84	0.20	16.77	19.08	0.19	0.03	99.00
THk3_groundmass_oliv_7	49.55	1.45	2.99	0.01	13.60	0.31	13.67	17.78	0.26	0.03	99.63
THk3_groundmass_oliv_9	51.56	0.77	3.09	0.10	7.54	0.19	16.31	19.89	0.24	0.00	99.68

Appendix E – Olivine Transects

<i>Transect</i>	<i>Distance (μm)</i>	<i>SiO₂</i>	<i>TiO₂</i>	<i>Al₂O₃</i>	<i>Cr₂O₃</i>	<i>FeO</i>	<i>MnO</i>	<i>MgO</i>	<i>CaO</i>	<i>Na₂O</i>	<i>K₂O</i>	<i>Total</i>
THa2.ol_macro1_transect_	0	36.67	0.04	0.03	0.00	31.45	0.42	31.11	0.47	0.02	0.00	100.21
	5	37.17	0.03	0.12	0.00	28.51	0.38	33.47	0.40	0.01	0.00	100.09
	10	37.69	0.03	0.03	0.00	26.96	0.35	34.97	0.39	0.00	0.00	100.43
	15	38.17	0.03	0.04	0.00	25.84	0.35	36.14	0.38	0.01	-0.01	100.97
	20	37.17	0.01	0.23	0.01	24.35	0.33	35.36	0.36	-0.01	0.00	97.82
	25	38.43	0.01	0.03	0.01	23.91	0.33	37.61	0.34	-0.01	-0.01	100.66
	30	38.68	0.03	0.03	0.01	23.02	0.32	38.31	0.35	0.01	0.00	100.75
	35	38.79	0.02	0.03	0.01	22.24	0.31	39.02	0.35	-0.01	-0.01	100.77
	40	27.30	0.02	0.45	0.01	16.47	0.21	27.00	0.28	0.01	0.00	71.75

Transect	Distance (μm)	SiO_2	TiO_2	Al_2O_3	Cr_2O_3	FeO	MnO	MgO	CaO	Na_2O	K_2O	Total
	45	38.91	0.01	0.04	0.01	20.83	0.30	40.13	0.34	-0.01	-0.02	100.56
	50	39.28	-0.01	0.05	0.01	20.31	0.29	40.73	0.35	0.01	0.00	101.03
	55	39.26	0.00	0.06	0.02	19.70	0.26	41.19	0.36	0.00	0.01	100.86
	60	39.42	0.02	0.05	0.01	18.97	0.26	41.85	0.35	0.01	0.00	100.95
	65	39.53	0.01	0.03	0.02	18.28	0.25	42.42	0.37	0.01	0.02	100.94
	70	39.57	0.02	0.03	0.02	17.68	0.25	42.77	0.35	0.01	-0.01	100.71
	75	39.70	0.01	0.04	0.01	17.20	0.23	43.15	0.35	0.00	-0.01	100.69
	80	39.82	0.02	0.04	0.02	16.79	0.23	43.51	0.35	0.01	0.01	100.79
	85	39.92	0.00	0.04	0.02	16.43	0.23	43.98	0.35	0.01	0.01	101.00
	90	40.02	0.01	0.02	0.02	16.06	0.23	44.20	0.37	-0.01	0.00	100.93
	95	39.95	0.01	0.04	0.02	15.81	0.22	44.38	0.36	0.01	0.00	100.82
	100	40.10	0.00	0.03	0.01	15.45	0.23	44.61	0.38	0.01	0.00	100.83
	105	40.22	0.01	0.04	0.02	15.28	0.22	44.73	0.38	0.00	-0.01	100.90
	110	40.24	0.01	0.04	0.02	15.10	0.23	45.00	0.41	0.01	0.01	101.07
	115	40.26	0.00	0.04	0.02	14.92	0.20	45.20	0.39	0.01	0.00	101.05
	120	40.18	0.00	0.05	0.02	14.81	0.21	45.24	0.39	0.01	-0.01	100.90
	125	40.30	0.01	0.05	0.02	14.69	0.22	45.30	0.37	0.01	0.02	100.98
	130	40.47	0.01	0.03	0.01	14.70	0.21	45.42	0.35	0.00	0.01	101.22
	135	40.69	0.02	0.05	0.01	14.51	0.22	43.15	0.36	0.02	-0.01	99.02
	140	40.22	0.02	0.04	0.02	14.58	0.22	45.33	0.34	0.01	0.00	100.77
	145	40.26	0.01	0.04	0.02	14.47	0.21	45.46	0.37	0.01	-0.01	100.85
	150	40.36	0.01	0.03	0.02	14.51	0.21	45.53	0.37	0.01	0.00	101.06
	170	40.38	0.01	0.04	0.02	14.49	0.21	45.52	0.36	-0.01	0.00	101.04
	190	40.35	0.01	0.04	0.02	14.36	0.22	45.57	0.38	0.00	0.00	100.95
	210	40.42	-0.01	0.04	0.02	14.29	0.22	45.55	0.36	0.01	-0.01	100.90
	231	40.35	0.00	0.04	0.02	14.36	0.21	45.48	0.40	0.00	0.02	100.88
	251	40.47	-0.01	0.05	0.01	14.26	0.21	45.47	0.37	0.01	0.01	100.86
	271	40.33	0.00	0.05	0.02	14.30	0.20	45.47	0.39	0.01	-0.01	100.77
	291	40.18	0.02	0.04	0.02	14.37	0.21	45.53	0.37	0.00	-0.01	100.74
	311	40.39	0.00	0.04	0.02	14.35	0.21	45.69	0.36	0.00	0.00	101.05
	331	40.45	0.02	0.04	0.02	14.37	0.22	45.75	0.36	0.01	-0.01	101.25
	351	40.43	-0.01	0.04	0.02	14.42	0.21	45.67	0.36	0.00	0.01	101.15
	372	40.48	-0.01	0.05	0.02	14.38	0.21	45.77	0.38	0.00	0.01	101.31
	392	40.43	0.02	0.04	0.01	14.36	0.22	45.58	0.35	-0.01	0.01	101.02
	412	40.00	0.01	0.03	0.02	14.32	0.21	45.42	0.35	0.00	0.00	100.37
	432	40.37	0.01	0.06	0.01	14.40	0.22	45.80	0.37	0.01	0.01	101.26
THa2_ol_macro2_transect_	0	37.32	0.06	0.04	0.00	28.42	0.41	33.62	0.36	0.01	0.01	100.23
	5	37.95	0.03	0.02	0.01	25.89	0.36	35.89	0.38	0.00	-0.01	100.52

Transect	Distance (μm)	SiO_2	TiO_2	Al_2O_3	Cr_2O_3	FeO	MnO	MgO	CaO	Na_2O	K_2O	Total
	10	38.07	0.05	0.03	0.00	24.98	0.36	36.81	0.36	0.00	0.00	100.67
	15	38.37	0.02	0.04	0.01	23.45	0.33	38.03	0.37	0.02	0.01	100.66
	20	38.68	0.01	0.03	0.01	21.54	0.30	39.48	0.34	0.00	0.01	100.41
	25	39.09	0.01	0.04	0.02	19.71	0.27	41.06	0.36	0.01	0.01	100.57
	30	39.44	0.01	0.03	0.02	18.42	0.26	42.16	0.35	0.01	0.00	100.72
	35	39.73	0.00	0.04	0.01	17.18	0.24	43.12	0.40	-0.01	0.01	100.75
	40	39.83	0.01	0.05	0.02	16.55	0.25	43.81	0.37	0.01	0.00	100.90
	45	39.69	0.01	0.02	0.01	15.99	0.24	44.22	0.39	-0.01	0.00	100.57
	50	39.88	0.02	0.03	0.01	16.01	0.23	44.31	0.39	0.00	0.01	100.90
	55	39.85	0.01	0.03	0.02	15.93	0.24	44.16	0.39	0.01	0.01	100.65
	60	39.89	0.01	0.03	0.02	16.02	0.24	44.13	0.38	0.01	0.01	100.72
	65	39.71	0.01	0.02	0.02	16.21	0.24	43.96	0.36	0.01	0.01	100.55
	70	39.69	0.01	0.04	0.02	16.58	0.25	43.74	0.37	0.02	0.00	100.71
	75	39.77	0.00	0.03	0.02	16.74	0.25	43.47	0.33	0.00	0.01	100.62
	80	39.62	0.00	0.03	0.02	17.05	0.26	43.30	0.35	0.00	0.01	100.64
	85	39.58	0.00	0.05	0.02	17.40	0.27	43.01	0.35	0.02	-0.01	100.68
	90	39.60	-0.01	0.03	0.01	17.67	0.26	42.95	0.36	0.00	0.01	100.89
	95	39.40	0.00	0.03	0.01	17.87	0.26	42.56	0.37	0.00	0.00	100.50
	100	39.46	0.01	0.03	0.01	18.21	0.29	42.40	0.34	0.01	0.01	100.75
	105	39.39	0.02	0.04	0.01	18.43	0.29	42.12	0.37	0.01	0.01	100.69
	110	39.30	0.01	0.03	0.00	18.73	0.27	41.92	0.34	0.01	0.00	100.60
	115	39.27	0.01	0.04	0.00	19.11	0.30	41.73	0.34	0.02	-0.02	100.81
	120	38.88	0.03	0.03	0.00	18.96	0.28	41.11	0.33	0.01	0.00	99.63
	125	39.00	0.00	0.03	0.00	19.45	0.29	40.84	0.33	0.00	-0.01	99.94
	130	39.12	0.01	0.04	0.00	19.80	0.31	41.20	0.31	0.00	-0.01	100.80
	135	39.01	0.03	0.03	0.00	19.90	0.31	41.07	0.30	-0.02	-0.01	100.67
	140	39.21	0.03	0.03	0.00	19.99	0.29	40.91	0.31	0.00	0.00	100.78
	145	39.01	0.02	0.03	0.00	20.27	0.30	40.84	0.32	0.01	0.00	100.81
	150	38.94	0.01	0.03	0.01	20.31	0.31	40.63	0.31	-0.01	0.01	100.55
	165	39.06	0.01	0.03	0.00	20.69	0.31	40.38	0.31	0.00	0.00	100.79
	181	38.95	0.02	0.03	0.00	20.97	0.32	40.08	0.31	0.00	0.00	100.70
	196	38.90	0.01	0.02	0.00	21.19	0.31	40.05	0.30	0.01	0.02	100.82
	212	38.91	0.02	0.04	0.01	21.29	0.32	39.99	0.32	-0.01	0.00	100.89
	227	38.84	0.01	0.03	0.00	21.19	0.33	39.92	0.29	0.01	0.01	100.62
	243	38.96	0.01	0.02	0.00	21.16	0.31	39.82	0.30	0.01	0.00	100.60
	258	38.83	0.02	0.03	0.00	21.22	0.32	39.86	0.31	0.00	0.01	100.61
	274	38.75	0.02	0.03	0.00	21.51	0.32	39.73	0.32	0.00	0.00	100.67
	289	38.80	0.02	0.02	0.00	21.68	0.33	39.29	0.33	0.00	0.01	100.49

<i>Transect</i>	<i>Distance (μm)</i>	<i>SiO₂</i>	<i>TiO₂</i>	<i>Al₂O₃</i>	<i>Cr₂O₃</i>	<i>FeO</i>	<i>MnO</i>	<i>MgO</i>	<i>CaO</i>	<i>Na₂O</i>	<i>K₂O</i>	<i>Total</i>
THa2_ol_macro3_transect_	0	37.63	0.08	0.03	0.00	27.91	0.37	34.26	0.37	-0.01	-0.01	100.65
	10	37.97	0.04	0.03	0.00	26.00	0.35	35.94	0.37	0.00	-0.01	100.71
	20	38.11	0.02	0.02	0.01	25.24	0.34	36.55	0.34	0.01	0.01	100.64
	30	38.40	0.02	0.03	0.00	23.99	0.32	37.52	0.32	0.01	0.02	100.62
	40	38.53	0.02	0.03	0.01	23.06	0.31	38.44	0.34	0.00	-0.01	100.74
	50	35.43	0.02	0.15	0.00	21.21	0.30	34.97	0.33	0.01	0.00	92.43
	60	38.74	0.02	0.02	0.01	21.82	0.31	39.11	0.35	0.00	0.00	100.37
	70	38.96	0.00	0.04	0.01	21.90	0.31	39.37	0.35	-0.01	0.00	100.95
	80	38.71	0.02	0.03	0.01	22.14	0.31	39.13	0.35	0.00	0.00	100.70
	90	38.68	0.04	0.05	0.00	22.43	0.34	38.70	0.35	0.01	0.00	100.59
	100	38.67	0.03	0.03	0.00	22.99	0.34	38.49	0.31	0.02	0.00	100.88
	135	38.30	-0.01	0.03	0.01	23.90	0.36	37.61	0.29	0.00	-0.01	100.50
	171	38.28	0.02	0.04	0.00	24.31	0.35	37.31	0.31	0.00	0.01	100.64
	206	38.29	0.02	0.02	0.01	24.33	0.35	37.19	0.31	-0.01	-0.01	100.51
	241	38.57	0.02	0.02	0.00	23.67	0.35	37.85	0.31	0.00	-0.01	100.80
	251	36.56	0.03	0.07	0.01	22.64	0.32	35.67	0.31	0.01	0.02	95.63
	261	38.49	0.03	0.04	0.00	23.94	0.35	37.71	0.30	0.00	0.01	100.87
	271	38.37	0.00	0.03	0.00	24.45	0.35	37.24	0.32	0.00	-0.01	100.75
	281	38.28	-0.01	0.03	0.01	25.05	0.35	36.70	0.34	0.01	0.00	100.77
	291	38.24	0.04	0.03	0.01	25.40	0.35	36.29	0.35	0.01	-0.01	100.71
	301	38.03	0.03	0.03	0.00	25.62	0.35	35.98	0.38	0.00	0.00	100.43
	311	38.06	0.04	0.06	0.00	25.66	0.37	36.14	0.38	0.00	0.00	100.72
	321	37.98	0.03	0.05	0.00	25.92	0.37	35.60	0.35	0.00	0.00	100.30
	331	37.81	0.02	0.03	0.00	26.64	0.36	35.28	0.38	0.01	0.02	100.55
	341	37.04	0.04	0.01	0.00	29.90	0.41	31.93	0.44	0.00	0.00	99.78
THd3a_ol_macro1_transect_	0	37.16	0.02	0.03	0.00	27.79	0.39	33.77	0.38	0.01	0.02	99.57
	5	37.13	0.01	0.02	0.01	26.86	0.37	34.14	0.35	0.02	0.01	98.93
	10	37.45	0.01	0.02	0.00	26.35	0.38	34.93	0.36	0.00	0.00	99.50
	15	37.73	0.02	0.03	0.00	25.61	0.36	35.57	0.36	0.00	0.00	99.68
	20	37.96	0.01	0.02	0.00	25.04	0.35	36.02	0.34	0.02	0.00	99.76
	25	37.94	0.02	0.02	0.00	24.39	0.35	36.83	0.34	0.00	-0.01	99.89
	30	38.00	0.03	0.04	0.01	23.81	0.32	36.90	0.33	0.02	0.02	99.48
	35	38.28	0.01	0.03	0.01	23.04	0.33	37.89	0.32	0.00	0.01	99.93
	40	38.42	0.02	0.04	0.00	22.32	0.30	38.59	0.32	0.00	0.01	100.03
	45	38.60	0.02	0.03	0.01	21.67	0.31	39.05	0.33	0.00	0.01	100.01
	50	38.70	0.04	0.03	0.01	20.92	0.30	39.54	0.32	0.00	0.01	99.87
	55	38.86	0.02	0.04	0.02	19.98	0.27	40.19	0.34	0.01	0.00	99.71
	60	39.01	0.01	0.04	0.01	19.23	0.26	40.99	0.34	0.01	0.00	99.90

<i>Transect</i>	<i>Distance (µm)</i>	<i>SiO₂</i>	<i>TiO₂</i>	<i>Al₂O₃</i>	<i>Cr₂O₃</i>	<i>FeO</i>	<i>MnO</i>	<i>MgO</i>	<i>CaO</i>	<i>Na₂O</i>	<i>K₂O</i>	<i>Total</i>
	65	39.28	0.00	0.03	0.02	18.61	0.25	41.48	0.34	0.00	0.01	100.02
	70	39.30	0.01	0.03	0.02	18.12	0.24	42.02	0.33	0.01	0.00	100.08
	75	39.45	0.01	0.05	0.02	17.30	0.25	42.39	0.34	0.01	0.01	99.82
	80	39.42	0.01	0.04	0.03	16.95	0.24	42.94	0.36	0.00	0.02	100.00
	85	39.49	0.01	0.03	0.02	16.53	0.25	43.24	0.35	0.01	0.00	99.92
	90	39.59	0.01	0.04	0.03	16.06	0.24	43.51	0.34	0.01	0.00	99.81
	95	39.51	0.00	0.04	0.02	15.58	0.23	43.38	0.35	0.02	0.02	99.16
	100	39.76	0.02	0.03	0.03	15.47	0.23	43.70	0.36	0.02	0.01	99.61
	105	39.83	0.00	0.04	0.02	15.29	0.21	44.22	0.36	0.03	0.00	100.00
	110	39.82	0.00	0.03	0.02	15.14	0.22	44.54	0.34	0.01	-0.02	100.12
	115	40.01	0.01	0.05	0.02	14.98	0.22	44.55	0.37	0.00	0.01	100.22
	120	39.93	0.02	0.05	0.02	14.73	0.22	44.69	0.35	0.02	0.00	100.02
	125	40.00	0.01	0.03	0.02	14.69	0.22	44.78	0.38	0.00	0.00	100.13
	130	39.92	0.02	0.04	0.02	14.71	0.22	44.84	0.36	0.00	0.01	100.13
	135	39.98	0.01	0.02	0.01	14.47	0.22	44.98	0.38	0.00	0.00	100.07
	140	40.11	0.02	0.03	0.02	14.46	0.21	44.98	0.36	0.00	0.01	100.21
	145	39.99	0.01	0.03	0.01	14.42	0.21	45.04	0.36	0.01	0.01	100.09
	150	40.08	0.00	0.03	0.02	14.48	0.21	45.02	0.36	0.02	0.01	100.24
	179	40.16	0.00	0.03	0.02	14.39	0.22	45.05	0.37	0.01	0.00	100.25
	208	39.95	0.01	0.05	0.01	14.47	0.22	44.82	0.37	0.02	0.04	99.96
	237	40.26	0.01	0.04	0.01	14.66	0.22	45.03	0.38	0.00	0.01	100.62
	266	40.14	0.00	0.03	0.01	14.90	0.23	44.96	0.39	0.01	0.01	100.68
	295	40.07	0.00	0.04	0.01	14.92	0.23	44.86	0.38	0.01	0.00	100.52
	324	39.89	0.01	0.05	0.01	15.03	0.23	44.83	0.39	0.00	0.00	100.45
	353	40.00	0.00	0.04	0.01	15.14	0.23	44.58	0.38	0.01	0.00	100.39
	382	40.04	0.02	0.02	0.01	15.18	0.23	44.53	0.38	0.01	-0.01	100.42
	411	40.05	0.00	0.04	0.01	15.29	0.24	44.50	0.39	0.01	0.01	100.53
	440	39.96	0.01	0.04	0.01	15.19	0.23	44.39	0.36	0.00	0.00	100.20
	469	39.99	0.01	0.04	0.01	15.41	0.24	44.51	0.38	0.01	0.02	100.63
	498	39.97	0.01	0.04	0.01	15.29	0.24	44.36	0.36	0.02	0.00	100.31
	527	39.93	0.02	0.03	0.01	15.47	0.21	44.50	0.38	0.00	0.00	100.57
	556	39.93	0.01	0.04	0.01	15.24	0.22	44.36	0.36	0.01	-0.01	100.18
	585	40.05	0.00	0.03	0.01	15.36	0.22	44.50	0.39	0.01	0.00	100.56
	614	39.86	0.00	0.03	0.01	15.39	0.22	44.40	0.41	0.01	0.00	100.34
	643	40.05	0.01	0.03	0.01	15.27	0.23	44.34	0.38	0.02	0.00	100.35
	672	40.01	0.02	0.04	0.01	15.34	0.24	44.61	0.36	0.01	0.00	100.64
	701	40.18	0.02	0.04	0.01	15.28	0.22	44.59	0.36	0.01	0.00	100.72
THd3a.ol_macro2_transect_	0	37.73	0.02	0.02	0.00	29.50	0.39	32.49	0.39	0.00	0.00	100.53

Transect	Distance (μm)	SiO_2	TiO_2	Al_2O_3	Cr_2O_3	FeO	MnO	MgO	CaO	Na_2O	K_2O	Total
	5	37.77	0.03	0.02	0.00	28.09	0.39	33.68	0.40	0.01	0.00	100.40
	10	37.81	0.00	0.03	0.00	27.59	0.38	34.22	0.40	0.01	0.00	100.46
	15	38.03	0.02	0.04	0.00	26.98	0.37	34.65	0.37	0.01	0.00	100.46
	20	38.08	0.00	0.02	0.00	26.54	0.37	35.06	0.39	0.01	0.01	100.49
	25	38.13	0.02	0.02	0.01	26.12	0.35	35.58	0.38	0.00	0.01	100.62
	31	38.12	0.01	0.02	0.00	25.46	0.34	35.72	0.37	0.01	0.00	100.07
	36	38.30	0.01	0.02	0.00	25.02	0.36	36.16	0.35	0.01	0.00	100.23
	40	38.38	0.00	0.04	0.00	24.63	0.32	36.49	0.36	0.00	0.01	100.24
	45	38.57	-0.01	0.03	0.01	23.97	0.32	37.15	0.35	0.01	-0.01	100.42
	50	38.63	0.03	0.02	0.01	23.50	0.32	37.68	0.32	0.00	0.00	100.52
	55	38.70	-0.01	0.04	0.00	22.78	0.31	38.11	0.34	0.01	-0.01	100.30
	60	38.70	0.02	0.03	0.01	22.19	0.30	38.52	0.36	0.01	0.00	100.13
	65	39.01	0.02	0.03	0.01	21.55	0.29	39.25	0.38	0.01	0.00	100.55
	70	38.97	0.00	0.04	0.02	20.89	0.30	39.75	0.38	0.01	0.00	100.35
	75	39.11	0.00	0.04	0.01	20.21	0.28	40.25	0.37	0.01	0.00	100.27
	80	39.26	0.01	0.04	0.01	19.65	0.26	40.76	0.35	0.01	0.01	100.36
	85	39.47	-0.01	0.03	0.02	18.99	0.26	41.39	0.35	0.01	0.00	100.51
	90	39.41	0.01	0.05	0.01	18.40	0.24	41.67	0.37	0.00	0.01	100.17
	95	39.71	0.01	0.03	0.01	17.93	0.24	42.28	0.37	0.00	0.00	100.58
	100	39.64	0.01	0.03	0.01	17.37	0.24	42.53	0.36	-0.01	0.01	100.21
	105	39.93	0.00	0.04	0.01	16.81	0.24	42.99	0.36	0.00	-0.01	100.39
	110	39.96	0.00	0.03	0.02	16.55	0.24	43.37	0.36	0.00	-0.01	100.52
	115	39.99	0.00	0.04	0.02	16.14	0.23	43.69	0.36	0.02	0.01	100.50
	120	39.98	0.00	0.04	0.02	15.88	0.23	43.82	0.36	0.00	0.02	100.34
	125	40.22	0.02	0.04	0.01	15.54	0.21	43.93	0.38	0.00	0.00	100.35
	130	40.17	0.00	0.03	0.01	15.38	0.22	44.18	0.35	0.00	0.00	100.35
	135	40.13	0.00	0.04	0.01	15.25	0.22	44.53	0.35	0.00	0.01	100.54
	140	40.24	0.02	0.04	0.02	15.13	0.22	44.63	0.36	0.00	0.00	100.66
	145	40.37	0.01	0.04	0.02	14.99	0.23	44.70	0.34	0.00	-0.01	100.69
	150	40.25	0.01	0.03	0.01	14.82	0.21	44.68	0.34	0.01	0.01	100.36
	173	40.37	0.00	0.03	0.02	14.59	0.22	45.05	0.35	0.01	-0.03	100.64
	197	40.26	0.02	0.04	0.02	14.59	0.22	44.88	0.38	0.01	-0.01	100.41
	220	40.17	0.01	0.03	0.01	14.66	0.22	44.97	0.37	0.00	0.02	100.46
	243	40.45	0.01	0.04	0.01	14.63	0.23	44.83	0.37	0.01	-0.01	100.58
	266	40.18	0.02	0.05	0.01	14.76	0.23	44.79	0.37	0.00	0.00	100.43
	290	40.06	0.03	0.05	0.02	14.89	0.21	44.77	0.39	0.01	0.01	100.44
	313	40.21	0.02	0.04	0.02	14.80	0.24	44.69	0.39	0.00	-0.01	100.41
	336	40.11	0.01	0.05	0.02	14.96	0.23	44.70	0.38	0.01	-0.01	100.46

Transect	Distance (μm)	SiO_2	TiO_2	Al_2O_3	Cr_2O_3	FeO	MnO	MgO	CaO	Na_2O	K_2O	Total
THd3a_ol_macro4_transect_	359	40.09	0.01	0.03	0.02	15.03	0.22	44.51	0.40	0.02	0.00	100.33
	382	40.08	0.01	0.04	0.02	15.01	0.22	44.62	0.42	0.01	0.01	100.43
	406	39.95	0.00	0.04	0.01	15.00	0.22	44.55	0.37	0.01	0.01	100.18
	429	40.20	-0.01	0.03	0.01	15.26	0.23	44.57	0.38	0.00	0.01	100.69
	452	40.17	0.01	0.04	0.01	15.24	0.24	44.56	0.38	0.00	0.01	100.66
	475	40.21	0.00	0.05	0.01	15.22	0.23	44.43	0.38	0.01	-0.01	100.54
THd3a_ol_macro4_transect_	0	37.68	0.07	0.02	0.01	28.04	0.40	34.00	0.35	0.01	0.01	100.58
	5	37.81	0.06	0.02	0.00	27.17	0.38	34.81	0.35	-0.01	-0.01	100.60
	10	37.99	0.02	0.03	0.00	26.28	0.37	35.49	0.34	0.00	0.01	100.54
	15	38.18	0.03	0.05	0.01	25.46	0.35	36.05	0.33	0.01	0.02	100.48
	20	38.43	0.01	0.03	0.02	24.54	0.34	36.91	0.32	0.01	0.01	100.62
	25	38.59	0.04	0.03	0.02	23.38	0.32	37.76	0.30	-0.01	0.01	100.44
	30	38.79	0.01	0.03	0.02	22.47	0.31	38.64	0.33	0.01	0.00	100.60
	35	39.00	0.02	0.03	0.02	21.63	0.29	39.43	0.32	0.02	-0.01	100.75
	40	39.19	0.02	0.03	0.02	20.50	0.28	40.20	0.31	0.02	0.02	100.60
	45	39.28	0.00	0.04	0.02	19.72	0.27	40.97	0.33	0.00	-0.01	100.62
	50	39.52	0.02	0.04	0.01	18.89	0.27	41.59	0.34	0.00	0.00	100.67
	55	39.55	0.00	0.03	0.02	18.16	0.26	42.22	0.32	0.00	-0.02	100.55
	60	23.68	0.01	0.07	0.01	11.87	0.17	29.85	0.24	0.01	0.00	65.91
	65	39.84	0.00	0.03	0.02	17.13	0.25	43.17	0.33	0.00	0.00	100.78
	70	39.84	0.03	0.04	0.02	16.71	0.23	43.55	0.34	0.00	-0.02	100.77
	75	40.12	0.02	0.04	0.02	16.12	0.24	43.87	0.35	0.02	0.00	100.79
	80	40.19	-0.01	0.03	0.02	15.73	0.23	44.23	0.36	0.00	-0.01	100.80
	85	40.09	0.02	0.03	0.02	15.28	0.23	44.41	0.37	0.00	-0.01	100.45
	90	40.28	0.00	0.04	0.02	15.06	0.22	44.67	0.38	-0.01	0.02	100.70
	95	40.12	0.02	0.05	0.02	14.84	0.22	44.89	0.34	0.00	0.00	100.50
	100	40.22	0.00	0.03	0.02	14.74	0.21	45.03	0.36	0.00	0.01	100.63
	105	40.36	0.03	0.03	0.02	14.61	0.22	45.21	0.36	0.01	-0.01	100.83
	110	40.46	0.00	0.04	0.03	14.41	0.21	45.24	0.37	0.00	0.00	100.76
	115	40.26	0.02	0.04	0.02	14.36	0.20	45.27	0.38	0.00	0.00	100.55
	120	40.34	0.00	0.03	0.02	14.31	0.22	45.29	0.36	0.00	0.00	100.58
	125	40.36	0.00	0.05	0.02	14.34	0.21	45.50	0.38	0.00	0.00	100.86
	130	40.44	0.01	0.04	0.02	14.25	0.21	45.41	0.37	-0.01	0.02	100.77
	135	40.39	0.00	0.05	0.02	14.24	0.22	45.50	0.36	0.00	0.01	100.80
	140	40.21	0.02	0.04	0.02	14.16	0.22	45.50	0.36	0.00	0.00	100.53
	145	40.42	-0.01	0.04	0.02	14.15	0.22	45.44	0.38	0.00	0.00	100.67
	150	40.38	0.00	0.04	0.03	14.16	0.20	45.59	0.35	-0.01	-0.01	100.74
	165	40.38	0.01	0.04	0.02	14.21	0.21	45.69	0.34	0.01	0.00	100.91

Transect	Distance (μm)	SiO_2	TiO_2	Al_2O_3	Cr_2O_3	FeO	MnO	MgO	CaO	Na_2O	K_2O	Total
	179	40.59	0.02	0.02	0.02	14.15	0.22	45.69	0.36	0.00	0.01	101.07
	194	40.44	-0.01	0.03	0.02	14.09	0.21	45.68	0.38	0.01	-0.01	100.87
	208	40.48	0.01	0.03	0.02	14.10	0.21	45.59	0.37	0.01	0.00	100.82
	223	40.33	0.01	0.02	0.02	13.94	0.20	45.62	0.35	-0.01	0.00	100.49
	237	40.43	-0.01	0.04	0.02	14.09	0.22	45.55	0.36	0.01	0.00	100.72
	252	40.40	0.00	0.03	0.02	13.96	0.21	45.58	0.38	0.00	0.00	100.60
	266	40.42	0.02	0.03	0.02	14.06	0.20	45.65	0.38	0.01	0.00	100.79
	281	40.43	0.00	0.03	0.02	13.98	0.20	45.56	0.38	0.00	-0.01	100.60
THd3a_ol_micro2_transect_	0	37.70	0.01	0.03	0.01	27.06	0.38	34.39	0.40	0.00	-0.02	99.98
	5	37.87	0.03	0.03	0.00	26.43	0.35	35.19	0.37	-0.01	0.00	100.28
	10	38.09	0.01	0.03	0.01	25.38	0.36	36.16	0.36	0.01	0.01	100.43
	15	38.38	0.01	0.02	0.01	24.38	0.33	36.91	0.32	0.01	0.00	100.37
	20	38.55	0.02	0.02	0.01	23.21	0.33	37.72	0.37	0.02	0.00	100.25
	25	38.63	0.04	0.03	0.01	22.38	0.31	38.49	0.31	0.02	-0.01	100.21
	30	39.12	0.00	0.03	0.01	21.59	0.32	39.59	0.33	-0.01	0.00	101.00
	35	38.99	0.02	0.03	0.01	20.63	0.28	40.05	0.33	0.00	0.02	100.35
	40	39.20	0.00	0.02	0.01	20.04	0.27	40.72	0.32	0.01	-0.01	100.60
	45	39.45	0.01	0.04	0.02	19.18	0.28	41.28	0.34	0.01	-0.01	100.60
	50	39.39	0.01	0.04	0.02	18.30	0.27	41.92	0.36	-0.01	0.00	100.30
	55	39.65	0.01	0.03	0.01	18.00	0.25	42.26	0.35	0.00	0.01	100.57
	60	39.81	-0.01	0.03	0.02	17.29	0.25	42.75	0.35	0.00	-0.01	100.49
	65	39.87	-0.01	0.04	0.02	16.95	0.25	43.06	0.35	0.02	0.01	100.57
	70	39.66	-0.01	0.04	0.02	16.61	0.24	43.38	0.37	0.00	-0.01	100.33
	75	39.89	0.01	0.04	0.01	16.31	0.24	43.61	0.33	0.00	0.01	100.45
	80	40.00	0.02	0.03	0.02	15.98	0.23	43.83	0.36	0.01	0.02	100.51
	85	39.75	0.00	0.05	0.02	15.57	0.22	42.88	0.48	0.03	-0.01	99.00
	90	39.64	0.00	0.03	0.02	15.42	0.22	44.17	0.36	0.00	0.00	99.86
	95	40.05	0.03	0.04	0.02	15.30	0.22	44.47	0.38	0.01	0.00	100.52
	100	40.14	0.01	0.03	0.02	15.02	0.21	44.65	0.39	0.00	0.01	100.48
	105	40.27	0.00	0.02	0.02	14.88	0.22	44.74	0.35	0.01	0.01	100.53
	110	40.11	0.01	0.03	0.02	14.78	0.22	44.84	0.35	0.01	0.01	100.38
	115	40.04	-0.01	0.03	0.02	14.74	0.22	45.06	0.37	0.01	0.01	100.50
	120	40.24	0.00	0.02	0.03	14.59	0.23	45.06	0.37	0.00	0.00	100.54
	125	40.31	0.00	0.03	0.02	14.57	0.21	45.16	0.36	0.01	0.00	100.67
	130	40.14	0.02	0.04	0.02	14.48	0.23	45.12	0.36	-0.01	0.00	100.41
	135	40.12	0.01	0.05	0.02	14.46	0.22	45.16	0.37	0.01	0.01	100.42
	140	40.29	0.03	0.04	0.02	14.40	0.21	45.37	0.36	0.01	0.02	100.75
	145	40.25	0.00	0.03	0.02	14.31	0.21	45.31	0.37	0.01	0.01	100.52

Transect	Distance (μm)	SiO_2	TiO_2	Al_2O_3	Cr_2O_3	FeO	MnO	MgO	CaO	Na_2O	K_2O	Total
	150	40.41	0.01	0.03	0.02	14.36	0.22	45.31	0.35	-0.01	-0.01	100.71
	177	40.26	0.01	0.02	0.02	14.26	0.21	45.41	0.34	0.02	0.01	100.55
	203	40.41	0.02	0.04	0.02	14.27	0.22	45.42	0.38	0.00	0.00	100.78
	230	40.27	0.01	0.04	0.02	14.21	0.22	45.35	0.37	0.01	0.02	100.51
	256	40.28	-0.01	0.03	0.02	14.36	0.22	45.43	0.38	0.01	0.01	100.74
	283	40.30	-0.01	0.04	0.02	14.40	0.21	45.14	0.37	0.00	-0.01	100.48
	309	40.19	0.01	0.04	0.02	14.70	0.21	44.91	0.36	0.00	0.03	100.47
	336	40.13	0.01	0.03	0.02	14.91	0.21	44.70	0.38	-0.01	0.01	100.41
	363	39.98	0.02	0.03	0.02	15.54	0.23	44.24	0.34	0.00	0.02	100.42
	389	39.74	-0.01	0.05	0.02	16.36	0.25	43.56	0.35	0.01	0.01	100.34
	394	39.37	0.00	0.04	0.02	16.35	0.24	42.77	0.72	0.01	0.03	99.54
	399	39.83	0.01	0.03	0.02	16.95	0.23	43.14	0.34	0.00	0.01	100.56
	404	39.76	0.00	0.04	0.02	17.16	0.25	43.05	0.34	0.01	0.01	100.65
	409	39.67	0.01	0.03	0.01	17.41	0.25	42.84	0.33	-0.01	0.01	100.57
	414	39.69	0.02	0.02	0.02	17.63	0.25	42.53	0.34	0.01	0.00	100.50
	419	39.08	-0.01	0.03	0.02	18.01	0.25	42.18	0.33	0.01	0.02	99.93
	424	39.37	0.00	0.04	0.01	18.27	0.25	42.11	0.33	0.00	0.01	100.42
	429	39.41	0.01	0.02	0.01	18.56	0.27	42.02	0.34	-0.01	0.00	100.63
	434	39.25	0.04	0.03	0.01	18.66	0.24	41.63	0.33	0.00	0.01	100.21
	439	39.08	0.00	0.03	0.01	18.91	0.26	41.41	0.33	0.00	0.01	100.04
	444	39.18	0.01	0.03	0.01	19.29	0.27	41.21	0.31	0.00	0.01	100.33
	449	39.24	0.01	0.03	0.01	19.64	0.28	40.92	0.34	0.00	0.00	100.47
	454	39.01	0.01	0.04	0.01	19.95	0.29	40.66	0.33	0.01	0.00	100.32
	459	39.00	0.01	0.02	0.01	20.36	0.28	40.25	0.30	0.02	0.00	100.26
	464	38.79	0.00	0.03	0.01	20.55	0.28	39.80	0.38	0.01	0.00	99.84
	469	38.73	0.01	0.04	0.00	21.05	0.28	39.66	0.34	0.00	0.01	100.12
	474	38.63	-0.02	0.02	0.00	21.32	0.30	39.22	0.32	0.00	0.02	99.84
	479	38.60	0.00	0.03	0.01	21.83	0.31	38.84	0.31	0.01	0.01	99.96
	484	38.64	0.02	0.03	0.01	22.52	0.32	38.63	0.31	0.00	0.01	100.49
	489	38.51	0.01	0.01	0.00	22.89	0.32	38.33	0.31	0.00	0.00	100.39
	494	38.29	0.01	0.03	0.00	23.27	0.31	37.75	0.31	0.01	0.00	100.01
	499	38.10	0.00	0.02	0.01	23.86	0.34	37.16	0.32	0.01	0.01	99.82
	504	38.17	0.01	0.04	0.01	24.41	0.34	36.78	0.32	0.01	0.00	100.09
	509	37.98	0.01	0.04	0.01	24.98	0.35	36.32	0.34	0.00	0.02	100.04
	514	38.01	0.02	0.03	0.00	25.64	0.34	35.79	0.34	0.01	0.00	100.20
	519	37.72	0.02	0.03	0.00	26.18	0.35	35.18	0.34	0.01	0.04	99.88
	524	32.28	0.03	0.19	0.00	23.37	0.31	26.63	0.29	0.01	0.04	83.14
	529	37.71	0.02	0.03	0.00	27.50	0.38	34.22	0.37	0.02	0.02	100.28

<i>Transect</i>	<i>Distance (µm)</i>	<i>SiO₂</i>	<i>TiO₂</i>	<i>Al₂O₃</i>	<i>Cr₂O₃</i>	<i>FeO</i>	<i>MnO</i>	<i>MgO</i>	<i>CaO</i>	<i>Na₂O</i>	<i>K₂O</i>	<i>Total</i>
	534	37.36	0.03	0.02	0.00	28.66	0.40	33.32	0.37	0.01	0.00	100.16
	539	34.33	0.07	0.01	0.00	44.19	0.59	19.61	0.35	0.00	0.02	99.17
THd3a_ol_micro5_transect_	0	36.50	0.10	0.02	0.00	32.86	0.44	30.00	0.32	0.01	-0.01	100.26
	5	37.66	0.09	0.03	0.01	27.76	0.37	34.20	0.33	0.00	-0.01	100.45
	10	37.95	0.07	0.02	0.00	26.50	0.36	35.33	0.34	0.00	0.00	100.57
	15	38.19	0.05	0.04	0.00	25.17	0.35	36.38	0.33	0.01	-0.01	100.52
	20	38.44	0.02	0.03	0.00	23.77	0.32	37.59	0.32	-0.01	-0.02	100.49
	25	38.66	0.02	0.03	0.01	22.37	0.32	38.66	0.30	0.02	0.00	100.38
	30	38.95	0.03	0.03	0.01	21.11	0.30	39.60	0.32	0.02	0.00	100.39
	35	39.25	0.02	0.03	0.01	20.12	0.28	40.75	0.32	0.01	0.01	100.80
	40	39.36	0.00	0.03	0.01	19.11	0.29	41.36	0.32	0.00	-0.01	100.49
	45	39.56	0.01	0.04	0.02	18.22	0.27	42.20	0.31	0.01	0.02	100.67
	50	39.79	0.01	0.05	0.02	17.49	0.24	42.74	0.32	0.01	0.01	100.69
	55	39.76	0.00	0.04	0.03	16.93	0.25	43.11	0.33	0.01	0.00	100.45
	60	39.83	0.02	0.03	0.02	16.62	0.24	43.57	0.36	-0.01	0.02	100.71
	65	40.10	0.01	0.02	0.02	16.17	0.23	43.83	0.37	0.00	-0.02	100.75
	70	40.12	0.01	0.04	0.02	15.76	0.23	44.22	0.36	0.00	0.01	100.79
	75	40.14	0.02	0.04	0.02	15.40	0.23	45.22	0.36	0.00	0.00	101.43
	80	25.97	0.00	0.18	0.01	7.92	0.11	24.47	0.18	0.00	-0.01	58.85
	85	40.03	0.00	0.03	0.02	15.02	0.23	44.43	0.37	-0.01	0.01	100.15
	90	40.16	0.00	0.03	0.02	14.69	0.22	44.78	0.38	0.00	0.00	100.28
	95	40.26	0.01	0.03	0.02	14.51	0.21	44.88	0.36	0.00	-0.01	100.28
	100	40.30	0.00	0.03	0.02	14.48	0.21	45.15	0.37	0.00	0.01	100.58
	105	40.23	0.01	0.02	0.02	14.28	0.22	45.29	0.36	0.00	0.00	100.43
	110	40.33	0.01	0.05	0.02	14.17	0.21	45.29	0.37	0.00	0.00	100.45
	115	40.33	0.00	0.03	0.02	14.11	0.21	45.50	0.38	-0.01	0.01	100.60
	120	40.40	0.02	0.03	0.02	14.09	0.21	45.52	0.39	0.00	0.01	100.69
	125	40.32	0.00	0.04	0.01	13.88	0.21	45.51	0.36	0.02	-0.01	100.36
	130	40.32	0.01	0.05	0.03	14.02	0.21	45.62	0.37	0.00	0.00	100.62
	135	40.16	0.00	0.04	0.03	13.94	0.20	45.65	0.36	0.00	0.00	100.39
	140	40.50	0.01	0.03	0.02	13.85	0.21	45.60	0.35	0.00	0.00	100.56
	145	40.45	-0.01	0.03	0.02	13.86	0.22	45.71	0.36	0.00	-0.01	100.65
	150	40.43	0.00	0.03	0.02	13.77	0.21	45.66	0.36	0.00	0.00	100.48
	180	40.39	0.00	0.03	0.02	13.85	0.21	45.77	0.37	0.00	0.01	100.64
	211	40.41	0.01	0.04	0.02	13.83	0.20	45.69	0.38	0.01	0.01	100.58
	241	40.44	0.01	0.03	0.02	13.70	0.21	45.67	0.36	0.01	0.01	100.47
	271	40.37	0.00	0.04	0.02	13.90	0.21	45.82	0.35	0.00	0.01	100.71
	301	40.39	-0.01	0.05	0.02	13.69	0.20	45.77	0.40	0.00	0.02	100.54

<i>Transect</i>	<i>Distance (µm)</i>	<i>SiO₂</i>	<i>TiO₂</i>	<i>Al₂O₃</i>	<i>Cr₂O₃</i>	<i>FeO</i>	<i>MnO</i>	<i>MgO</i>	<i>CaO</i>	<i>Na₂O</i>	<i>K₂O</i>	<i>Total</i>
	332	40.46	0.00	0.04	0.01	13.70	0.20	45.69	0.37	0.01	0.01	100.49
	362	40.35	0.00	0.04	0.02	13.79	0.20	45.87	0.36	0.00	0.00	100.64
	392	40.45	0.00	0.03	0.03	13.80	0.19	45.87	0.35	0.00	0.00	100.73
	422	40.35	-0.01	0.03	0.01	13.72	0.21	45.74	0.36	0.01	-0.01	100.42
	453	40.34	0.00	0.03	0.02	13.84	0.20	45.77	0.37	0.00	0.02	100.60
	483	40.41	0.01	0.03	0.02	13.74	0.21	45.95	0.35	-0.01	0.00	100.73
	513	40.36	-0.01	0.04	0.02	13.88	0.21	45.79	0.38	0.00	0.00	100.68
	543	40.43	0.01	0.03	0.02	13.80	0.21	45.95	0.38	0.00	-0.01	100.82
	574	40.34	0.01	0.02	0.02	13.85	0.21	45.85	0.36	0.01	0.01	100.67
	604	40.46	0.01	0.03	0.02	13.82	0.22	45.90	0.37	-0.01	0.01	100.83
	634	40.50	-0.01	0.05	0.02	13.81	0.21	45.94	0.36	0.00	-0.01	100.89
	664	40.43	0.01	0.04	0.02	13.79	0.22	45.93	0.36	-0.01	0.00	100.81
	695	40.42	0.01	0.05	0.03	13.80	0.21	45.85	0.38	0.01	0.00	100.75
	725	40.60	0.00	0.03	0.02	13.87	0.20	45.80	0.37	0.00	0.00	100.89
THde2.ol_macro1_transect_	0	38.96	0.03	0.03	0.00	21.52	0.31	39.27	0.36	-0.01	0.01	100.49
	10	39.00	0.00	0.02	0.01	20.89	0.29	39.85	0.39	0.01	0.01	100.46
	20	39.09	0.00	0.03	0.01	20.26	0.28	40.42	0.38	0.00	0.00	100.46
	30	39.27	0.01	0.02	0.01	19.58	0.26	41.04	0.36	0.01	-0.01	100.56
	40	39.26	-0.01	0.03	0.01	18.68	0.27	41.79	0.35	0.00	0.02	100.40
	50	39.27	0.03	0.03	0.01	17.91	0.25	42.35	0.37	0.00	0.01	100.23
	60	40.20	0.00	0.02	0.01	17.09	0.25	43.23	0.35	0.00	0.00	101.16
	70	39.45	0.01	0.04	0.01	16.67	0.24	42.96	0.39	0.00	-0.01	99.78
	80	39.74	0.02	0.04	0.01	16.29	0.23	43.63	0.39	0.01	-0.01	100.35
	90	39.83	-0.01	0.03	0.02	15.54	0.24	43.89	0.37	0.02	0.02	99.96
	100	39.22	0.00	0.02	0.02	14.87	0.22	43.15	0.38	0.03	0.04	97.95
	110	40.07	0.02	0.05	0.01	15.05	0.22	44.61	0.39	0.00	0.00	100.42
	120	40.30	0.02	0.04	0.02	14.75	0.23	44.98	0.37	0.01	0.01	100.73
	130	40.26	0.01	0.05	0.02	14.59	0.22	45.13	0.38	0.02	0.00	100.67
	140	40.16	0.00	0.04	0.02	14.51	0.22	45.14	0.39	0.00	-0.01	100.48
	150	40.18	0.01	0.04	0.02	14.40	0.22	45.31	0.38	-0.01	0.01	100.58
	178	40.17	0.01	0.04	0.02	14.00	0.21	45.17	0.40	0.01	0.01	100.04
	206	40.22	-0.01	0.05	0.02	13.88	0.20	45.68	0.38	0.00	0.00	100.43
	233	40.12	0.01	0.04	0.02	13.75	0.21	45.57	0.38	0.00	0.00	100.11
	261	40.09	-0.01	0.05	0.02	13.53	0.20	45.58	0.37	0.01	0.01	99.86
	289	40.33	0.01	0.05	0.03	13.50	0.21	45.93	0.37	0.00	0.01	100.45
	316	40.24	-0.01	0.05	0.03	13.51	0.20	45.88	0.38	0.00	0.00	100.29
	344	40.31	0.02	0.04	0.02	13.33	0.21	45.95	0.39	0.02	0.00	100.29
	372	40.19	0.00	0.05	0.03	13.36	0.20	45.83	0.39	0.02	-0.01	100.06

Transect	Distance (μm)	SiO_2	TiO_2	Al_2O_3	Cr_2O_3	FeO	MnO	MgO	CaO	Na_2O	K_2O	Total
	400	40.06	0.01	0.04	0.03	13.38	0.19	45.71	0.38	0.01	0.00	99.82
	427	40.43	0.01	0.07	0.03	13.47	0.20	45.87	0.40	0.01	0.01	100.50
	455	40.34	0.01	0.06	0.03	13.38	0.21	45.96	0.40	0.00	0.00	100.38
	483	40.27	0.01	0.04	0.02	13.42	0.20	45.94	0.37	0.02	-0.01	100.29
	510	40.33	0.00	0.06	0.03	13.33	0.19	45.84	0.39	0.01	0.00	100.18
	538	40.00	0.00	0.04	0.02	13.21	0.19	45.66	0.38	0.00	0.00	99.50
THde2.ol_macro2_transect_	0	38.81	0.02	0.03	0.01	21.11	0.31	39.57	0.41	0.01	0.00	100.29
	5	39.10	0.02	0.03	0.01	20.37	0.31	40.33	0.38	0.01	-0.01	100.55
	10	39.20	0.02	0.03	0.01	19.66	0.29	40.82	0.36	0.01	0.00	100.41
	15	39.15	0.00	0.04	0.01	18.94	0.26	41.28	0.39	0.02	-0.01	100.10
	20	39.37	0.01	0.05	0.02	18.30	0.25	42.05	0.38	0.02	0.01	100.45
	25	39.52	0.01	0.06	0.02	17.57	0.25	42.63	0.34	0.03	0.00	100.43
	30	39.77	0.00	0.04	0.02	16.81	0.24	43.17	0.37	0.01	0.01	100.44
	35	39.87	0.02	0.04	0.02	16.48	0.23	43.65	0.37	0.01	0.01	100.70
	40	39.96	0.02	0.05	0.02	15.74	0.24	44.19	0.33	0.01	0.01	100.57
	45	40.16	0.02	0.06	0.02	15.26	0.23	44.57	0.37	0.01	-0.01	100.70
	50	40.15	0.00	0.04	0.03	14.86	0.21	44.90	0.36	0.01	0.00	100.55
	55	40.19	-0.02	0.03	0.02	14.36	0.22	45.17	0.37	0.01	0.00	100.36
	60	40.44	-0.01	0.06	0.02	14.14	0.21	45.38	0.37	0.01	0.00	100.63
	65	40.42	0.00	0.09	0.02	13.85	0.19	45.60	0.36	0.02	0.01	100.57
	70	40.27	0.00	0.05	0.03	13.68	0.20	45.71	0.38	0.01	-0.01	100.33
	75	40.35	0.00	0.06	0.03	13.51	0.20	46.07	0.37	0.00	0.03	100.63
	80	40.47	0.01	0.04	0.02	13.51	0.20	46.12	0.37	0.00	0.01	100.77
	85	40.59	-0.01	0.05	0.03	13.30	0.20	46.38	0.38	0.01	0.01	100.93
	90	40.58	0.01	0.05	0.02	13.17	0.19	46.49	0.37	0.01	0.02	100.92
	95	40.57	-0.01	0.05	0.02	13.01	0.18	46.47	0.39	0.04	0.02	100.76
	100	40.55	0.00	0.06	0.03	12.95	0.21	46.53	0.37	0.02	0.01	100.72
	105	40.63	0.00	0.04	0.03	12.86	0.18	46.96	0.39	0.02	0.01	101.13
	110	39.85	0.01	0.06	0.02	12.72	0.18	47.99	0.38	0.04	0.03	101.29
	115	41.00	0.41	1.82	0.06	6.32	0.14	15.03	14.72	0.17	0.01	79.68
	120	43.93	0.12	22.25	0.00	1.89	0.03	0.85	10.58	2.24	0.06	81.94
	125	15.69	0.10	6.77	0.01	1.90	0.04	2.95	4.02	0.68	0.05	32.19
	130	41.91	0.03	0.99	0.03	11.75	0.16	42.74	0.73	0.29	0.13	98.75
	135	38.26	0.01	0.05	0.03	12.51	0.18	44.98	0.39	0.02	0.02	96.45
	140	40.33	0.00	0.04	0.03	12.71	0.20	46.14	0.37	0.01	0.00	99.83
	145	40.34	0.01	0.03	0.02	12.72	0.18	46.42	0.39	0.01	0.01	100.14
	150	40.46	0.00	0.05	0.03	12.69	0.18	46.62	0.38	0.02	-0.01	100.43
	155	40.46	0.00	0.04	0.02	12.69	0.18	46.56	0.36	0.00	0.01	100.33

Transect	Distance (μm)	<i>SiO₂</i>	<i>TiO₂</i>	<i>Al₂O₃</i>	<i>Cr₂O₃</i>	<i>FeO</i>	<i>MnO</i>	<i>MgO</i>	<i>CaO</i>	<i>Na₂O</i>	<i>K₂O</i>	Total
	160	40.41	0.01	0.05	0.02	12.65	0.18	46.56	0.38	0.01	0.00	100.27
	165	40.50	0.02	0.05	0.03	12.66	0.18	46.61	0.37	0.02	0.01	100.44
	170	40.55	-0.01	0.04	0.02	12.75	0.19	46.65	0.37	0.01	0.01	100.61
	175	40.47	-0.01	0.05	0.02	12.66	0.18	46.60	0.39	0.01	0.01	100.39
	180	40.24	0.01	0.04	0.03	12.67	0.19	46.54	0.38	0.01	0.00	100.09
	185	40.60	-0.01	0.05	0.02	12.65	0.18	46.62	0.37	0.00	0.02	100.52
	190	40.55	0.01	0.04	0.02	12.70	0.18	46.68	0.38	0.00	0.00	100.57
	195	40.32	0.00	0.04	0.02	12.63	0.20	46.44	0.38	0.01	-0.01	100.03
	200	40.37	-0.01	0.05	0.02	12.64	0.19	45.54	0.41	0.03	0.00	99.25
	223	40.57	0.02	0.04	0.02	12.71	0.19	46.76	0.38	0.00	0.00	100.69
	246	40.28	0.01	0.06	0.02	12.52	0.18	46.38	0.42	0.03	0.01	99.91
	269	40.18	-0.01	0.06	0.03	12.28	0.19	45.39	0.49	0.06	0.02	98.68
	292	40.59	0.01	0.04	0.03	12.64	0.18	46.70	0.38	0.00	0.01	100.58
	315	39.18	0.00	0.28	0.02	11.93	0.19	44.57	1.13	0.09	0.05	97.45
	338	40.43	0.01	0.05	0.02	12.51	0.18	46.75	0.40	0.02	0.00	100.39
	361	40.74	0.01	0.04	0.02	12.62	0.18	46.84	0.36	0.01	0.00	100.81
	384	40.52	0.01	0.06	0.03	12.49	0.18	46.73	0.40	0.01	0.01	100.45
	407	44.08	0.01	0.09	0.03	12.30	0.19	48.17	0.38	0.02	0.01	105.28
	430	40.27	0.02	0.04	0.03	12.56	0.18	46.41	0.38	0.01	0.00	99.90
	453	40.41	0.02	0.05	0.03	12.50	0.17	46.73	0.36	0.00	0.01	100.28
	476	40.42	0.00	0.05	0.02	12.48	0.19	46.52	0.37	0.01	-0.01	100.06
	499	40.50	-0.01	0.04	0.03	12.54	0.18	46.47	0.38	0.01	0.00	100.15
	522	40.57	0.02	0.06	0.03	12.47	0.19	46.46	0.37	0.02	0.03	100.21
THde2.ol_macro3_transect_	0	38.70	0.04	0.03	0.00	21.99	0.31	39.32	0.43	0.00	0.00	100.82
	5	38.92	0.02	0.04	0.01	21.35	0.31	39.79	0.40	0.00	0.00	100.83
	10	39.00	0.00	0.03	0.00	20.60	0.30	40.27	0.41	0.01	-0.01	100.62
	15	39.07	-0.01	0.03	0.01	20.19	0.30	40.74	0.39	-0.01	0.02	100.75
	20	39.21	0.01	0.03	0.01	19.52	0.28	41.30	0.39	-0.02	0.01	100.76
	25	39.53	0.01	0.03	0.01	18.62	0.27	41.85	0.37	0.00	0.00	100.68
	30	39.64	-0.01	0.03	0.01	18.23	0.26	42.30	0.36	-0.01	0.00	100.83
	35	39.78	0.00	0.04	0.02	17.66	0.26	42.80	0.36	-0.01	0.01	100.92
	40	39.79	0.00	0.04	0.02	17.13	0.24	43.13	0.37	0.00	0.00	100.73
	45	39.95	0.02	0.04	0.02	16.71	0.24	43.61	0.37	0.02	0.00	100.96
	50	39.82	0.01	0.04	0.02	16.29	0.24	43.88	0.36	0.01	-0.01	100.66
	55	39.97	-0.01	0.05	0.02	15.81	0.22	44.06	0.36	0.02	0.01	100.50
	60	39.94	0.01	0.04	0.02	15.63	0.23	44.47	0.35	0.00	0.00	100.69
	65	40.00	-0.01	0.04	0.02	15.28	0.22	44.49	0.36	0.00	0.01	100.42
	70	8.61	0.00	0.06	0.00	3.28	0.05	9.34	0.12	0.00	0.00	21.46

Transect	Distance (μm)	<i>SiO₂</i>	<i>TiO₂</i>	<i>Al₂O₃</i>	<i>Cr₂O₃</i>	<i>FeO</i>	<i>MnO</i>	<i>MgO</i>	<i>CaO</i>	<i>Na₂O</i>	<i>K₂O</i>	Total
	75	41.07	0.03	0.03	0.02	14.99	0.23	45.67	0.36	0.00	0.00	102.41
	80	40.27	0.02	0.03	0.02	14.83	0.21	45.06	0.39	0.00	0.00	100.82
	85	40.36	0.01	0.04	0.02	14.87	0.22	45.22	0.38	0.01	0.01	101.15
	90	40.43	0.01	0.03	0.02	14.64	0.21	45.22	0.37	0.00	0.00	100.94
	95	40.26	0.00	0.05	0.02	14.46	0.21	45.30	0.38	0.01	0.00	100.69
	100	40.40	0.01	0.03	0.02	14.45	0.22	45.34	0.37	0.00	0.01	100.85
	105	40.32	0.01	0.02	0.02	14.34	0.21	45.36	0.37	0.00	0.01	100.66
	110	40.47	0.03	0.04	0.02	14.49	0.22	45.54	0.38	0.01	0.00	101.20
	115	40.47	0.01	0.04	0.02	14.24	0.21	45.67	0.35	0.01	0.00	101.02
	120	40.47	0.02	0.04	0.02	14.14	0.21	45.61	0.38	0.00	0.00	100.90
	125	40.31	0.01	0.05	0.02	14.16	0.21	45.62	0.36	0.00	-0.02	100.73
	130	40.42	-0.01	0.05	0.02	14.00	0.20	45.58	0.38	-0.01	-0.01	100.64
	135	40.57	-0.01	0.04	0.02	14.03	0.21	45.70	0.38	0.01	0.00	100.97
	140	40.50	0.00	0.03	0.02	14.00	0.21	45.70	0.37	0.00	-0.01	100.83
	145	40.45	0.01	0.04	0.02	13.98	0.20	45.66	0.35	0.00	0.02	100.73
	150	40.35	-0.01	0.06	0.03	14.00	0.21	45.80	0.36	0.01	0.00	100.81
	175	40.36	-0.01	0.03	0.02	13.85	0.21	45.96	0.39	0.03	0.00	100.85
	200	40.36	0.00	0.03	0.03	13.92	0.20	45.84	0.36	0.00	0.00	100.75
	225	40.45	0.00	0.04	0.02	13.87	0.21	45.79	0.39	0.00	0.00	100.78
	251	40.30	0.02	0.05	0.02	13.81	0.20	45.89	0.37	-0.01	0.00	100.67
	276	40.35	0.00	0.05	0.02	13.83	0.22	45.84	0.37	0.01	0.00	100.69
	301	40.40	0.00	0.04	0.02	13.87	0.21	45.89	0.39	0.00	0.00	100.81
	326	40.36	0.01	0.04	0.02	13.89	0.21	45.80	0.36	0.00	-0.01	100.69
	351	40.27	0.00	0.03	0.02	13.80	0.20	45.77	0.41	0.00	0.01	100.51
	376	40.34	-0.02	0.03	0.02	13.83	0.21	45.76	0.39	0.00	0.01	100.59
	401	40.23	0.01	0.04	0.02	13.93	0.20	45.70	0.38	0.00	0.00	100.49
	427	40.38	0.00	0.04	0.02	13.84	0.21	45.64	0.38	-0.01	0.02	100.52
	452	40.34	0.01	0.04	0.02	13.82	0.20	45.67	0.38	0.01	0.00	100.48
	477	40.44	0.00	0.05	0.02	13.85	0.21	45.66	0.36	0.03	0.02	100.64
	502	40.40	0.01	0.05	0.02	13.97	0.21	45.70	0.38	0.00	0.00	100.74
THf3b_oliv_macro1_transect_	0	39.39	0.03	0.03	0.01	19.01	0.27	41.49	0.40	0.01	-0.01	100.63
	5	39.53	0.01	0.02	0.01	18.61	0.25	41.94	0.34	0.01	-0.01	100.72
	10	39.57	0.01	0.04	0.01	18.20	0.26	42.35	0.34	0.01	0.00	100.79
	15	39.73	0.01	0.05	0.01	17.79	0.25	43.08	0.34	0.00	0.00	101.26
	20	39.84	0.02	0.06	0.01	17.48	0.25	42.70	0.36	-0.01	-0.01	100.71
	25	39.91	0.02	0.04	0.01	17.28	0.25	43.08	0.34	-0.01	-0.01	100.93
	30	40.05	0.00	0.04	0.02	16.90	0.25	43.37	0.35	0.00	0.00	100.97
	35	40.05	0.00	0.03	0.02	16.49	0.24	43.79	0.35	0.01	0.00	100.98

Transect	Distance (μm)	SiO_2	TiO_2	Al_2O_3	Cr_2O_3	FeO	MnO	MgO	CaO	Na_2O	K_2O	Total
	40	39.92	0.01	0.03	0.02	16.19	0.24	43.85	0.32	0.01	-0.01	100.58
	45	40.04	-0.01	0.03	0.02	15.94	0.23	44.16	0.32	-0.01	0.00	100.73
	50	40.19	0.00	0.03	0.02	15.87	0.24	44.34	0.35	0.00	0.01	101.05
	55	40.27	0.01	0.02	0.01	15.67	0.23	44.49	0.35	0.01	-0.01	101.06
	60	40.33	-0.01	0.02	0.02	15.31	0.23	44.61	0.38	0.00	0.00	100.90
	65	40.37	0.01	0.04	0.02	15.18	0.22	44.76	0.34	0.00	0.00	100.95
	70	40.33	0.04	0.04	0.02	14.93	0.22	44.97	0.35	0.01	0.01	100.90
	75	40.41	-0.01	0.04	0.02	14.85	0.22	45.25	0.36	0.01	-0.01	101.16
	80	40.28	0.01	0.05	0.03	14.54	0.21	45.21	0.35	0.00	-0.01	100.67
	85	40.38	0.01	0.04	0.02	14.46	0.21	45.20	0.37	0.00	-0.01	100.69
	90	40.54	0.00	0.03	0.02	14.44	0.22	45.48	0.35	0.00	0.01	101.10
	95	40.46	0.02	0.05	0.02	14.26	0.20	45.52	0.37	0.01	0.01	100.90
	100	40.46	0.01	0.04	0.02	14.18	0.21	45.62	0.35	0.01	-0.01	100.89
	105	40.61	0.04	0.04	0.02	14.06	0.21	45.67	0.36	-0.01	0.00	101.01
	110	40.31	0.00	0.03	0.02	14.05	0.20	45.83	0.37	0.02	-0.01	100.82
	115	40.56	0.00	0.03	0.02	13.90	0.21	45.84	0.37	0.00	-0.02	100.93
	120	40.46	-0.01	0.05	0.03	13.94	0.19	45.86	0.36	0.00	0.00	100.89
	125	40.69	0.03	0.05	0.02	13.92	0.20	46.08	0.35	0.00	0.00	101.34
	130	40.60	-0.01	0.04	0.02	13.92	0.19	45.88	0.36	0.00	0.01	101.03
	135	40.63	0.01	0.06	0.02	13.80	0.21	45.84	0.37	-0.01	0.01	100.93
	140	40.56	0.00	0.04	0.03	13.76	0.20	45.96	0.35	0.01	0.01	100.91
	145	40.60	0.00	0.04	0.02	13.68	0.21	45.99	0.37	-0.01	-0.01	100.91
	150	40.52	0.01	0.05	0.02	13.64	0.21	46.03	0.36	0.00	0.00	100.84
	179	40.77	0.02	0.05	0.02	13.44	0.20	46.27	0.39	0.01	0.01	101.16
	207	40.73	0.02	0.04	0.02	13.27	0.20	46.25	0.35	0.00	0.00	100.90
	236	40.76	0.01	0.04	0.03	13.25	0.21	46.43	0.37	0.00	0.00	101.09
	265	40.68	0.01	0.04	0.02	13.13	0.21	46.52	0.37	0.00	-0.01	100.97
	294	40.64	0.01	0.04	0.03	13.15	0.20	46.61	0.37	0.00	0.01	101.06
	322	40.69	0.00	0.03	0.02	13.11	0.20	46.66	0.41	0.00	0.00	101.13
	351	40.90	-0.01	0.04	0.03	13.11	0.18	46.80	0.36	0.01	0.01	101.43
	380	40.63	-0.01	0.04	0.02	13.09	0.19	46.45	0.35	0.00	0.02	100.78
	408	40.64	0.00	0.04	0.03	13.05	0.19	46.53	0.37	-0.01	0.00	100.85
	437	40.58	-0.01	0.05	0.02	13.03	0.19	46.52	0.38	0.01	0.01	100.78
	466	40.54	0.01	0.05	0.02	12.94	0.18	46.60	0.37	0.01	0.00	100.73
	495	40.57	0.02	0.04	0.02	13.07	0.19	46.66	0.37	0.00	-0.01	100.94
	523	40.59	0.00	0.04	0.02	12.99	0.18	46.62	0.36	0.00	0.01	100.81
	552	40.61	-0.01	0.03	0.02	12.97	0.20	46.76	0.37	0.00	0.00	100.95
THf3b_oliv_macro2_transect_	0	38.81	-0.01	0.04	0.01	21.41	0.31	39.51	0.38	-0.01	0.00	100.46

<i>Transect</i>	<i>Distance (µm)</i>	<i>SiO₂</i>	<i>TiO₂</i>	<i>Al₂O₃</i>	<i>Cr₂O₃</i>	<i>FeO</i>	<i>MnO</i>	<i>MgO</i>	<i>CaO</i>	<i>Na₂O</i>	<i>K₂O</i>	<i>Total</i>
	5	39.09	0.03	0.03	0.01	21.04	0.31	39.88	0.37	0.01	0.01	100.77
	10	38.80	0.02	0.09	0.00	20.63	0.30	39.82	0.35	0.01	0.01	100.03
	15	39.40	0.02	0.06	0.01	20.30	0.29	40.85	0.35	0.01	0.02	101.30
	20	39.26	0.00	0.02	0.01	20.06	0.28	40.84	0.35	-0.01	0.00	100.83
	25	39.21	0.03	0.03	0.01	19.69	0.29	41.29	0.36	0.01	0.00	100.93
	30	39.47	-0.01	0.03	0.01	19.30	0.27	41.53	0.34	0.01	0.00	100.96
	35	39.39	0.01	0.03	0.01	19.02	0.27	41.64	0.33	0.01	0.01	100.70
	40	39.49	0.01	0.02	0.02	18.86	0.28	41.76	0.36	0.00	0.02	100.81
	45	39.73	0.01	0.04	0.01	18.75	0.27	41.98	0.33	-0.01	-0.01	101.11
	50	39.63	-0.01	0.04	0.01	18.46	0.27	42.18	0.36	0.00	-0.01	100.93
	55	39.57	0.00	0.04	0.01	18.31	0.26	42.46	0.36	0.01	0.00	101.02
	60	39.51	0.01	0.04	0.02	18.09	0.25	42.41	0.35	0.00	0.00	100.68
	65	39.62	0.01	0.02	0.02	18.00	0.25	42.67	0.35	-0.01	0.00	100.94
	70	39.75	0.02	0.05	0.01	17.68	0.24	42.75	0.37	0.00	-0.01	100.87
	75	39.83	0.00	0.02	0.02	17.52	0.25	42.88	0.35	-0.01	0.01	100.87
	80	39.73	0.00	0.03	0.01	17.40	0.25	43.07	0.36	0.01	0.00	100.86
	85	39.96	0.01	0.03	0.01	17.39	0.24	43.03	0.34	0.00	0.00	101.01
	90	39.88	0.00	0.05	0.01	17.20	0.24	43.20	0.36	0.01	0.03	100.96
	95	39.95	0.01	0.04	0.01	16.99	0.24	43.30	0.35	0.02	-0.01	100.91
	100	39.96	0.00	0.03	0.02	16.92	0.25	43.32	0.35	0.01	0.02	100.87
	105	39.90	0.00	0.04	0.02	16.73	0.23	43.22	0.32	0.00	0.01	100.47
	110	39.47	0.00	0.05	0.01	16.52	0.22	42.77	0.34	0.00	0.01	99.39
	115	40.41	0.01	0.04	0.01	16.49	0.23	43.51	0.38	-0.01	-0.01	101.08
	120	38.44	0.01	0.12	0.01	15.97	0.22	40.85	0.34	0.01	-0.01	95.97
	125	19.26	0.00	0.67	0.01	8.20	0.11	24.68	0.23	0.01	0.01	53.17
	130	39.69	0.00	0.04	0.02	16.21	0.23	43.63	0.36	0.00	0.00	100.18
	135	39.82	0.01	0.06	0.02	16.10	0.24	43.90	0.35	0.00	-0.01	100.49
	140	39.91	0.01	0.04	0.02	16.15	0.22	44.12	0.36	0.00	-0.01	100.83
	145	40.18	-0.01	0.04	0.02	15.90	0.22	44.21	0.37	0.01	-0.01	100.94
	150	39.95	0.01	0.05	0.02	15.83	0.22	44.23	0.34	0.00	0.00	100.64
	176	40.17	0.01	0.04	0.01	15.20	0.21	44.78	0.34	0.00	0.01	100.77
	202	40.30	-0.01	0.05	0.02	14.73	0.21	45.33	0.37	0.02	0.00	101.01
	227	40.41	0.02	0.04	0.02	14.35	0.22	45.56	0.37	-0.01	0.00	100.99
	253	40.30	0.01	0.04	0.02	14.13	0.21	45.67	0.36	0.00	0.00	100.74
	279	40.49	0.01	0.05	0.02	13.90	0.19	46.01	0.35	0.00	0.00	101.02
	305	40.39	0.02	0.04	0.03	13.77	0.20	46.01	0.37	-0.01	0.00	100.83
	330	40.54	0.00	0.03	0.02	13.60	0.20	46.14	0.34	0.02	-0.01	100.89
	356	40.45	0.01	0.05	0.02	13.53	0.21	46.09	0.37	0.00	-0.01	100.72

Transect	Distance (μm)	SiO_2	TiO_2	Al_2O_3	Cr_2O_3	FeO	MnO	MgO	CaO	Na_2O	K_2O	Total
	382	40.63	0.01	0.04	0.02	13.44	0.20	46.26	0.37	-0.01	0.01	100.98
	408	40.56	-0.01	0.03	0.03	13.42	0.20	46.28	0.36	0.00	-0.01	100.89
	433	40.64	0.01	0.05	0.03	13.35	0.20	46.38	0.35	0.01	0.00	101.02
	459	40.65	-0.01	0.03	0.02	13.27	0.20	46.36	0.38	0.00	0.00	100.91
	485	40.65	0.00	0.03	0.02	13.25	0.21	46.50	0.40	0.01	0.01	101.08
	511	40.66	-0.01	0.05	0.02	13.12	0.20	46.44	0.37	0.00	-0.01	100.85
THi3_oliv_macro1_transect_	0	38.76	0.02	0.03	0.01	22.87	0.30	38.52	0.32	0.00	0.01	100.82
	5	39.51	-0.01	0.02	0.01	18.74	0.28	41.79	0.35	0.01	0.00	100.71
	10	40.00	0.01	0.03	0.01	16.94	0.25	43.32	0.37	0.00	-0.01	100.92
	15	40.06	0.02	0.03	0.01	16.14	0.23	43.95	0.36	0.00	0.01	100.79
	20	40.29	0.01	0.04	0.00	16.00	0.23	44.22	0.38	-0.01	0.00	101.16
	25	39.95	0.02	0.02	0.01	15.75	0.24	44.43	0.38	-0.01	-0.01	100.80
	30	40.08	0.01	0.03	0.02	15.65	0.22	44.32	0.37	0.00	0.00	100.69
	35	39.92	0.01	0.02	0.01	15.82	0.23	44.47	0.37	0.00	0.00	100.84
	40	40.13	0.01	0.04	0.01	15.71	0.22	44.53	0.35	0.02	0.00	101.01
	45	40.03	0.02	0.02	0.01	15.76	0.25	44.46	0.37	0.01	0.01	100.93
	50	40.05	0.00	0.03	0.01	15.73	0.23	44.52	0.34	0.02	-0.01	100.91
	55	40.16	0.02	0.03	0.01	15.72	0.23	44.46	0.36	0.00	-0.01	100.99
	60	40.11	0.02	0.03	0.01	15.58	0.24	44.36	0.37	0.01	0.00	100.72
	65	40.04	0.00	0.03	0.01	15.76	0.24	44.34	0.36	0.01	0.01	100.81
	70	40.10	0.01	0.03	0.01	15.75	0.23	44.45	0.35	0.02	-0.01	100.94
	75	39.47	0.01	0.05	0.01	15.72	0.24	43.63	0.38	0.02	0.00	99.52
	80	39.99	0.00	0.03	0.01	15.66	0.23	44.29	0.35	0.01	0.01	100.58
	85	14.28	0.02	0.15	0.01	8.86	0.13	17.81	0.23	0.01	-0.01	41.48
	90	40.13	0.01	0.04	0.01	15.76	0.24	44.40	0.37	0.00	-0.01	100.96
	95	40.08	0.01	0.03	0.01	15.63	0.23	44.29	0.36	0.01	0.00	100.65
	100	40.14	-0.01	0.03	0.01	15.72	0.23	44.38	0.37	-0.01	0.00	100.88
	105	40.01	0.02	0.04	0.01	15.72	0.23	44.28	0.37	0.00	0.01	100.69
	110	40.12	0.03	0.04	0.01	15.87	0.24	44.42	0.37	0.00	0.00	101.11
	115	39.92	0.00	0.04	0.01	15.83	0.24	44.54	0.34	0.00	0.01	100.94
	120	39.96	-0.01	0.03	0.01	15.74	0.23	42.89	0.40	0.01	0.00	99.26
	125	40.28	0.01	0.03	0.02	15.75	0.24	44.23	0.37	0.00	0.00	100.92
	130	40.18	0.03	0.03	0.01	15.79	0.24	44.30	0.34	0.00	0.01	100.92
	135	40.27	0.03	0.04	0.01	15.92	0.24	44.48	0.37	-0.01	-0.01	101.36
	140	40.11	0.02	0.02	0.01	15.76	0.24	44.23	0.35	-0.01	-0.01	100.73
	145	40.28	0.00	0.04	0.01	15.80	0.23	44.38	0.36	0.00	0.01	101.10
	150	40.01	0.01	0.05	0.01	15.72	0.23	44.35	0.36	-0.01	0.00	100.74
	172	40.08	0.01	0.05	0.01	15.84	0.24	44.36	0.37	0.00	0.01	100.98

<i>Transect</i>	<i>Distance (μm)</i>	<i>SiO₂</i>	<i>TiO₂</i>	<i>Al₂O₃</i>	<i>Cr₂O₃</i>	<i>FeO</i>	<i>MnO</i>	<i>MgO</i>	<i>CaO</i>	<i>Na₂O</i>	<i>K₂O</i>	<i>Total</i>
	194	40.06	0.02	0.05	0.01	15.83	0.24	44.42	0.34	0.01	0.00	100.97
	215	39.99	0.01	0.04	0.01	15.79	0.24	44.41	0.34	0.02	0.01	100.86
	237	40.19	-0.01	0.03	0.01	15.80	0.24	44.48	0.36	0.00	0.00	101.11
	259	40.20	-0.01	0.05	0.01	15.88	0.23	44.67	0.35	0.00	0.00	101.39
	281	40.16	0.03	0.03	0.01	15.87	0.24	44.38	0.34	0.00	0.00	101.05
	303	40.08	0.01	0.06	0.02	15.83	0.23	44.54	0.38	0.00	-0.02	101.15
	324	39.63	-0.01	0.05	0.02	15.58	0.24	44.12	0.34	-0.01	0.00	99.98
	346	40.06	-0.01	0.04	0.01	15.78	0.23	44.43	0.37	0.01	0.00	100.93
THj2_oliv_macro1_transect_	0	37.63	0.09	0.03	0.00	28.90	0.41	33.67	0.39	0.01	0.01	101.14
	5	38.13	0.06	0.02	0.00	26.91	0.39	35.34	0.37	0.00	0.01	101.22
	10	38.31	0.05	0.03	0.01	26.17	0.37	35.98	0.37	-0.01	0.01	101.29
	15	36.43	0.01	0.06	0.00	24.56	0.34	35.39	0.33	0.00	0.00	97.12
	20	36.74	0.01	0.04	0.00	23.76	0.35	35.08	0.32	0.01	-0.01	96.30
	25	38.57	0.02	0.02	0.01	24.04	0.34	37.66	0.34	0.00	-0.01	101.00
	30	38.45	0.01	0.02	0.00	23.35	0.35	38.77	0.35	0.01	0.00	101.31
	35	38.09	0.00	0.06	0.01	22.37	0.32	36.93	0.33	0.00	0.01	98.13
	40	37.47	0.03	0.05	-0.01	21.61	0.31	37.00	0.34	0.01	-0.01	96.81
	45	39.04	0.01	0.02	0.00	21.63	0.30	39.31	0.33	0.00	0.01	100.66
	50	39.16	0.01	0.02	0.01	21.50	0.32	39.73	0.34	0.01	0.00	101.10
	55	39.34	0.03	0.03	0.01	20.68	0.29	40.31	0.36	0.01	0.00	101.06
	60	39.38	0.01	0.04	0.01	20.15	0.28	40.70	0.35	0.01	0.00	100.94
	65	39.53	0.00	0.02	0.01	19.68	0.28	41.11	0.32	0.00	0.01	100.96
	70	39.55	0.01	0.04	0.01	19.31	0.27	41.51	0.36	0.00	0.01	101.06
	75	39.64	-0.01	0.03	0.00	18.98	0.27	41.71	0.34	0.00	-0.01	100.97
	80	39.75	-0.01	0.03	0.01	18.64	0.27	42.07	0.36	0.00	0.00	101.13
	85	39.46	0.00	0.04	0.01	18.12	0.27	41.53	0.42	0.01	0.01	99.86
	90	39.97	-0.01	0.03	0.01	18.12	0.26	42.51	0.34	0.00	0.02	101.24
	95	39.87	0.00	0.02	0.01	17.82	0.26	42.74	0.34	0.01	-0.01	101.09
	100	39.78	0.02	0.04	0.01	17.58	0.26	42.97	0.34	0.02	0.00	101.02
	105	39.73	0.00	0.03	0.01	17.45	0.26	43.00	0.36	0.00	-0.01	100.84
	110	39.69	0.00	0.03	0.02	17.17	0.25	43.02	0.37	0.00	0.01	100.55
	115	39.94	0.02	0.03	0.01	17.25	0.25	43.18	0.35	0.00	0.00	101.03
	120	39.86	0.00	0.03	0.01	17.27	0.25	43.29	0.34	0.00	-0.01	101.06
	125	39.87	0.00	0.05	0.01	17.06	0.25	43.31	0.33	0.00	0.01	100.88
	130	39.86	0.01	0.03	0.01	17.06	0.25	43.47	0.37	0.00	0.00	101.05
	135	39.99	0.00	0.04	0.01	16.96	0.25	43.42	0.37	0.02	-0.01	101.06
	140	40.00	0.01	0.03	0.00	16.95	0.24	43.58	0.36	0.00	0.01	101.18
	145	39.93	0.02	0.04	0.01	17.06	0.23	43.74	0.37	0.01	0.01	101.42

Transect	Distance (μm)	SiO_2	TiO_2	Al_2O_3	Cr_2O_3	FeO	MnO	MgO	CaO	Na_2O	K_2O	Total
	150	40.02	-0.01	0.02	0.01	16.83	0.24	43.71	0.34	0.02	-0.01	101.18
	158	40.11	0.02	0.03	0.02	16.82	0.26	43.76	0.37	0.00	0.01	101.40
	166	40.10	0.00	0.03	0.01	16.80	0.25	43.78	0.34	0.00	-0.01	101.32
	174	40.23	0.02	0.03	0.01	16.80	0.24	43.93	0.35	0.00	-0.01	101.62
	182	40.50	0.00	0.03	0.01	16.64	0.25	44.86	0.37	0.01	0.00	102.65
	190	39.68	0.03	0.03	0.01	16.54	0.25	43.38	0.34	0.00	-0.02	100.26
	198	40.04	0.01	0.04	0.01	16.58	0.25	43.92	0.37	-0.01	0.01	101.21
	206	40.15	0.03	0.04	0.01	16.54	0.24	44.01	0.37	-0.01	-0.01	101.39
	214	40.19	0.02	0.03	0.01	16.49	0.25	44.11	0.37	0.01	-0.01	101.47
	222	39.93	0.02	0.02	0.01	16.41	0.25	44.11	0.36	0.00	0.00	101.11
THj2_oliv_macro2_transect_	0	37.84	0.04	0.02	0.01	27.22	0.39	34.63	0.39	0.01	0.01	100.54
	5	37.88	0.03	0.01	0.00	26.47	0.37	35.52	0.35	0.00	0.00	100.63
	10	38.18	0.02	0.01	-0.01	25.57	0.37	36.17	0.36	0.00	0.01	100.69
	15	38.60	0.02	0.02	0.00	24.39	0.35	37.22	0.33	0.01	0.01	100.95
	20	38.59	0.01	0.05	0.01	23.32	0.33	38.18	0.32	-0.01	0.02	100.83
	25	38.92	0.01	0.02	0.00	22.15	0.31	39.29	0.32	0.00	-0.01	101.01
	30	39.00	0.03	0.03	0.01	21.16	0.30	39.89	0.32	0.01	0.01	100.76
	35	39.08	0.04	0.02	0.00	20.31	0.28	40.74	0.33	0.01	0.03	100.85
	40	39.44	0.00	0.03	0.00	19.57	0.28	41.40	0.36	0.02	0.02	101.12
	45	39.47	0.00	0.04	0.01	18.71	0.26	41.93	0.36	0.01	0.01	100.79
	50	39.66	0.02	0.03	0.01	18.23	0.26	42.51	0.35	0.01	0.00	101.07
	55	39.68	0.00	0.05	0.00	17.88	0.25	42.85	0.34	-0.02	0.02	101.08
	60	39.88	0.01	0.02	0.01	17.50	0.26	43.10	0.35	0.01	0.00	101.14
	65	39.87	0.03	0.05	0.01	17.30	0.26	43.40	0.35	-0.01	-0.01	101.27
	70	39.77	-0.01	0.02	0.01	17.23	0.25	43.52	0.35	0.01	0.01	101.16
	75	39.87	0.00	0.03	0.01	17.16	0.25	43.51	0.38	0.01	-0.01	101.22
	80	39.97	0.01	0.04	0.01	16.99	0.26	43.58	0.36	0.01	0.00	101.23
	85	39.88	-0.01	0.04	0.01	16.89	0.25	43.60	0.37	0.00	0.00	101.04
	90	39.99	0.00	0.03	0.02	16.88	0.24	43.80	0.34	0.01	0.00	101.30
	95	40.10	0.01	0.03	0.01	16.79	0.24	43.87	0.38	0.00	-0.01	101.44
	100	39.98	0.01	0.03	0.01	16.79	0.25	43.88	0.37	0.00	-0.01	101.33
	105	39.93	0.03	0.03	0.01	16.65	0.24	44.06	0.37	0.01	0.00	101.34
	110	40.22	0.00	0.03	0.01	16.50	0.25	43.96	0.38	-0.01	-0.02	101.35
	115	40.17	0.01	0.02	0.01	16.56	0.25	44.07	0.34	0.01	0.00	101.42
	120	40.44	0.02	0.03	0.01	16.43	0.25	44.55	0.36	-0.01	0.00	102.09
	125	30.95	0.02	0.14	0.01	10.93	0.15	33.23	0.26	0.00	-0.01	75.69
	130	30.08	0.05	0.19	0.01	14.06	0.20	23.11	0.40	0.01	0.03	68.14
	135	38.41	0.01	0.07	0.01	15.97	0.23	41.35	0.35	0.01	0.00	96.40

<i>Transect</i>	<i>Distance (μm)</i>	<i>SiO₂</i>	<i>TiO₂</i>	<i>Al₂O₃</i>	<i>Cr₂O₃</i>	<i>FeO</i>	<i>MnO</i>	<i>MgO</i>	<i>CaO</i>	<i>Na₂O</i>	<i>K₂O</i>	<i>Total</i>
	140	39.87	0.01	0.04	0.00	16.23	0.24	43.88	0.35	0.00	0.00	100.64
	145	39.93	0.02	0.03	0.01	16.30	0.24	43.92	0.35	0.00	0.00	100.81
	150	40.11	0.01	0.03	0.02	16.28	0.24	42.50	0.35	0.01	-0.01	99.54
	170	39.96	0.01	0.03	0.01	16.31	0.24	44.09	0.37	0.00	0.01	101.03
	190	39.99	0.02	0.05	0.01	16.29	0.24	44.24	0.36	0.01	-0.02	101.21
	210	40.64	0.02	0.05	0.01	16.17	0.24	45.63	0.35	0.01	0.01	103.11
	230	39.89	0.00	0.03	0.01	16.31	0.24	43.95	0.33	0.00	0.00	100.76
	250	39.93	0.01	0.04	0.01	16.10	0.24	44.15	0.35	0.01	0.00	100.83
	270	39.91	0.01	0.04	0.02	16.15	0.24	44.06	0.36	-0.01	0.00	100.77
	290	40.06	0.02	0.03	0.01	16.06	0.24	44.23	0.36	0.00	0.02	101.03
	310	39.96	0.03	0.03	0.01	16.09	0.25	44.21	0.37	0.01	0.00	100.96
	330	40.08	0.00	0.04	0.01	16.19	0.24	44.28	0.37	0.02	0.01	101.21
	350	40.32	0.01	0.03	0.01	16.21	0.24	44.34	0.34	0.01	0.00	101.50
	370	32.49	0.02	0.03	0.01	13.51	0.20	35.64	0.31	0.00	0.01	82.21
	390	40.06	0.00	0.03	0.01	16.22	0.24	44.04	0.38	0.00	0.01	100.99
	410	39.95	0.01	0.05	0.00	16.15	0.24	44.14	0.34	0.01	0.02	100.91
	430	40.13	0.00	0.04	0.01	16.31	0.24	44.08	0.35	0.00	-0.01	101.16
THj2_oliv_macro3_transect_	0	49.95	1.55	2.32	0.01	14.23	0.32	12.58	18.33	0.32	0.02	99.62
	11	50.70	1.35	2.67	0.01	11.52	0.27	14.04	19.21	0.30	0.02	100.09
	21	52.11	0.89	2.00	0.02	8.97	0.21	15.77	19.87	0.24	-0.01	100.08
	32	51.56	1.10	2.43	0.01	9.82	0.24	15.14	19.80	0.27	-0.01	100.37
	42	52.08	0.96	2.16	0.03	8.84	0.22	15.67	20.19	0.22	0.00	100.36
	53	52.00	0.92	2.14	0.03	8.74	0.20	15.64	20.18	0.24	-0.01	100.08
	63	51.31	0.96	2.23	0.02	8.57	0.21	15.40	20.27	0.25	0.01	99.23
	74	51.82	0.86	2.85	0.07	6.99	0.15	16.08	21.01	0.23	-0.01	100.06
	84	51.66	0.87	2.99	0.07	6.85	0.15	16.02	21.22	0.22	-0.01	100.05
	95	49.62	1.67	3.88	0.02	9.30	0.20	13.96	20.77	0.35	0.01	99.76
	106	45.82	1.38	3.05	0.01	9.06	0.22	12.08	19.51	0.29	0.00	91.41
	116	49.92	1.52	3.42	0.00	9.56	0.23	13.96	20.68	0.33	0.01	99.63
	127	50.57	1.28	3.09	0.00	9.08	0.22	14.39	20.81	0.31	0.00	99.74
	137	50.62	1.25	3.17	0.00	8.97	0.21	14.50	20.96	0.31	0.00	99.99
	148	50.78	1.16	2.89	0.00	9.03	0.21	14.69	20.70	0.30	0.01	99.76
	158	51.97	0.40	1.23	0.00	10.83	0.31	14.08	20.04	0.29	0.01	99.16
	169	52.26	0.46	1.24	0.00	11.36	0.33	13.89	20.24	0.31	-0.01	100.09
	179	52.48	0.36	1.05	-0.01	11.43	0.33	13.97	20.26	0.32	-0.01	100.20
	190	52.63	0.41	1.15	0.00	11.47	0.33	13.86	20.41	0.30	0.02	100.57
	201	52.35	0.41	1.14	0.01	11.51	0.34	13.85	20.25	0.31	-0.01	100.15
	211	52.24	0.43	1.15	0.00	11.66	0.35	13.88	20.19	0.30	0.00	100.19
	222	52.20	0.50	1.40	0.00	11.61	0.35	13.73	20.15	0.30	0.00	100.22

Appendix F – Annotated Fe-Mg Interdiffusion Code (R Notebook)

Note: `~~{r}` and `~~` indicate the start and end of a chunk, which can be run independently within R Studio. Comments are italicized.

```
---
```

```
title: "Fe-Mg Diffusion in Olivine (Costa,2008)"
```

```
output: html_notebook
```

```
---
```

This is an [R Markdown](http://rmarkdown.rstudio.com) Notebook. When you execute code within the notebook, the results appear beneath the code.

This code is modified from the mathematica code of Costa 2008. Annotations are modified from those found within.

```
```{r Import Relevant Packages, message=FALSE}
```

```
library(ggthemes)
library(ggplot2)
library(RColorBrewer)
library(gridExtra)
library(tidyverse)
library(GGally)
library(extrafont)
library(ggrepel)
library(cowplot)
library(ggalt)
library(readxl)
library(grid)
library(dplyr)
library(viridis)
library(ggsci)
library(wesanderson)
library(ggpubr)
library(reshape2)
library(pracma)
library(data.table)
```
```

Clear Global Environment to avoid memory effects from previous calculations

```
```{r}
rm(list = ls())
```
```

```

Import .csv file
**FOR BEST RESULTS/LEAST HEADACHES USE A FILE WHICH:      **
**1. Has two columns labelled "Dist" and "Fo" respectively **  

**2. Has NO N/A values  

``{r}
Tung_OI_Transects <- read.csv("~/Diffusion Modeling/Tung_Transects/Tung_OI_Transects.csv", header = TRUE, sep = ',')
``

``{r}
TungOITransects_Split <- split(Tung_OI_Transects, Tung_OI_Transects$Sample.Name)
``

``{r}
Transect_Name <- "THj2_oliv_macro2_transect_"

datafo <- TungOITransects_Split[[Transect_Name]][,c(6,29)]

colnames(datafo) <- c("Dist", "Fo")
datafo$Dist <- abs(max(datafo$Dist) - datafo$Dist)

datafo <- datafo[order(datafo[,1]),]    # These two lines ensure the data is in a consistent order where
rownames(datafo) <- 1:nrow(datafo)    # x = 0 is in row 1
``

Plot Fo vs. Distance
``{r}
ggplot() +
  geom_line(aes(x = datafo$Dist, y = datafo$Fo), col = "blue") +
  labs(x = "Distance (μm)", y = "Fo %")
``

``{r}
Fomin = min(datafo$Fo) # Good idea to check these values before beginning.
Fomax = max(datafo$Fo)

Fomin
Fomax
``
```

Set-up Grid, Number of Iterations, and Max Number of Days

```
```{r}
dx = 5 # Set Grid step (μm)
dt = 60 # Set Time step (s)
R1=dt/(dx^2) # Dummy variable used later for stability check
Maxdays = 3600 # Set the maximum number of days the code will run
titer=1440 # Number of iterations per day. 1440 = 1 iteration/minute.
````
```

Normalize to the number of gridpoints we have chosen (=dataf0).

```
```{r}
dataf0 = dataf0
dataf0 = dataf0$Dist/dx
````
```

The larger the number of gridpoints the more detailed will be the result but the longer time it will take to do the calculation.

The number of gridpoints has to be an integer number so the command round() is applied.

```
```{r}
ttlength = max(dataf0$Dist) # Set the length of the model based on the profile measurement
ttgrid = round(ttlength/dx, digits = 0) # Number of grid points based on dx and length of profile
````
```

*(a,b,c)x = Cos of the angle between the electron microprobe traverse and the (a,b,c) axes of the crystal.
fO2 shown with respect to the Log NNO oxygen buffer of Huebner and Sato (1970)*

```
```{r}
PRES = 2000 # Pressure in bars
Temp = 1153 # Temp in C
logfO2 = 9.36 - (24930/(273.15+Temp))+(0.046*((PRES-1)/(273.15+Temp)))
fO2 = 10^logfO2 # fO2 in bars
minFo = min(dataf0$Fo) # Lowest Fo in profile. Used for stability check.
ax = round(cos(deg2rad(90))) # Values for determining axes based on angle between
bx = round(cos(deg2rad(90))) # the transect and crystal axes
cx = cos(deg2rad(0)) # Use round(cos(deg2rad(90)), digits = 0) to get an exact 0 value
````
```

Plot to check the row number of the inflection point

```
```{r}
ggplot() +
 geom_line(aes(x = c(1:nrow(dataf0)), y = dataf0$Fo), col = "blue") +
 labs(x = "Grid Step", y = "Fo %")
````
```

```

``{r}
InfPt = 20          # Inflection point, analysis/row number where the core ends.

NNO = 9.36 - (24930/(273.15+Temp))+(0.046*((PRES-1)/(273.15+Temp))) # Log oxygen fugacity calculation from Huebner and Sato (1970)

deltaNNO = log10(fO2)-NNO    # Comparison to the NNO buffer calculated from P and T Inputs.
deltaNNO
```

```

*Diffusion coefficient data for Fe-Mg (DFo) from Dohmen and Chakraborty (2007a), with corrections of Dohmen and Chakraborty (2007b). Using diffusion parameters for fO<sub>2</sub> > 10<sup>-15</sup> bar, for lower fO<sub>2</sub> see publications.*  
*DFo(a,b,c) = Fe-Mg diffusion coefficient parallel to (a,b,c) axis in μm<sup>2</sup>s<sup>-1</sup>.*

*The only variable that changes with time is the concentration and thus we have created a new set of diffusion coefficients without the dependence and this will be directly incorporated in the diffusion loop.*

*DFox= diffusion coefficient parallel to the electron microprobe traverse.*

*DFoxd= expression of DFo without the compositional dependence used to speed up the loop below.*

```

``{r}
DFoc = (10^-9.21)*((fO2/10^-12)^(1/6))*(10^(3*(0.9-0.01*minFo)))*exp(-(201000+(PRES-1)*7*(10^-6)*(10^5))/(8.314*(Temp+273.15)))*(10^12)

```

DFoa = DFoc/6.

DFob = DFoc/6.

DFocd = (10^-9.21)\*((fO2/10^-12)^(1/6))\*exp(-(201000+(PRES-1)\*7\*(10^-6)\*(10^5))/(8.314\*(Temp+273.15)))\*(10^12)

DFoad = DFocd/6.

DFobd = DFocd/6.

DFoxd = (DFoad\*ax<sup>2</sup>) + (DFobd\*bx<sup>2</sup>) + (DFocd\*cx<sup>2</sup>)

DFox = DFoxd\*(10^(3\*(0.9-0.01\*minFo)))

DFoc

R1\*DFox

*The stability criteria for the implicit method is that δt/δx<sup>2</sup>\*DFox < 0.5.*

*δt/δx<sup>2</sup> = R1 = dummy variable to speed up the loop below.*

*Choosing the initial distribution (in this case homogeneous and equal to Foini) of Fo (= cFo) and seeding the diffusion coefficients for the initial distribution (= DIFFo)*

```

```{r}
Foini = mean(datafo$Fo[1:InfPt])           # Set the Inflection point at the edge of the core.
                                              # The initial left(core) Fo boundary is set by taking the
                                              # average value up to the inflection point
cFo = matrix(Foini, nrow = ttgrid + 1, ncol = 2)
cFo[,1] = (0:ttgrid)

Foini
```

```{r}
ggplot() +
  geom_line(aes(x = datanfo, y = datafo$Fo), col = "blue") +
  geom_line(aes(x = cFo[,1], y = cFo[,2]), col = "red")
```

DIFFo is the Diffusion Coefficient

```{r}
DIFFo = matrix(0, nrow = ttgrid + 1, ncol = 2)
DIFFo[,1] = (0:ttgrid)

for (i in 0:ttgrid+1) {
  DIFFo[i,2] = DFoxd*10^(3*(0.9-0.01*(cFo[i,2])))
}

DIFFoBound = DFoxd*10^(3*(0.9-0.01*(minFo)))
DIFFoBound
```

```{r}
ggplot() +
  geom_line(aes(x = DIFFo[,1],y = DIFFo[,2]), col = "green") +
  coord_cartesian(ylim=c(0, 0.001)) +
  labs(x = "Grid Point", y = "Diffusion Coefficient")
```

Initializing some matrices to be filled later

```{r}
NRMSE = matrix(0, nrow = Maxdays, ncol = 1)
FoHold = matrix(0, nrow = ttgrid + 1, ncol = Maxdays)
```

```

*Diffusion Calculation in the form of nested loops.*

```
```{r message=FALSE, warning=FALSE}
for (f in 1:Maxdays){      # Set up to run Maxdays*itтерation where dx*ttiter = 1 day
  for (i in 0:ttiter){
    bFo = cFo
    cFo[1,2] = cFo[2,2]
    #cFo[tgrid+1,2] = min(datafo$Fo)  # Boundary Condition, set equal to min(datafo$Fo) if assuming rim equilibrium with groundmass
    for (j in 1:tgrid + 1){
      DIFFo[j,2] = DFoxd*10^(3*(0.9-0.01*(cFo[j,2])))
    }
    for(k in 1:tgrid + 1){
      if(k == 1){
        cFo[k,2] = bFo[k,2] + R1*((DIFFo[k+1,2]-DIFFo[k,2])*(bFo[k+1,2]-bFo[k,2]))+(DIFFo[k,2]*(bFo[k+1,2]-(2*bFo[k,2])+Foini)))
      }
      if(k > 1 && k < tgrid){
        cFo[k,2] = bFo[k,2] + R1*((DIFFo[k+1,2]-DIFFo[k,2])*(bFo[k+1,2]-bFo[k,2]))+(DIFFo[k,2]*(bFo[k+1,2]-(2*bFo[k,2])+bFo[k-1,2])))
      }
      if(k == tgrid){
        cFo[k,2] = bFo[k,2] + R1*((DIFFoBound-DIFFo[k,2])*(minFo-bFo[k,2]))+(DIFFo[k,2]*(minFo-(2*bFo[k,2])+bFo[k-1,2])))
      }
      if(k == tgrid + 1){
        cFo[k,2] = minFo
      }
    }
  }
  FoHold[,f] = cFo[,2]
  NRMSE[f,1] = ((sqrt(mean((datafo[,2] - cFo[c(1,round(datanfo)),2])^2)))/(max(datafo[,2]) - min(datafo[,2])))
  if(f > 2 && NRMSE[f,1] > NRMSE[f-1,1] && NRMSE[f-1,1] < NRMSE[f-2,1]){
    NRMSEFinal = round(NRMSE[f-1,1], digits = 4)
    PredDays = f-1
    print(PredDays)
    break
  }
}
```
Plotting Set-up
```{r}
ModelPlotInterval = PredDays/10  # Set number of days between plotted models

FoHold.Clipped <- data.frame(FoHold[,0:PredDays])  #Clip Data frame to end of model run
```

```

FoHold.Clipped$Distance = c(0:ttgrid)*dx           #Add distance Column for Plotting
FoHold.Intervals =
  FoHold.Clipped[,seq(0,PredDays,ModelPlotInterval)] #Create Data Frame with desired intervals for plotting. ncol = PredDays/Model Plot Interval
  FoHold.Intervals$Distance = c(0:ttgrid)*dx          #Add distance Column for plotting

FoHold.Melt <- melt(FoHold.Intervals,id.vars = "Distance")

pal = plasma(ncol(FoHold.Intervals)-1)

lblspce = 0.75
LgndHt = 0.5
```
Plotting result
```{r}
ModelPlot = ggplot() +
  #geom_point(data = datafo, aes(datafo$Dist, datafo$Fo), shape = 1, color = "blue") +
  #geom_smooth(data = datafo, aes(datafo$Dist, datafo$Fo), method = "loess",color = "blue") +
  geom_line(data = FoHold.Clipped, aes(FoHold.Clipped$Distance, FoHold.Clipped[,1]), color = "navy", size = 1) +
  geom_line(data = FoHold.Melt, aes(x = Distance, y = value, col = variable),) +
  geom_line(data = FoHold.Clipped, aes(FoHold.Clipped$Distance, FoHold.Clipped[,PredDays]), color = "black", size = 1) +
  geom_point(data = datafo, aes(datafo$Dist, datafo$Fo), shape = 1, color = "blue") +
  coord_cartesian(xlim=c(0, round(max(datafo$Dist), digits = -1) + 10), ylim = c(min(datafo$Fo), max(datafo$Fo))) +
  scale_color_manual(values = pal) +
  labs(x = "Distance (\u00b5m)", y = "% Fo",
       color = "", shape = "", fill = "") +
  theme_bw() +
  theme(axis.title.x=element_text(size = 24, family = "Avenir"),
        axis.title.y=element_text(size = 24, family = "Avenir"),
        axis.text.x=element_text(size=20, family = "Avenir"),
        axis.text.y=element_text(size=20, family = "Avenir"),
        legend.position = "none") +
  annotate(geom = "text", x = 0, y = min(datafo$Fo) + LgndHt + (8*lblspce), label = "Transect = ", hjust = 0) +
  annotate(geom = "text", x = (max(datafo$Dist)/8)^3, y = min(datafo$Fo) + LgndHt + (8*lblspce), label = Transect_Name, hjust = 0) +
  annotate(geom = "text", x = 0, y = min(datafo$Fo) + LgndHt + (7*lblspce), label = "Total Time (days) = ", hjust = 0) +
  annotate(geom = "text", x = (max(datafo$Dist)/8)^3, y = min(datafo$Fo) + LgndHt + (7*lblspce), label = PredDays, hjust = 0) +
  annotate(geom = "text", x = 0, y = min(datafo$Fo) + LgndHt + (6*lblspce), label = "Plotted Interval (days) = ", hjust = 0) +
  annotate(geom = "text", x = (max(datafo$Dist)/8)^3, y = min(datafo$Fo) + LgndHt + (6*lblspce), label = ModelPlotInterval, hjust = 0) +
  annotate(geom = "text", x = 0, y = min(datafo$Fo) + LgndHt + (5*lblspce), label = "Axis = ", hjust = 0) +
  annotate(geom = "text", x = (max(datafo$Dist)/8)^3, y = min(datafo$Fo) + LgndHt + (5*lblspce), label = paste(ax,bx,cx), hjust = 0) +
  annotate(geom = "text", x = 0, y = min(datafo$Fo) + LgndHt + (4*lblspce), label = "log(fO2) = ", hjust = 0) +

```

```
annotate(geom = "text", x = (max(datafo$Dist)/8)*3, y = min(datafo$Fo) + LgndHt + (4*lblspce), label = round(logfO2, digits = 3), hjust = 0) +
  annotate(geom = "text", x = 0, y = min(datafo$Fo) + LgndHt + (3*lblspce), label = "T(°C) = ", hjust = 0) +
  annotate(geom = "text", x = (max(datafo$Dist)/8)*3, y = min(datafo$Fo) + LgndHt + (3*lblspce), label = Temp, hjust = 0) +
  annotate(geom = "text", x = 0, y = min(datafo$Fo) + LgndHt + (2*lblspce), label = "P(kbar) = ", hjust = 0) +
  annotate(geom = "text", x = (max(datafo$Dist)/8)*3, y = min(datafo$Fo) + LgndHt + (2*lblspce), label = formatC(signif(PRES/1000,digits=2),
  digits=2, format="fg", flag="#"), hjust = 0) +
  annotate(geom = "text", x = 0, y = min(datafo$Fo) + LgndHt + (1*lblspce), label = "NRMSE = ", hjust = 0) +
  annotate(geom = "text", x = (max(datafo$Dist)/8)*3, y = min(datafo$Fo) + LgndHt + (1*lblspce), label = NRMSEFinal, hjust = 0)
ModelPlot
```

```

## Appendix G – Diffusion and Thermobarometry Equations

Oxygen Fugacity Equation (Huebner and Sato, 1970; Costa, 2008)

$$fO_2 = 9.36 - \left( \frac{24930}{273.15 + T} \right) + \left( 0.046 * \left( \frac{P - 1}{273.15 + T} \right) \right)$$

Diffusion Coefficient (Costa, 2008)

$$D_{\text{Fe-Mg}} = 10^{-9.21} \cdot \left( \frac{f_{O_2}}{10^{-7}} \right)^{1/6} \cdot 10^{3(X_{\text{Fe}} - 0.1)} \exp \left( -\frac{201000 + (P - 10^5) \cdot 7 \cdot 10^{-6}}{RT} \right)$$

Finite Difference Equation (Costa, 2008)

$$\text{New } Fo_{[k,2]} = Fo_{[k,2]} + \frac{\delta t}{\delta x^2} * (((D_{[k+1,2]} - D_{[k,2]}) * (Fo_{[k+1,2]} - Fo_{[k,2]})) + (D_{[k,2]} * (Fo_{[k+1,2]} - (2 * Fo_{[k,2]} + Fo_{[k-1,2]}))))$$

Plagioclase Thermometer (Druitt et al., 2012)

$$T(\text{°K}) = 855 + \left( 400 * \frac{An - 40}{80 - 40} \right)$$

Liquid Thermobarometer (Yang et al., 1996; Putirka, 2008)

$$T(\text{°C}) = -583 + 3141 \left[ X_{\text{SiO}_2}^{\text{liq}} \right] + 15779 \left[ X_{\text{Al}_2\text{O}_3}^{\text{liq}} \right] + 1338.6 \left[ X_{\text{MgO}}^{\text{liq}} \right] \\ - 31440 \left[ X_{\text{SiO}_2}^{\text{liq}} \cdot X_{\text{Al}_2\text{O}_3}^{\text{liq}} \right] + 77.67 \left[ P(\text{GPa}) \right]$$

Ti-in-melt predictor from Ti in plagioclase (Bindeman et al., 1996)

$$Ti_{\text{melt(ppm)}} = (TiO_2 * 0.59951) / \frac{\exp(-28.9(An/100) - 15.4)}{0.008314 * T(\text{°K})}$$